Dissertation zur Erlangung des Doktorgrades
der Fakultät für Chemie und Pharmazie
der Ludwig-Maximilians-Universität München

A New Player in mTOR Regulation: Introducing FKBP51

Andreas Matthias März

aus

Starnberg

2011

Erklärung

Diese Dissertation wurde im Sinne von § 13 Abs. 3 bzw. 4 der Promotionsordnung vom 29. Januar 1998 (in der Fassung der sechsten Änderungssatzung vom 16. August 2010) von Herrn Prof. Dr. C. Turck betreut und vor der Fakultät für Chemie und Pharmazie vertreten.

Ehrenwörtliche Versicherung

Diese Dissertation wurde selbständig, ohne unerlaubte Hilfe erarbeitet.

München, den 31.05.2011

.....
Andreas März

Dissertation eingereicht am: 31.05.2011

1. Gutachter: Prof. Dr. C. Turck
2. Gutachter: Prof. Dr. R. Beckmann

Mündliche Prüfung am: 23.01.2012

This thesis was made at the Max Planck Institute of Psychiatry in the research group „chemical genomics“ under supervision of Dr. Felix Hausch.

Poster presentations:

“Frontiers in Medicinal Chemistry”, March 2 – 5 2008, University of Regensburg:

Kozany C, **März A**, Hausch F:
Characterization of FKBP51 and FKBP52 by High Throughput-Compatible Fluorescence Polarization Assays

“Signal Transduction and Disease”, September 27 – 30 2009, RWTH Aachen:

März A, Bracher A, Hausch F:
A new player in mTOR regulation: Introducing FKBP51

Publications:

Kozany C, **März A**, Kress C, Hausch F.

Fluorescent probes to characterise FK506-binding proteins.
Chembiochem. 2009 May 25;10(8):1402-10.

März A, Bracher A, Hausch F

Large FK506-Binding Proteins Shape the Pharmacology of Rapamycin.
(manuscript in preparation)

Oral presentation:

A New Player in mTOR Regulation: Introducing FKBP51
Institute seminar, November 5 2009

Table of contents

1 – Introduction:

1.1 – FKBPs: big family with huge functional diversity

The FK506 binding proteins (FKBPs) are members of the family of immunophilin proteins and display peptidyl prolyl cis-trans isomerase activity (PPIase)[1, 2]. This enzymatic action plays a role in the folding of numerous proteins as the interconversion of peptide bonds (like Xaa-proline) often is a rate-limiting step [3] (see figure 1.1). The process is accelerated by binding of the target sequence at the active site of the FKBP and stabilization of the transition state by hydrogen bonds during isomerization [4]. Generally, the effectiveness of PPIases tends to be low, demanding high concentrations of these proteins. The same is true for the PPIase-independent chaperone function of some FKBPs that includes binding of non-native proteins, inhibition of unwanted inter- and intramolecular interactions and separation of productive and non-productive folding steps [5].

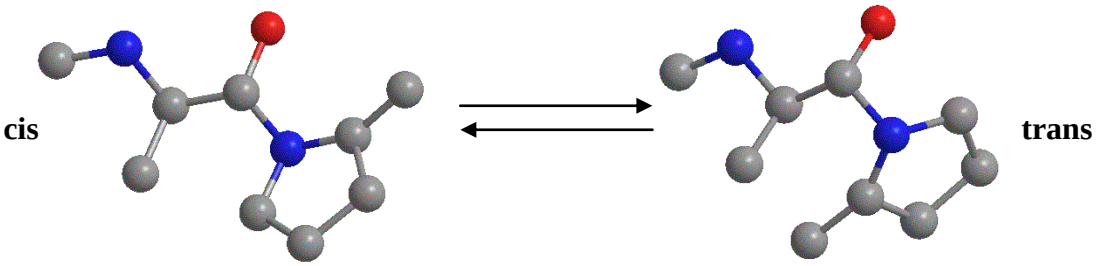

Figure 1.1: FKBPs possess peptidyl-prolyl-cis-trans-isomerase activity
Schematic representation of cis-trans isomerization of the peptide bond between proline and the adjacent residue. Blue: Nitrogen; red: carbonyl oxygen of peptide bond.

Apart from their role in protein maturation, the diverse members of the FKBP protein family also act as receptors of the natural compounds FK506 and rapamycin: by formation of the FKBP12*FK506 complex, not only the PPIase activity of FKBP but also the phosphatase activity of the secondary target calcineurin is inhibited [6, 7]. A blockage of calcineurin causes reduced activation of the transcription factor NF-AT that stimulates IL-2 expression and thereby promotes activation of T-cells [8]. In contrast, the complex of FKBP12 and rapamycin inhibits the action of the kinase mTOR that results in general reduction of protein biosynthesis and cell growth [9-11]. Interestingly, FKBP12 is more abundant in nerve tissue than in the immune cells [12], and its expression is especially strong after nerve injury [13].

Thus, a neuro-protective or even neurotrophic effect of FKBP12 is supposed [14] as rapamycin enhances neurite outgrowth in certain neurons [15].

FKBP proteins with higher molecular weight contain several domains, including ones with PPIase and FK506 binding capability (FKBD), domains for interaction with Hsp90 (TPR/tetratricopeptide domain) [16, 17] and domains for putative interaction with calmodulin (calmodulin-binding domain (CBD)). Figure 1.2 provides an overview of important FKBPs and their domain structure.

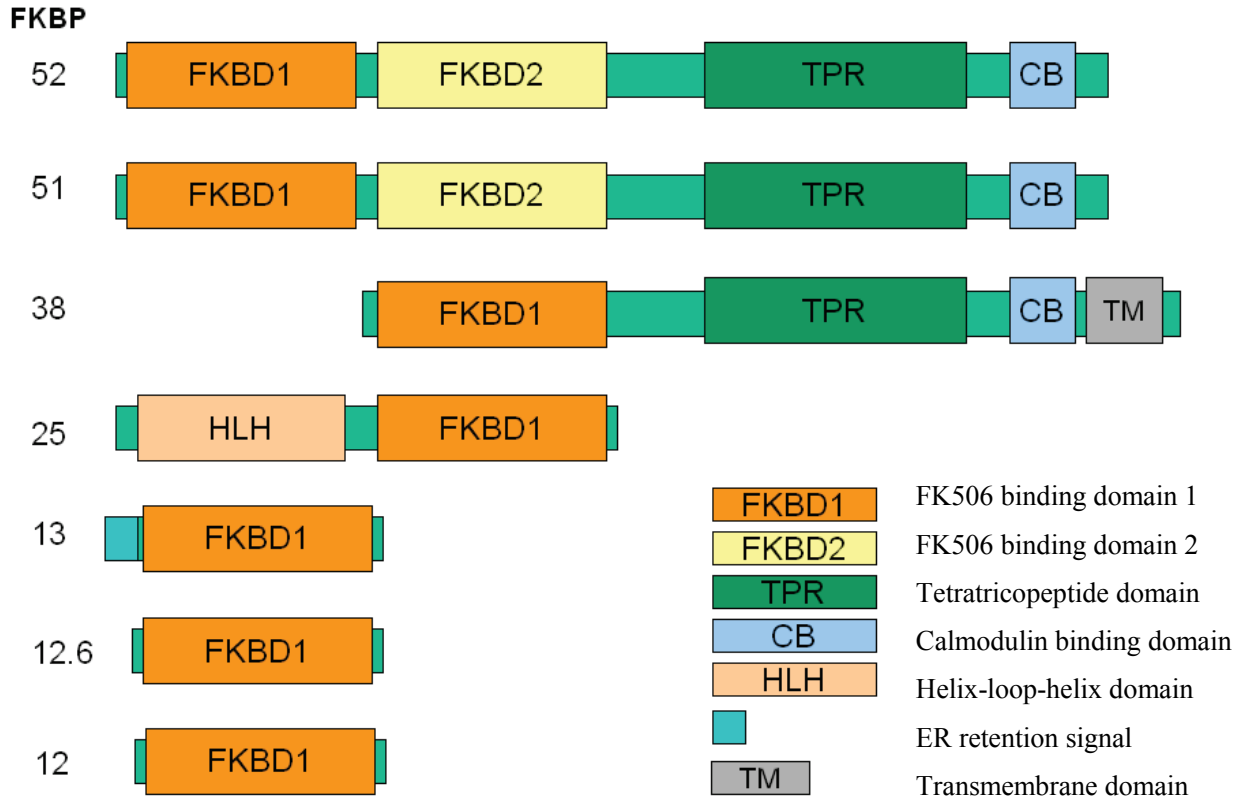

Figure 1.2: Larger FKBPs contain several domains

Simplified scheme of the domain structures of human FKBPs.

N-Terminus: left; C-Terminus: right.

1.1.1 – FKBP12: the archetype of the family

The prototypic member of the FKBP family, FKBP12, consists of a single FKBD domain [18] and is almost ubiquitously expressed in all human tissues [19]. The protein binds FK506 and rapamycin with very high affinity (K_d: 0.2 and 0.4 nM) [20], is stabilized by formation of the complex and inhibits the target protein within the ternary complex with calcineurin or

mTOR [6, 21]. Structurally, the FKBD domains are dominated by an amphipathic, five-stranded ß-sheet that has a right-handed twist and turns around a central alpha-helix. In most cases, a hydrophobic pocket forms the binding pocket for FK506 and rapamycin [18, 22, 23].
Other cellular proteins are influenced by FKBP12 as well: an interaction between FKBP12 and the ryanodine receptor [24, 25], one of the main calcium influx channels of the endoplasmatic reticulum, results in a better performance of the channel [26]. The phosphorylation status of inositol-1,4,5-triphosphate receptor (IP_3R) is also regulated by the phosphatase calcineurin that in turn is recruited to the receptor via FKBP12 [27]. FKBP12 represents a natural ligand of the TGF-ß receptor 1 [28] and stabilizes its inactive conformation [29, 30]. Altogether, the protein plays an important role either by interacting with target proteins itself or by mediating protein-protein interactions, resulting in altered regulation of the binding partner.
Another finding supports this model of FKBP action: in brain-restricted FKBP12 knockout mice, interactions between Raptor and mTOR seem to be stronger than in wild type mice, resulting in increased basal mTOR and S6Kinase phosphorylation. On a behavioural level, the mice show better contextual fear memory and display abnormal repetition [31].
In a cell culture model of Parkinson's disease, the reduction of FKBP12 resulted in reduced aggregation of alpha-synuclein and protected cells from cell death [32], thus providing an explanation for neuroregenerative and neuroprotective properties of FKBP proteins. On the other hand, researchers had shown before that FKBP12 mRNA cannot be detected in human neuroblastoma cells; nevertheless, a protective effect of FK506 and a non-immunosuppressive analogue could be observed which must be at least partially FKBP12-independent [33].

1.1.2 – FKBP51 and FKBP52: the multi-domain members

FKBP51 was initially isolated from murine T-cells [34] and murine adipocytes [35] where its expression is specifically induced during final steps of differentiation. Further characterization revealed that the protein contains PPIase activity, binds to FK506 and rapamycin, but does not inhibit calcineurin activity [36]. This large FKBP12 homologue is expressed in a multitude of human tissues, often even in molar excess compared to FKBP12 [19]. FKBP51 is a multi-domain protein: the TPR domain plays an important role in mediating interactions with Hsp70/90 [37, 38], while only one of the two FKBD (FK506/Rapamycin binding) domains displays PPIase activity [16].

One of the best-studied functions of FKBP51 is its ability to reduce hormone binding affinity of the glucocorticoid receptor. In accordance with this finding some monkey species are hyposensitive to cortisol, and FKBP51 is overexpressed in some of their tissues [39, 40]. The monkey version of the protein displays stronger inhibitory effects on hormone binding of the receptor compared to human FKBP51 [41]. In spite of structure determination so far no exact mechanism could be determined that explains the different effects of FKBP51 variants [42].

The expression of FKBP51 can be strongly increased by corticosteroids [43, 44]. Therefore a feedback mechanism for adjusting the glucocorticoid susceptibility is created by the fact that FKBP51 reduces the activity of the glucocorticoid receptor [45],[46]. This neuroendocrine circuit is part of the HPA (hypothalamic – pituitary – adrenal) axis which can be considered as one main regulator of the stress response.

At the MPI of Psychiatry it has been found that polymorphisms within the FKBP51-encoding gene (*FKBP5*) seem to increase the risk of relapse into depressive episodes and attenuate patients' response to antidepressive treatment [47, 48]. Additionally, *FKBP5* gene mutations seem to influence the response of healthy subjects upon psychosocial stress [49]. In african-american patients, a correlation between single nucleotide polymorphisms in the *FKBP5* gene and abuse-induced suicide was established [50]. Another study revealed that genetic variability in *FKBP5* might increase the number of depressive episodes in bipolar subjects [51]. Altogether these results implicate an important role of FKBP51 in HPA axis dysregulation and suggest that targeting the protein might be beneficial for treatment of depressed patients.

FKBP51 expression is influenced by other steroid hormones as well, suggesting an importance of the protein in the regulation of glucocorticoid, progesterone and androgen receptors [52]. Concerning the latter, an especially interesting role of FKBP51 has been identified in prostate cancer cells, as the co-chaperone seems to promote androgen receptor complex formation and increases its activity [53, 54].

Furthermore, decreased FKBP51 expression in old age seems to contribute to memory impairment in mice [55]. Similarly, the co-chaperone is involved in stabilization of the Tau protein, causing its hyperphosphorylation and aggregation. As a consequence, senile plaques, a hallmark of Alzheimer's disease, are stabilized [56].

Very recently, FKBP51 has been proposed as a negative regulator of the Akt signaling pathway: it functions as a scaffolding protein to recruit the phosphatase PHLPP to Akt, resulting in decreased survival signaling. Thus, certain cell lines are more susceptible to

chemotherapeuticals. Interestingly, FKBP51 is downregulated in a number of cancer cell lines [57]. A possible role as a tumour suppressor protein still has to be established.

The large immunophilin **FKBP52** (or synonymously Hsp56) was originally characterized in 1992 as a protein with four clearly distinguishable domains that are arranged like in FKBP51 [58-60]. Again, the first PPIase domain exhibits enzymatic activity and binds FK506 and rapamycin, while FKBD2 shows extremely low activity and does not bind the natural compounds. There can be also found a putative ATP/GTP binding site whose function is not yet well characterized [61].

Additionally, FKBP52 contains a phosphorylation site that can be modified by casein kinase II and changes the Hsp90 binding ability [62]. Furthermore the protein represents the cellular factor that binds a single-stranded region of the genome of the adeno-associated virus (AAV) and inhibits DNA synthesis [63]. This inhibitory effect can be modified by dephosphorylation of specific Ser/Thr/Tyr residues in FKBP52 [64]. The cellular expression of FKBP52 can be induced by heat-shock, and the promoter region of the corresponding gene contains a consensus sequence for binding of the heat-shock transcription factor in rabbits [65].

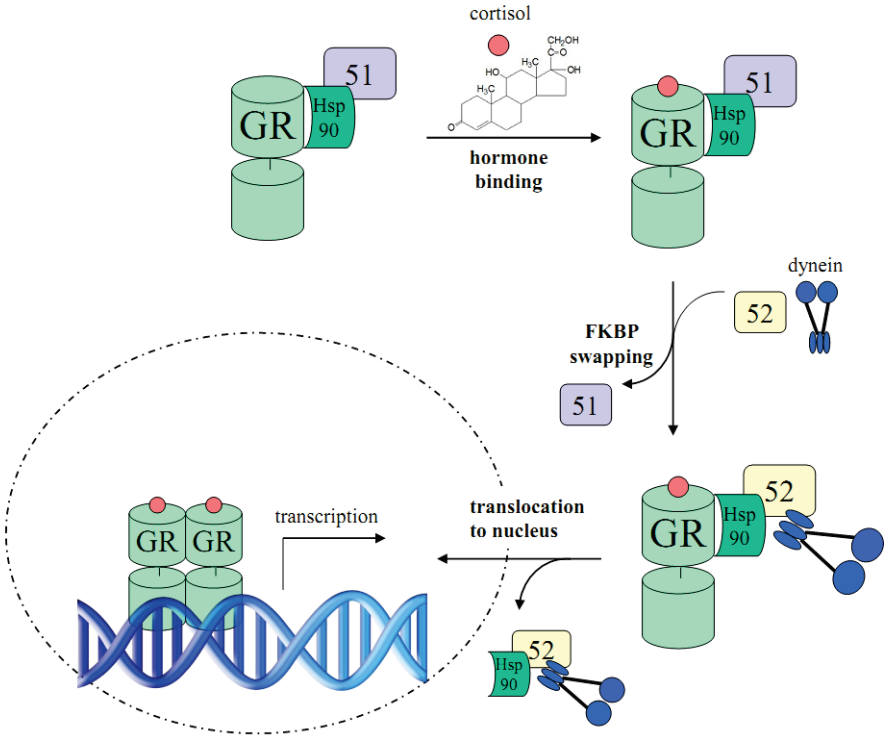

Figure 1.3: Exchange of FKBP51/52 occurs during maturation of the glucocorticoid receptor

FKBP51 and FKBP52 play different roles during the assembly cycle of the glucocorticoid receptor (GR): while FKBP51 (51) reduces hormone binding, FKBP52 (52) is involved in recruiting dynein to the complex and allowing nuclear translocation.

Just like FKBP51, FKBP52 is part of the glucocorticoid receptor complex and plays a role during functional maturation of the receptor: it interacts with Hsp90 and Hsp70; these proteins themselves recruit and displace co-chaperons (FKBP51, FKBP52, Hip, Hop, Chip) [66]. In a yeast model system it could be demonstrated that by expression of human FKBP52 the hormone-dependent transcriptional activity of the glucocorticoid receptor could be increased significantly [67]. For this effect, the TPR and PPIase domains of FKBP must be present [68]. FKBP52 also binds via its PPIase domain to the motor protein dynein which is connected to microtubuli and accelerates the translocation of protein from the cytoplasm into the nucleus [69, 70]. Importantly, a crucial step during receptor activation seems to be the exchange of bound FKBP51 with FKBP52 ("switching"; see figure 1.3) [71].
Recently, FKBP52 was found to bind to the hyperphosphorylated form of tau protein and inhibits its function and accumulation. This "anti-tau activity" may play a role in protecting neurons against degenerative diseases [72].

1.1.3 – FKBP12.6, FKBP13 and FKBP25: the less popular ones

The immunophilin **FKBP12.6** is very similar to its close relative FKBP12: the sequence identity is 85%, and the inhibition of calcineurin activity *in vitro* is similarly effective as the one of FKBP12 [73, 74]. The proteins exhibit highly overlapping functions *in vivo* as they both bind ryanodine receptors with high affinity. FKBP12.6 interacts preferentially with the ryanodine receptor in heart muscle cells [75]. Binding of the FKBP to the receptor stabilizes its closed conformation and influences cooperative interactions between receptor subunits. Mutagenesis experiments revealed that PPIase activity is not involved in this function of FKBPs [76].
Knockout of the FKBP12.6 gene resulted in a cardiac hypertrophy in male mice; the organs of females were normal. Obviously oestrogen seems to have protective influences on this issue. Nevertheless, both genders similarly display dysfunction of calcium release in myocardial cells [77].

The immunophilin **FKBP13** has strong homology to FKBP12; within the active centre of the PPIase domain it is even completely conserved [78]. The protein carries an N-terminal retention sequence which keeps the protein in the lumen of the endoplasmatic reticulum. Therefore a role of FKBP13 in the folding of newly synthesized proteins is proposed [79]. In

yeast a homologous protein is known [80]: its expression is increased by an unfolded-protein-response (UPR) element in the 5' region of the gene in presence of denatured proteins in the ER [81, 82].
As first physiological binding partner the homologue of the erythrocyte membrane cytoskeletal protein 4.1 was identified [83]. The interaction occurs via a histidyl-prolyl moiety in the membrane protein. As FKBP13 interacts with a homologue as well, it is discussed whether the protein is a general component of membrane scaffolds.

The immunophilin **FKBP25** is different from other FKBPs with respect to its ligand binding characteristics: it binds rapamycin (K_d = 0.9 nM) with much higher affinity than FK506 (K_d = 160 nM) [84-86]. This preference can be explained structurally by differences in the 50S loop region, by the flexibility of an insertion within the 40S loop and the substitution of a residue within the ligand binding pocket [87].
Moreover, in contrast to other FKBPs, FKBP25 displays a highly hydrophilic N-terminal domain that has no identity to other known proteins. This domain consists of a helix-loop-helix motif with a high proportion of charged amino acids. A nuclear localization signal is located in that area as well as different residues that can be phosphorylated by casein kinase II; as FKBP25 forms a stable complex with the kinase, it can be found mainly in the nucleus [88].
The biological relevancy of the protein is still largely unknown. It is well understood that expression of FKBP25 is negatively regulated by the tumour suppressor protein p53 [89]. There are reports about FKBP25 interacting with the N-Terminus of histone deacetylases (HDAC1 and HDAC2) and the transcription factor YY1, modifying its DNA binding capability [90]. Furthermore, the "High Mobility Group" protein HMG II and the GTP binding protein Rab5 were identified as potential binding partners [91]; the latter binds to the phosphorylated isoform of FKBP25. Whether the PPIase activity plays a crucial role in this process or whether other mechanisms are more meaningful could not yet be resolved. Likewise, there are no findings at all about which genes could be regulated differentially by the influence of FKBP25.

1.2 – Rapamycin and the Target of Rapamycin (TOR): inextricably linked

The macrolidic small molecule rapamycin (also: Sirolimus) was originally isolated from the bacterial species *Streptomyces hygroscopicus* in the 1970s and was named after the location, the Easter Island (Rapa Nui) [92-94]. The fungicidal action of the natural compound was discovered first [95], while its effects against transplanted tumours [96] and its immune-suppressive action [97] were observed later. The latter was confirmed in organ transplantation experiments with animals [98] which demonstrated that rapamycin reduces allograft rejection. In the 1990s, the natural compound proved its effectiveness in clinical trials after kidney transplantations in humans [99]. In 1997 rapamycin was finally approved by the FDA as trade brand "Rapamune" for human application. Furthermore, rapamycin-coated stents are widely used in patients suffering from vascular obliteration as the anti-proliferative effect of the natural compound can prevent restenosis effectively [100-102].

Structural similarities of rapamycin and the compound FK506 as well as their shared immunosuppressive effect gave rise to the suggestion that both natural compounds make use of related mechanisms of action: it could be demonstrated that rapamycin and FK506 bind to the co-chaperones of the FKBP family with high affinity [18, 103]. Surprisingly, two different signaling pathways in T-lymphocytes are affected by rapamycin and FK506, respectively [20]: while the complex of FKBP12 and FK506 binds and inhibits the protein phosphatase calcineurin [6], a yeast gene was discovered that causes a resistance against rapamycin when mutated. Therefore the gene was named "Target of Rapamycin" (TOR) [104, 105]. Further analysis of the gene product identified the protein as a member of the family of PI3K-like kinases [105] which are involved in regulation of cell cycle progression [106]. Later on, a homologous mTOR complex was identified in mammalian cells [107] which activates protein biosynthesis by phosphorylation of the translational regulators 4E-BP1 and S6Kinase in a mitogen-dependent manner [10, 108, 109]. The physiological relevancy of the protein is stressed by the fact that a homozygous knockout of mTOR is lethal in an early stage of mouse embryonic development [110].

The crystal structure of FKBP12 in complex with rapamycin and the rapamycin-binding domain of mTOR (FRB domain) was solved in order to further assess the allosteric mechanism of rapamycin action (see figure 1.4). It turned out that there is a direct blockage of the FRB domain of mTOR by FKBP12 that might influence interactions with actual substrates [23, 111]. Interestingly, direct protein-protein interactions play a subordinate role within this complex; rapamycin itself forms mostly hydrophobic contacts to amino acids of

FRB on one side of the macrolide, and interactions to residues in FKBP12 on the other side. For the latter contacts, defined loop structures of FKBP12 are especially important, harboring numerous H-bonds that strengthen the interaction.

The molecular mechanisms of kinase inhibition are not yet known: whether complex formation with FKBP12 blocks substrate binding sites or whether FKBP12*rapamycin directly interacts with the kinase domain still must be determined. Recent discoveries suggest that FKBP12*rapamycin interferes with oligomerization of mTOR, resulting in abolished activity of the obligatorily dimeric kinase [112].

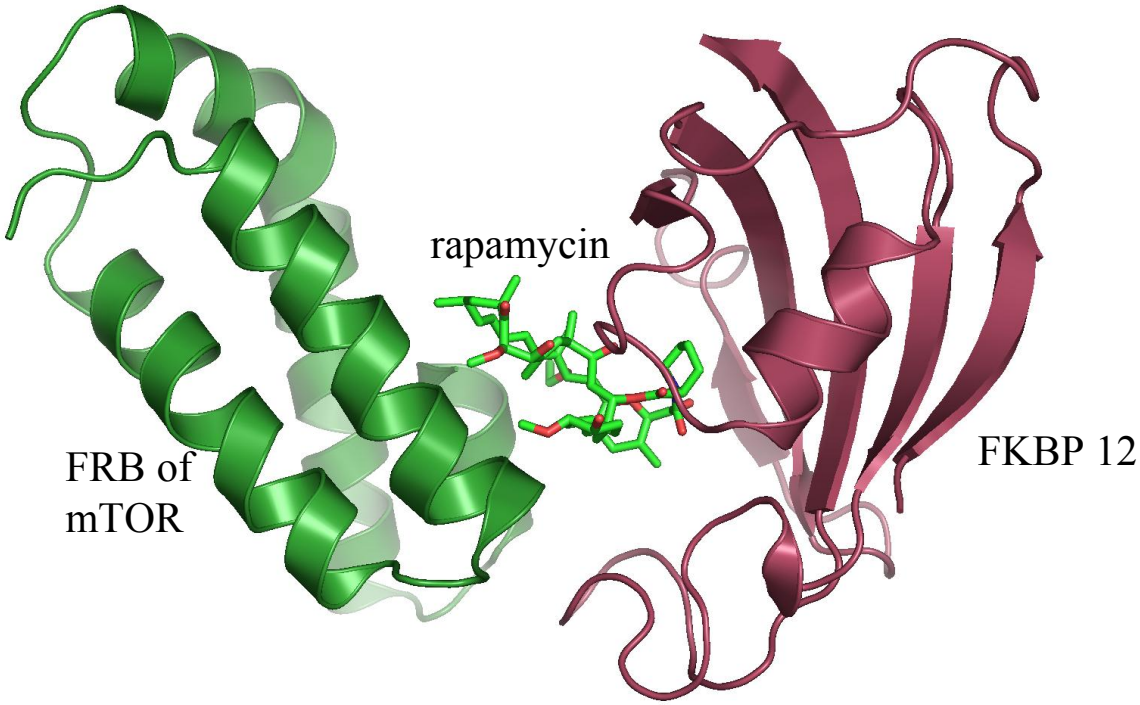

Figure 1.4: Rapamycin binds to FKBP12 and complexes the FRB domain of mTOR
Cartoon representation of the crystal structure "2fap" [111]:
ternary complex of FRB (green)*rapamycin (green, sticks; oxygen atoms red)*FKBP12 (red)

This dogma of FKBP12 being the only relevant rapamycin-dependent mTOR regulator was not challenged until recently: Bai and colleagues demonstrated that mTORC1 regulation via Rheb is mainly mediated by FKBP protein 38 [113]. They claim that FKBP38 represents an intrinsic inhibitor of mTOR kinase activity and binds to FRB domain in a similar way as the FKBP12*rapamycin complex. This binding seems to take place in absence of rapamycin as well. Mechanistically, the GTP-bound form of Rheb interacts with FKBP38 and reduces its inhibitory action on mTOR. Wang and Fonseca refuted those findings: they were unable to observe any inhibition of mTOR signaling by FKBP38 [114]. Furthermore, Uhlenbrock and

colleagues could not detect any interaction of Rheb with FKBP38 [115]. Thus, the hypothesis of FKBP38 contributing crucially to mTORC1 regulation cannot be sustained.

Recently, a novel mTOR inhibitor, a small molecule named "torin1", has been developed: Torin1 is a highly potent and selective ATP-competitive inhibitor that directly targets the active site of mTOR kinase [116]. It affects cell growth and proliferation with higher efficiency than rapamycin and acts on both mTOR complexes similarly. Importantly, the use of torin1 in mTORC1 inhibition revealed rapamycin-insensitive functions of the complex, mainly involving phosphorylation of the mTOR substrate 4E-BP1 [117]. With Ku-0063794, another compound has been discovered that inhibits mTOR kinase activity [118]. Finally, the small molecule inhibitors PP242 and PP30 ("TORKinibs") exhibit low-nanomolar mTOR affinity and affect mTOR to a further extent than rapamycin does [119]. Generally, these active-site inhibitors exert more direct effects than the allosteric inhibitor rapamycin whose inhibitory effect might be dependent on further factors like FKBP availability and binding competition.

1.3 – mTOR complexes: composition defines substrates

The Ser/Thr kinase mTOR is a large protein that has a molecular weight of around 290 kDa and consists of several domains (see scheme in figure 1.5) [120]. A PI3K-related domain is located at the C-terminus and is highly conserved among eukaryotes [121]. This domain plays a crucial role because it contributes the kinase activity to mTOR [109, 122]. In immediate vicinity the small FRB domain (FKBP12-rapamycin-binding) can be found [21] which comprises 11 kDa and provides the capability of rapamycin binding by its 4-helix-bundle structure [23, 123]. N-terminally, 20 HEAT repeats are located that contain each two interacting alpha helices and a variable spacer region [120]. These repeats provide binding sites for different cofactors (Raptor, Rictor) and substrates (4E-BP1, S6Kinase) [124]. Finally, mTOR contains two domains named FAT and FATC; the latter might play a role in sensing the intracellular redox potential and in adjusting mTOR structure by formation of a disulfide bond [125].

Figure 1.5: The PI3K-like kinase mTOR is a multi-domain protein

Schematic representation of the domain structure of mTOR; left side: N-Terminus; right side: C-terminus

Just like in yeast, the protein mTOR can be found in two distinct complexes: in mTORC1 and mTORC2 [104, 126]. mTORC1 is mainly involved in sensing energy and nutrition in dependence of cellular signals and in adjusting protein biosynthesis and cell growth accordingly [127]. This first complex consists of mTOR, mLST8 (GßL) and Raptor [128]. Although it does not contain enzymatic activity, Raptor ("regulatory associated protein of TOR") is an essential component of mTORC1. It rather functions as a scaffold and supports mTOR in recruitment of substrates [129]: insulin stimulates binding of 4E-BP1 to the complex. Raptor includes three HEAT repeats and seven WD40 units for interaction with binding partners. Nevertheless, its association with mTOR is very dynamic: under conditions of nutrient deficiency, the binding of Raptor to mTOR gets stronger [130] while rapamycin treatment reduces this interaction [131]. Detergents can also interfere with the binding.

Another important part of mTOR complex is the protein mLST8 which consists of WD40 units almost completely. By utilizing these units, it interacts with the kinase domain of mTOR. Initially it was assumed that LST8 exerts regulatory effects on mTOR [128]; but knockout experiments revealed that the protein is not essential for proper function [132].

mTORC1 enhances cell growth by phosphorylation of proteins that are involved in regulation of protein translation, gene expression and autophagy. The most important substrates of mTOR are regulators of protein translation, namely the eIF4E-binding protein (4E-BP1) [108] and the ribosomal p70 S6Kinase (S6K) [10]. Both proteins occupy key positions within the cap-dependent protein biosynthesis machinery and are regulated reciprocally: S6K, a positive regulator of translation, is activated by phosphorylation, while the translational inhibitor 4E-BP1 is inactivated by mTORC1.

4E-BP1 binds to the initiation factor eIF4E and thereby inhibits the formation of a complex that allows initiation of translation by unwinding the 5' ends of mRNA [133]. A phosphorylation by mTOR inactivates 4E-BP1, causing release of eIF4E and increase of mRNA translation at the ribosomes [134]. Active S6Kinase phosphorylates different proteins within the ribosomal subunits, mainly initiation factors and elongation factors. These events trigger the assembly of the translation machinery [135]. Both mTORC1 substrates contain a conserved 5 amino acid sequence, a so-called "TOR-signaling motif" (TOS motif) that mediates the interaction with Raptor [136].

By cryo-electron microscopy, the three-dimensional structure of mTORC1 complexes has been revealed at low resolution [112]: it turns out that mTORC1 forms dimers with a central cavity. The interface areas are stabilized by mTOR-Raptor interactions. Other components, like mLST8 and PRAS40, are bound to the outside portion of the complex. When rapamycin

is added in presence of FKBP12, the complex binds to one mTORC1 dimer, resulting in conformational changes that weaken the interaction between mTOR and Raptor. As phosphorylation of 4E-BP1 is abolished in presence of rapamycin, it is assumed that it demands the presence of one mTORC1 dimer. Maybe, 4E-BP1 is bound to one monomer, while the phosphorylation is performed by the adjacent monomer.

Within the mTORC2 complex, mTOR can be found together with mLST8, Rictor and Sin1 [137, 138] while the latter two are exclusive components of this complex. The kinase activity of TORC2 cannot be reduced by acute application of rapamycin, and binding of FKBP12*rapamycin does not occur [126]. Presumably the components of mTORC2 complex block binding of FKBP12*rapamycin to the FRB domain of mTOR. Under conditions of prolonged rapamycin treatment, reduced formation of TORC2 might occur as newly synthesized TOR protein is sequestered [139].

Rictor, the rapamycin-insensitive companion of mTOR, is a large protein of 190 kDa. Its function within the mTORC2 complex is still widely unknown. Obviously the protein is comparable to Raptor in TORC1: it represents a scaffold for assembly of the different components and may be involved in substrate binding [140]. A heterozygous knockout of Rictor causes lethality of mice in the tenth week of embryonic development [132]. This implicates physiological importance of the protein.

mTORC2 complex exerts an important regulatory influence on Akt kinase: it phosphorylates Akt together with PDK1 kinase within a hydrophobic motif and allows its complete activation [141]. Is it not clear whether the two activating kinases can work independently. Anyway, Akt kinase is most active when it is phosphorylated twice [142]. This phosphorylation state is also used as a measure for mTORC2 activity.

Some functions of the mTORC2 complex are not yet understood completely. Clearly, the complex has regulatory effects on actin accumulation and therefore on cytoskeleton dynamics [143]. This effect might be mediated by proteins of the Rho family of small GTPases and protein kinase C (PKC). Regulatory pathways which act upstream of mTORC2 and contribute to its activation or inhibition are not yet well characterized.

Recently, it has been reported that mTORC2 associates with ribosomes, and that this interaction is necessary for activation of the complex [144]. Thus, mTORC2 activation can be reduced in static cells, because the number of ribosomes in a cell is proportional to its growth activity.

1.4 – PI3K/Akt/mTOR signaling pathway: integrator of multiple signals

One important function of the mTORC1 complex consists of initiating cell growth in presence of growth factors or insulin. During this process, signaling pathways are triggered which include the kinases Akt (protein kinase B, PKB) and mTOR as major effectors. These proteins crucially co-determine survival of a cell and thus regulate processes like growth, proliferation and apoptosis [145].

After activation of the insulin receptor by hormone binding, this growth factor triggers an important growth-mediating signaling pathway, namely the PI3K/Akt kinase pathway. During this process, activation of phosphatidyl inositol 3 kinase (PI3K) occurs that in turn produces the second messengers PIP3 (phosphatidyl-inositol-3,4,5-triphosphate) and PIP2 (phosphatidyl-inositol-3,4-diphosphate) [146]. They stimulate recruitment of the kinase Akt by its PH (Pleckstrin Homology) domain and induce membrane localization of the protein [147]. There, Akt is phosphorylated by the kinases PDK1 and PDK2 at the regulatory amino acid residues T308 and S473; this activates Akt completely. Recently PDK2 (3-phosphoinositid-dependent protein kinase 2) was identified as the rapamycin-independently regulated mTOR complex mTORC2 [141].

Akt kinase phosphorylates the tumour suppressor proteins TSC1/2 at several positions and thereby causes a reduction of inhibitory effects on mTOR [148]. This event actually increases the activity of mTORC1 complex and stimulates protein biosynthesis via its substrates 4E-BP1 and S6Kinase. The complete signaling pathway is referred to as Insulin-PI3K-Akt-TSC-mTORC1-S6K1/4E-BP1 (see figure 1.6).

The important role of the tumour suppressor proteins TSC1 and TSC2 (Tuberous Sclerosis Protein 1 und 2) can be clarified by the fact that inactivating mutations cause development of tuberous sclerosis [149]. The proteins TSC1 and TSC2 form a functional complex in which TSC1 mainly exerts stabilizing action while TSC2 acts as GTPase activating protein (GAP) on subordinate targets. A crucial role of the complex is the inhibition of mTORC1: if the activity of the TSC proteins is lost, hyperactivation of mTOR complex 1 is induced which results in excessive cell growth and tumour formation.

Target of the GTPase activating action of TSC1/TSC2 complex is the small regulatory GTPase Rheb (Ras-homolog enriched in brain). TSC2 activates Rheb's intrinsic GTPase and converts it to its inactive, GDP-bound state [150, 151]. In turn Rheb acts as positive regulator of mTORC1, activating its kinase function [152]. This can be verified by overexpressing Rheb which leads to increased phosphorylation of 4E-BP1 and S6Kinase.

PRAS40 (proline-rich Akt substrate 40 kDa, [153]) represents another important regulator of mTORC1 activity and transfers mitogen-dependent signals directly to mTOR without a detour via the TSC complex [154]. In its hypophosphorylated form, PRAS40 acts as a direct inhibitor of mTOR kinase activity; when it becomes phosphorylated by Akt kinase, its inhibitory action decreases [155]. Normally, PRAS40 interacts with mTOR via Raptor [156] and thereby competes with other substrates for binding to the kinase [157].

As increased mTOR activity leads to higher biosynthesis of ribosomes and protein translation rates, and as these processes entail significant energy consumption, mTOR must have a mechanism to detect the current energy level of the cell. The AMP-activated protein kinase AMPK serves as such a sensor of cellular ATP concentration and detects the AMP/ATP ratio. At high AMP concentrations the kinase is activated by direct AMP binding and phosphorylates TSC2 which in turn reduces mTORC1 activity via Rheb [158, 159].

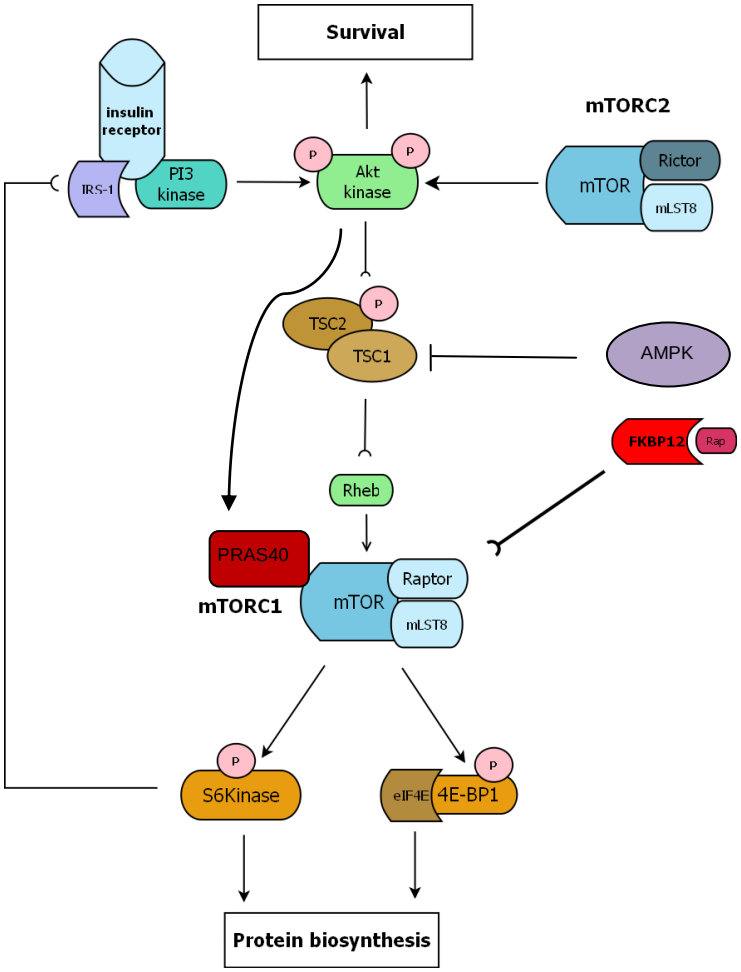

Figure 1.6: mTOR senses different stimuli by integrating several upstream components

Simplified representation of the PI3 kinase-Akt-mTOR signaling pathway.

After successful activation of S6Kinase by mTORC1 the Akt signaling pathway is dampened by S6K1-dependent negative feedback inhibition [160]: S6Kinase directly phosphorylates IRS-1 (insulin receptor substrate 1) and thereby hinders its bridging function between the insulin receptor and PI3Kinase, also by promoting its degradation [161]. This auto-regulatory connection within the complex PI3K/Akt/mTORC1 signaling pathway serves as a tool for fine-tuning of insulin sensitivity.
Recently, DEPTOR has been identified as a novel interaction partner of mTOR that inhibits kinase activity. Its expression is directly regulated and suppressed by mTORC1 and mTORC2 [162, 163]. DEPTOR expression levels are relatively low in different human cancer cell lines. In some types of myeloma cells, the protein seems to be overexpressed, leading to Akt activation and maintenance of survival.

The influence of amino acids on mTORC1 regulation is well characterized, but the underlying mechanisms were enigmatic for a long time. Recently, Sancak [164] and Li [165] discovered that mTORC1 interacts with members of the family of GTP-binding Rag proteins: these proteins form heterodimers, and amino acid supplementation converts them into a GTP-bound state. Once activated, RagB interacts directly with the mTORC1 component Raptor [164]. Another protein complex, called Ragulator, binds to Rag and triggers its translocation to lysosomes. As a consequence, mTORC1 is recruited to this compartment, where it is enabled to interact with membrane-bound Rheb, resulting in mTOR activation. Altogether, activated Rag mediates the interaction of mTORC1 and its activator at the surface of lysosomes [166].

During the process of autophagy, cellular proteins and whole organelles are degraded in order to provide basic building blocks for cellular metabolism and regeneration, especially in times of starvation. Autophagy is essential for cell survival as it prevents cell death or damage [167]. Under conditions of amino acid abundance, mTORC1 also plays an important role in suppressing autophagy: via Raptor, it recruits the kinase ULK1, phosphorylates it and hereby inhibits its autophagy-inducing function [168]. When amino acids are missing and the cell is starving, mTORC1 is inactive, and the hypophosphorylated ULK1 complex translocates to the autophagosome in order to initiate the process [169].

1.5 – mTOR carries on signals by phosphorylating three main substrates

1.5.1 – 4E-BP1: many phosphorylation sites, one kinase?

Protein synthesis, a process tightly controlled in eukaryotes, is triggered mainly by mitogens, like insulin, amino acids and growth factors [170]. As a first crucial step, the 40S subunit of the ribosome must be recruited to mRNA which is done by the assembly of a "translation initiation complex" at the 5' 7-methyl guanosine cap structure [171, 172]. One key component of this complex is the initiation factor eIF4E whose availability is regulated by sequestration of its binding protein 4E-BP1 (PHAS-I) [173, 174]. In its hypophosphorylated form, 4E-BP1 is active and binds to eIF4E [175]. After sequential phosphorylation of its multiple phosphorylation sites, 4E-BP1 is inactivated and releases eIF4E which in turn initiates cap-dependent translation [134].

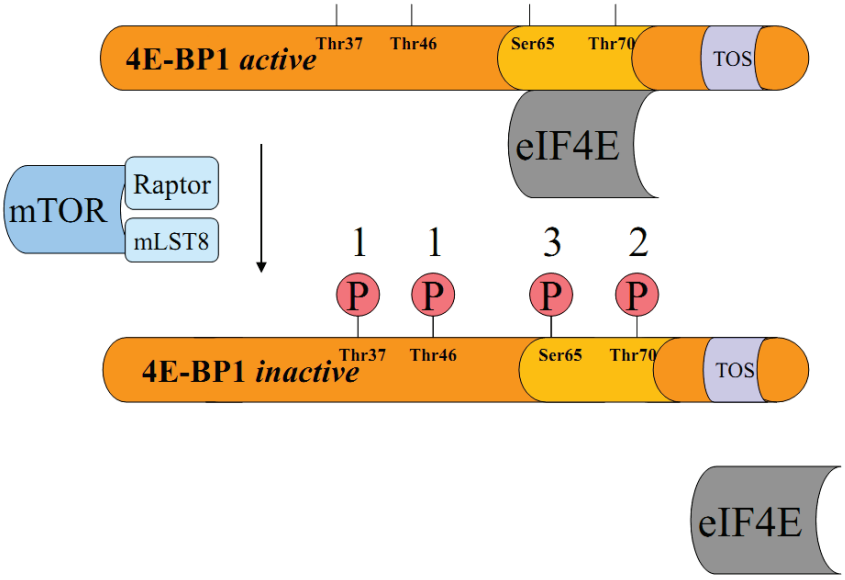

Figure 1.7: 4E-BP1 is inactivated by sequential phosphorylation events
Schematic representation of 4E-BP1 phosphorylation sites; order of phosphorylation events by mTORC1 is indicated. Under *in vivo* conditions, phosphorylation of S65 and T70 is rapamycin-sensitive.

Four phosphorylation sites seem to be crucial for regulation of 4E-BP1 (T37, T46, S65, T70) because they are regulated via growth signals (especially insulin) [176]. Furthermore, these sites are conserved evolutionarily and within the family of 4E-binding proteins [177]. As 4E-BP1 contains a C-terminal TOS motif, it is a substrate of mTORC1 [178] and is phosphorylated by the kinase in a strictly hierarchical manner: first, the residues T37 and T46 are modified by mTORC1, creating the basis for phosphorylation of T70 [179]. Lastly, Ser65

is phosphorylated, resulting in total loss of eIF4E binding [180] (see figure 1.7). The pairs of phospho-residues seem to modulate 4E-BP1 activity in a cooperative way: the first two residues are not sufficient for inactivation, while pS65 and pT70 alone cannot inhibit binding of 4E-BP1 to eIF4 completely [181].

Interestingly, only S65 and T70 phosphorylation can be reduced by rapamycin treatment *in vivo*; T37 and T46 do hardly respond to mTORC1 inhibition by the small molecule and do not depend on the TOS motif [182, 183]. Under *in vitro* conditions, mTORC1 phosphorylates T37/T46, while it has little effect on the phosphorylation state of S65/T70 [184]. Thus, speculations about mTORC1 not being the only kinase that regulates the different phosphorylation sites in 4E-BP1 cannot be maintained. It rather must be assumed that some of the mTORC1 functions cannot be affected by rapamycin.

Rapamycin inhibition of mTOR activity has different effects on the substrates 4E-BP1 and S6Kinase in some cell types (e.g. HEK293 and HeLa cells). While T389 phosphorylation of S6Kinase is abolished reliably after short or long-term rapamycin treatment, regulation appears much more complicated for 4E-BP1. Here, phosphorylation of the critical residues S37/S46 is reduced during the first six hours of rapamycin treatment. Afterwards, the phosphorylation recovers, resulting in hyperphosphorylated 4E-BP1 at 12 hours of treatment, accompanied by high levels of cap-dependent protein translation in absence of active S6Kinase [185, 186]. As the TOS motif of 4E-BP1 and mTORC1 are necessary to induce this hyperphosphorylation, it is speculated whether some functions of mTORC1 are rapamycin-insensitive. Some mechanisms have been proposed that might explain these differences, involving binding or release of regulatory proteins like PRAS40 to mTORC1 [157], changes in phosphorylation state of Raptor [187, 188] or post-translational modifications of mTOR itself.

1.5.2 – p70 S6Kinase: more than just a regulator of translation

p70 S6Kinase1 is a member of the AGC family of serine/threonine protein kinases and is present in mammalian cells as two isoforms. These isoforms are produced from the same transcript by differential translation and are regulated similarly [189]. The larger protein S6K1L (p85 S6K) carries an N-terminal extension that contains signals for nuclear localization, while the small isoform S6K1S (p70 S6K) is mainly present in the cytoplasm [190]. A second S6Kinase, named S6K2, is highly identical to S6K1 especially within the

catalytic and the autoinhibitory domain [191]. Both S6K1 and S6K2 are present ubiquitously in mammalian tissues. The amino acid sequence of S6K1 is totally conserved within mammals, while S6K2 displays alterations [192].

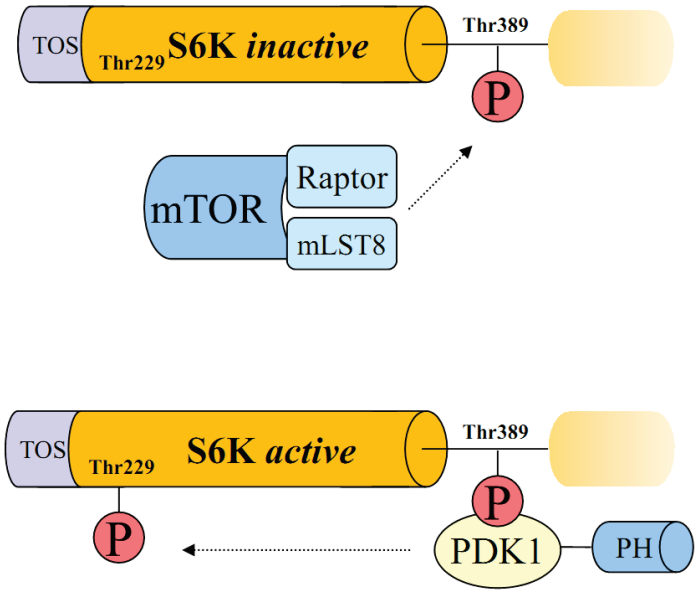

Figure 1.8: S6Kinase is activated by two phosphorylation steps

Schematic representation of S6Kinase phosphorylation sites and involved kinases (adapted from Pearce et al. [193]).

The activity of S6K is mainly regulated by the canonical IR-PI3K-Akt-TSC-mTOR signaling pathway in response to stimuli like growth factors, mitogens and nutrients. During activation, the kinase is phosphorylated in a complex manner at multiple serine and threonine residues within the C-terminal regulatory domain and the kinase domain (see figure 1.8): first, T389 is phosphorylated by mTOR in a TOS-motif dependent way [136]. This phospho-threonine serves as a binding site for the kinase PDK1, whose action leads to phosphorylation of T229 within the catalytic activation loop [194]. Additionally, the nucleocytoplasmatic shuttling of the isoforms seems to be regulated by phosphorylation events [195]. S6K1 regulates a lot of effector proteins by direct phosphorylation, among them ribosomal proteins (S6, IF-4B and the eEF2 kinase [196, 197]), transcription factors (CREM) and proteins involved in cell survival (Bad1, PDCD4) [198]. IRS (insulin receptor substrate) phosphorylation serves as a mechanism of negative feedback and causes inhibition of the whole pathway [160, 199].

The termination of S6K signaling is mainly mediated by three mechanisms: first, association with the protein phosphatases PP2A and PP1 leads to dephosphorylation of specific sites and renders the kinase inactive [200]. Secondly, recent studies suggest that the cellular S6K protein levels might be regulated by ubiquitin-dependent degradation in an unknown manner

[201]. Lastly, the activation of the tumour suppressors PTEN and TSC1/2 inhibit mTOR activity which in turn reduces S6K activation [202].

The kinase passes on an anabolic signal in order to influence cell size and growth by affecting protein translation and cellular energy levels. Insulin and insulin-like growth factor 1 signaling (IIS) pathway and the mTOR pathway play a role in regulation of life span in lower organisms and in mice [203]. In flies, variant forms of S6K seem to influence fat metabolism, immune response and longevity [204]. Recently it has been demonstrated that S6K1-knockout mice show an increased life span and are less prone to age-related disease. These effects are caused by gene expression patterns that are similar to the ones seen during caloric restriction and are connected to activity of AMP-activated protein kinase (AMPK) [205]. Furthermore, in a transgenic mouse model of Alzheimer's Disease, mTOR inhibition by rapamycin and resulting S6Kinase inactivation decelerated Aß protein accumulation and disease progression. These effects are mainly caused by increased autophagy of affected cells [206].

Recently, an interaction of the prolyl isomerase Pin1 with S6K in hepatocarcinoma cells has been described. Overexpression of Pin1 increases insulin-dependent S6K phosphorylation, resulting in enhanced cell transformation and tumorigenesis [207].

1.5.3 – Akt/PKB: connecting the mTOR complexes

The Akt protein kinases (alternatively: Protein Kinases B) are involved in regulation of a variety of cellular processes, including survival, growth and metabolism. This is mainly achieved by three different, but nevertheless highly homologous isoforms (Akt1, 2 and 3) [208] which share a common mechanism of activation but act on different downstream substrates. The Akt proteins are integrated in the insulin-PI3K signaling pathway which is activated upon reception of extra-cellular stimuli like growth factor or insulin [209]. As a consequence of PI3K activity, the concentration of PIP3 within the plasma membrane increases and allows recruitment of Akt to the membrane [210]. This re-localization triggers phosphorylation of two residues of Akt (T308 within the catalytic domain and S473 within the C-terminal hydrophobic domain) by the kinases PDK1 [211] and mTORC2 [141], respectively (see figure 1.9). Once activated, Akt phosphorylates a lot of different substrates independently of the cellular localization. By phosphorylating the protein BAD [212], the transcription factor FOXO3 [213] and the pro-caspase9 [214], Akt inhibits proapoptotic processes and promotes cell survival. By alleviating the inhibitory action of the tumour suppressor protein TSC2 [215] and PRAS40 [155], Akt activates mTORC1 signaling and thus

promotes cell growth via promotion of ribosomal protein biosynthesis. Cell cycle progression can also be accelerated by Akt-mediated phosphorylation of the cyclin-dependent kinase inhibitor $p27^{Kip1}$ [216].

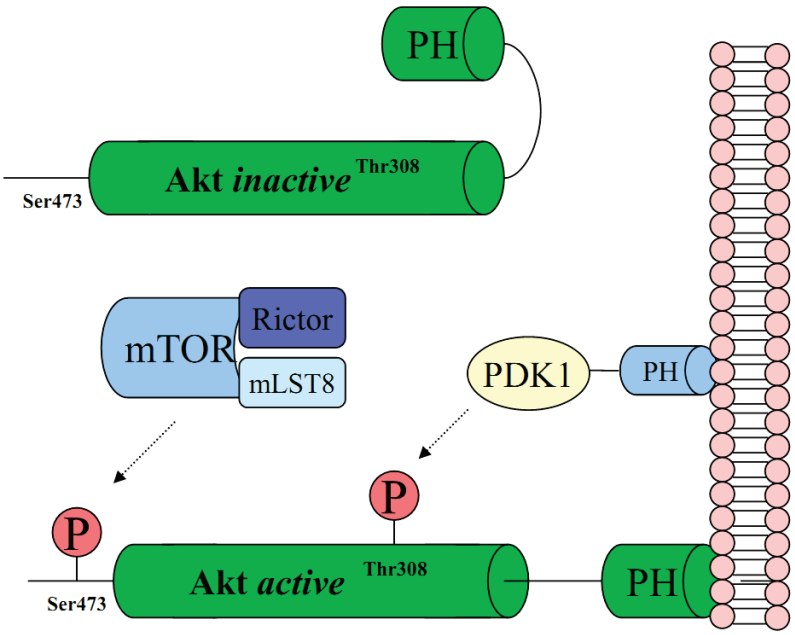

Figure 1.9: Akt kinase is activated by membrane recruitment and two phosphorylation steps
Schematic representation of Akt kinase phosphorylation sites, involved kinases and cellular localization (adapted from Pearce et al. [193]).

The importance of Akt kinase action on cellular processes has been demonstrated very clearly by knockout experiments in mice: animals missing Akt1 display impaired growth during all stages of development [217] and increased rates of apoptosis on a cellular level [218]. Akt2 knockout results in a phenotype characterized by insulin resistance and subsequent hyperglycemia, accompanied by the loss of pancreatic ß-cells. In male mice, a severe form of diabetes occurs [219, 220]. Mice lacking Akt3 show impairment in brain development [221], but are otherwise healthy. Combined knockout experiments indicate that some functions overlap and thus can be compensated by other isoforms, especially by the indispensable Akt1 [222]. Other tasks seem to be exclusive to certain Akt isoforms.

1.6 – Rapamycin in cancer treatment: promising in combination

As PI3K/Akt/mTOR signaling is crucially involved in regulation of cell growth, proliferation and survival, hyperactivity of this pathway can be commonly found in a variety of human cancers (reviewed in [223]). Very often, mutations or silencing of the tumour-suppressor PTEN are responsible for excessive signaling; this can be observed in cancers including glioblastoma [224], melanoma [225], hepatocellular carcinoma [226] and cancers of lung, thyroid [227] and renal cells [228]. In some cases, there are additional factors, like PI3K mutations (especially deletions within the autoregulatory domain) that contribute to malignancy [229]. Although a single deregulated protein can be sufficient for cancer development, there are several different factors involved in hyperactivation of mTOR signaling in ovarian or breast cancer cells: here, aberrant Akt2 activation or overexpression are frequently found in addition to PTEN and PI3K mutations [230]. Interestingly, no malignant mutations of the kinase mTOR itself are reported.

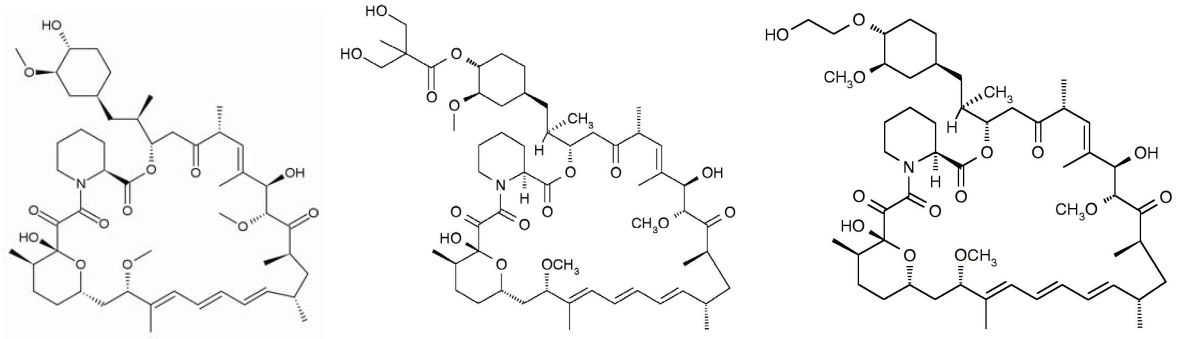

Rapamycin (Sirolimus) Temsirolimus Everolimus

Figure 1.10: Rapalogues share the same core structure

Structures of rapamycin and the two analogues temsirolimus and everolimus which carry different substitution at the cyclohexyl moiety.

A general anti-proliferative effect of rapamycin has been reported for a panel of different cancer cells in mouse models [231]. To increase oral bio-availability and compound concentration in the target organs, several rapamycin analogues ("Rapalogues") were developed (see figure 1.10). Some of these derivatives are metabolized to form rapamycin and therefore exhibit similar modes of action as the original compound concerning mTOR inhibition; others seem to exert additional FKBP-independent effects at high concentrations [232]. Preclinical studies, mainly using mouse models, verified the effectiveness of rapamycin

and its homologues: in mouse xenograft, the rapamycin-derivative everolimus was able to reduce growth of different human tumour transplants, mainly by affecting angiogenesis via VEGF signaling [233, 234]. In a mouse model of neuroendocrine tumours, rapamycin reduced tumour growth significantly and increased survival [235]. Interestingly, the effects of rapamycin can be further increased by co-administration of the PI3K inhibitor LY294002 which reduces rapamycin-induced Akt hyperphosphorylation in human T-cell leukaemia [236], but not in melanoma cells [237]. Temsirolimus turned out to be a promising candidate in clinical trials with patients suffering from kidney carcinoma [238-240]. The compound was also successfully tested in model systems of human breast cancer, where it exerted anti-proliferative effects mainly by reducing cyclin D and c-myc protein levels [241]. Similarly, everolimus is currently studied in several clinical trial targeting neuroendocrine tumours and renal cell carcinoma [242]. Unfortunately, the degree of rapamycin/rapalogue sensitivity varies greatly between different cell lines, rendering some of them totally resistant. As marker proteins for prediction of sensitivity, S6Kinase protein levels and activation state of Akt have been proposed for breast cancer cells [243].
For temsirolimus and everolimus, clinical trials with cancer patients have been carried out, and promising results have been obtained [244]: treatment regimen could be adjusted in order to prevent side-effects (rash, mucositis, anorexia and fatigue), and survival rates could be increased especially with temsirolimus in patients suffering from renal cell carcinoma [245]. In mantle cell lymphoma, the compound worked in 38% of all patients and slightly delayed disease progression [246]. Nevertheless, in many cases a combinational therapy using both mTOR inhibitors and MAPK inhibitors (such as sorafenib) is preferable, as activation of MAPK signaling overrides mTOR inhibition in some types of cancers [247].

Due to complexity of PI3K/Akt/mTOR signaling, many mechanisms have been detected that generate resistance to rapamycin and rapalogues: first of all, mutations of FKBP12 (predominantly D37G, [248-250]) reduce rapamycin binding affinity. This is also true for mutations in the FRB domain of mTOR (namely S2035I, [21]) which largely prevent FKBP12*rapamycin binding and thus abolish mTOR inhibition [251]. Secondly, the ratio of the initiation factor eIF4E and its inhibitor 4E-BP1 seems to be an indicator of tumour malignancy as either overexpression of eIF4E [252] or down-regulation of 4E-BP1 [253] increases the tendency of malign degeneration of cancer cells. Next, p53 status is known to influence the response of mouse embryonic fibroblast (MEF) cells after rapamycin treatment: if the tumour suppressor protein is mutated and not functional, rapamycin triggers a stress-

induced apoptotic pathway, resulting in rapid cell death. Cells that express active p53 are protected against this effect of rapamycin [254]. ABC-transporters, like P-glycoprotein, are involved in generation of multi-drug-resistant phenotypes: rapamycin (as well as FK506 and cyclosporin A) has been reported to reverse drug-resistance by binding to the receptors and inhibiting their ATP hydrolyzing activity. Thus, the small molecules might also be substrates for transport [255, 256]. Another important mechanism of rapamycin resistance includes angiogenesis: as mTOR signaling regulates cap-dependent protein translation, concentration of HIF-1α (hypoxia inducible factor 1α) might be lowered after rapamycin treatment, resulting in reduced VEGF (vascular endothelial growth factor) release. As a result, growth of tumour xenografts in mouse models is inhibited significantly, although the original cells are resistant to rapamycin under cell culture conditions [231, 257, 258]. Finally, the application of growth factors (like insulin or IGF-I) suppresses rapamycin-mediated apoptosis. This happens mainly by triggering pathways involving Akt kinase which lead to inactivation of the protein Bad; Bad normally exerts pro-apoptotic effects [259].

1.7 – Aim of the project:

During the last two decades, the kinase mTOR turned out to be a central player in the regulation of cellular processes: it integrates mitogen-activated signaling pathways via PI3K/Akt kinase, energy-level dependent regulation via AMPKinase and allows inhibition via FKBP12*rapamycin. All these processes mediate modifications of mTOR activity and thereby induce fine-tuning of downstream processes like initiation of translation, ribosomal biogenesis, autophagy and actin organisation.
The family of FK506-binding proteins comprises several functionally heterogeneous members that display high homology within their FK domains. This part of the protein is responsible for binding of the natural compound rapamycin, and it exerts PPIase activity. Thus, one could postulate that apart from FKBP12 other FKBPs might bind to the FRB domain of mTOR in presence of rapamycin and influence the kinase in a defined manner.

Therefore this research project is dedicated to theses central questions: which members of the FKBP protein family bind to mTOR in a rapamycin-dependent manner? Does this interaction exert regulatory effects on mTOR kinase activity?

A more profound characterization of the molecular mode of rapamycin action is crucial for a better understanding of its pharmacological effects in different tissues. This in turn could form the basis for the development of rapamycin-derivatives which are FKBP subtype-selective and therefore might allow mTOR inhibition in a cell type- or context-dependent manner. Eventually, this development might produce compounds that could allow mTOR inhibition without exerting the classical immunosuppressive action of rapamycin as a critical side effect.

2 – Materials:

2.1 – Oligonucleotide primers:

For amplification and cloning of FKBP nucleotide sequences the following oligonucleotide primers and cloning strategies were used together with the indicated vectors:

Name	Sequence (5'–3')	Amplificat	Cloning strategy
Eco-FKBP12-Start	AAAGAATTC**ATGGGAG TGCAGGTGGAAACC**	Human FKBP12 (Accession: NM_000801), 324 bp	With *Eco*RI and *Sal*I in pPROEx-HTa and pYX424 → pProExHta-FKBP12, pYX424-FKBP12
FKBP12-Stop-Sal	CCCGTCGACTCA**TTCCA GTTTTAGAAGCTCC**		
FKBP12.6-EcoRI-forward	CCGGAATTC **ATGGGCGTGGAGATC GAG**	Human FKBP12.6 (NM_004116), 360 bp	With *Eco*RI and *Xho*I in pPROEx-HTa and pYX424 → pProExHta-FKBP12.6, pYX424-FKBP12.6
FKBP12.6-XhoI-reverse	GCTCGAGTCA**CTCTAA GTTGAGCAGCTC**		
FKBP13-EcoRI-forward	CCGGAATTC**AAAAGG AAGCTGCAGATCGG**	Human FKBP13 (NM_004470), aa 27 – 142, 348 bp	With *Eco*RI and *Xho*I in pPROEx-HTa and pYX424 → pProExHta-FKBP13, pYX424-FKBP13
FKBP13-XhoI-reverse	GCTCGAGTTA**CAGCTC AGTTCGTCGCTC**		
FKBP25-EcoRI-forward	CCGGAATTC**ATGGCGG CGGCCGTTCC**	Human FKBP25 (NM_002013), 675 bp	With *Eco*RI and *Xho*I in pPROEx-HTa and pYX424 → pProExHta-FKBP25, pYX424-FKBP25
FKBP25-XhoI-forward	GCTCGAGTCA**ATCAAT ATCCACTAATTC**		
FKBP51-NcoI-forward	GGCCATGGGG**ATGACA CTGATGAAGG**	Human FKBP51 (NM_004117), 1374 bp	With *Nco*I and *Xho*I in pProEx-HTa and pYX242 → pProExHta-FKBP51, pYX424-FKBP51
FKBP51-XhoI-reverse	GCCTCGAGTCA**TACGT GGCCCTCAGGTTTCTC**		
FKBP52-NcoI-forward	GCGCCATGGGG**ATGAC AGCCGAGGAG**	Human FKBP52 (NM_002014), 1380 bp	With *Nco*I and *Xho*I in pProEx-HTa and pYX424 → pProExHta-FKBP52, pYX424-FKBP52
FKBP52-XhoI-reverse	GCCTCGAGTCA**TGCTT CTGTCGAACAAG**		
FKBP51-FK1-EcoRI-forward	CGGAATTC**ATGACTAC TGATGAAGGTGC**	Human FKBP51 (NM_004117), fragment aa 1-140, 420 bp	With *Eco*RI and *Sal*I in pPROEx-HTa and pXY424 → pProExHta-FKBP51 FK1, pYX424-FKBP51 FK1
FKBP51-FK1-SalI-reverse	GCAGTCGAC**TCTCCTT TGAAATCAAGGAGC** – 3'		
FKBP52-FK1-EcoRI-forward	CCGAATTC**ATGACAGC CGAGGAGATG**	Human FKBP52 (NM_002014), Fragment aa 1- 140, 420 bp	With *Eco*RI and *Sal*I in pPROEx-HTa and pYX424 → pProExHta-FKBP52 FK1, pYX424-FKBP52 FK1
FKBP52-FK1-SalI-reverse	GTCGAC TCA**TTCTCCCTTAAAC TCAAACAACTC**		

Table 2.1: Oligonucleotide primers and cloning strategies used for generation of FKBP plasmids

The restriction sites are underlined, coding sequences are bold.

cDNA templates for human FKBP12, FKBP51 and FKBP52 were kindly provided by Dr. Theo Rein. Plasmids containing ORFs of FKBP12.6, FKBP13 and FKBP25 were a kind gift of Dr. Gunter Fischer. cDNA of human mTOR was provided by Prof. Jie Chen (see table 2.7).

The following primers were used for generation of FRB constructs and FRB variants:

Name	Sequence	Amplificat	Cloning strategy
His-FRB-forw-EcoRI	5' - CGGAAT TC**ATGGAGA TGTGGCATGAAGG** – 3'	Human FRAP1 (TOR; NM_004958), aa 2025 - 2114	With *Eco*RI and *Xho*I in pPROEx-Hta → pProExHta-FRB
His-FRB-rev-XhoI	5' - GCTCGA GCCTTA**CTG CTTTGAGATTCG** – 3'		
GST-FRB-forward-BamHI	5' - GCGGATCC**ATGGAGATG TGGCATGAA**		With *Bam*HI and *Eco*RI in pGEX-4T2 → pGEX-4T2-FRB
GST-FRB-rev-EcoRI	5' – CGGAATTCTTA**CTGCTTT GAGATTCGTCGG** – 3'		

Table 2.2: Oligonucleotide primers and cloning strategies used for generation of FRB plasmids

The primers used for amplification of EGFP variants read as follows:

Name	Sequence	Amplificat	Cloning strategy
EGFP-KasI-forw	5' - GGCGCC **ATG GTG AG C AAG GGC GAG GA** – 3'	EGFP in vector pEGFP-N1 (Accession Number U55762), bp 789 - 1395	With *Kas*I and *Nco*I in pPROEx-Hta → pProExHta-EGFP
EGFP-NcoI-rev	5'-CCATGG **CCTTGTACAGCTCGTCC ATGCCGAG** – 3'		

Table 2.3: Oligonucleotide primers and cloning strategies used for generation of EGFP plasmids

For generation of plasmids for FKBP expression in mammalian cells, the following primers were used:

Name	Sequence (5'–3')	Amplificat	Cloning strategy
12-FLAG-Eco-forward	CGGAATTCATGGACTACAAGGACGATGACGATAAG **ATGGGAGTGCAGGTGGAAACCATC**	Human FKBP12 (Accession: NM_000801), 324 bp	With *Eco*RI and *Xho*I in pcDNA3 → pcDNA3-FLAG-FKBP12
12-XhoI-Stop-reverse	GG CTCGAG TCA**TTCCAGTTTTAGAAGCTCCACA**		
12.6-FLAG-Eco-forward	CGGAATTCATGGACTACAAGGACGATGACGATAAG**ATGGGCGTGGAGATCGAGACCATC**	Human FKBP12.6 (NM_004116), 360 bp	With *Eco*RI and *Xho*I in pcDNA3 → pcDNA3-FLAG-FKBP12.6
12.6-XhoI-Stop-reverse	GGCTCGAGTCAC**TCTAAGTTGAGCAGCTCC**		
13ab26-FLAG-Eco-forward	CGGAATTCATGGACTACAAGGACGATGACGATAAGAAAAGG**AAGCTGCAG ATCGGGGTC**	Human FKBP13 (NM_004470), aa 26 – 142, 348 bp	With *Eco*RI and *Xho*I in pcDNA3 → pcDNA3-FLAG-FKBP13
13-XhoI-Stop-reverse	GGCTCGAGTCA**CAGCTCAGTTCGTCGCTC**		
25-FLAG-Eco-forward	CGGAATTCATGGACTACAAGGACGATGACGATAAG**ATGGCGGCGGCCGTTCCACAGCGG**	Human FKBP25 (NM_002013), 675 bp	With *Eco*RI and *Xho*I in pcDNA3 → pcDNA3-FLAG-FKBP25
25-XhoI-Stop-reverse	GG CTCGAG TCA**ATCAATATCCACTAATTCCACTT**		
FKBP51 in pcDNA3	TTTTGGTACCCCCACCATGGACTACAAGGACGATGACGATAAG**ACTACTGATGAAGGTGCC**	Human FKBP51 (NM_004117), 1374 bp	With *Xba*I and *Kpn*I in pcDNA3 → pcDNA3-FLAG-FKBP51
3´FKBP51 in pGem	GCGGTACCTCA**TACGTGGCCCTCAGGTTTCTC**		
FKBP52 in pcDNA3	TTTTGGTACCATGGACTACAAGGACGATGACGATAAG**ACAGCCGAGGAGAT**	Human FKBP52 (NM_002014), 1380 bp	With *Xba*I and *Kpn*I in pcDNA3 → pcDNA3-FLAG-FKBP52
3´FKBP52 in pGem4	GCGGTACCTCA**TGCTTCTGTCGAACAAG**		

Table 2.4: Oligonucleotide primers and cloning strategies used for generation of FKBP expression plasmids

2.2 – Expression vectors:

The following commercial vectors were used for protein expression in bacteria and yeast cultures:

Name	Size	Usage	Provides resistance / auxotrophy	Manufacturer
pProEx-Hta	4779 bp	Expression of proteins with N-terminal hexahistidin tag in *E. coli*	Ampicillin	Invitrogen (Karlsruhe)
pGex-4T2	4970 bp	Expression of proteins as N-terminal GST-Fusion in *E. coli*	Ampicillin	GE Healthcare (München)
pYX223	7.6 kbp	Inducible overexpression of proteins in *S. cerevisiae*	Ampicillin in *E. coli*; Histidine auxotrophy in *S. cerevisiae*	Novagen/Merck (Darmstadt)

Table 2.5: Vectors used for protein expression

The following commercially available protein expression plasmids were used for experiments in mammalian cell cultures:

Name	Vector	Size	Protein expression (from *species*)	Order number	Resistance in *E. coli*	Manufacturer
pRK5-FLAG-DEPTOR	pRK5	7050 bp	Expression of FLAG-tagged DEPTOR (*H. sapiens*)	21334	Ampicillin	Addgene (Cambridge, USA)
pRK5-myc-Raptor	pRK5	10754 bp	Expression of myc-tagged Raptor (*H. sapiens*)	1859	Ampicillin	Addgene (Cambridge, USA)
pRK5-myc-Rictor	pRK5	10454 bp	Expression of myc-tagged Rictor (*H. sapiens*)	11367	Ampicillin	Addgene (Cambridge, USA)
pRK7-HA-S6K1-WT	pRK7	6200 bp	Expression of HA-tagged S6 Kinase 1 (*R. norvegicus*)	8984	Ampicillin	Addgene (Cambridge, USA)

Table 2.6: Expression vectors used for protein expression in mammalian cells

The plasmids for overexpression of FLAG-tagged human mTOR and the mutant S2035T were a kind gift of Prof. Jie Chen (UCLA, Riverside, USA):

Name	Vector	Size	Protein expression (from *species*)	Resistance in *E. coli*
pcDNA3-FLAG-mTOR	pcDNA3	13225 bp	Expression of FLAG-tagged mTOR (*H. sapiens*)	Ampicillin
pcDNA3-FLAG-mTOR S2035T	pcDNA3	13225 bp	Expression of FLAG-tagged mTOR, mutant S2035T (*H. sapiens*)	Ampicillin

Table 2.7: Expression vectors used for mTOR expression in mammalian cells

2.3 - Primary antibodies:

For protein detection in immunoblotting experiments, the following primary antibodies were diluted in buffered protein solution (BSA or milk powder):

Name	Antigene sequence	IgG subtype from species	Dilution factor and used solution	Manufacturer
α-4E-BP1 phospho S65	Peptide around phospho S65	IgG, monoclonal, from rabbit	1:1000 in 5% (w/v) BSA in TBS	Cell Signaling (Danvers, MA, USA)
α-4E-BP1 phospho T37/46	Peptide around phospho T37/46	IgG, monoclonal, from rabbit	1:1000 in 5% (w/v) BSA in TBS	Cell Signaling (Danvers, MA, USA)
α-6xHis tag	Hexahistidyl peptide	IgG, polyclonal, from rabbit	1:1000 in 5% (w/v) milk powder in TBS	Abcam (Cambridge, UK)
α-Actin	Not known	IgG, polyclonal, from rabbit	1:5000 in 5% (w/v) milk powder in TBS	Abcam (Cambridge, UK)
α-Akt kinase (pan)	C-terminal sequence of mouse Akt	IgG, monoclonal, from rabbit	1:1000 in 5% (w/v) milk powder in TBS	Cell Signaling (Danvers, MA, USA)
α-Akt phospho S473	Peptide around phospho S473	IgG, monoclonal, from rabbit	1:1000 in 5% (w/v) BSA in TBS	Cell Signaling (Danvers, MA, USA)
α-FKBP12	Not known	IgG, polyclonal, from rabbit	1:1000 in 5% (w/v) milk powder in TBS	Abcam (Cambridge, UK)
α-FKBP12.6	Aa 1-81 FKBP12.6	IgG1, monoclonal, from mouse	1:500 in 5% (w/v) milk powder in TBS	Abcam (Cambridge, UK)
α-FKBP13	Not known	IgG, polyclonal, from rabbit	1:1000 in 5% (w/v) milk powder in TBS	Proteintech Group (Chicago, IL, USA)
α-FKBP25	Peptide from aa1-100	IgG, polyclonal, from rabbit	1:1000 in 5% (w/v) milk powder in TBS	Abcam (Cambridge, UK)
α-FKBP38	Not known	IgG, polyclonal, from rabbit	1:1000 in 5% (w/v) milk powder in TBS	Abcam (Cambridge, UK)
α-FKBP51	Peptide from aa 407-457	IgG, polyclonal, from rabbit	1:5000 in 5% (w/v) milk powder in TBS	Bethyl Laboratories (Montgomery, TX, USA)
α-FKBP52	Peptide from aa 400-440	IgG, polyclonal, from rabbit	1:5000 in 5% (w/v) milk powder in TBS	Bethyl Laboratories (Montgomery, TX, USA)
α-FLAG	DYKDDDDK	IgG1, monoclonal, from mouse	1:1000 in 5% (w/v) milk powder in TBS	Sigma (Saint Louis, MS, USA)
α-HA	YPYDVPDYA	IgG1, monoclonal, from mouse	1:1000 in 5% (w/v) milk powder in TBS	Roche Diagnostics (Mannheim)
α-mTOR	Not known	IgG, polyclonal, from rabbit	1:1000 in 5% (w/v) milk powder in TBS	Cell Signaling (Danvers, MA, USA)
α-MYC	EQKLISEEDL	IgG2a, monoclonal, from mouse	1:1000 in 5% (w/v) milk powder in TBS	Cell Signaling (Danvers, MA, USA)

α-p70 S6 kinase	C-terminus of human p70 S6 kinase	IgG, polyclonal, from rabbit	1:1000 in 5% (w/v) milk powder in TBS	Cell Signaling (Danvers, MA, USA)
α-p70 S6K phospho T389	Peptide around phospho T389	IgG, polyclonal, from rabbit	1:1000 in 5% (w/v) BSA in TBS	Cell Signaling (Danvers, MA, USA)
α-Raptor	Not known	IgG, polyclonal, from rabbit	1:1000 in 5% (w/v) milk powder in TBS	Cell Signaling (Danvers, MA, USA)
α-Rictor	Peptide around K1125 of human Rictor	IgG, polyclonal, from rabbit	1:1000 in 5% (w/v) milk powder in TBS	Cell Signaling (Danvers, MA, USA)

Table 2.8: Primary antibodies used in immunoblotting experiments and their properties

2.4 – Secondary antibodies:

The following secondary antibodies were used in immunoblotting experiments:

Name	Conjugation	IgG subtype from species	Dilution factor and used solution	Manufacturer
Mouse IgG	Horseradish peroxidase	Polyclonal, IgG, H&L, from goat	1:3500 in 5% (w/v) milk powder in TBS	Abcam (Cambridge, UK)
Rabbit IgG	Horseradish peroxidase	Polyclonal, IgG, H&L, from goat	1:3500 in 5% (w/v) milk powder in TBS	Abcam (Cambridge, UK)
Goat IgG	Horseradish peroxidase	Polyclonal, IgG, H&L, from donkey	1:3500 in 5% (w/v) milk powder in TBS	Abcam (Cambridge, UK)

Table 2.9: Secondary antibodies used in immunoblotting experiments

2.5 – Bacterial strains:

While *Escherichia Coli* strain DH5α was used especially for cloning of PCR products and for preparation of plasmid DNA, the strain BL21(DE3) is suitable for heterologous protein expression. The strains were purchased from Invitrogen (Karlsruhe) and display the following genotypes:

Strain	Genotype
DH5α	F' Phi80dlacZ ΔM15 Δ(lacZYA-argF)U169 deoR recA1 endA1 hsdR17(rK-mK+)phoA supE44 lambda- thi-1
BL21(DE3)pLysS	F–, *omp*T, *hsd*S_B (r_B–, m_B–), *dcm*, *gal*, λ(DE3), pLysS, Cm^r.

Table 2.10: Bacterial strains used for cloning and expression experiments

2.6 – Yeast strains:

Saccharomyces cerevisiae wild type yeast cells and FKBP deletion mutants (provided by Euroscarf, Frankfurt) were used. The genotypes are as follows:

	Accession Number	Name of the strain	Mating type	Genotype	Deletion
Wild type	Y10000	BY4742	Mat a	his3D1; leu2D0; lys2D0; ura3D0;	/
Mutant	Y12941	BY4742	Mat a	his3D1; leu2D0; lys2D0; ura3D0; YNL135c::kanMX4	YNL135c (=FPR1)

Table 2.11: Yeast strains used for complementation assay

2.7 – Mammalian cell lines:

The following mammalian cell lines were used:

Name	Description	Origin	Provided by	ATCC Number
HeLa	Cervix adenocarcinoma cells	*H. sapiens*	Dr. T. Rein	CCL-2
HEK293	Embryonic kidney cells	*H. sapiens*	Dr. T. Rein	CRL-1573

Table 2.12: Mammalian cell lines used for different experiments

2.8 – Media and additives for cell culture:

The following media were used to maintain mammalian cell cultures:

Name	Contains	Used for	Manufacturer
Dulbecco's Modified Eagle Medium	4.5 g/l glucose, L-glutamine	HeLa, HEK,	Gibco-Invitrogen (Karlsruhe)
Dulbecco's Phosphate Buffered Saline		all cell lines	Gibco-Invitrogen (Karlsruhe)
Heat Inactivated Fetal Calf Serum (FCS)		all cell lines	Gibco-Invitrogen (Karlsruhe)
Pen Strep	5000 U/ml Penicillin, 5000 U/ml streptomycin	all cell lines	Gibco-Invitrogen (Karlsruhe)
0.25% Trypsin-EDTA		all cell lines	Gibco-Invitrogen (Karlsruhe)

Table 2.13: Media and additives used for cell culture experiments

2.9 – siRNA:

siRNA for RNAi experiments in HeLa cells was purchased from Thermo Fischer Scientific Dharmacon (Schwerte):

Name	Target	Targeting sequence
ON-TARGETplus Non-targeting Pool	Control (non-targeting)	unknown
ON-TARGETplus siRNA J-009494-07-0005	Human FKBP1A (=FKBP12; NM_0540145)	GAGCCAAACUGACUAUAUC

Table 2.14: siRNA used for knockdown experiments

2.10 - Chemicals:

The chemicals used for this work are listed below and were purchased from the indicated companies:

Acryl amid	Roth (Karlsruhe)
Adenosine 5´-Triphosphat	Roth (Karlsruhe)
Adenine	Roth (Karlsruhe)
Agarose SeaKem	Biozym (Oldendorf)
Agar-Agar	Roth (Karlsruhe)
Ammonium peroxodisulfate	Roth (Karlsruhe)
Ammonium sulfate	Roth (Karlsruhe)
Ampicillin	Roth (Karlsruhe)
Anti-FLAG M2 Affinity Gel	Sigma (Steinheim)
Anti-HA-Agarose	Sigma (Steinheim)
Bisacryl amid	Roth (Karlsruhe)
Boric acid	Calbiochem (San Diego, CA, USA)
Bradford reagent	Bio Rad (München)
Brilliant Blue R250	Roth (Karlsruhe)
Bromophenol Blue	Merck (Darmstadt)
Calciumchloride	Roth (Karlsruhe)
3-[(3-Cholamidopropyl)dimethylammonio]-1-propanesulfonate (CHAPS)	Roth (Karlsruhe)
p-Coumaric acid	Sigma-Aldrich (Steinheim)
Desoxynucleotide mix	NEB (Frankfurt am Main)
DharmaFECT 2 transfection reagent	Thermo Fischer Scientific (Schwerte)
Dimethyl sulfoxide (DMSO)	Roth (Karlsruhe)
1,4-Dithiotreitole	Roth (Karlsruhe)
EDTA (Titriplex III)	Merck (Darmstadt)
Ethidium bromide	Roth (Karlsruhe)
Everolimus	Molcan (Toronto, Canada)
EZview Red Anti-c-MYC Affinity Gel	Sigma (Steinheim)
FK506	Fujisawa Pharmaceuticals (Osaka, Japan)
FLAG peptide	Sigma (Steinheim)

D-(+)-Galactose	Roth (Karlsruhe)
D-(+)-Glucose	Roth (Karlsruhe)
Glycerol (86-88% (v/v))	Roth (Karlsruhe)
Glycerol phosphate	Roth (Karlsruhe)
Glycine	Roth (Karlsruhe)
GST ProCatch Sepharose	Miltenyi Biotech (Bergisch Gladbach)
HA peptide	Sigma (Steinheim)
Hepes	Biomol (Hamburg)
L-Histidine	Roth (Karlsruhe)
Imidazole	Roth (Karlsruhe)
Isopropyl-beta-D-thiogalactopyranoside (IPTG)	Roth (Karlsruhe)
LB medium (Luria/Miller)	Roth (Karlsruhe)
L-Leucine	Roth (Karlsruhe)
Lipofectamine 2000	Invitrogen (Karlsruhe)
Lithium acetate (LiAc)	Alfa Aesar (Karlsruhe)
Lithium chloride	Merck (Darmstadt)
Luminol	Roth (Karlsruhe)
L-Lysine hydrochloride	Roth (Karlsruhe)
LY94002	NEB (Frankfurt am Main)
Magnesium chloride	Merck (Darmstadt)
2-Mercaptoethanol	Merck (Darmstadt)
Milk powder	Roth (Karlsruhe)
MYC peptide	Sigma (Steinheim)
Ni-NTA agarose	Qiagen (Hilden)
Peptone from casein	Roth (Karlsruhe)
Phenylmethylsulfonyl fluoride (PMSF)	Molekula (Vaterstetten)
PI-103	Calbiochem (San Diego, CA, USA)
Polyethylenglycole 4000	Roth (Karlsruhe)
Ponceau S	Roth (Karlsruhe)
Protease inhibitor cocktail	Sigma (Steinheim)
Protein A resin	GenScript (Piscataway, USA)
Rapamycin (Lot #R020)	Cfm (Marktredwitz)
Saccharose	Merck (Darmstadt)
Salmon Sperm Carrier DNA	Gibco-Invitrogen (Karlsruhe)

Sodium chloride (NaCl)	Roth (Karlsruhe)
Sodium dodecylsulfat (SDS)	Merck-Schuchardt (Hohenbrunn)
Sodium orthovanadate	Fluka Sigma-Aldrich (Steinheim)
Sodium pyrophosphate dibasic	Fluka Sigma-Aldrich (Steinheim)
N,N,N',N'-Tetramethylethylenediamine (TEMED)	Roth (Karlsruhe)
Torin1	provided by D. Sabatini
Trichloro acetic acid	Roth (Karlsruhe)
Tris(hydroxymethyl)-aminomethane	Merck (Darmstadt)
Triton X-100	Roth (Karlsruhe)
Tween 20	Bio-Rad (München)
L-Tryptophan	Roth (Karlsruhe)
Uracil	Fluka Sigma-Aldrich (Steinheim)
X-OMAT EX-II Developer	Kodak (Stuttgart)
X-OMAT EX-II Fixer	Kodak (Stuttgart)
Yeast extract	Roth (Karlsruhe)
Yeast Nitrogen Base	Fluka Sigma-Aldrich (Steinheim)
Zotarolimus	Molcan (Toronto, Canada)
Zotarolimus isomer	Molcan (Toronto, Canada)

2.11 - Enzymes:

The enzyms that were used for different assays are listed below:

Akt1/PKB$_\alpha$ (inactive)	Millipore (Schwalbach)
Antarctic Phosphatase	NEB (Frankfurt am Main)
Immunoglobulin G (bovine)	Thermo Fischer Scientific (Schwerte)
Insulin solution, human	Sigma-Aldrich (Steinheim)
Lysozyme	Roth (Karlsruhe)
Phusion High Fidelity Taq Polymerase	NEB (Frankfurt am Main)
Restriction endonucleases	NEB (Frankfurt am Main)
T4-DNA Ligase	NEB (Frankfurt am Main)
Taq Polymerase	NEB (Frankfurt am Main)
TEV protease	homemade; plasmid provided by Dr. A. Bracher

2.12 - Kits:

The following kits were used for DNA purification and FRET assays according to the manufacturer's recommendations:

CellTiter-Glo Luminescent Cell Viability Assay	Promega (Mannheim)
Genopure Plasmid Midi Kit	Roche (Mannheim)
High Yield PCR Clean-up/Gel Extraction Kit	SLG (Gauting)
High Yield Plasmid Mini Kit	SLG (Gauting)
HTRF Phospho Akt (Ser473)	Cis bio GmbH (Berlin)
LanthaScreen TR-FRET Assay	Invitrogen (Karlsruhe)
Nucleobond AX Mega Kit	Macherey-Nagel (Düren)

2.13 - Markers:

For size quantification of protein and DNA samples, the following standards were used:

1 kb DNA Ladder	NEB (Frankfurt am Main)
Page Ruler Plus Prestained Protein Ladder	MBI Fermentas (St. Leon-Rot)
Unstained Protein Molecular Weight Marker	MBI Fermentas (St. Leon-Rot)

2.14 - Equipment:

The following machines and lab items were utilized:

Äkta Purifier chromatography system	GE Healthcare (München)
Centrifuge 6K15	Sigma (Osterode)
Centrifuge Avanti J-25, Rotor JA-20	Beckman (Krefeld)
Centrifuge Biofuge pico	Heraeus (Mannheim)
Centrifuge Universal 30 F	Hettich (Tuttlingen)
CO_2 incubator HeraCell	Fischer Thermo Scientific (Schwerte)
Developer machine	3M (Neuss)

Electrophoresis power supply	Pharmacia/GE Healthcare (München)
Flat bed scanner PrecisionScan	HP GmbH (Böblingen)
Gel Dryer 583	Bio Rad (München)
Gel electrophoresis chambers	PeqLab GmbH (Erlangen)
Gel electrophoresis system XCell Sure Lock	Invitrogen (Karlsruhe)
HiLoad 16/60 Superdex 75 pg	GE Healthcare (München)
Ice machine ZBE 150-MT	Ziegra (Isernhagen)
Incubation shaker Innova 4000	NewBrunswick (Edison, NJ, USA)
Incubator Polymax 1040	Heidolph Instruments (Schwabach)
Magnet stirer RCT basic	IKA Labortechnik (Staufen)
Microscope DM IL	Leica (Wetzlar)
PCR cycler Gene Amp 9700	Applied Biosystems (Darmstadt)
pH meter WTW 538	WTW (Weilheim)
Pipettor Pipetus akku	Hirschmann Laborgeräte (Eberstadt)
Power Supply Power Pac 300	Bio Rad (München)
Precision scales Master Pro LP4200S	Sartorius (Göttingen)
Reader Tecan GENios Pro	Tecan (Crailsheim)
Refrigerator	Liebherr (Biberach)
Shaking table SM25A	Edmund Bühler (Hechingen)
Thermomixer comfort	Eppendorf (Hamburg)
Ultrapure water dispenser PureLab ultra	Elga Lab Water (Celle)
Ultrasound Sonifier 450	Branson (Dietzenbach-Steinberg)
UV transilluminator	Faust (Meckenheim)
UV/VIS spectrophotometer DU 530	Beckman (Krefeld)
Vortexer Mini-Shaker MS2	IKA Labortechnik (Staufen)
Water bath GfL 1002	GfL (Burgwedel)
Work bench LaminAir HB2448	Heraeus (Mannheim)

2.15 - Consumables:

384-well plates, low-binding surface	Corning (Kaiserslautern)
96-well plates, low-binding surface	Corning (Kaiserslautern)
96-well plates, transparent	Greiner Bio-One (Kremsmünster, AT)
Cell scraper 25 cm	Sarstedt (Nümbrecht)
Cellstar serological pipettes	Greiner Bio-One (Kremsmünster, AT)
Centricon 10 kDa	Millipore (Schwalbach)
Chromatography column 5 ml	Bio Rad (München)
Falcon 6-well plates	BectonDickinson (Franklin Lakes,USA)
Glass beads	Sigma (Steinheim)
Medical X-Ray film Super RX	Fujifilm Corporation (Düsseldorf)
Millex Stringe Filter 0.22 µm	Millipore (Schwalbach)
Nunclon Surface cell culture dishes	Nunc A/S (Roskilde, DK)
Protran BA 83 Nitrocellulose	Whatman (Dassel)
Rotilabo Blotting paper	Carl Roth (Karlsruhe)
SDS Mini gel cassettes	Invitrogen (Karlsruhe)
SnakeSkin Dialysis Tubing 3,500 MWCO	Pierce/Fisher Thermo Scientific (Bonn)
Test tubes	Sarstedt (Nümbrecht)

2.16 – Software:

For data collection and analysis, the following PC programs were used:

COOT /CCP4	STFC
Chimera	UCSF, Conrad Huang [261]
Gimp 2.4.7	Spencer Kimball, Peter Mattis
PyMol 0.99	DeLano Scientific
SigmaPlot 10	Systat Software (Erkrath)
Word, Excel 2000	Microsoft (München)

3 – Methods:

3.1 – Standard cloning techniques:

3.1.1 – Polymerase chain reaction (PCR):

For a standard PCR reaction the following components were combined in a 0.2 ml PCR tube and a total volume of 50 µl:

400 µmol	dNTP mix (stock: 20 mM)
100 nmol	primer forward (Metabion, Planegg)
100 nmol	primer reverse
100 ng	plasmid DNA template
1 U	Phusion "High Fidelity" Taq polymerase
5 µl	10x Phusion High-Fidelity buffer

The polymerase chain reaction was performed in a thermo cycler following a defined time and temperature profile. Per 1 kb of polymerization, 1 minute elongation time was scheduled. Annealing temperature was chosen according to primer melting temperature.

step 1:	300 seconds	92°C	initial denaturation
step 2:	40 seconds	92°C	denaturation
step 3:	40 seconds	50-65°C	annealing
step 4:	30-120 seconds	72°C	elongation
		30 repeats of steps 2-4	
step 5:	300 seconds	72°C	final elongation

3.1.2– Analysis and purification of PCR products:

3.1.2.1 – Agarose gel electrophoresis:

TBE buffer: 90 mM boric acid; 2.5mM EDTA; 90 mM Tris/HCl, pH 8.3

DNA sample buffer: 40% (w/v) saccharose; 0.25% (w/v) bromophenol blue
20 mM EDTA, pH 8.0

To prepare an agarose gel, an appropriate amount of agarose (normally: 0.5 to 1.5 grams to yield 0.5 – 1.5% gels) was mixed with 100 ml TBE buffer and boiled in a microwave oven until it had dissolved completely. After the solution had cooled down to 60°C, 3 µl of ethidium bromide solution were added and mixed thoroughly. Then, the solution was poured into a gel tray. Air bubbles were removed, and the comb was put in place. After 30 minutes, the gel had solidified and was transferred to a gel chamber containing TBE buffer. The DNA samples (normally: 5 µl of a 100 ng/µl solution) were mixed with an equal amount of DNA sample buffer and were filled into the gel wells. Separation of DNA was performed by applying a current of 200 mA for 30 minutes (or until desired separation is achieved).

3.1.2.2 – Isolation of DNA fragments:

The PCR products were visualized as gel bands using an UV transilluminator and documented photographically, before the bands were excised with a scalpel. The „High Yield PCR and Gel Extraction Kit“ was used according to the manufacturer's recommendations to isolate DNA from the gel slices. Usually concentrations of 30 – 50 µg DNA / ml were obtained (determined by standard UV measurement at 260 nm and 280 nm; 1 A_{260} = 50 ng/µl; optimal ratio A_{260}/A_{280} between 1.8 and 2.0).

3.1.3 – DNA restriction:

For restriction of vector DNA and PCR products, the following components were combined:

1 µg	vector DNA (100 µg/ml)	
10 U	restriction enzyme 1 (20 U/µl)	
10 U	restriction enzyme 2 (20 U/µl)	
2 µl	10x restriction buffer	
	bidest. H_2O	ad 20 µl

alternatively:

1 µg	PCR product (50 µg/ml)	
20 U	restriction enzyme 1 (20 U/µl)	
20 U	restriction enzyme 2 (20 U/µl)	
4 µl	10x restriction buffer	
	bidest. H_2O	ad 40 µl

For the enzyme combination *EcoR*I/*Xho*I, the buffer „EcoRI“ was used. For *Nco*I/*Xba*I and *Nco*I/*Sal*I, NEB buffer II was utilized. The restriction mixtures of PCR products were incubated for 2 hours at 37°C, while the ones of the vectors were incubated at 37°C over night.
To avoid re-ligation of single-cut vector, the vector restriction mixtures were supplemented with 1 µl of Antarctic Phosphatase (1 U/µl) and 2 µl of the corresponding 10x AP buffer. After 30 minutes of incubation at 37°C the samples were subjected to DNA purification using the „Gel Extraction Kit“. DNA concentrations of around 25 µg/ml were obtained; around 50% of the original amount of DNA were lost during the procedure.
5 µl of the purified DNA samples were separated by gel electrophoresis (1.0% agarose gel) to check for contamination and yield.

3.1.4 – DNA ligation:

For ligation, vector DNA and PCR product were combined in a 1:3 ratio following the manufacturer's recommendations. A typical ligation mixture contained the following components:

1 µg	vector DNA (25 µg/ml)	
3 µg	PCR product (25 µg/ml)	
10 U	T4 DNA ligase (20 U/µl)	
1 µl	10x ligation buffer	
	bidest. H_2O	ad 10 µl

The mixture was incubated over night at 16°C. If an optimization of the reaction was necessary, a higher amount of PCR product was used. Alternatively, the concentration of ligase and/or the incubation time was increased.

3.1.5 - Transformation into *E. coli* DH5α and BL21:

3.1.5.1 – Preparation of competent cells:

To prepare transformation-competent *E. coli* cells, 50 ml of sterile LB medium were inoculated with a small amount of glycerol stock and incubated over night at 37°C on a

shaking platform (200 rpm). 25 ml of this over-night culture were used to inoculate 500 ml of sterile LB medium. This culture was grown at 37°C until an OD_{600} of 0.3 was reached.
Cells were harvested by 15 minutes of centrifugation at 5000 g and 4°C. The pellet was resuspended slowly and gently in 125 ml of cold, sterile 100 mM $MgCl_2$ solution. After another centrifugation step (5000 g, 4°C, 15 minutes), the bacteria were resuspended in 25 ml of sterile 100 mM $CaCl_2$ solution before another 200 ml 100 mM $CaCl_2$ solution were added. The mixture was incubated on ice for 20 minutes. The cells were harvested again (4000 g, 4°C, 10 minutes) and resuspended in 10 ml of 100 mM $CaCl_2$ solution with 10% glycerol (w/w). Finally, 100µl aliquots of the cell suspension were shock-frozen in liquid nitrogen and stored at -80°C until usage.

3.1.5.2 – Transformation procedure:

5 µl of the ligation reaction were added to 50 µl of thawed competent *E. coli* and mixed carefully. The cells were incubated for 30 minutes on ice and were exposed to a heat shock of 42°C in a water bath for 60 seconds. After addition of 500 µl LB medium, the transformation mixture was grown at 37°C for 60 minutes on a shaking platform. Finally, the cells were harvested by short centrifugation, plated of LB agar plates containing antibiotics (100 µg/ml ampicillin or 50 µg/ml kanamycin) and incubated over night at 37°C.

3.1.6 – PCR colony screening:

To identify successfully transformed clones, single colonies on LB agar plates were picked and resuspended in 20 µl of sterile water. 2 µl of this suspension were used as DNA template in a standard PCR reaction. Thus, the PCR mixtures contained the following components:

400 µmol	dNTP mix (20 mM stock)	
100 nmol	vector-specific primer forward (Metabion, Planegg)	
100 nmol	vector-specific primer reverse	
2 µl	clone suspension	
1 U	Taq polymerase	
2 µl	10x PCR buffer	
	bidest. H_2O	ad 20 µl

The PCR mixtures were subjected to a standard temperature profile with reduced annealing temperature in a thermo cycler (300 s 92°C; 25 cycles of 40 s 92°C, 40 s 52°C, 90 s 72°C; 300 s 72°C).
Afterwards, the samples were analyzed on a 1.5% agarose gel. Short amplificats of around 200 bp reflected the presence of empty vector, while DNA bands of higher molecular weight represented a successfully ligated insert.
Positive clones were inoculated in 5 ml of antibiotic-supplemented sterile LB medium and incubated over night at 37°C with shaking (200 rpm). Plasmid preparation was performed using a MiniPrep Kit, following the manufacturer's protocol. UV determination revealed a yield of around 100 µg plasmid DNA per ml solution.

3.1.7 – Restriction control:

To further verify successful cloning, plasmid DNA was subjected to enzymatic restriction. During this control assay the same restriction enzymes are used as for cloning; therefore the insert is cut out of the vector.
The digestion mixtures contained the following components:

1 µg	plasmid DNA (100 µg/ml)
10 U	restriction enzyme 1 (20 U/µl)
10 U	restriction enzyme 2 (20 U/µl)
2 µl	10x restriction buffer
	bidest. H_2O ad 20 µl

The restriction mixtures were incubated at 37°C for 60 minutes and analyzed on a 1.5% agarose gel. Preparations of plasmid DNA with insert were saved while plasmids without inserts were discarded.

3.1.8 – DNA sequencing:

For final approval of positive clones the plasmid DNA was sequenced using the chain termination sequencing technique and standard vector-specific primers. This service was provided by the "Microchemistry Core Facility" at the MPI of Biochemistry in Martinsried. The obtained sequences were compared to corresponding references in order to exclude base pair deletions and point mutations.

3.2 – Heterologous protein expression:

3.2.1 – Expression of proteins with hexahistidin tag:

3.2.1.1 – *E. coli* culture:

Plasmid DNA encoding a specific hexahistidin tagged protein was transformed into the expression strain *E. coli* BL21. 3 l of sterile LB medium, supplemented with the appropriate antibiotics, were inoculated with an over night culture (maximal OD_{600}: 0.1) and incubated at 37°C on a shaking platform. As soon as an optical density of 0.5 was reached, protein expression was induced by addition of 1.8 ml 1 M IPTG (final concentration: 600 µM). After further 3 hours of incubation, the cells were harvested by centrifugation in a Sigma centrifuge at 4000 g and 4°C for 15 minutes.

3.2.1.2 – Cell lysis:

Lysis buffer:	50 mM Hepes; pH 8.0; 300 mM NaCl; 20 mM imidazole; 1 mM PMSF; 1 mg/ml lysozyme

All further purification steps were carried out at 4°C or on ice.
The cell pellet was resuspended in 50 ml lysis buffer and incubated on ice for 30 minutes. Treatment with an ultrasound sonifier was performed to complete cell lysis (8 cycles: 15 seconds ultrasound in impulses, 15 seconds break; intensity: 5). To remove insoluble material, the lysate was centrifuged for 40 minutes at 4°C and 15000 g in a Beckman centrifuge.

3.2.1.3 – Purification on nickel NTA sepharose:

Washing buffer:	50 mM Hepes, pH 8.0; 30 mM NaCl; 50 mM imidazole; 10% glycerol (v/v)
Elution buffer:	50 mM Hepes, pH 8.0; 30 mM NaCl; 500 mM imidazole; 10% glycerol (v/v)

5 ml nickel NTA resin were resuspended in 50 ml water and pelleted again by 5 minutes of centrifugation at 2500 g. Washing was repeated twice with each 50 ml lysis buffer.
The cleared lysate was added to the resin and incubated for 3 hours with agitation at 4°C. Afterwards, the beads were pelleted by centrifugation (2500 g, 4°C), and the supernatant was discarded. The resin was resuspended in 50 ml washing buffer, incubated shortly and pelleted by centrifugation. This washing step was repeated twice.
Next, the resin was resuspended in 5 ml washing buffer and transferred into a 5-ml chromatography column. As soon as the washing buffer had drained totally, 5 ml elution buffer were added. The eluate was collected in 0.5 ml fractions and checked for protein content by Bradford assay (see section 3.3.2).

3.2.1.4 – Purification on anti-FLAG affinity resin:

TBS: 50 mM Tris; 150 mM NaCl; pH 7.5
Elution buffer: 100 µg/ml FLAG peptide in TBS

For FKBP51, analysis of elution fractions revealed an insufficient purity of the preparation. A second purification step had to be performed, taking advantage of the C-terminally fused FLAG peptide. This peptide (sequence: DYKDDDDK) binds to specific antibodies with high affinity and therefore allows binding of FLAG fusion proteins to immuno-affinity resin in which the antibodies are bound covalently to a sepharose matrix.
1 ml of resuspended “ANTI-FLAG immuno-affinity resin” was transferred to a 5-ml plastic column and washed with 10 ml TBS. Then the pooled protein-containing fractions of the Ni-NTA purification were loaded onto the column. After the flow through was completed, the resin material was washed with TBS until no protein could be detected any more in the washing buffer by Bradford assay. By addition of elution buffer the FKBP51-FLAG protein was released from the resin and collected in different fractions. Once again, protein content was quantified by Bradford assay, and protein-containing fractions were pooled.

3.2.1.5 – Analysis of purified proteins by SDS gel electrophoresis:

3.2.1.5.1 – Casting SDS gels:

SDS running buffer: 25 mM Tris/HCl, pH 8.3; 250 mM glycine; 0.1% (w/v) SDS

SDS sample buffer 2x: 125 mM Tris/HCl; 10% (v/v) 2-mercaptoethanol;
"Lämmli buffer" [262] 4% (w/v) SDS; 0.004% (w/v) bromophenol Blue

Resolving gel**:** 380 mM Tris/HCl, pH 8.8; 0.1% (w/v) sodium dodecylsulfate;
10-16% (w/v) acryl amid; 0.2 – 0.3% (w/v) bisacryl amid;
0.12% (v/v) TEMED; 0.06% (w/v) ammonium peroxydisulfate

Stacking gel**:** 375 mM Tris/HCl, pH 6.8; 0.1% (w/v) sodium dodeclysulfate
5% (w/v) acryl amid; 0.2 – 0.3% (w/v) bisacryl amid
0.2% (v/v) TEMED; 0,06% (w/v) ammonium peroxydisulfate (APS)

Coomassie staining solution: 40% (v/v) ethanol, 10% (v/v) acetic acid
0.01% (w/v) coomassie brilliant blue

Coomassie destaining solution: 40% (v/v) ethanol, 10% (v/v) acetic acid

Acryl amid mix was prepared using 30% (w/v) acryl amid and 0.6% (w/v) bisacryl amid. For two mini gels of the indicated acryl amid concentration, following components were combined:

final concentration	acryl amid mix	H_2O bidest.	TEMED	1 M Tris, pH 8.8	10% (w/v) SDS	10 % (w/v) APS
10%	4.7 ml	3.9 ml	17 µl	5.4 ml	140 µl	85 µl
12%	5.7 ml	3.0 ml	17 µl	5.4 ml	140 µl	85 µl
16%	7.6 ml	1 ml	17 µl	5.4 ml	140 µl	85 µl

Table 3.1: Components and necessary amounts for 2 "mini" SDS gels

Ammonium peroxydisulfate and TEMED were added lastly because they induce radical formation and start the polymerization. The gel solution was filled into a commercially available mini gel cassette and was covered carefully with water. After the polymerization was completed, water was removed, and the gel cassettes were filled with stacking gel solution. Finally, 12 or 15-well combs were inserted.

3.2.1.5.2 – Preparation of samples and gel run:

Samples of the protein-containing fractions were diluted in SDS sample buffer and incubated at 95°C for 5 minutes to achieve denaturation. The samples were then loaded into the gel

wells and separated using a current of 30 mA in the "XCell SureLock Gel System" for approximately 60 minutes. Protein patterns were visualized by treatment with Coomassie staining solution for 30 minutes, followed by destaining in the destaining solution under mild agitation. The gel was put on a sheet of blotting paper and was conserved using a gel dryer. Finally, it was digitalized on a flatbed scanner.
Alternatively, the gel was subjected to immunoblotting procedure (see section 3.7.3).

3.2.2 – Proteins as GST fusion:

PBS:	137 mM NaCl; 2.7 mM KCl;
	4.3 mM Na_2HPO_4; 1.47 mM KH_2PO_4; pH 7.4
Lysis buffer:	PBS; 1 mM PMSF; 1 mg/ml lysozyme
Elution buffer:	PBS; 10 mM glutathione; 10% glycerol

Generally, the expression of GST fusion proteins was performed in the same way as for His-tagged proteins; instead of Nickel NTA beads, GST ProCatch Sepharose was used as affinity resin together with the above mentioned lysis, washing and elution buffers as recommended by the manufacturer. 2 ml of resin were used for 50 ml of bacterial lysate.

3.3 – Determination of protein concentration:

3.3.1 – UV absorption:

Because of the presence of aromatic amino acids (tyrosine, phenylalanine, tryptophan), protein solutions display absorption of ultra-violet light. The maximum of absorption is usually at 280 nm. The Law of Lambert-Beer provides a connection between protein concentration and its UV absorption value:

$\mathbf{A = \varepsilon\ c\ d}$, being: A: absorption at 280 nm
ε: absorption coefficient solution
d: path length (depth of the cuvette) [cm]
c: protein concentration [M]

The absorption coefficient of a protein can be deduced from its amino acid sequence as it depends mainly on the number of aromatic amino acids. The values for all expressed proteins can be found in appendix (see section 6.1). These values were computed using the ExPASy tools „ProtParam“ with the amino acid sequence as input.
Determination of UV absorption was performed in a Beckman photometer. For calibration the quartz cuvette was filled with 100 µl of elution buffer, and a blank value was recorded. Afterwards, the protein samples were measured in the same manner. If necessary the samples were diluted in elution buffer to give A_{280} values between 0.1 and 1.0. Protein concentration can be calculated using the formula $c = A / (\varepsilon \cdot d)$, being d = 1 cm**.**

3.3.2 – Bradford assay [263]:

In order to determine protein concentrations, a colorimetric assay according to Bradford is used routinely. This assay is based on an absorption shift of the dye “Coomassie Brilliant Blue” from red to blue after protein binding. Thus, the increase of absorption at 595 nm is directly proportional to the protein concentration of the sample. After determination of a reference array the concentration of every kind of protein sample can be determined.
The assay was performed in transparent 96-well plates. Each well was filled with 100 µl of a 20% (v/v) dilution of Bradford reagent in bidest. H_2O. For a reference array 0, 1, 2, 3, 4 and 5 µl of IgG (concentration: 1.4 mg/ml) were added and mixed thoroughly. The actual protein samples were diluted 1:10 in water if addition of 1 µl of undiluted sample resulted in excessive blue staining. 1 µl of the dilution was added to each well and mixed thoroughly.
After 10 minutes of incubation all wells were read out in a Tecan “GENios Pro” reader with standard settings:

Measurement mode: Absorbance, endpoint;
Wavelength: 595 nm;
Number of reads: 10 reads;
3 s of orbital shaking before measurement.

The optical density at 595 nm was plotted against the known protein concentration of the references, and a trend line was fitted. Using the linear equation of this trend line in Excel, the concentrations of the protein samples could be determined (after applying the corresponding dilution factors).

3.4 – Protein crystallization:

3.4.1 – Tobacco etch virus (TEV) protease digestion:

TEV cleavage buffer:	50 mM Tris/HCl, pH 8.0
	0.5 mM EDTA
	1 mM DTT

All proteins that were purified using the expression vector pPRO-ExHta still carried an N-terminal hexahistidin tag which could influence the performance of proteins in downstream assays. In order to assure maximum wild type-like behavior, the purification tags of the proteins had to be removed. This is a standard procedure to prepare proteins for protein crystallization and structure determination.

First, the Nickel-NTA-purified proteins were dialyzed twice against 2 l TBS for two hours. The exclusion size of the dialysis tubes was 3.5 kDa; thus the imidazole concentration of the protein samples was reduced efficiently. Protein concentrations were controlled by measurement of UV absorption at 280 nm.

To start protease cleavage, the protein samples were mixed with Tobacco Etch Virus protease (recombinantly expressed as his-tagged protein in *E. coli* BL21 and purified using standard Ni-NTA chromatography) in a molar ratio of 1:100. After addition of 10x cleavage buffer and DTT the mixtures were incubated over night at 4°C. A typical batch contained the following components:

100 nmol	FKBP51 FK1 (stock: 200 µM)
10 nmol	TEV protease (stock: 20 µM)
1:1000	1 M DTT
	10x TEV buffer

Progress of the cleavage reaction was checked by SDS gel analysis. If cleavage was incomplete, incubation time was extended by another 24 hours.

To remove contaminating protease and cleaved his-tag, the samples were incubated with an appropriate amount of Nickel-NTA beads (normally: 1/10 of total volume) for one hour. After short centrifugation at 4000 g, the supernatant was transferred to another tube and extracted

once again with Nickel-NTA beads. After the beads were pelleted, the supernatant was cleared by passing it through a 0.22 µm syringe filter and analyzed on a SDS gel.

3.4.2 – Reconstitution of ternary complexes:

In order to create the respective ternary complexes of FRB and FK1 FKBP51/52 *in vitro*, rapamycin was added to an equimolar mixture of the two protein components. The macrolide was used in slight excess to ensure maximum yield of complex.
A typical mixture contained the following compounds:

each 1 µmol	FK1 FKBP51/52 and FRB
1.2 µmol	rapamycin

As the affinity of the FKBP*rapamycin complex to FRB is presumably very high, formation of ternary complexes occurs instantaneously; therefore incubation time was kept short (5 minutes).

3.4.3 – Gel filtration chromatography:

As excessive rapamycin and unbound FKBP or FRB fractions had to be removed, the reconstitution mixture was submitted to another purification step. Since the proteins were all untagged, affinity chromatography could not be used; instead, gel filtration chromatography using a "HiLoad Superdex" column appeared suitable as this application permits the separation of a protein mixture based on the size of the single components.
The column matrix consists of dextran which is bound covalently to cross-linked agarose. The average particle size is 34 µm. Therefore small proteins penetrate into the pores and are retained while the migration of large proteins and complexes is relatively undisturbed. Since the ternary complex is twice as large as the individual proteins, its separation was expected to be relatively simple: presumably, the ternary complex is eluted faster than its individual components.
To start the purification procedure, the complex mixture was loaded via the injection valve into the super loop of the "Äkta Purifier" chromatography system. Afterwards, the solution was injected with a flow rate of 0.3 ml/min onto the "Superdex HiLoad 16/60" column which had been equilibrated with two column volumes of TBS before.

The running buffer TBS was pumped with a constant flow rate of 0.3 ml/min over the column, until all fractions were eluted completely at around 120 ml (corresponding to one column volume). By automatic recording of UV absorption at 280 nm by the Äkta system, the protein containing fractions could be determined.

3.4.4 – Protein crystallization:

The crystallization of the ternary complexes FRB*rapamycin*FK1 FKBP51 and FRB*rapamycin*FK1 FKBP52 was accomplished in co-operation with Dr. Andreas Bracher (MPI for biochemistry, Martinsried).

To prepare initial screening for suitable crystallization conditions, the pooled Äkta fractions were concentrated in a Centricon tube (exclusion size: 10 kDa) by centrifugation at 15.000 g and 4°C until a protein concentration of 20 mg/ml was reached (determination after Bradford). In the department of structural cell biology (Elena Conti, MPI of Biochemistry, Martinsried) three “complex screens” of each 120 conditions including different buffers and precipitates were performed in nano-drop format. A “Phoenix Nanodispenser” robot performed all necessary pipetting steps in a completely automated manner. Digital imaging was also accomplished by an automated system; evaluation of the pictures occurred online.

After 24 hours the first conditions were identified which allowed growth of single crystals. These conditions were further varied in a 24-well format and assayed in 2 µl drops on cover slips in siliconized wells. The plates were incubated at 20°C, and crystal growth was controlled microscopically.

To harvest the crystals, they were transferred into a drop of precipitation buffer (supplemented with 10% (v/v) glycerol) using a fine manipulation loop. After 10 minutes of equilibration in the new buffer environment, the crystal was transferred into a drop of cryobuffer containing 20% (v/v) glycerol. After another 10 minutes of incubation, the crystal was positioned as centrically and parallel to the loop as possible and quick-frozen in liquid nitrogen in a Dewar vessel. A magnetically sticking protective cap was put onto the mounting plate of the loop in order to prevent mechanical damage of the crystal. All manipulations of the crystal had to be accomplished strictly under liquid nitrogen since the crystal would have thawed immediately after exposition to air and thus would have become useless.

The mounting plate with the crystal was kept in a sampler cassette in liquid nitrogen until it was needed for x-ray diffraction analysis at the synchrotron. Well-shaped, preferably big

crystals were used for X-ray exposure at beamline ID19 at the ESFR (European Synchrotron Radiation Facility) in Grenoble.
For data processing and evaluation, the CCP4 software suite [264] was used: Data integration was done using Mosflm [265], data reduction was carried out by SCALA [266], and molecular replacement was performed using Arp Warp [267]; the crystal structure of the ternary complex FRB*C15-(R)-methylthienyl-Rapamycin*FKBP12 (PDB entry: 3fap) was used as an initial model. Graphical fitting and model building was done using COOT [268]. For intermediate refinement of the structures, Refmac [269] was executed (5 cycles, 1.45 – 20 Å resolution range, weighting term 0.1, refine isotropic temperature factors). Finally, waters were added to the structure (peaks greater than 3sigma in the difference map).

3.5 – Protein assays:

3.5.1 – Fluorescence polarization assay:

3.5.1.1 – Principle of the assay:

Fluorescence polarization assays are used to determine binding interactions between a protein and a fluorescent ligand. Here, an important parameter is the decoupling between excited and emitted photon polarization which occurs when a molecule displays rotational diffusion. This diffusion (or tumbling) reaches its maximum when the fluorophor performs free rotation in a solution; it decreases when the fluorophor builds a complex with a protein as binding partner because the resulting complex is much larger and moves more slowly. Thus, the difference is biggest when the free molecule binds to a large protein partner [270].
Practically, fluorescence polarization is determined by measurement of the intensity of parallel polarized light and perpendicularly polarized light. The following equation describes how P values are calculated mathematically:

$$\mathbf{P = (I_{parallel} - I_{perpendicular}) / (I_{parallel} + I_{perpendicular})}$$

being: P: fluorescence polarization
$I_{parallel}$: intensity of parallel polarized light emission
$I_{perpendicular}$: intensity of perpendicularly polarized light emission

To determinate protein activity or the portion of active protein in the mixture, an „active site titration" was performed: during this procedure the fluorescent FKBP ligands CK97 and CK182 (see figure 3.1) were titrated in different concentrations against FKBP protein. In accordance with the law of mass action the EC_{50} value should rise linearly with increasing ligand concentrations; this EC_{50} can be considered as the mean effective concentration, and it indicates at which ligand concentration half of the protein is bound. If the ligand concentration is plotted against the associated EC_{50} values, one obtains a straight line whose upward slope ideally is 0.5, and whose y axis intercept corresponds to the binding affinity of the protein that is independent of the ligand concentration (possibly: k_d).

$$[\text{Protein}] + [\text{Ligand}] \rightleftharpoons [\text{Protein*Ligand}]$$

$$k_d = [\text{Protein}] * [\text{Ligand}] / [\text{Protein*Ligand}]$$

3.5.1.2 – Experimental procedure: active site titration

Assay buffer: 50 mM Hepes, pH 7.7; 30 mM NaCl; 0.01% (v/v) Tween20

In a 96-well low-binding Corning plate, a serial dilution of FKBP protein was prepared. To this end, 23 wells in two rows were filled with each 50 µl of assay buffer. Another well contained 100 µl of a 20 µM dilution of the respective FKBP protein in assay buffer. From this well, 50 µl were transferred to the first well containing 50 µl of buffer and mixed well. Again, 50 µl were transferred to the next well. This transfer was repeated until the 1:1 dilution series of the protein was completed. The last well contained pure buffer.
10 µl of these dilutions were pipetted into a 386-well low-binding plate before 10 µl of a CK97 or CK182 dilution in assay buffer were added (double final concentration). For an active site titration, at least 5 different final concentrations of ligand were tested: 5, 50, 100, 150 and 200 nM. Altogether, for every tested FKBP protein 5 dilution series with each 24 wells and each 5 different CK97 and CK182 concentrations were prepared.
After 15 minutes of incubation at room temperature, a Tecan reader was used to determine fluorescence polarization values. The following settings were used:

Mode: Fluorescence Polarisation, end point
Wavelengths: Excitation: 485 nm; Emission: 535 nm
Number of reads: 10; Integration time: 100 µs

A plot of mP units against the protein concentration created a dose-response curve that could be analyzed by "Four-Parameter-logistic-curve" fitting in SigmaPlot. This analysis also revealed EC_{50} values that represent a protein concentration at which half of the protein is bound to ligand. The formula looks as follows:

$$y = \text{bot} + \frac{(\text{top} - \text{bot})}{1+(\text{“x”}/IC_{50})^{\text{slope}}}$$

bot = minimum mP value
top = maximum mP value

The calculated EC_{50} values were plotted against the corresponding CK97 or CK182 concentration. This provided the opportunity to determine EC_{50} values by linear regression which are independent of the ligand concentration. They could be regarded as theoretical K_d values. The following equation gives the theoretical approach:

$$EC_{50} = m\ [CK97/182] + „K_d“$$

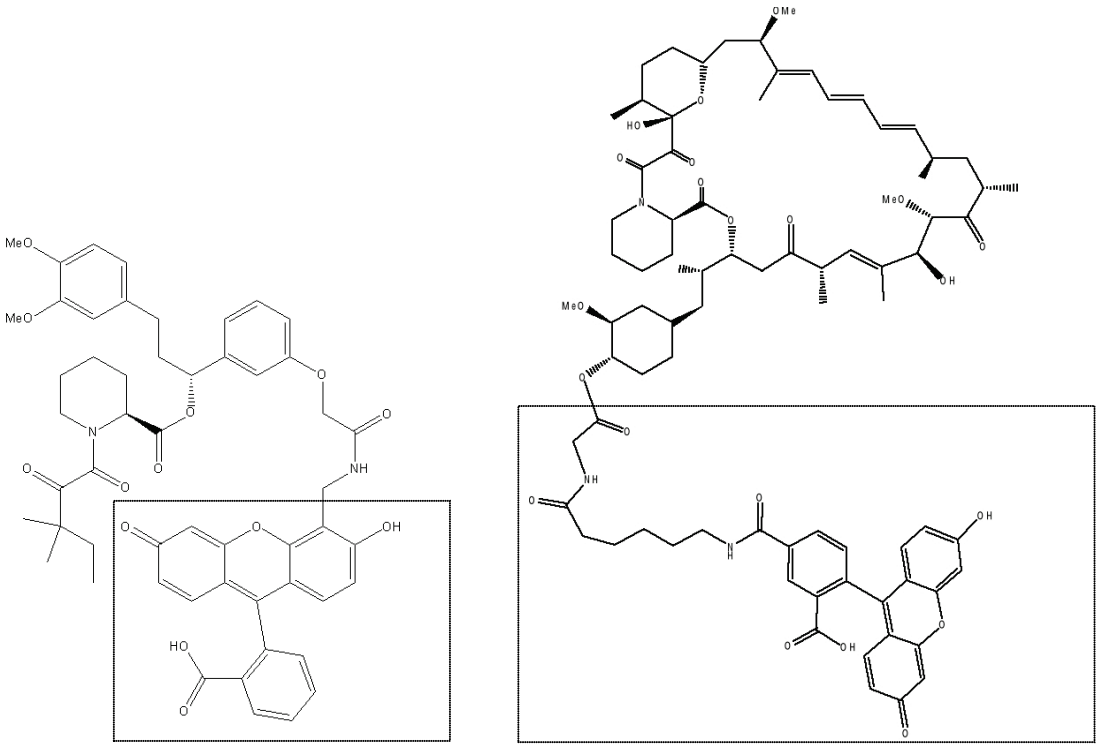

CK182 **CK97**

Figure 3.1: Fluorescent tracers CK182 and CK97 were used for active site titration

CK182 has been synthesized by coupling CK85 to a fluorescein derivative. CK97 contains a hexanoic acid spacer between the rapamycin moiety and the fluorescein (fluorophor in box). These two compounds were provided by C. Kress, RG Hausch, MPI of Psychiatry.

3.5.2 – FRET binding assay:

FRET (Fluorescence Resonance Energy Transfer) is a quantum-mechanical phenomenon that involves energy transfer between two chromophores [271] and provides an elegant tool to characterize protein-protein interactions. Basically the concept describes the energy transfer between two partners that is possible just when they are located in close proximity with correct orientation. If such a system of interacting chromophores is excited with light energy of the absorption wavelength of the donor, it will transfer energy to the acceptor which thereby emits light on a wavelength different from the one of the donor. Thus, it is possible to determine the extent of energy transfer by measuring the intensity of light emission at acceptor wavelength and to deduce the intensity of the underlying protein-protein interaction.
The time-resolved FRET assay that was used to investigate the interaction between FKBPs and FRB was originally developed by Invitrogen and is based on a Terbium-labelled anti-GST antibody and a GFP (green fluorescent protein) acceptor. As GST fusion protein, GST-FRB was used while all FKBPs were utilized as N-terminal EGFP-fusions (EnhancedGFP) in the assay.

The assay was performed following the manufacturer's recommendations: in a total volume of 10 µl, 5 µl of rapamycin dilution (1:1 dilution in TR-FRET dilution buffer, starting at 4 µM) were combined with 5 µl of protein mixture in low-binding 384-well plates. The protein mixture contained variable amounts of the following components in dilution buffer:

5 nM	GST-FRB
25 nM – 100 nM	EGFP-FKBP
2.5 nM – 5 nM	Tb-labelled anti-GST antibody

After 15 minutes of incubation, the wells were read out using a Tecan "GENios Pro" reader with the following settings:

Measurement mode: Fluorescence Intensity, endpoint
FRET 1: Excitation: 340 nm; Emission: 495 nm
FRET 2: Excitation: 340 nm; Emission: 520 nm
Integration: 100 µs lag time; 200 µs integration time
Number of flashes: 10

The two emission intensities were plotted as ratio (520nm/495nm) against the rapamycin concentration. Then, an EC_{50} value was calculated by using the „Four-Parameter-Logistic-Curve“-Fitting in SigmaPlot. This value corresponds to the rapamycin concentration at which the half-maximum concentration of the FRB*FKBP complex is present.

3.5.3 – FRET mTOR kinase activity assay:

The commercial “LanthaScreen mTOR Activity Assay“ was used to determine mTOR activity in presence of FKBP proteins and rapamycin. The assay was performed according to the manufacturer’s recommendations. Basically, the assay detects 4E-BP1 phosphorylation by a phospho-specific Terbium-labelled antibody. Energy transfer occurs between the antibody and the EGFP-N-Terminus of the mTOR substrate 4E-BP1.

Assay buffer: 50 mM Hepes, pH 7.5; 0.01% (v/v) Tween 20;
1 mM EGTA; 10 mM $MnCl_2$; 2 mM DTT.

To prepare a rapamycin master dilution series, each 40 µl of DMSO were provided in 12 tubes. To the first tube 0.8 µl 10 mM rapamycin solution in DMSO were added to achieve a final concentration of 200 µM. 20 µl of this solution were transferred to tube number 2 and mixed well. If this procedure was repeated with the following tubes, a dilution series was obtained in which the rapamycin concentration decreased by 33% in consecutive tubes.
To avoid issues concerning rapamycin solubility in water and to assure constant DMSO concentration in all assay wells, a 1:50 dilution was prepared by adding each 1 µl of the DMSO master dilution to 49 µl of assay buffer. The resulting dilution series ranged from 4 µM rapamycin to 0.
In a total volume of 10 µl per well, 2.5 µl of rapamycin dilution (in assay buffer; starting at 4 µM; 2% (v/v) DMSO), 5 µl kinase dilution and 2.5 µl substrate mix were combined. For this purpose, 384-well low-binding plates were used. After mixing the plate was incubated for 60 minutes at room temperature. By addition of 10 µl antibody mix the reaction was stopped. Another incubation step of 30 minutes at room temperature was carried out.

The following volumes and final concentrations were used for a test series with 12 wells:

		final concentration
Kinase dilution:	0.7 µl 1:100 mTOR dilution	
	0.6 µl 10 µM FKBP	50 nM
	ad 60 µl with assay buffer	
Substrate mix:	0.6 µl 2 mM ATP	10 µM
	0.5 µl 90 µM EGFP-4E-BP1	400 nM
	ad 30 µl with assay buffer	
Antibody mix:	0.7 µl 0.33 µM Tb-Anti-P-antibody	1 nM
	5 µl 500 mM EDTA	10 mM
	ad 120 µl with assay buffer	

Reading of FRET intensities was performed using a Tecan reader as recommended by the manual. The reader settings were taken over from FRET binding assays (see section 3.5.2). Fluorescence intensities at 520 nm and 495 nm were recorded, and their ratio (A_{520}/A_{495}) was plotted against the corresponding rapamycin concentration. Once again the IC_{50} values of the test series was determined using „Four-Parameter-Logistic-Curve“-Fitting in SigmaPlot.

3.5.4 – GST pulldown assay:

GST pulldown assays are widely used to detect protein-protein interactions *in vitro*. For this procedure a tagged protein can be captured on resin material, forming a complex that allows simple fishing of interacting proteins. To do that, the resin is incubated with putative protein binding partners and washed thoroughly to reduce unspecific binding. By SDS-PAGE analysis all proteins that are bound to the resin can be resolved and identified.

To determine FKBP binding to the FRB domain of mTOR, FRB was expressed as GST fusion and bound to glutathione sepharose resin. After addition of different FKBP proteins, successful formation of a ternary complex of FRB*rapamycin*FKBP was analyzed.

1 µM GST-FRB and FKBP (0.5 - 1.5 µM) were combined in 100 µl PBS with 1 µM rapamycin and incubated for 30 minutes at room temperature. 50 µl of glutathione resin were added, mixed well and pelleted by centrifugation for 5 minutes at 1000 g. The resin was washed three times with each 500 µl PBS. Then, it was treated with 20 µl 1x SDS sample buffer and incubated at 95°C for 5 minutes in order to denature and release proteins from the resin. To pellet the resin, the samples were centrifuged for 1 minute at 1000 g. Finally, the supernatant was subjected to SDS gel electrophoresis and analyzed by Coomassie Brilliant Blue staining.

3.6 – Cell culture:

3.6.1 – Cell lines and growth conditions:

HeLa, HEK293 and MEF cells were generally kept at 37°C and 5% CO_2 in a humidified incubator. Cell growth occurred as adherent culture in standard 125cm^2 cell culture bottles. For HeLa, HEK293 and MEF cells, standard DMEM was supplemented with 10% fetal calf serum and 1% penicillin/streptomycin solution.

3.6.2 – Maintenance of cells:

When cell density at the ground of the cell culture bottles was too high for further cell division, the cell culture was split.
During this procedure, DMEM medium was removed, and the cells were washed with approximately 10 ml of PBS under mild agitation. After the PBS was removed, 500 µl of trypsin/EDTA dilution was added and distributed evenly. Cells were incubated for 5 minutes at 37°C (or until all cells detached from the plastic surface), resuspended in 10 ml DMEM medium and singularized by pipetting up and down. To get rid of residual trypsin, the suspension was centrifuged for 5 minutes at 1000 g, and the cell pellet was resuspended in fresh DMEM/10% FCS. The cell suspension was then distributed into several bottles, culture dishes or 6-well plates. Finally, the original volume was re-established by filling up with DMEM/10% FCS.

3.6.3 – Cell transfection:

3.6.3.1 – Transfection with Lipofectamine 2000 reagent:

To introduce expression plasmids into eukaryotic cells, lipofection is widely used as a convenient method. During the transfection procedure, plasmid DNA is packed into lipid vesicles which fuse with the phospholipid bilayer of cells and thus deliver the DNA into the interior. The transfection reagent Lipofectamine 2000 consists of polycationic lipids. Compared to other lipid-based transfection methods, very high transfection yields can be achieved.

Transfections were performed as recommended by the manufacturer. In detail, the following components were used for transfection of a 10 cm cell culture dish with cells (80% confluency):

24 µg plasmid DNA (Midi-Prep)	in 1.5 ml DMEM medium
60 µl Lipofectamine 2000	in 1.5 ml DMEM medium

After 5 minutes of incubation at room temperature, the two components were combined and mixed thoroughly. During the following 20 minutes of incubation time, formation of DNA lipid vesicles occurred.
The cells were prepared for transfection by washing them with PBS and supplying them with 7 ml DMEM. 3 ml of the transfection mixture were added drop wise and carefully to the cells. The dishes were swayed mildly and incubated at 37°C and 5% CO_2 in the incubator. After 5 hours, 10 ml of DMEM with 20% FCS were added to improve cell growth. 40 hours later the cells were harvested or treated as indicated.

3.6.3.2 – Transfection using calcium phosphate $Ca_3(PO_4)_2$:

2xHBS buffer: 0.1 M Hepes, 0.56 M NaCl, 3 mM Na_2HPO_4, pH 7.0

Compared to commercial lipid-based reagents, this alternative transfection method is a bit less effective, but much cheaper. During the procedure, plasmid DNA is diluted in $CaCl_2$ solution and mixed with Hepes buffered saline (HBS) [272]. This triggers the formation of a fine precipitate of positively charged calcium ions and negatively charged phosphate ions which bind the DNA on its surface. This complex formation facilitates introduction of DNA into cells. The exact mechanism of the process is not yet fully understood. As the yield of successfully transfected cells is variable, this method is used mainly when high transfection efficiency is not necessary.
Cells were plated on 10 cm dishes to give 60-70% confluence on the day of transfection. 10 µg of DNA were diluted in 1.1 ml of sterile water, and 155 µl 2 M $CaCl_2$ were added. While this solution was gently mixed, 1250 µl of 2xHBS were added drop wise. Immediately after, the whole mixture was given directly and drop wise to the cells. After an incubation of 24 hours at 37°C and 5% CO_2 in an incubator, the medium was removed. The cells were washed with

PBS, supplied with DMEM/10% FCS and incubated for another 24 hours. Then cells were harvested or used in other assays.

3.6.3.3 – Transfection of siRNA:

For FKBP12 knockdown experiments, we transfected HeLa cells as recommended by the manufacturer. Shortly, 0.5 µl 2 µM siRNA were diluted in 9.5 µl DMEM, and 0.5 µl of DharmaFECT 2 were diluted in 9.5 µl DMEM. After 5 minutes, the solutions were combined and mixed. 20 minutes later, the mixture was added to HeLa cells in a 96-well containing 80 µl DMEM (final volume: 100 µl). After 48 h, cells were washed with PBS and lysed by addition of 50 µl 1x SDS sample buffer. Samples were boiled for 5 minutes and analyzed by SDS-PAGE /immunoblotting.

3.6.4 – Starvation and stimulation of cells:

In order to stimulate mTOR signaling and phosphorylation of downstream targets, transfected or untreated cells were starved: for this purpose, normal medium was removed, cells were washed once with PBS and fed with starvation medium (DMEM with 1% antibiotics). After at least 16 hours of serum starvation, amino acid starvation can be performed by replacing medium with PBS for 30 minutes. Afterwards, cells are kept in DMEM with 10% FCS and/or 100 nM insulin. Simultaneously, rapamycin was added to the wells (range: 0 – 100 nM) to inhibit S6Kinase phosphorylation to different extents. After one hour of incubation at 37°C and 5% CO_2, the cells were washed twice with PBS and harvested.
For stimulation of mTORC2 and subsequent Akt phosphorylation, addition of 100 nM insulin and incubation for 2 h is sufficient.

3.7 – Co-immunoprecipitation:

3.7.1 – Lysis of eukaryotic cells:

Lysis buffer: 40 mM Hepes, pH 7.5; 120 mM NaCl; 1 mM EDTA;
10 mM sodium pyrophosphate; 10 mM glycerol phosphate;
0.5 mM sodium orthovanadate; 50 mM NaF; 0.3% (w/v) CHAPS;
1% (v/v) protease inhibitor cocktail

To harvest transfected cells in a 10 cm dish, the dishes were put on ice and washed three times with ice-cold PBS. All liquid was drained as thoroughly as possible before 500 µl of lysis buffer were added. The cells were removed from the surface using a cell scraper, and the suspension was transferred to a pre-cooled reaction tube. This lysis mixture was then incubated for 20 minutes at 4°C with vigorous shaking (1200 rpm) before it was cleared by 20 minutes of centrifugation at 13 000 g and 4°C in a tabletop centrifuge. The supernatant was transferred to another tube and analyzed for total protein concentration by Bradford assay.

3.7.2 – Immunoprecipitation:

3.7.2.1 – IP with protein A resin and antibody:

Cell lysate, containing 500 µg total protein, was treated with 1 µg anti-mTOR antibody and incubated over night at 4°C with mild agitation. To prepare the resin, 20 µl of Protein A/G-coupled sepharose beads were mixed thoroughly and washed twice with PBS and finally added to the lysate. The mixture was incubated for 4 hours at 4°C under agitation, before the resin was pelleted at 13.000 g and 4°C for 30 seconds in a tabletop centrifuge. The supernatant was removed immediately, and a sample was analyzed as “flow through” on an SDS gel. The pelleted beads were washed four times with each 1 ml lysis buffer.
To elute bound protein, the resin was resuspended in 20 µl 2x SDS sample buffer and incubated for 5 minutes at 95°C. Finally, the suspension was centrifuged at 13 000 for 60 seconds to pellet the resin. 10 µl of the supernatant were subjected to SDS gel electrophoresis.

3.7.2.2 – IP with FLAG/HA/MYC affinity resin:

IP elution buffer:	150 µg/ml FLAG peptide in TBS 100 µg/ml HA or MYC peptide in TBS

Anti-FLAG/HA/MYC affinity resin contains the corresponding antibody covalently linked to the resin material. Like this, the material can simply be used to extract tagged proteins from lysates. As the binding does not depend on quality or quantity of a primary antibody, yields are optimized, and handling is much easier. The resin can be regenerated and re-used several times.

To prepare the material for use, the affinity resin was washed three times with TBS. An amount of 1.5 mg total protein in cell lysate were combined with 50 µl of 50% resin suspension on ice and incubated for 2 hours at 4°C under agitation. After 2 minutes of centrifugation at 10 000 g and 4°C, the supernatant was removed; a sample was kept and analyzed as flow through on the SDS gel. The pelleted resin was washed 5 times with each 1 ml lysis buffer.

For elution of bound proteins, the resin was resuspended in 30 µl FLAG/HA/MYC elution buffer and incubated for 10 minutes at 4°C under agitation. The mixture was shortly centrifuged to pellet the beads. The supernatant was supplemented with an equal volume of 2x SDS sample buffer and incubated at 95°C for 5 minutes. 15 µl of this mixture were separated on a SDS gel.

3.7.3 – Immunoblotting:

Blotting buffer:	20 mM Tris; 150 mM glycine; 0.02% (w/v) SDS; 20% (v/v) methanol
Ponceau S:	0.5% (w/v) Ponceau S; 3% (v/v) acetic acid
TBS-T:	TBS; 0.05% (v/v) Tween 20
5% milk powder:	TBS-T; 5% (w/v) skimmed milk powder
10% milk powder:	TBS-T; 10% (w/v) skimmed milk powder
Primary antibody:	2 µg antibody in 2 ml 5% milk powder (1:1000)
Secondary antibody:	1 µg antibody in 5 ml 10% milk powder (1:5000)
ECL1:	100 mM Tris/HCl, pH 8.5; 440 mg/l Luminol, 150 mg/l P-Coumaric acid
ECL2:	100 mM Tris/HCl, pH 8.5; 30% (v/v) H_2O_2

The immunoblotting procedure was performed according to recommendations of Invitrogen: After the SDS gel run was completed, the gel was put on a sheet of pre-soaked nitrocellulose membrane Protran BA 83 of the same size. A sheet of wet blotting paper was put on each side, and the pile was positioned with blotting sponges in the blotting chamber "XCell II Blot Module". The chamber was filled with blotting buffer before protein transfer was started by applying a current of 400 mA for 70 minutes.

Afterwards, the membrane was stained in Ponceau S solution for 2 minutes and then destained in water to an appropriate degree. Successful blotting was confirmed by complete transfer of all pre-stained molecular marker bands. Well positions were marked before the membrane was destained completely in distilled water.

To block unspecific antibody binding sites, the blot was incubated in 5% skimmed milk powder solution for 60 minutes at room temperature. After a short washing step with TBS-T, the membrane was kept over night at 4°C with mild agitation in a dilution of the primary antibody. Superfluous and unspecifically bound antibody was removed by washing three times for 5 minutes with large volumes of TBS-T. Next, the membrane was incubated in a dilution of the secondary antibody for 60 minutes at room temperature. Antibody probing was completed by further three washing steps (each 5 minutes, large volumes of TBS-T).

The luminescence reaction was started by combining 2 ml ECL1 and 2 ml ECL2, and adding the mixture immediately to the membrane. After 1 minute of incubation the blot was wrapped in cling foil, drained completely and put into an X-ray cassette. In the darkroom a sheet of medical X-ray film Super RX was put on the membrane under safelight conditions. The sheet was exposed to the blot for up to five minute in the closed cassette. The film was developed using a developer machine. Finally, the labels and markers were transferred to the film.

3.8 – Yeast complementation assay:

3.8.1 – Preparation of media:

YPD medium:	1% (w/v) yeast extract; 2% (w/v) peptone; 2% (w/v) glucose
SD medium:	0.5% (w/v) ammonium sulfate;
	0.17% (w/v) yeast nitrogen base; 2% (w/v) glucose
SG medium:	0.5% (w/v) ammonium sulfate; 0.17% (w/v) yeast nitrogen base;
	2% (w/v) galactose

SD minimum medium was supplemented with amino acids to allow growth of auxotrophy mutants. For yeast transformed with the vector pYX242 lysine, leucine and uracil were added, while the vector pYX233 demands histidine, lysine and uracil. The following table gives an overview over the used amounts:

Amino acid	Final concentration (mg/l)	Stock solution (per 100 ml ddH_2O)	ml stock solution per 1 l SD-Medium
Uracil	20	200 mg	10 ml
L-Tryptophan	20	1 g	2 ml
L-Histidine/HCl	20	1 g	2 ml
L-Lysine/HCl	50	1 g	5 ml
L-Leucine	60	1 g	6 ml

Table 3.2: Amino acid supplementation in yeast growth media

The amino acid stock solutions were autoclaved and stored at 4°C. The uracil solution was checked for precipitation before use and warmed in a water bath if necessary.

3.8.2 – Yeast cultures:

The yeast strains were plated on SD plates and incubated for several days at 30°C. As soon as enough cell material was available, the yeast cells were collected with a sterile inoculating loop and resuspended in 15% (v/v) glycerol. The glycerol stocks were stored at –80°C and served as backup.
Both strains were also grown as liquid cultures. For this purpose, a single colony was transferred from an agar plate to 50 ml SD medium in a sterile flask. After some days the cell density (OD_{600}) increased, and the cells were ready for further treatment.

3.8.3 – Yeast transformation:

To generate a preparatory culture, 20 ml YPD medium were inoculated with the desired yeast strain and incubated over night at 30°C and 200 rpm on an orbital shaker. 5 ml of this culture were added to 50 ml YPD medium and shaken at 30°C until an optical density of 0.6 was reached. The yeast cells were then pelleted for 5 minutes in a sterile 50 ml tube at 2000 g and

resuspended in 25 ml of sterile water. After repetition of the previous centrifugation step, the water was removed, and the cells were resuspended in 1 ml of 100 mM lithium acetate (LiAc). The mixture was centrifuged at maximum speed for 15 seconds to pellet the cells. After the supernatant was discarded, the pellets were resuspended in 400 µl 100 mM LiAc and aliquoted à 50 µl. Once again the cells were pelleted, and the supernatant was removed.
The transformation mix contained the following components which were added to the cells in the indicated order:

240 µl	50% (w/v) PEG
36 µl	1 M LiAc
25 µg	SS DNA (salmon sperm carrier DNA, denatured at 95°C for 5 minutes)
5 µg	plasmid DNA, diluted in 70 µl of sterile water

The samples were mixed thoroughly until the cell pellets were dissolved completely. Next, the cells were incubated for 30 minutes at 30°C on a rocking platform. A heat shock was applied by rising the temperature to 42°C for 20 minutes. The cells were then pelleted by 15 seconds of centrifugation at 7000 g before the supernatant was discarded, and the pellet was resuspended carefully in 30 µl of sterile water. The cell suspension was spread on agar plates with the appropriate selective medium and incubated for several days.

3.8.4 – Yeast colony PCR:

Yeast colony screen was done as described in section 3.1.6 for *E. coli* cells. Instead of bacteria colonies, a small amount of resuspended yeast colony was used as DNA template for PCR, together with appropriate vector-specific primers.

3.8.5 – Lysis of yeast cells:

Using a saturated starter culture, yeast cells were incubated in 50 ml of SD medium and grown at 30°C on a shaking platform until an OD_{600} of 1.0 was reached. The cells were harvested by centrifugation for 10 minutes at 2000 g and 4°C, resuspended in 1 ml 10 mM sodium azide and incubated on ice. By centrifugation of 1 minute at 14000 g, the cells were pelleted again. The supernatant was discarded, and the pellet was resuspended in 200 µl 1x SDS sample buffer. The mixture was incubated on a heating block at 96°C for 10 minutes,

before 200 µl of washed glass beads were added. To allow effective disruption of the yeast cells, the samples were vortexed vigorously for 2 minutes. Using a 21 gauge needle, a hole was poked into the bottom of the sample tubes, and the tubes were placed into fresh tubes. By centrifugation at 2000 g for 10 seconds, the liquid was expelled into the bottom tube. While the beads could be discarded, the liquid fraction was centrifuged at 14000 g for 2 minutes to pellet any insoluble material. A defined volume of the supernatant was loaded into SDS gels and subjected to SDS-PAGE and immunoblotting as described before.

3.8.6 – Complementation assay procedure:

Successfully transformed deletion mutants were distributed on glucose-containing SD plates and on galactose-containing SG plates, supplemented with 5 µM rapamycin. Hereby, the glucose plates served as control, while the galactose plates induced expression of FKBP and thus potentially influenced rapamycin susceptibility. The plates were each separated into eight segments (one clone per segment) and incubated at 30°C for several days. The colonies were documented photographically, and growth behavior of the yeast clones was directly compared.

3.8.7 – Yeast growth curves:

In order to evaluate growth of the individual yeast transformants more exactly, optical density of yeast suspension culture was recorded over 48 hours. To do that, the respective clone was inoculated in 150 µl SD medium (with an appropriate amino acid supplementation) on a transparent 96 well plate and incubated in a Tecan reader at 30°C. The initial OD was not higher than 0.1 in any of the wells.
By using an appropriate reader program, the absorption at 595 nm was determined every 180 minutes. After 15 measurements the upper plateau of the hyperbolic growth curve was reached in most cases, and the experiment was stopped.

Reader settings:	Absorbance, endpoint
	Wavelength: 595 nm
	Number of reads: 10; time between move & read: 1 ms

The growth curve was obtained by plotting the OD values against time (in minutes) in an Excel worksheet.

3.9 – *In vitro* kinase assay:

Procedure for immunoprecipitation of mTOR complex 1:

For mTORC1 preparation, HEK293 or HeLa cells were plated in 10 cm dishes and were transfected using $Ca_3(PO_4)_2$ with 30 µg of myc-Raptor plasmid. The following day, cells were starved by changing medium to simple DMEM without serum. After another 16-24 h, amino acid starvation was performed by incubating cells in TBS for 30 minutes. Finally, cells were stimulated by addition of DMEM with serum/insulin/amino acids for 60 minutes.
Cells were washed twice with TBS and lysed in 500 µl of CHAPS-containing lysis buffer (see section 3.7.1). Lysates were shaken for 30 minutes at 4°C, then centrifuged for 15 minutes at full speed and 4°C. While the pellets were discarded, 100 µl of "EZview Red Anti-c-Myc Affinity Gel" were added to the supernatant; then, the samples were rotated at 4°C for 2 h.
The beads were collected by centrifugation (8000 rpm, 1 minute), washed six times with each 1 ml of lysis buffer (without protease inhibitor mix). The immunoprecipitates were eluted by addition of 100 µl elution buffer (TBS with 100 µg/ml MYC peptide) and gentle shaking at 4°C for 10 minutes.

Procedure for immunoprecipitation of HA-S6K:

Lysis buffer: 40 mM Hepes, pH 7.5; 120 mM NaCl; 1 mM EDTA;
10 mM sodium pyrophosphate; 10 mM glycerol phosphate;
0.5 mM sodium orthovanadate; 50 mM NaF; 1% (v/v) Triton X-100
1% (v/v) protease inhibitor cocktail

HEK293 cells in 10 cm dishes were transfected using $Ca_3(PO4)_2$ with 30 µg of HA-S6Kinase plasmid. After 24 h, cells were starved with simple DMEM without serum. The following day, cells were incubated in TBS for 60 minutes. Addition of rapamycin (final concentration: 100 nM) ensures total dephosphorylation of S6Kinase.

Cells were washed twice with TBS and lysed in 500 µl of lysis buffer. After 30 minutes of shaking at 4°C, the lysates were centrifuged for 15 minutes at full speed and 4°C. 100 µl of monoclonal Anti-HA agarose were added to the supernatant before the samples were rotated at 4°C for 2 h.
The beads were spun down and washed excessively with each 1 ml of Triton buffer. Elution was performed by addition of 100 µl TBS with 200 µg/ml HA peptide and gentle shaking at 4°C for 10 minutes.

In vitro kinase assay:

Kinase buffer: 20 mM Tris/HCl, pH 7.4
10 mM MgCl2
0.2 mM ATP

Generally, the assay conditions are identical for the mTOR substrates 4E-BP1, S6Kinase and Akt kinase. Recombinant 4E-BP1 and pulled-down S6Kinase were combined with mTORC1 eluate.

In a total volume of 40 µl, the following components were mixed:

a. 8 µl 5x kinase buffer
b. 20 ng recombinant EGFP-4E-BP1
   or 5 µl HA-S6K IP eluate
c. 2-5 µl of mTORC1 IP eluate
d. bidest. H_2O ad 40 µl
e. 0.5 µl 4 µM rapamycin / torin1 (final concentration: 50 nM)
f. 1 µl 2 µM recombinant FKBP (final concentration: 50 nM)

The reaction was incubated at 37°C for 30 minutes and stopped by addition of 15 µl 4x SDS sample buffer and boiling for 5 minutes at 95°C.
The samples were resolved by SDS-PAGE on a 12% gel and analyzed by Western blotting using the appropriate anti-phospho antibody.

4 – Results:

4.1 – Recombinantly expressed FKBPs are functional:

4 .1.1 – FKBPs can be expressed successfully in *E. coli:*

For different *in vitro* activity and binding experiments, some members of the FKBP protein family were expressed in *E. coli* and purified using standard methods of affinity chromatography as previously described [60, 84, 273]. The integrity and purity of the His-tagged FKBP proteins were verified by performing gel runs on 16% SDS gels. Around 100 pmol of protein were loaded per lane to achieve satisfactory signal intensity.

Representative gel pictures are shown in figure 4.1.1A. It can be observed that the small FKBPs 12, 12.6 and 13 as well as the FK1 domains of FKBP51 and FKBP52 are relatively pure: the gel does not display any contaminating bands here. For the FKBPs of higher molecular weight (FKBP25, FKBP51, FKBP52), degradation bands and unspecific signals are more frequent, implying a higher degree of contamination. As the protein band of the correct size represents the main species in every case, it could be expected that the protein preparations exhibit reasonable activity in downstream assays. This was also further approved in active-site titrations (see section 4.1.2).

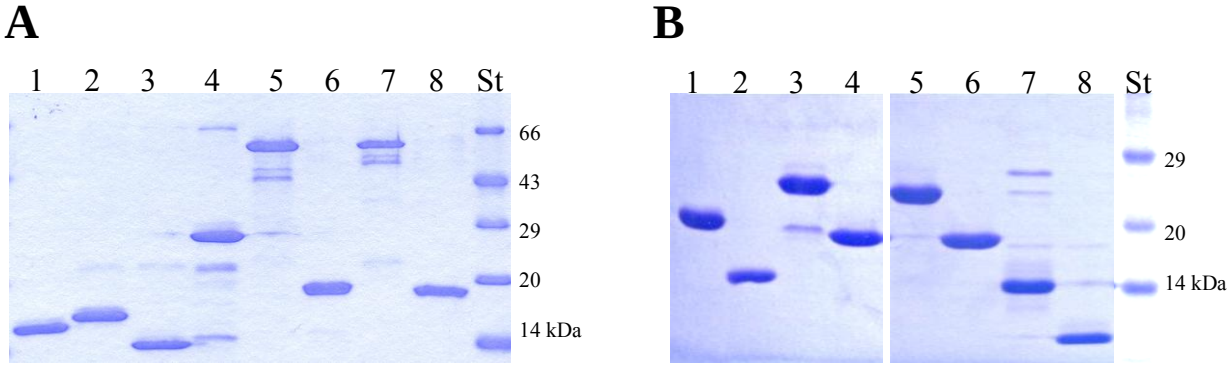

1: FKBP12
2: FKBP12.6
3: FKBP13
4: FKBP25
5: FKBP51
6: FKBP51 FK1
7: FKBP52
8: FKBP52 FK1

FKBP12 (1: with His-tag; 2: without His-tag)
FKBP51 FK1 (3: with His-tag; 4: without His-tag)
FKBP52 FK1 (5: with His-tag; 6: without His-tag)
FRB (7: with His-tag; 8: without His-tag)

Figure 4.1.1: Recombinantly expressed FKBPs are sufficiently pure

Representation of SDS protein gels stained with Coomassie Brilliant Blue.

(A) SDS gel of different FKBPs

(B) SDS gel demonstrating TEV cleavage of His-tags

For protein crystallization, FKBPs were treated with TEV protease to cleave off His-tags. The progress of this procedure was checked, too. The resulting gel picture shows the proteins before and after TEV treatment (see figure 4.1.1B). Notably, the excessive extraction procedure after cleavage increases purity of the proteins significantly.

For FRET binding assays, EGFP fusions proteins of several FKBPs were generated and expressed. Again, SDS gel analysis was performed in order to control their quality. As figure 4.1.2 reveals, the protein preparations contain contaminations: for the full-length FKBP51 and 52 fusion proteins (lane 7 and 8), at least one second species is present. The fusion proteins of the smaller FKBPs appear to be of higher purity. But as many of the protein assays to be performed allow big variations of protein concentration, the concentration of main product can be considered as sufficient for usage in downstream assays.

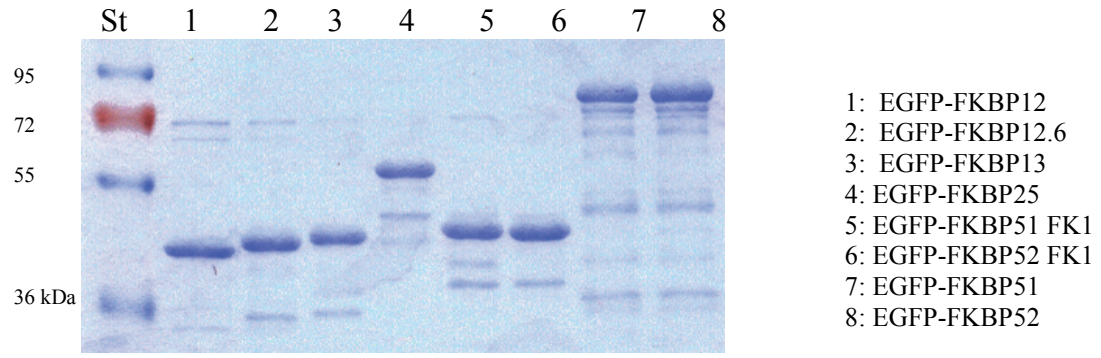

Figure 4.1.2: Recombinantly expressed EGFP fusion proteins are larger and less pure
Representation of an SDS gel stained with Coomassie Brilliant Blue. 50 pmol of each protein was analyzed. St: standard protein ladder.

4.1.2 – Recombinant FKBPs display high ligand-binding activity:

As the purification procedure can affect integrity and activity of expressed proteins in a negative way, these parameters must be checked before further use. For this purpose, “active site titration” with the synthetic fluorescein-labeled FKBP ligands CK97 and CK182 (“tracers”) was performed [274]. This experiment enables us to verify whether the concentration of purified proteins (determined by UV measurement) really corresponds to the concentration of active protein.
During the experiment, the FKBP is titrated against a fixed concentration of labeled ligand. This results in a classical binding curve with characteristic s-shape in a half-logarithmic plot

(see figure 4.1.3A). When the experiment is repeated with tracer concentrations higher than the K_d, the transition point of the curve shifts towards the right side for these high-affinity tracers and therefore towards higher FKBP concentrations. For each curve, EC_{50} values were determined by curve-fitting, and these values were plotted against the actual tracer concentrations. A line can be fit into the individual data points, and the intersection with the y axis can be determined by linear regression. The resulting EC_{50} value in absence of tracer can theoretically be considered as a K_d-like constant (see figure 4.1.3.B; FKBP13 and FKBP25 in section 6.2 of appendix).

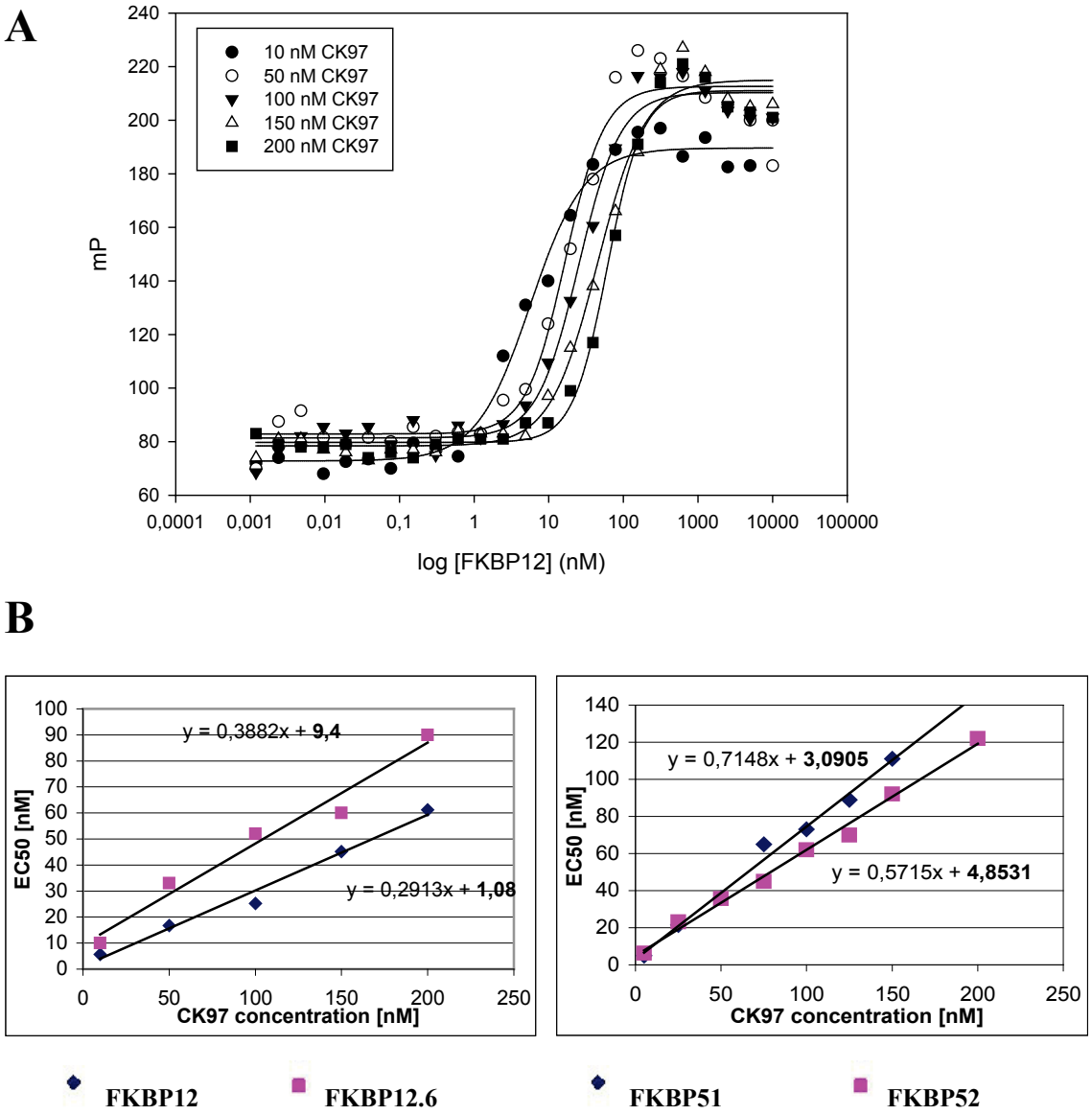

Figure 4.1.3: Tracers bind to FKBPs with high affinity

(A) Binding curves of titration of FKBP12 against 10-200 nM CK97; half-logarithmic plot

(B) Plot of calculated EC_{50} values against the actual tracer concentration; linear equation is shown, intersection with y-axis is printed in bold.

Altogether, the slope values of FKBP51 and FKBP52 are above the ideally expected value of 0.5. The other FKBPs display slope values below 0.5. Thus, the protein concentration determined by UV measurement must be corrected; the correction factor can be calculated by forming the quotient of 0.5 and the slope value. If the concentration value determined by UV measurement is multiplied with this factor, the corrected value can be obtained. This value is used to calculate protein amount that is utilized in all downstream protein assays.

The following table gives an overview of all determined values:

Protein	Slope	Correction factor	K_d	Protein concentration, UV-determined (µM)	Protein concentration, corrected (µM)
FKBP12	0.29	1.7	1.1	200	345
FKBP12.6	0.39	1.3	9.4	700	897
FKBP13	0.22	2.3	0.6	60	136
FKBP25	0.34	1.5	13	20	29
FK1 FKBP51	0.16	3.1	0.7	240	744
FKBP51	0.71	0.7	3.1	20	14
FK1 FKBP52	0.15	3.3	2.0	280	924
FKBP52	0.57	0.9	4.9	30	26

Table 4.1.1: Protein concentrations must be corrected corresponding to results of active-site-titration
Protein concentrations after UV determination and after correction for all tested FKBP proteins

4.1.3 – Competition assays reveal high-affinity binding of natural ligands:

After activity and actual protein concentration of purified FKBPs were verified, further fluorescence polarization assays with different ligands were performed. By titrating the proteins against a constant amount of fluorescent tracer (CK97, CK182), a binding curve was generated (see figure 4.1.4), and K_d values for the binding were calculated. The ideal tracer concentration for CK97 and CK182 was determined as 0.5 nM in previous experiments.

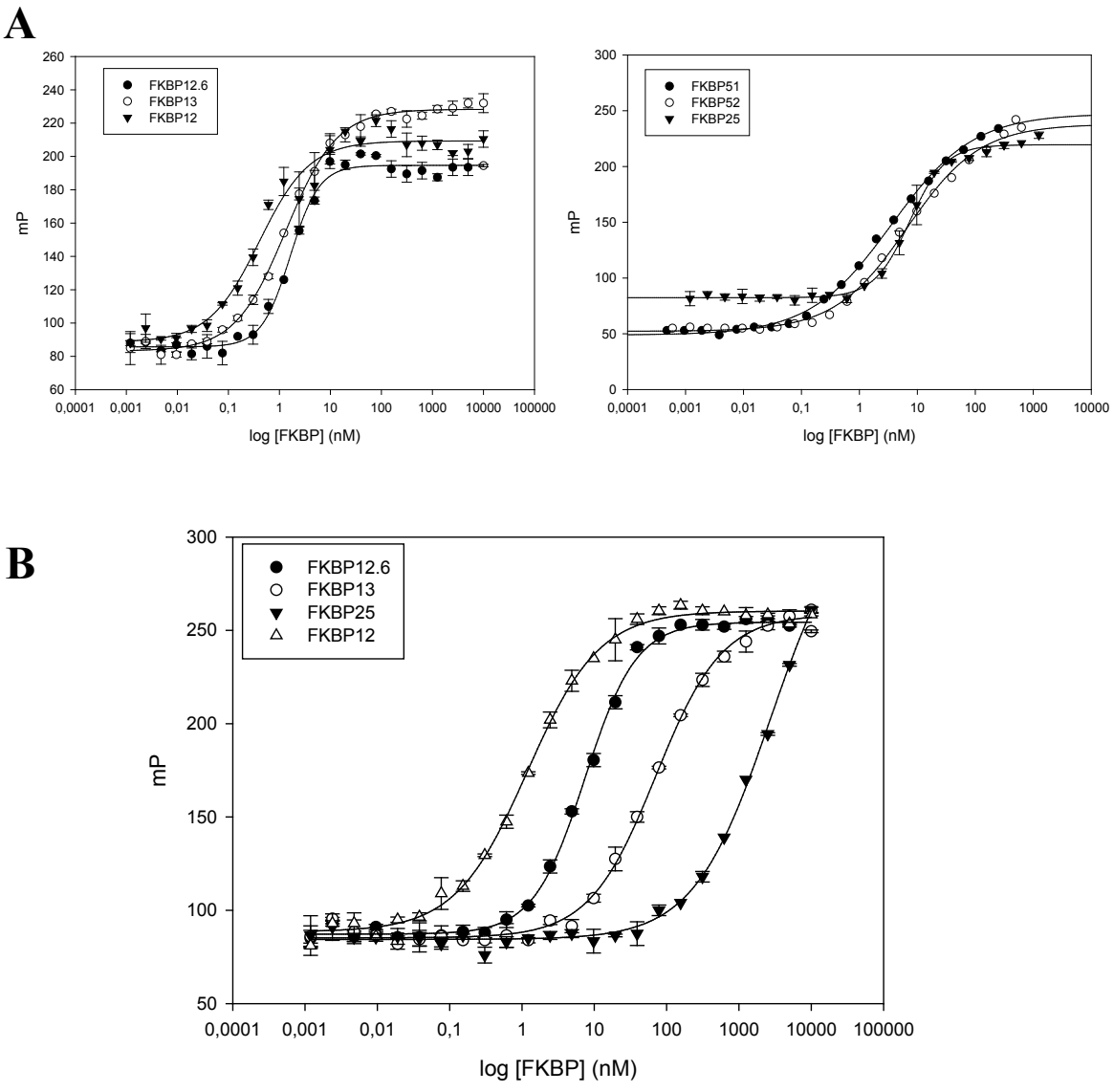

Figure 4.1.4: Fluorescein-labeled rapamycin and FK506 analogs bind to FKBPs with different affinities

Binding curves (half-logarithmic plot of protein concentration against fluorescence polarization anisotropy (mP)) for (A) 0.5 nM CK97 (B) 0.5 nM CK182

By fitting of the individual curves using "K_d fit" the dissociation constants of the binding were determined.

As expected, binding of the rapamycin derivative CK97 turned out to be highly affine for all tested FKBPs: K_d values cluster below 15 nM and even reach sub-nanomolar affinity for FKBP12 (see table 4.1.2). In contrast, the FK506/rapamycin analogue CK182 displayed low nanomolar binding only for FKBP12 and FKBP12.6; binding to FKBP13 was 10fold weaker, and the affinity to FKBP25 was in the μM range. This finding is in line with previous observations that showed a clear selectivity of FKBP25 for rapamycin compared to FK506.

Protein	K_d for binding to CK97 (nM)	K_d for binding to CK182 (nM)
FKBP12	0.2 ± 0.06	1.0 ± 0.09
FKBP12.6	1.3 ± 0.19	7.2 ± 0.49
FKBP13	2.9 ± 0.2	160 ± 9.2
FKBP25	13 ± 2	>2500
FKBP51	2.5 ± 0.4	n.d.
FKBP52	4.9 ± 0.6	n.d.

Table 4.1.2: Affinities of CK97 and CK182 are highly different for the tested FKBPs
Comparison of K_d values for CK97 and CK182 (in nM); medium deviation is indicated; n.d.: not determined.

In direct comparison to the K_d values determined by active-site titration (see table 4.1.1), K_d values for FKBP12, 13, 25, 51 and 52 are highly consistent. Only for FKBP12.6, a slight deviation could be detected (1.3 nM vs. 9.6 nM).

As the compounds CK97 and CK182 are modified by addition of a fluorescein moiety, their binding characteristics might differ from the ones of the natural products rapamycin and FK506: although fluorescein is not attached at sites involved in FKBP binding, it cannot be excluded that sterical hindrance alters accessibility of certain regions of the molecule.

To overcome this problem, competition assays were performed to evaluate K_i values for the unmodified ligands rapamycin, FK506 and CK85: during these experiments, protein and tracer concentrations are constant while a ligand (rapamycin, FK506 or CK85) is titrated to the mixture. With increasing ligand concentrations the tracer which is bound to the FKBP protein is replaced successively. The ligand concentration that displaces 50% of the tracer is referred to as "the IC_{50}" of the binding. The resulting binding curves are presented in figure 4.1.5. The detection limit of CK97 precluded a dilution of this tracer below its K_d. To account for this situation, the formula for curve fitting has been adjusted to conditions of FKBP concentration not being much smaller than K_d [274] (whole formula see appendix section 6.3).

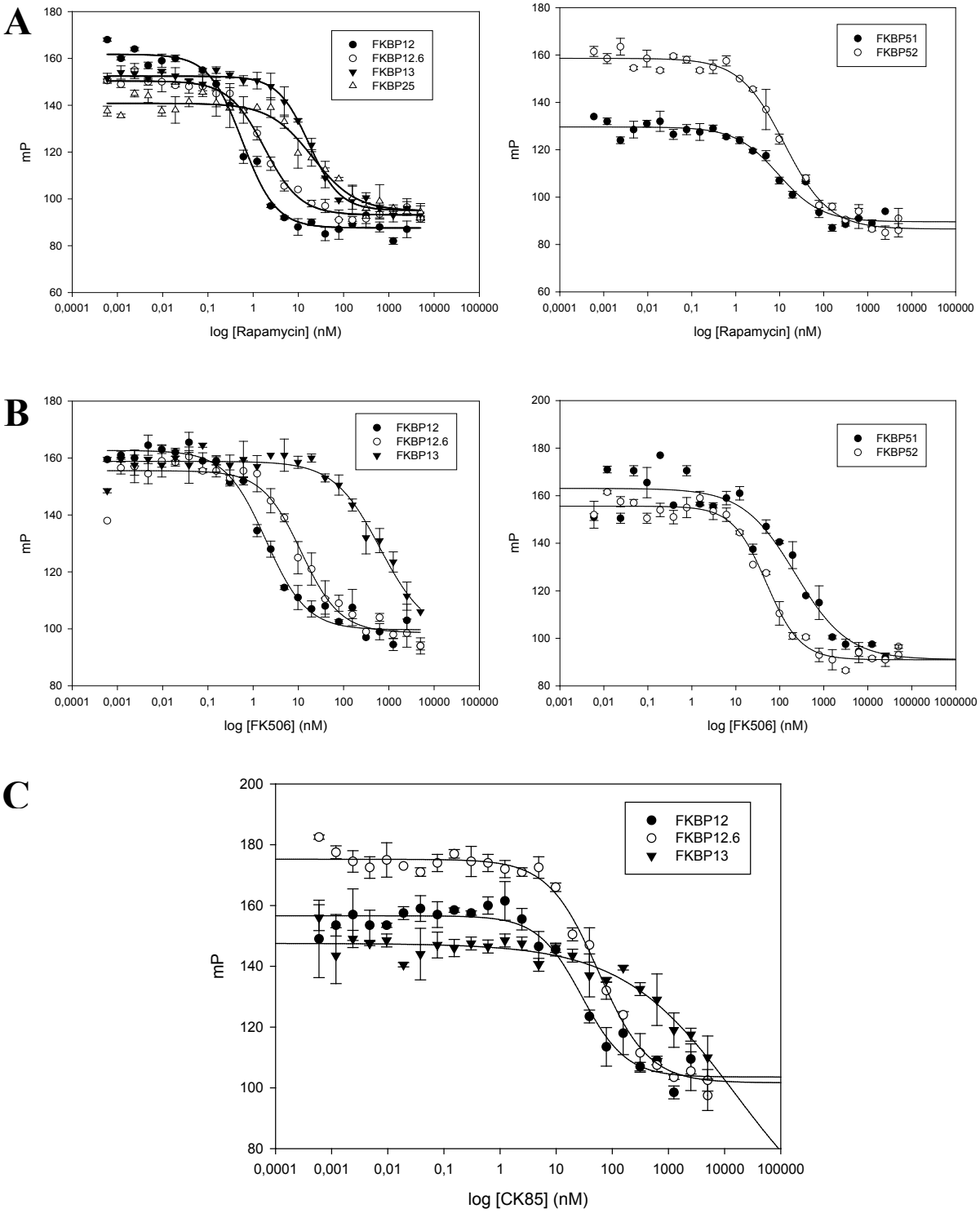

Figure 4.1.5: Competition assays reveal high affinity of natural ligands to FKBPs

Binding curves (half-logarithmic plot of ligand concentration against fluorescence polarization anisotropy (mP))

(A) 0.5 nM CK97 as tracer and rapamycin

(B) 0.5 nM CK97 as tracer and FK506

(C) 0.5 nM CK182 as tracer and CK85

By fitting of the individual curves by "K_d fit" (see appendix section 6.8 for exact formula) the dissociation constants of the binding were determined.

In table 4.1.3 the results of the series of experiments are shown: for FKBP12, affinity for both rapamycin and FK506 was highest, displaying values in the picomolar range. Similarly, FKBP12.6 was an excellent binder of both compounds. The larger FKBP12 homologues also show highly affine binding to rapamycin, ranging below 10 nM. For FK506, the values vary quite a lot: FKBP52 binds best with around 23 nM while the affinity of FKBP13 is 5fold less. FKBP25 could not be bound to FK506 at all. CK85, a simplified analogue of the FKBP binding moiety of rapamycin and FK506, bound to FKBP12 and FKBP12.6 with high affinity.

Protein	K_i Rapamycin (CK97) (nM)	K_i CK85 (CK182) (nM)	K_i FK506 (CK97) (nM)
FKBP12	0.6 ±0.17	12. 4 ±3.1	0.2 ±0.01
FKBP12.6	0.4 ±0.06	24.4 ±2.8	4.4 ±1.04
FKBP13	7.2 ±0.7	318 ±101	166 ±29.7
FKBP25	5.9 ±1.76	n.d.	n.d.
FKBP51	3.7 ± 0.9	n.d.	104 ± 14
FKBP52	4.2 ± 0.7	n.d.	23 ± 3

Table 4.1.3: Binding constants for unlabeled compounds rapamycin, CK85 and FK506
Comparison of K_d values for rapamycin, CK85 and FK506; in brackets: used tracer.
Median deviation is indicated; n.d.: not determined.

When the binding affinities of the labelled compound CK97 are compared to the natural product rapamycin (see tables 4.1.2 and 4.1.3), it turns out that the values are quite consistent: for FKBP12, the deviation is smallest (0.4 nM), while it is biggest for FKBP13 (4.3 nM) and FKBP25 (7.1 nM). FKBP51 and FKBP52 lie in-between with deviations of 1.2 nM and 0.7 nM. Altogether it can be stated that the fluorescein-modified compound reflects binding characteristics of the natural compound very well.

4.2 – Rapamycin induces binding of different FKBPs to FRB/mTOR *in vitro*:

4.2.1 – In GST pulldown assays, FRB/mTOR recruits FKBP*rapamycin complexes:

GST pulldown assays were performed in order to examine direct interaction of mTOR and FKBP51/52 under *in vitro* conditions; this has been demonstrated for FKBP12 before [275]. As full-length mTOR protein is quite large (around 290 kDa) and unstable in insolated form, it cannot be obtained easily. So we decided to perform the experiment with the FRB (FK506-rapamycin-binding domain) of mTOR which can be expressed as a GST-fusion protein with high yields [23]. As FKBP binding partners, we used recombinantly expressed FK1 domains of FKBP51 and FKBP52. The pulldown batches were separated by SDS PAGE and subjected to Coomassie staining.

On the gel image (see figure 4.2.1), pulldown eluates can be seen in lanes 2-6 and 8-12, while the load is present in lane 1. The latter represents the amount of protein that has been loaded onto the beads and thus can be eluted again. As there is less FRB protein detectable in the eluates than in the load, it can be concluded that there was loss of protein during the pulldown procedure, mainly caused by washing and insufficient elution. Importantly, the pulldown yields of FRB do not differ much and allow a comparison of the samples.

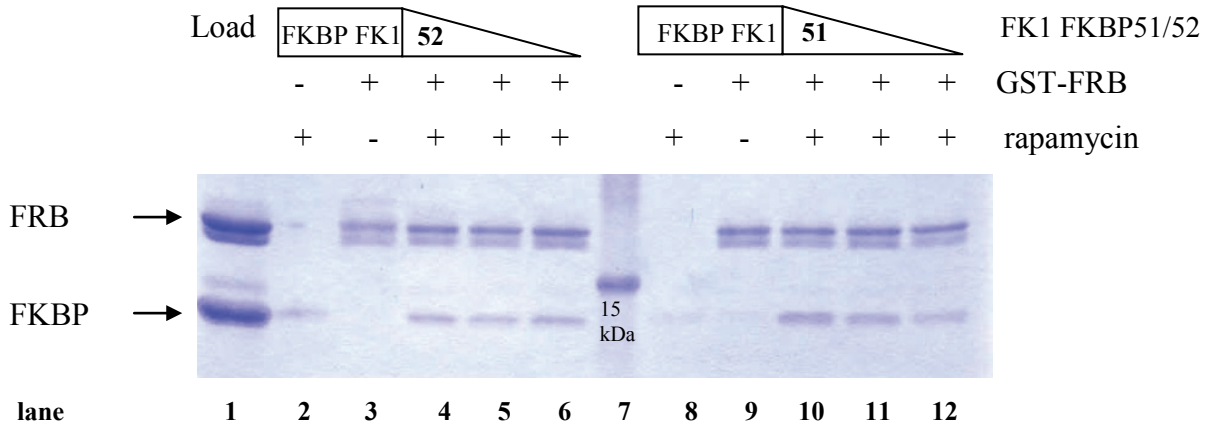

Figure 4.2.1: FK1 domains of FKBP51 and 52 bind to FRB in presence of rapamycin

For the GST pulldown assay, 0.5, 1.0 and 1.5 µM FK1 domains of FKBP51 and FKBP52 were incubated with 1 µM GST-FRB on GST beads in absence and presence of 1 µM rapamycin. After washing with TBS, the GST resin was boiled in 1x SDS sample buffer, and the supernatant was subjected to SDS-PAGE.

Lane 7: protein size marker (band of 15 kDa)

Lane 1: loading control: 1 µM GST-FRB and 1.5 µM FKBP52 FK1

Lanes 2/ 8: control for unspecific binding to beads: 1.5 µM FK1 FKBP51 or FKBP52 in absence of GST-FRB

The gel picture shows clearly that generally both the FK1 domain of FKBP51 and FKBP52 are able to bind to FRB domain of mTOR (lanes 4-6 for FK1 FKBP52 and 10-12 for FK1 FKBP51). At least for FKBP51, this binding seems to occur in a dose-dependent manner as the pulldown signal becomes more intensive with increasing FKBP concentrations. For FKBP52 such a result cannot be detected: binding appears to be similar at all three FKBP concentrations.

In absence of rapamycin the binding is abolished almost completely indicating that the interaction of FKBP51/52 with FRB is specific and mediated by rapamycin. Furthermore the FKBPs do not display unspecific binding to the GST beads when FRB is not present (lanes 2 and 8).

As the isolated FK1 domains may behave differently compared to the full-length proteins, the pulldown experiment was also performed with recombinant full-length FKBP51 and FKBP52. Representative SDS gel images are shown in figure 4.2.2.

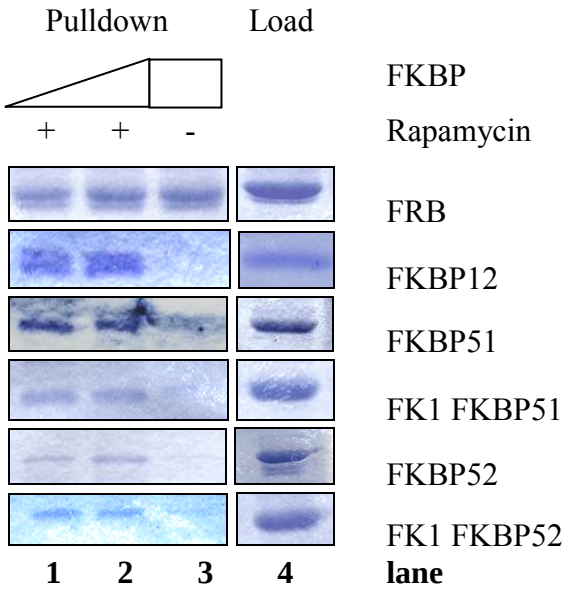

Figure 4.2.2: Full-length FKBPs interact with FRB in a rapamycin-dependent manner

SDS PAGE gel picture of GST pulldown assay; lanes 1-3: pulldown experiments; lane 4: loading control.
Lane 1: 1 µM FKBP and 1 µM GST-FRB; Lane 2: 2 µM FKBP and 1 µM GST-FRB;
Lane 3: 2 µM FKBP and 1 µM GST-FRB; Lane 4: 1 µM FKBP or 1 µM GST-FRB
FKBP12 load (lane 4) is taken from a second experiment performed under the same conditions.

First of all, it can be stated that all tested FKBP*rapamycin complexes bind to GST-FRB in GST pulldown experiments: in the rapamycin-dependent pulldown lanes (lanes 1-2) protein

bands can be detected for all five FKBPs. When compared to the load in lane 4, the concentration of FKBP protein in the pulldown lanes is considerably lower; a big amount of protein is lost during the pulldown procedure. Nevertheless, binding to GST-FRB in presence of rapamycin seems similarly strong for all FKBPs.
In the pulldown samples of lane 3, rapamycin has been omitted. Although there is a small amount of FKBP52 binding in the absence of rapamycin, it can be stated that signal intensity is much lower than in lanes 1 and 2 for all other FKBPs. Thus, binding of FKBP proteins to GST-FRB is indeed rapamycin-mediated.
Altogether, the signal strength in this simple assay is not sufficient to measure specificity and intensity of binding. A further, more exact characterization of protein interactions including. EC_{50} values can only be achieved with more advanced binding assays.

4.2.2 – *In vitro* FRET assay reveals high-affinity binding of FKBPs to FRB/mTOR:

A commercially available FRET-based assay was utilized to further investigate binding of FKBPs to the FRB domain of mTOR. For usage in this assay, FKBPs were expressed as EGFP fusion proteins, and FRB was modified by addition of a GST domain. The resulting FRET pair consists of EGFP and a Terbium-labelled anti-GST antibody. Rapamycin was added to induce binding of the two protein partners. In the assay mixture final concentrations of 5 nM GST-FRB and 100 nM EGFP-FKBP were used. Thereby the concentration of the FRB-fusion protein was in the range of the antibody (2.5 nM) while the FKBPs were added in huge excess. Thus it was ensured that the FKBP protein did not become the limiting factor during titration.
In order to obtain binding curves, a rapamycin titration was performed at constant protein concentrations. A half-logarithmic plot of the rapamycin concentration against the FRET ratios (Em_{520} / Em_{495}) produced dose-response curves (see figure 4.2.3A). The experiment was performed with EGFP fusions of 6 different FKBPs, and for all of them a rapamycin-dependent interaction with GST-FRB could be detected. The curves were analyzed in terms of EC_{50}, hill slope and plateaus. All obtained values are represented in table 4.2.3B.
Compared to the negative control EGFP (see appendix section 6.4), all EGFP-FKBP fusion proteins displayed highly affine binding to GST-FRB in the presence of rapamycin. EC_{50} values ranged from 4 – 26 nM. FKBP12, 13 and 25 had very similar affinities of around 5 nM which is in good agreement with a value of 12 nM for FKBP12 determined by

Banaszynski [276]. In contrast, the large FKBPs 51 and 52 showed a 5-fold lower binding strength. Interestingly, the isolated FK1 domain of FKBP51 displayed higher affinity to GST-FRB than the full-length protein. This was not the case for FK1 FKBP52.

A

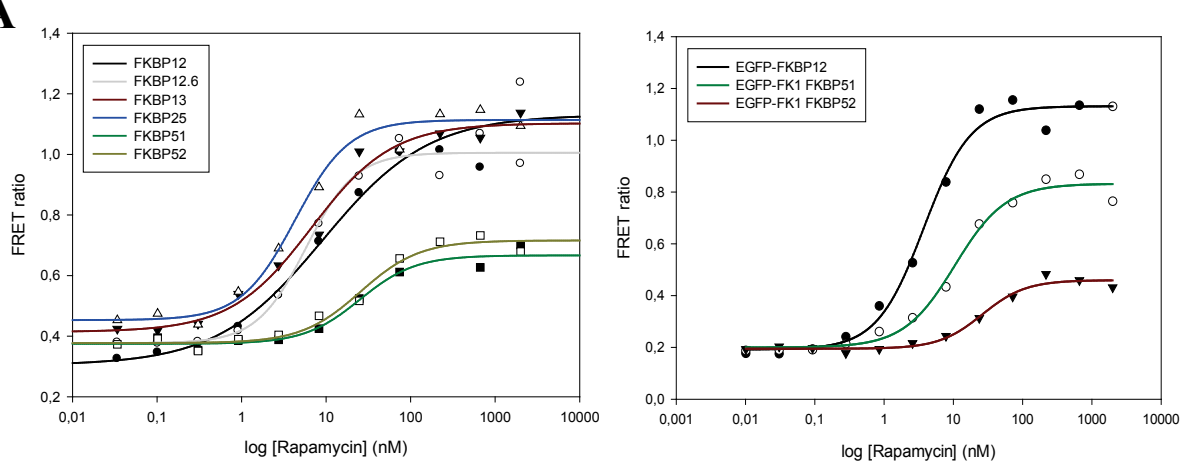

B

Protein	EC_{50} [nM]	Hill slope	Minimum	Maximum	Difference Max-Min
FKBP12	3.8 ± 0.6	- 1.3	0.2	1.1	0.9
FKBP12.6	5.6 ± 0.9	- 1.44	0.4	1.0	0.6
FKBP13	6.7 ± 1.6	- 0.9	0.4	1.1	0.7
FKBP25	4.3 ± 0.9	- 1.35	0.4	1.1	0.7
FKBP51	25 ± 6.7	- 1.3	0.4	0.7	0.3
FKBP52	25.5 ± 5.8	- 1.2	0.4	0.7	0.3
FK1 FKBP51	10.5 ± 1.8	-1.18	0.2	0.83	0.63
FK1 FKBP52	26.2 ± 5.6	-1.38	0.2	0.46	0.26

Figure 4.2.3: Six different FKBPs bind to FRB/mTOR with comparable affinity

(A) Half-logarithmic plot of the rapamycin concentration against the observed FRET ratio (Em 520 nm/ Em 495 nm). 5 nM GST-FRB, 100 nM EGFP-FKBPs and 2.5 nM of a Terbium-labelled anti-GST antibody were used. Rapamycin was titrated from 0 to 5 µM. Left panel: full-length FKBPs (●FKBP12; ○FKBP12.6; ▼FKBP13; ΔFKBP25; ■FKBP51; □FKBP52). Right panel: ● FKBP12 and FK1 domains of ○FKBP51 and ▼FKBP52.

(B) Table summarizing the constants obtained by analysis of the binding curves (FKBP12 curve from right panel).

This tendency can also be observed on the level of FRET efficiency: while FRET efficiency for FKBP12, 13 and 25 ranges over 0.7 units, the efficiency for FKBP51 and FKBP52 was only half as high. This might be explained by the size of the multi-domain proteins of around 80 kDa which might not allow formation of the ternary complex in the same way as for the small FKBPs. Maybe the distance between the FRET partners is increased which leads to a

less effective energy transfer. Possibly, sterical effects influence the orientation or hinder the binding of anti-GST antibodies in the complex, causing changes in the FRET ratio. Reduced purity of the EGFP-FKBP protein preparations (see SDS gel analysis in figure 4.1.2) might also contribute to this effect.

Next, different clinically used rapamycin analogues ("rapalogues") were tested for their binding affinities to different FKBPs. Again, formation of the ternary complex was assayed by measuring the FRET ratio between GST-FRB and EGFP-FKBP51/52 at different rapalogue concentrations. The resulting FRET binding curves are represented in figure 4.2.4.

A

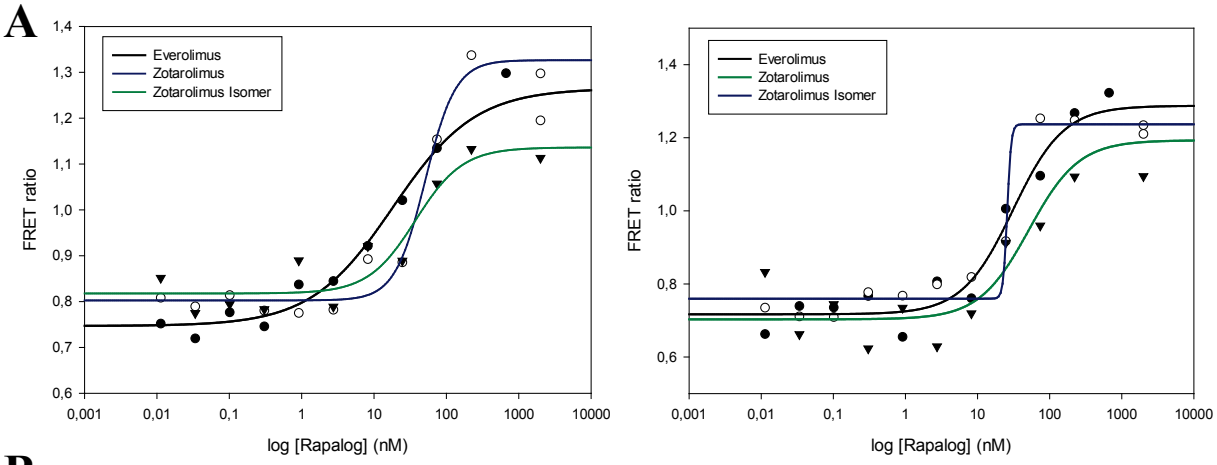

B

EC_{50} (nM)	Rapamycin	Zotarolimus	Everolimus	Zotarolimus Isomer
FKBP51	25	51	18	37
FKBP52	25.5	25	31	51

Figure 4.2.4: Rapalogues are able to induce interaction of FKBPs and FRB/mTOR

(A) Half-logarithmic plot of rapalogue-dependent FRET ratio of 10 nM GST-FRB and 50 nM EGFP-FKBP. Left panel: FKBP51; Right panel: FKBP52. ●Everolimus; ○Zotarolimus; ▲Zotarolimus isomer.

(B) Overview of EC_{50} values determined by FRET binding assays (values for rapamycin taken from figure 4.2.3B)

In summary, all three tested rapamycin derivatives induce formation of ternary complexes of FKBP51/52 and FRB successfully. Everolimus appears to even increase recruitment of FRB to FKBP51, while zotarolimus and its isomer reduce binding affinity. In the case of FKBP52, everolimus and zotarolimus are as good as rapamycin; only zotarolimus isomer displays

weaker complex induction capacity. Generally, we could not detect any significant preference of a rapalogue for FKBP51 over FKBP52.

4.2.3 – FK506 can compete for binding of rapamycin to the FKBP active site:

To demonstrate that the observed binding of FKBPs to FRB is really rapamycin-dependent, a competition with FK506 was performed. Hereby one can take advantage of the fact that rapamycin and FK506 compete for binding to FKBPs [277]. In doing so the affinity of both ligands is similarly high, ranking in the low nanomolar section [21].
A pre-incubation of FKBPs with an excess of FK506 (2 and 4 µM) was performed in order to saturate all binding sites. When FRB and rapamycin were added, the formation of the ternary complex was largely inhibited: not until very high rapamycin concentrations were reached, the equilibrium between rapamycin binding and FK506 dissociation shifted to free rapamycin, and the complex formation started (see figure 4.2.4). Thus, the observed shift of the binding curve to higher rapamycin concentrations can be considered as a reliable control for specificity and rapamycin-dependency of complex formation.

For FKBP12 the competition of ternary complex formation by FK506 was highly effective: the EC_{50} values shifted from 6 nM to >700 nM after pre-treatment with 2 µM FK506. EC_{50} values of more than 1 µM could be reached by doubling the FK506 concentration to 4 µM.
For FKBP51 an effect is clearly visible as well, although addition of FK506 did not cause a similarly big shift of the binding curve as in the case of FKBP12. Nevertheless, EC_{50} values of ~500 nM for 2 µM FK506 and ~800 nM in the presence of 4 µM FK506 suggest that a competition between the ligands for the same binding site takes place.
A similar effect could be observed for full-length FKBP52: the competition works reliably. When the EGFP-fusion of the FK1 domain was used instead of the full-length form of FKBP52, EC_{50} of binding was shifted from 26 nM to more than 1 µM. This indicates a strong inhibition of rapamycin-dependent binding to the FK1 domain by FK506; other domains are obviously not involved in these binding events.

Altogether, the competition experiments reveal that binding of FKBPs to the FRB domain of mTOR is indeed rapamycin-dependent, as affinity of the two protein partners can be lowered substantially by addition of an excess of FK506.

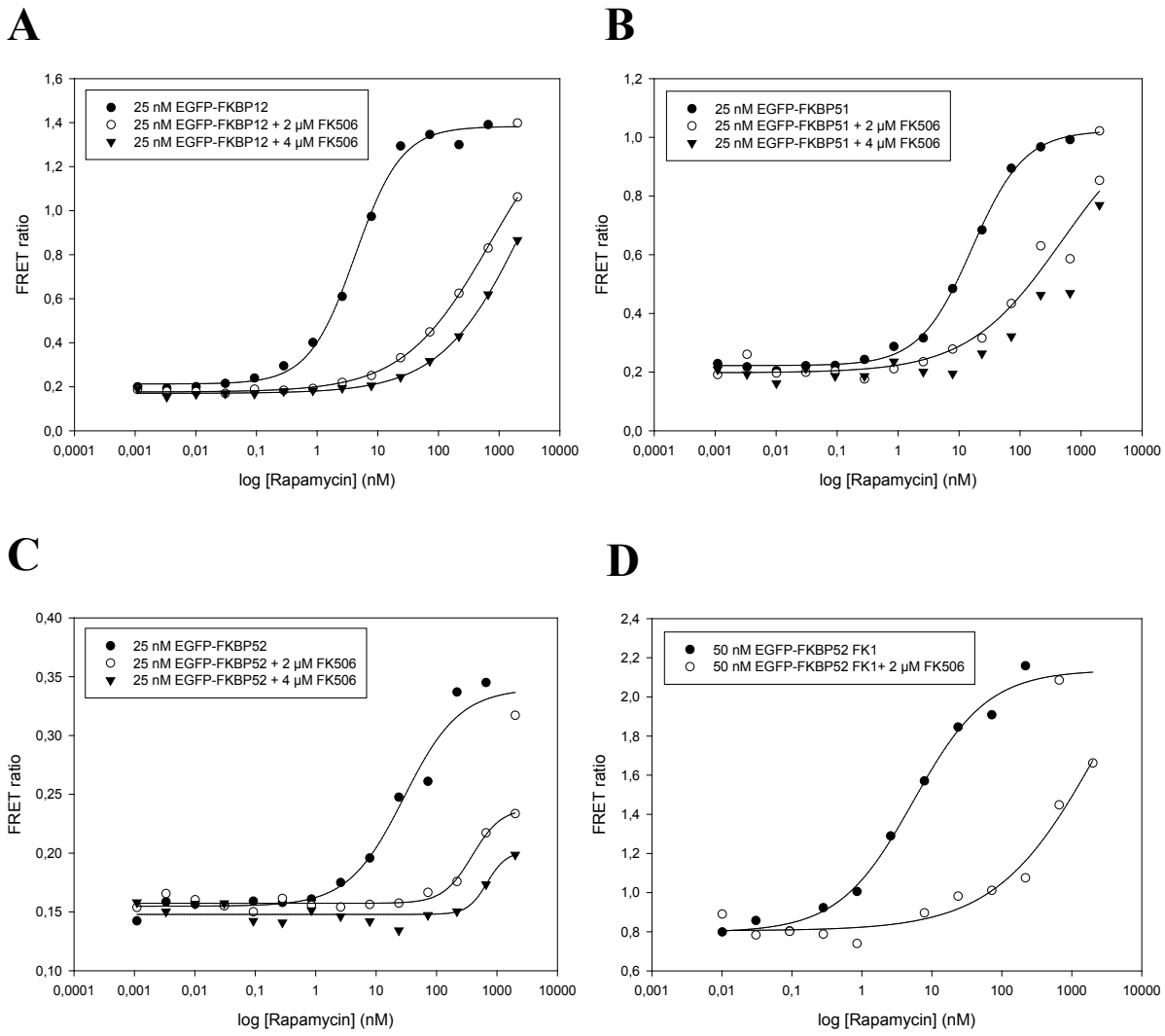

Figure 4.2.4: An excess of FK506 blocks formation of rapamycin-dependent ternary complexes

Half-logarithmic plot of the rapamycin concentration against the observed FRET ratio. The following binding partners were used in the respective FRET assay:

(A) 5 nM GST-FRB and 25 nM EGFP-FKBP12 (C) 5 nM GST-FRB and 25 nM EGFP-FKBP52

(B) 5 nM GST-FRB and 25 nM EGFP-FKBP51 (D) 5 nM GST-FRB and 50 nM FK1 FKBP52

FKBPs were pre-incubated with 0, 2 and 4 µM FK506 before the assay was started.

4.3 – mTOR activity can be inhibited *in vitro* by a variety of FKBPs:

4.3.1 – In a FRET activity assay, all FKBPs inhibit mTOR activity toward 4E-BP1:

In the previous experiments, we were able to demonstrate that formation of ternary complexes with rapamycin and FRB/mTOR *in vitro* is not restricted to FKBP12, but is successful with several tested FKBPs. Therefore, we then concentrated on the question whether these "alternative ternary complexes" exert inhibitory effects on the kinase mTOR, or whether this function is exclusive to FKBP12.

mTOR activity can be assessed easily by using a commercial *in vitro* FRET assay. The actual read-out is based on phosphorylation of the mTOR substrate 4E-BP1 which correlates directly to the activity of the heterologously expressed kinase (aa 1360-2549; N-terminally truncated product comprising FAT, FATC, FRB and PI3K-related kinase domain) [278]. As a positive control, the known mTOR inhibitors LY-294002 and PI-103 were titrated until kinase activity was totally abolished (see appendix section 6.5). Internally, we compared the inhibitory effects of different FKBPs with the one exerted by FKBP12 because its behavior is well known and characterized extensively.

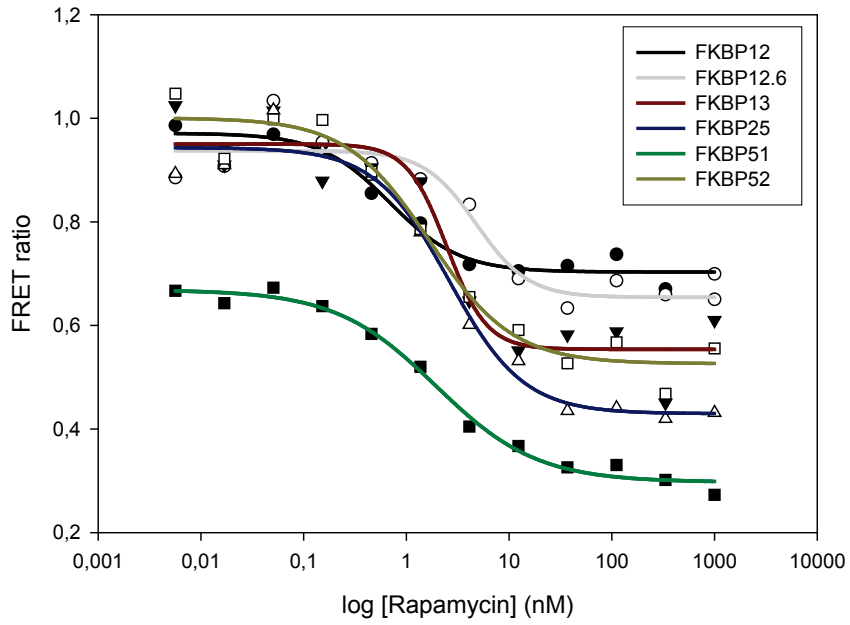

Figure 4.3.1: Six different FKBPs reduce mTOR activity with nanomolar IC_{50} values

Half-logarithmic plot of a rapamycin titration (0 – 1000 nM) against observed FRET ratio (Em 520 nm / Em 495 nm) in presence of 100 nM FKBP protein (●FKBP12; ○FKBP12.6; ▲FKBP13; ΔFKBP25; ■FKBP51; □FKBP52).

Figure 4.3.1 gives an overview of the inhibition curves of six different FKBPs. Their concentration was constant (100 nM) while rapamycin was titrated from 0 to 1 µM. For all tested FKBP proteins, a significant and rapamycin-dependent inhibition of mTOR activity could be observed.

The curves display maximum kinase activity at low rapamycin concentrations, resulting in a FRET ratio of around 1.0. When the concentration of the macrolide is increased, kinase activity is reduced; FRET ratio decreases accordingly and reaches a lower plateau of 0.3 – 0.5 at around 10 nM rapamycin. For the case of total mTOR kinase inhibition, FRET ratio could theoretically be close to zero. Such a total inhibition cannot be accomplished by rapamycin and FKBPs proteins.

Protein	IC_{50} (nM)	Minimum	Maximum	Difference Max-Min
FKBP12	**0.69** ± 0.17	0.7	1.0	0.3
FKBP12.6	**4.79** ± 1.76	0.65	0.94	0.29
FKBP13	**2.48** ± 0.82	0.55	0.95	0.4
FKBP25	**2.61** ± 0.57	0.43	0.94	0.51
FKBP51	**1.95** ± 0.36	0.3	0.67	0.37
FKBP52	**1.68** ± 0.51	0.53	1.0	0.47

Table 4.3.1: Overview of all parameters determined doing mTOR activity assays

The activity curves were characterized in terms of IC_{50} (see table 4.3.1). The data suggest that all examined FKBP proteins exert an inhibitory effect on mTOR kinase activity at nanomolar rapamycin concentrations. Furthermore, this inhibition seems to be highly effective; all IC_{50} values range below 5 nM.

FKBP12 inhibited mTOR activity in a rapamycin-dependent manner with an IC_{50} of 0.7 nM in our experiments. Reichling and colleagues determined a value of 4.3 nM under the same conditions [279]. Thus, it can be concluded that the assay works reliably, and that the minor deviation might be caused by different factors (e.g. serial rapamycin dilution).

FKBP51 exhibits a special behavior: the plateaus of maximum kinase activity and maximum inhibition are shifted downwards. Compared to the FKBPs with the largest margins of inhibition, the maximum mTOR activity in absence of rapamycin reaches a level that corresponds to 50% of activity for FKBP13 or FKBP25. Apparently FKBP51 inhibits mTOR

kinase activity directly and in a way that is independent of rapamycin. The macrolide intensifies the effect even further and allows most effective inhibition among all FKBPs. However, unspecific quenching of the FRET signal by FKBP51 cannot be excluded.

A direct comparison of the inhibition exerted by full-length FKBP51 and the FK1 domain reveals that the upper plateaus differ significantly, while IC_{50} values are similar (see figure 4.3.2). From these observations it could be concluded that only full-length FKBP51 displays an intrinsic rapamycin-independent inhibitory effect on mTOR. This effect therefore seems to be mediated by the FKBD2 and/or the TPR domain of FKBP51. This could be further checked by repeating this experiment with a truncated FKBP51$^{-FKBD2-TPR}$ construct. To control for read-out artefacts, FKBP51 could be added after the mTOR kinase assay under otherwise identical conditions.

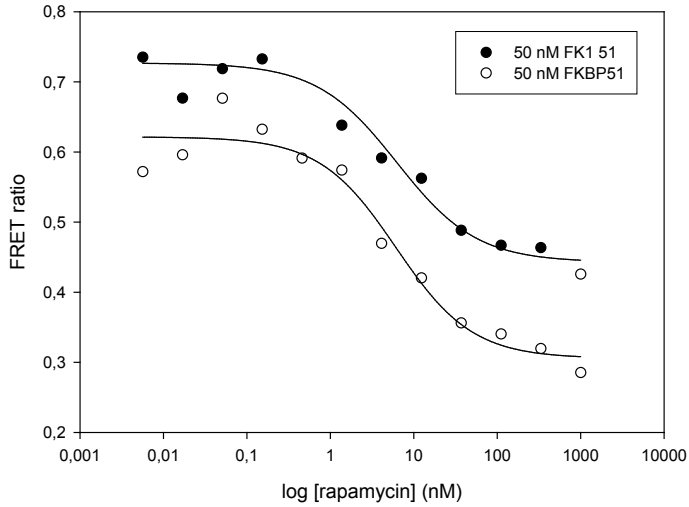

Figure 4.3.2: FK1 FKBP51 and full-length FKBP51 have different effects on mTOR kinase activity

mTOR inhibition was induced by 50 nM FK1 FKBP51 and 50 nM FKBP51. Rapamycin was titrated from 0 to 1 µM. A half-logarithmic plot of the rapamycin concentration against the respective FRET ratio (Em 520 nm / Em 495 nm) is shown.

4.3.2 – FKBPs reduce phosphorylation of mTOR targets 4E-BP1 and S6Kinase *in vitro:*

As the above described FRET-based mTOR *in vitro* activity assay uses isolated, truncated and recombinantly expressed mTOR protein and therefore does not allow a reliable characterization of mTOR complex components, we performed an *in vitro* kinase assay with intact mTORC1 [116, 179].

By expressing myc-tagged Raptor protein in HEK293 cells and by performing immunoprecipitation under conditions that preserve mTOR complex integrity, we isolated intact mTORC1 from living cells and used it directly in a kinase assay. As different FKBPs, rapamycin and other inhibitors could be added in a well-defined manner, we were able to assess mTOR activity under different conditions more precisely. As a general readout, we determined the phosphorylation status of both substrates 4E-BP1 and S6Kinase.

In order to assure general functionality and reliability of the assay, we examined 4E-BP1 and S6Kinase phosphorylation without FKBPs, in presence of rapamycin and in presence of both FKBP12 and rapamycin. In figure 4.3.3, the results of immunoblotting against phospho-proteins are presented: for both substrates, phosphorylation can only be detected in presence of mTORC1 (lanes 1/2 vs. 3) while there is very few background of unspecific 4E-BP1/S6Kinase detection. The ATP-competitive mTOR inhibitor torin1 [116] blocks phosphorylation very effectively (lane 5) while rapamycin has no effect in absence of FKBPs (lane 4). When FKBP12 is added, there is only a minor inhibitory effect on mTOR; together with rapamycin, kinase activity is blocked almost completely, resulting in largely reduced substrate phosphorylation. Altogether, the *in vitro* kinase assay seems suitable for detection of rapamycin-dependent FKBP effects on mTOR.

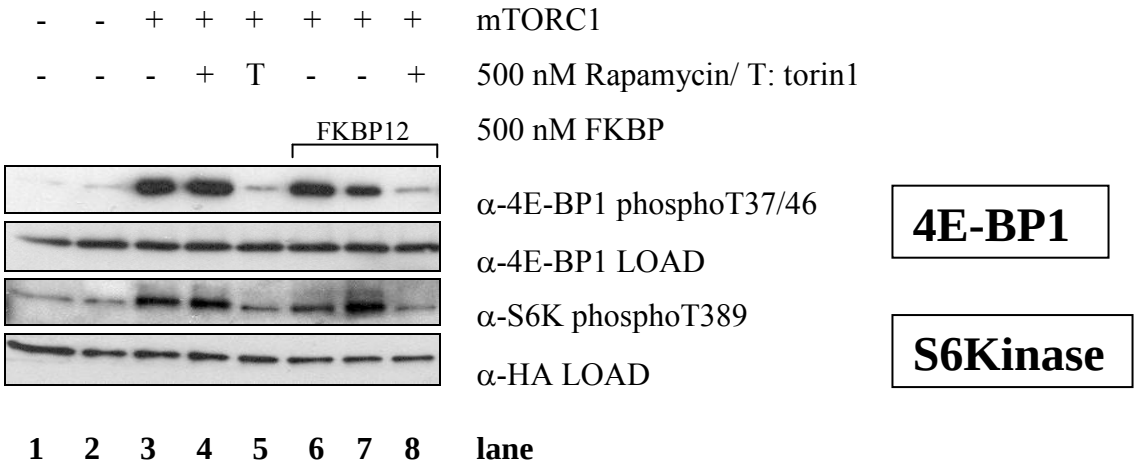

Figure 4.3.3: 4E-BP1 and S6Kinase phosphorylation can be inhibited by mTOR inhibitors and by FKBP12 in a rapamycin-dependent manner

In vitro kinase assay: 100 ng recombinant EGFP-4E-BP1 or 5 µl IP of HA-S6Kinase were incubated with mTORC1 IP, FKBP12 and rapamycin (as indicated) in ATP-containing kinase buffer for 30 minutes at 37°C. Reaction was stopped, and samples were resolved by SDS-PAGE and subjected to Western blotting.

We were mainly interested in comparing effects of FKBP12 to those exerted by FKBP51 and FKBP52, both in absence and in presence of rapamycin. FKBP13 and FKBP25 were neglected because their cellular localization [82, 88] argues against a regulatory function in the cytoplasm. Thus, we modified the above assay and added FKBP12, FKBP51 and FKBP52 at final concentrations of 500 nM in order to yield maximum inhibitory effects. Immunoblotting revealed phosphorylation patterns of 4E-BP1 and S6Kinase as presented in figure 4.3.4. As a control, total 4E-BP1/S6Kinase protein was assessed to assure uniform loading. Controls for unspecific effects exerted by rapamycin were included (see appendix section 6.5.2).

In presence of mTORC1, S6K and 4E-BP1 phosphorylation was established (lane 2) and could be blocked by torin1 more or less completely (lane 3). All samples containing FKBPs, but no rapamycin, displayed stable substrate phosphorylation compared to the controls (lanes 4, 5, 8, 9, 12, 13). Thus, no intrinsic inhibitory activity of FKBPs could be detected. When FKBPs were combined with the small molecule, phosphorylation of both 4E-BP1 and S6Kinase was greatly reduced (lanes 6, 7, 10, 11, 14, 15). The effects of all three FKBPs were comparable, and reduction of substrate phosphorylation was similar to the one achieved by torin1 (lane 3).

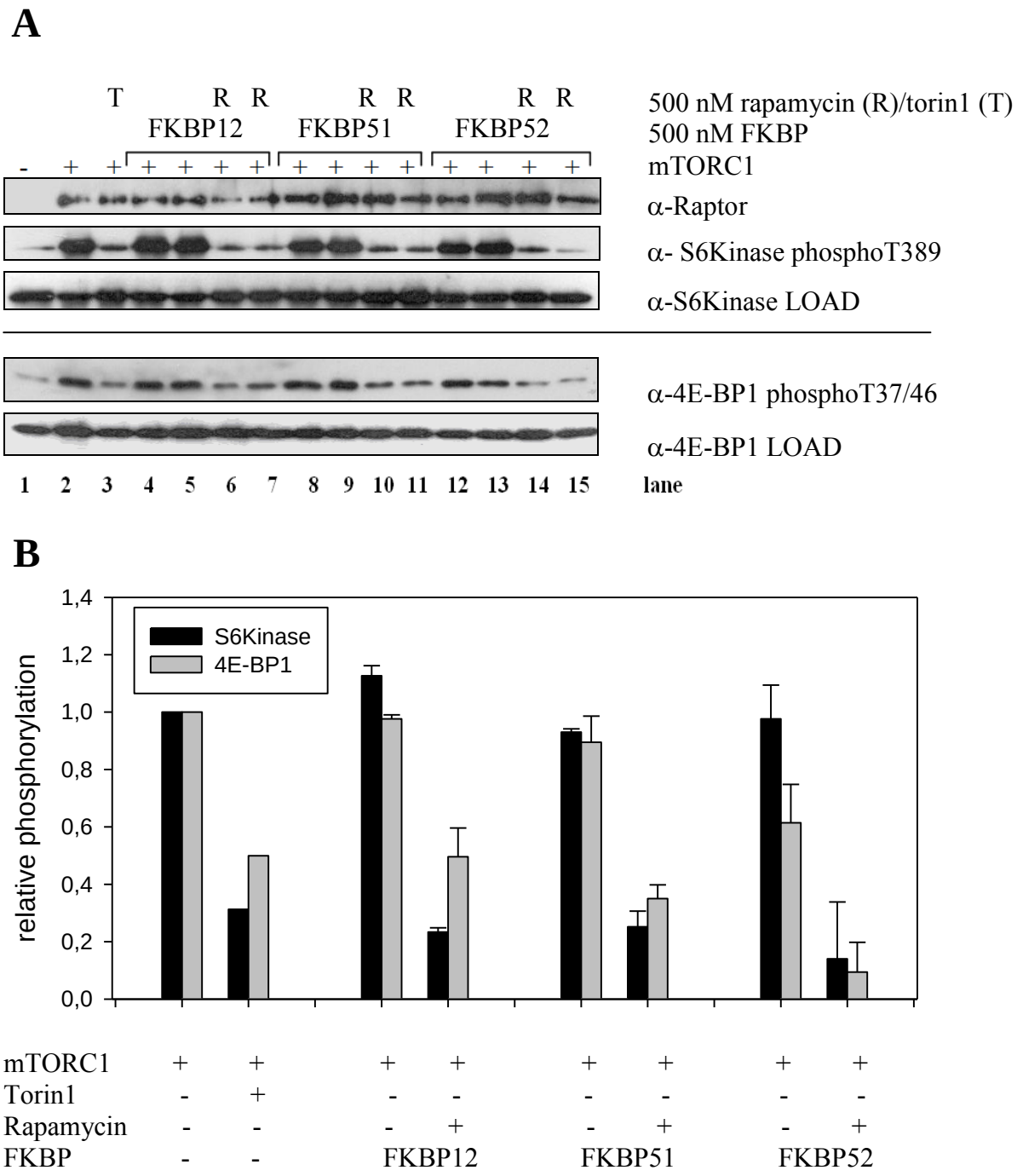

Figure 4.3.4: Inhibition of mTOR kinase activity is achieved by different FKBPs in *in vitro* kinase assays

In vitro kinase assay was performed with immunoprecipitated mTORC1 in presence of EGFP-4E-BP1 or HA-S6Kinase: IP eluate was combined with EGFP-4E-BP1/HA-S6Kinase, 500 nM of FKBP and 500 nM rapamycin in kinase buffer, incubated for 30 minutes at 37°C, boiled for 5 minutes and subjected to SDS-PAGE and immunoblotting analysis. 4E-BP1 phosphoT37/46 and S6Kinase phosphoT389 signal intensities were quantified and normalized to mTORC1-only treated sample (lane 2). As a control, 100 nM torin1 was used in the assay.

As full-length FKBP51 and FKBP52 seem to affect mTORC1 activity, we repeated the assay using FK1 domains instead. In figure 4.3.5, the resulting pattern of T37/46 phosphorylation is represented: just like in the previous experiment, FKBP12/51/52 exert an inhibitory effect on mTOR kinase activity, resulting in reduced 4E-BP1 phosphorylation. Again, this effect is clearly rapamycin-dependent. Interestingly, the FK1 domains of FKBP51 and FKBP52 cause a larger decrease of phosphorylation signal compared to the full-length proteins. This finding might indicate that for successful mTORC1 inhibition only the rapamycin-binding FK1 domain is necessary, while additional domains are rather counterproductive to this function (maybe by just increasing protein size).

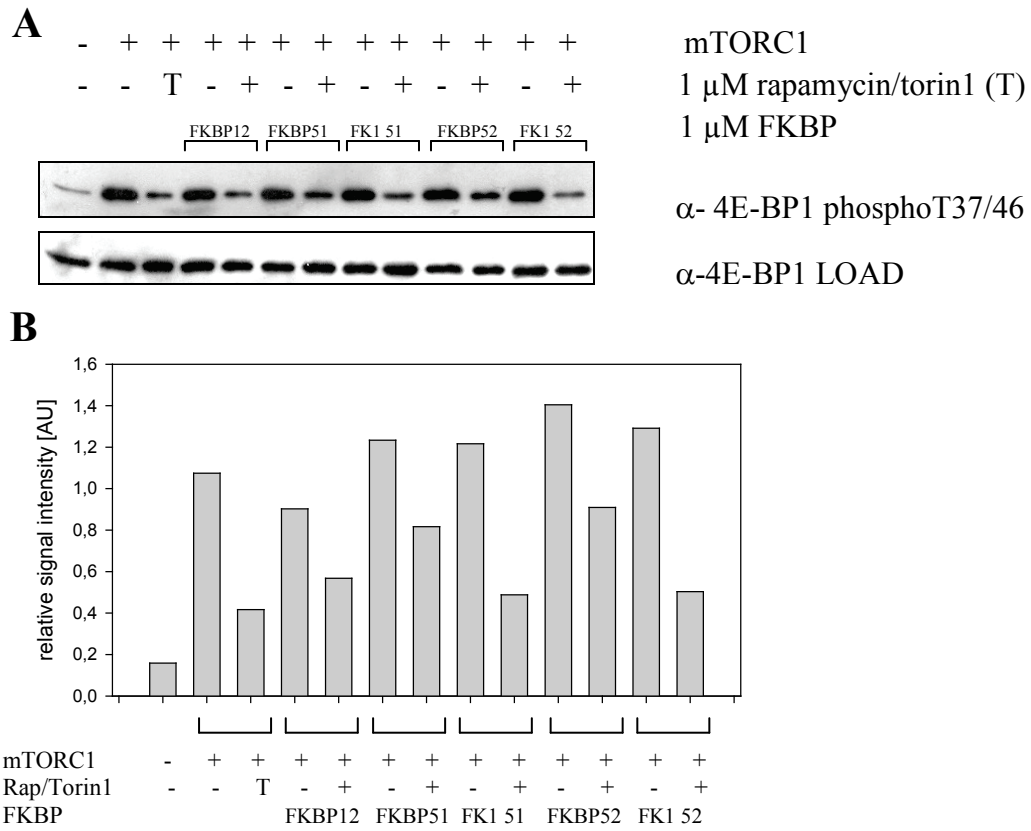

Figure 4.3.5: FK1 domains of FKBP51/52 are sufficient for mTORC1 inhibition

In vitro kinase assay was performed with immunoprecipitated mTORC1 in presence of 100 ng EGFP-4E-BP1. Anti-phosphoT37/46 signal intensity was quantified and normalized to load.

In summary, our *in vitro* kinase experiments revealed that intact mTOR complex 1 can be inhibited not only by FKBP12, but also by FKBP51 and FKBP52 in a rapamycin-dependent manner. Thereby, the FK1 domain of the large FKBPs is sufficient. As this effect is equal for all three FKBPs, and as it is highly rapamycin-dependent, it could be assumed that the underlying mechanism is the same in all cases.

4.4 – In yeast, FK1 FKBP51 can substitute FKBP12 in terms of mTOR inhibition:

4.4.1 – FK1 FKBP51 mimics effects of FKBP12 expression in FKBP-deficient yeast cells:

In order to create a eukaryotic model system for FKBP action on mTOR, we used the yeast strain Y12941. This strain lacks the FKBP12 homologue Fpr1, the only cytoplasmatic yeast FKBP. Therefore, this strain is insensitive to the anti-proliferative effect of rapamycin. In our experiment, we overexpressed human FKBP proteins in the yeast cells and determined their ability to compensate for the missing endogenous FKBP. It is well known that human and fungal FKBP12 rescue the system and thus restore the growth-inhibitory action of rapamycin [280, 281]. This finding served as a positive control to judge the effect of other FKBPs, but especially possible effects of FKBP51 and FKBP52. Galactose-induced FKBP expression was controlled by Western blotting of lysed yeast cells (see appendix section 6.9).

In figure 4.4.1, representative images of yeast cultures growing on SD agar plates are shown. The upper panel (A) displays yeast growth on SD medium without galactose which does not induce expression of human FKBPs. Since the deletion strain lacks endogenous FKBP, no binding partner was present that could mediate rapamycin action. Thus, no significant differences could be detected between the cultures growing on rapamycin-free plates or on rapamycin-containing plates.

The lower panel of images (figure 4.4.1B) represents yeast cultures that have been supplemented with galactose ("SG medium") and therefore expressed human FKBPs. In absence of rapamycin, no effect on yeast growth could be detected, just as expected. If the cells were grown on agar containing rapamycin, a clear reduction of growth could be observed for the cells expressing human FKBP12. This well-known effect could be reproduced successfully.

Interestingly, a similar effect is also present for FK1 FKBP51: the yeast cells that expressed the FK1 domain of human FKBP51 showed much slower growth on rapamycin-containing plates than control cells. This growth reduction was as strong as the one observed for FKBP12, and it was clearly rapamycin-dependent. Thus, FK1 FKBP51 can exert the same function as FKBP12 in this yeast complementation system. Altogether, growth effects could be observed for FKBP12 and FK1 FKBP51. These findings are presented and directly compared in figure 4.4.2, indicating that they are similarly effective.

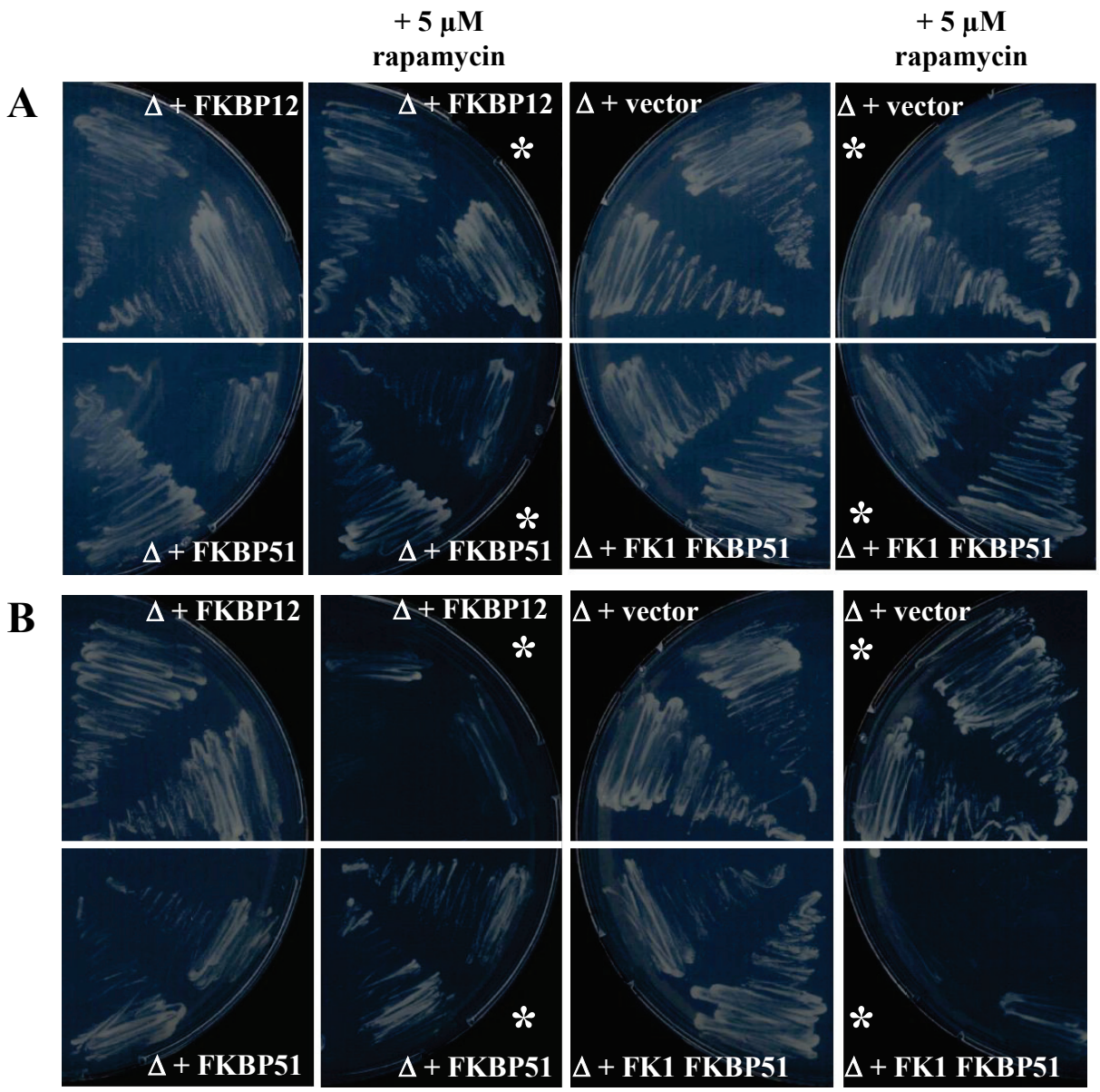

Figure 4.4.1: Human FKBPs have different effects on rapamycin-sensitivity of yeast cells

Yeast cells (FKBP deletion strain Y12941, short Δ) were transformed with the indicated expression vector (or empty vector as a control) and grown for 3 days at 30°C on glucose-containing SD medium or on galactose-containing SD medium (SG) to induce expression of FKBPs. 5 µM rapamycin were present on the plates marked by a star *. Each 2 individual clones are shown.

(A) Growth on SD medium (does not contain galactose; no induction of gene expression)

(B) Growth on SG medium (contains galactose: induction of FKBP expression)

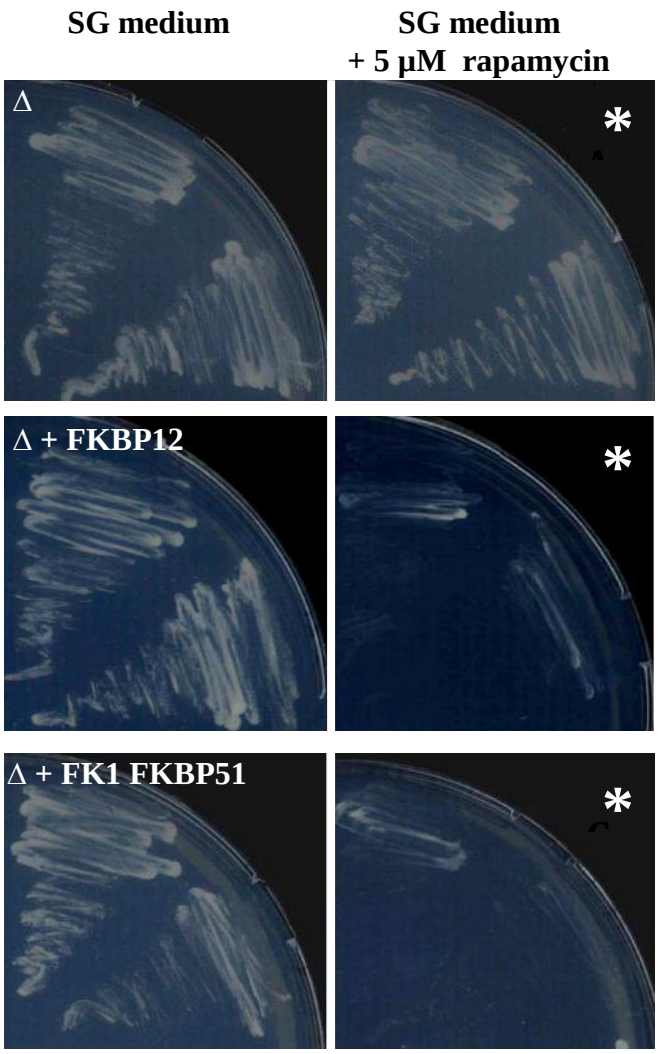

Figure 4.4.2: Yeast clones expressing human FK1 FKBP51 lose their rapamycin-resistance

Yeast cells (FKBP deletion strain Δ) were grown for 3 days at 30°C on galactose-containing SD medium. This medium induces expression of the respective FKBP gene on the transformed expression vector. Left panel shows yeast growth in absence of rapamycin, right panel shows growth in presence of 5 µM rapamycin (marked by a star *).

(A) Deletion mutants (2 individual clones)

(B) Deletion mutant with inducible FKBP12 expression

(C) Deletion mutant with inducible FK1 FKBP51 expression

For more intensive analysis, growth of the clones was also recorded as a function of time in order to obtain growth curves (see figure 4.4.3). This representation demonstrates more clearly that rapamycin resistance of the deletion mutant (red curves) can be abolished by overexpression of human FKBP12. As soon as the clone grew on rapamycin- and galactose-containing medium (SG) its growth was significantly reduced. In absence of rapamycin the

overexpression of the human protein caused only mild growth interference; this might be explained by mechanisms that directly influence the yeast cells' metabolism.

For FKBP12 and the FK1 domain of FKBP51 virtually identical growth curves were obtained. Thus, the FK1 domain of FKBP51 is able to function as a cellular receptor for rapamycin and induces cell cycle and growth arrest by inhibition of TOR complex in yeast. The expression of full-length FKBP51 in yeast deletion mutants leads to delayed growth; this effect is independent of rapamycin. Unfortunately it cannot be estimated whether the protein itself is toxic in yeast cells or whether it is a specific effect, mediated by mTOR.

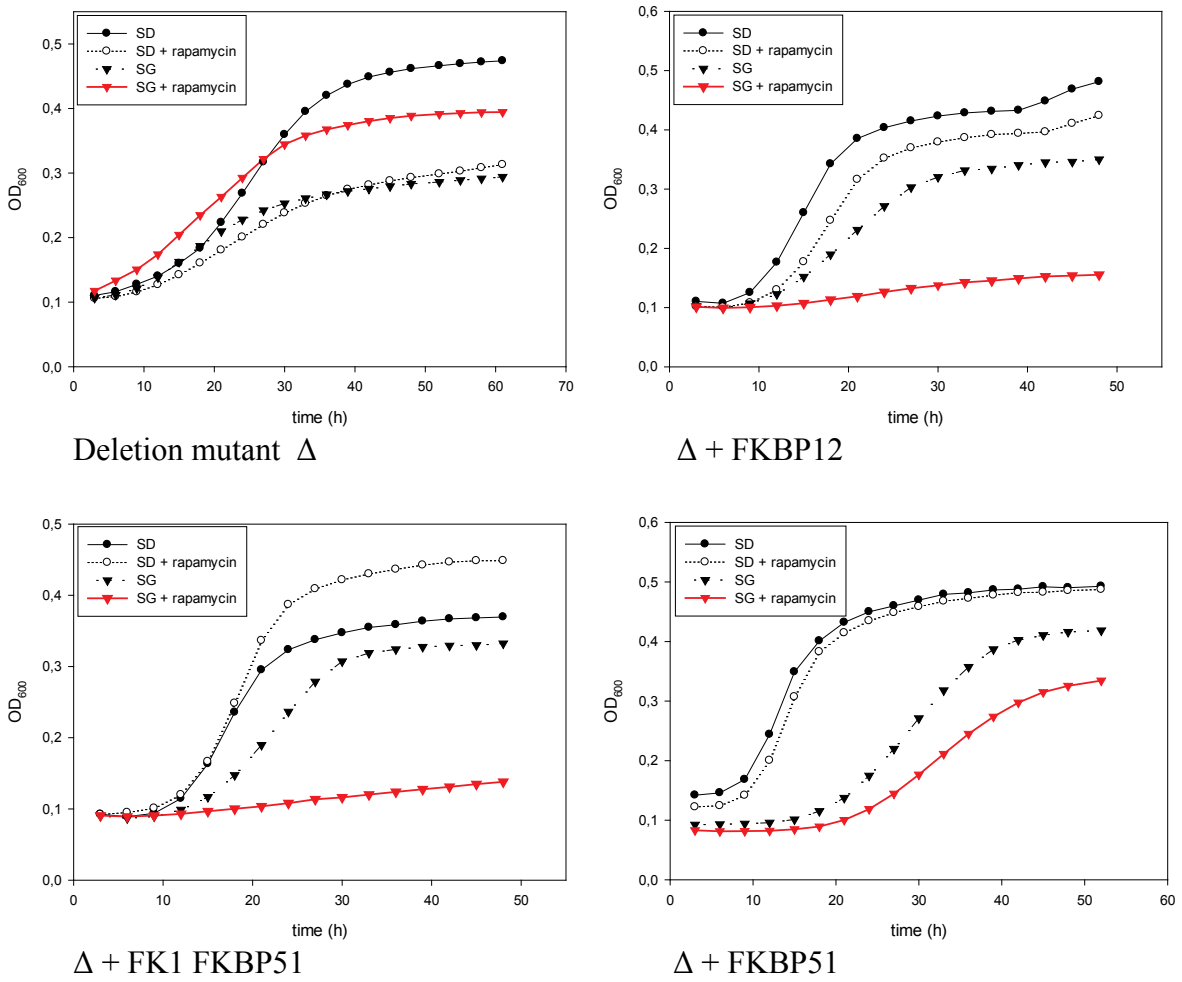

Figure 4.4.3: Yeast growth curves corroborate effect of FKBP12 and FK1 FKBP51

In glucose (SD) or galactose containing medium (SG), the indicated yeast clones were grown at 30°C in the presence or the absence of rapamycin (5 µM final concentration). OD_{600} was measured every 180 minutes and plotted against time.

In contrast to the FK1 domain of FKBP51, the highly homologous FK1 FKBP52 did not cause the same effects: when the protein was expressed in presence of rapamycin, no substantial change in growth rates compared to control conditions could be observed (see figure 4.4.4).

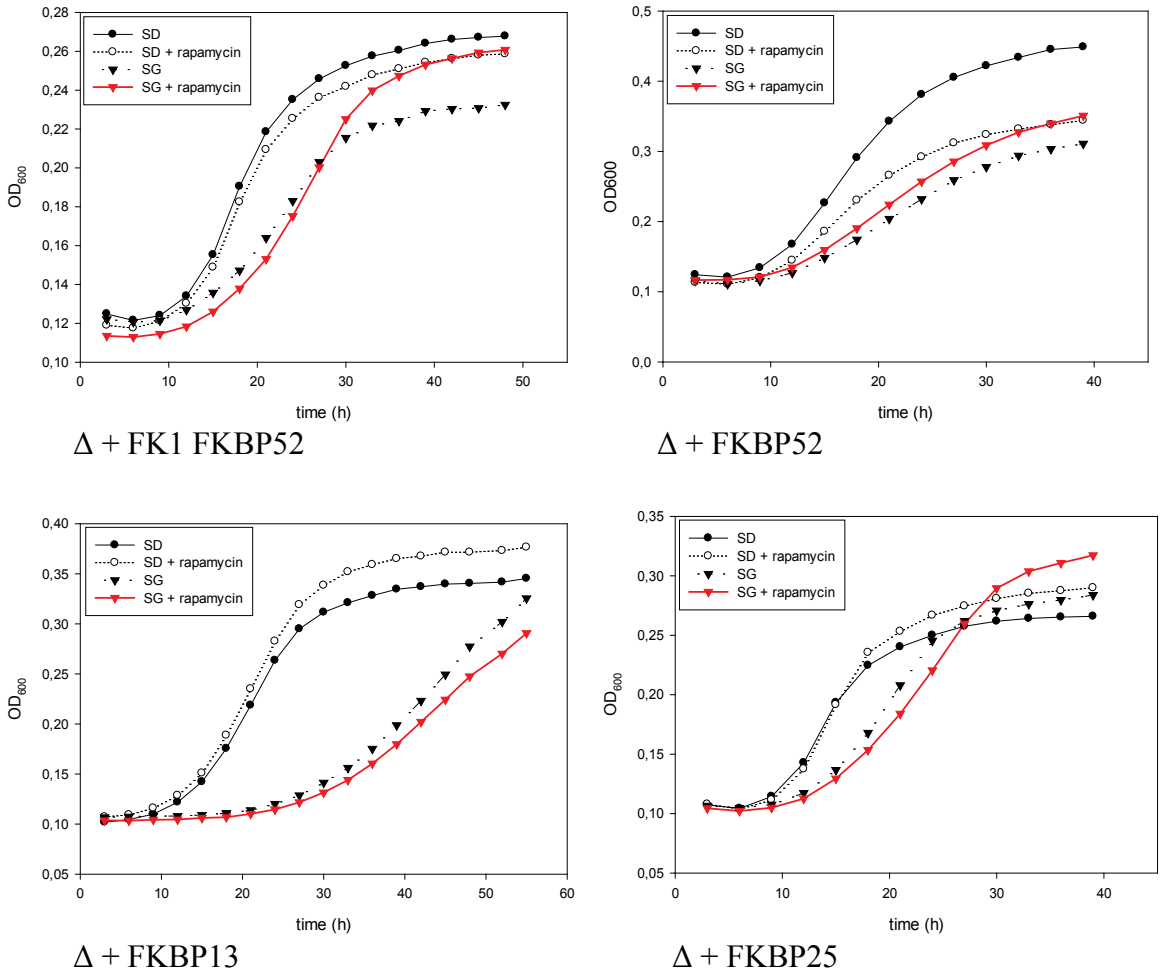

Figure 4.4.4: Not all FKBPs are able to complete the deletion system

The indicated yeast cultures were incbuated in glucose- or galactose-containing selective medium (with or without rapamycin) at 30°C. Optical density (OD_{600}) was measured every 180 minutes and was blotted as a function of time to generate growth curves.

The influence of human FKBP13 on deletion mutants is similar to the one of full-length FKBP51: cell growth slows down significantly when yeast express the protein. The presence of rapamycin does not have an additional effect. Thus, it could be assumed that FKBP13 acts as a cytotoxin that possibly masks any additional rapamycin-dependent effects. This result was obtained for full-length FKBP13 as well as for the truncated variant (lacking the N-terminal signal peptide; data not shown). Similarly, the overexpression of human FKBP25 had no effect on growth of the deletion mutants. Only a slight growth delay could be detected, but it cannot be considered as significant.
Also, it should be noted that technical reasons could account for the absence of rapamycin-induced effects in the experiments with FKBP52 or FKBP25. In particular, it is unclear whether these constructs were expressed functionally in sufficient amounts. For FKBP25, its nuclear location might explain the absence of any rapamycin-dependent effects.

Altogether, the results of the yeast complementation experiments demonstrate clearly that FKBP51 can substitute FKBP12 as the protein mediating rapamycin action *in vivo*. It can also be stated that the FK1 domain of FKBP51 is as effective in inducing rapamycin-dependent growth arrest in yeast cells as FKBP12.

4.5 – Crystal structures of three ternary complexes are highly similar:

4.5.1 – Ternary complexes can be purified and crystallized:

As the *in vitro* binding and the *in vivo* complementation assays both indicate a potential involvement of FKBP51 and FKBP52 in rapamycin-mediated mTOR regulation, we decided to compare the structures of these "alternative" ternary complexes with the original one containing FKBP12. Thus, the ternary complexes FRB*rapamycin*FK1 FKBP51 and FKBP52 were reconstituted *in vitro* using recombinantly expressed proteins and purified by gel filtration.

The UV elution profile of a column volume of 130 ml is shown in figure 4.5.1A: the main peak at 63 ml (1) can clearly be assigned to the ternary complex while the small shoulder at its side (2) consists of unbound FK1 and FRB domains. The degree of separation seems to be insufficient to divide these 12 kDa components from the 22 kDa complex. At around 130 ml, free rapamycin is eluted (3). This molecule has a weight of around 1 kDa and is retained by the column very efficiently.

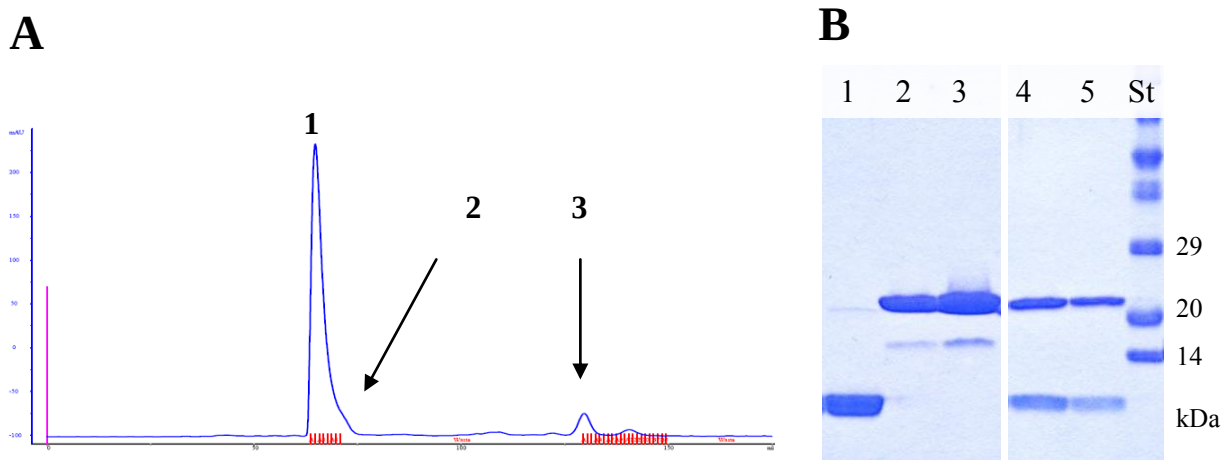

Figure 4.5.1: The ternary complexes were reconstituted and purified successfully

(A) Elution diagram represents a plot of the volume against the respective mAU absorption, recorded by the Äkta HPLC system. Important peaks are:

(1) Ternary complex FRB*rapamycin* FK1 FKBP51 (2) Unbound FK1 FKBP51 and FRB

(3) Unbound rapamycin

(B) Coomassie stained SDS gel; 100 pmol protein per lane were separated by gel electrophoresis:

(1) FRB (2) FK1 FKBP51 (3) FK1 FKBP52

(4) complex FRB*rapamycin* FK1 FKBP51 (5) complex FRB*rapamycin* FK1 FKBP52

(6) Protein size ladder

Integrity of both the single protein components and the ternary complexes was checked by SDS gel electrophoresis. The gel picture (see figure 4.5.1B) clearly shows two explicit bands in lanes 4 and 5 which correspond to the single ones in the lanes 1 and 2/3. This proves that the ternary complexes indeed form spontaneously after addition of rapamycin and that they are stable even during the process of purification.
Furthermore, the protein contaminations that can be seen in the lanes 2 and 3 disappear after gel filtration and cannot be detected in the final complexes. Thus, purity of the protein preparation, a major requirement for successful crystallization, is confirmed.

The structure of the complex FRB*rapamycin*FKBP12 has been solved at high resolution (2.2 Å; [111]). Unfortunately, the buffer conditions and the used precipitant can vary extremely even between highly homologous proteins. Thus, the following standard screens were performed using robotics at the department of structural cell biology (E. Conti, MPI of Biochemistry, Martinsried) in order to determine appropriate conditions for crystallization:

Protein Complex Suite
Protein Complex Suite 2
Index Screen

During this procedure, two conditions appeared especially suitable to promote crystal growth. These conditions were selected for further optimization:

FRB*rapamycin*FK1 FKBP51: 40% PPG-400; 0.1 M BisTris, pH 6.5;
20% PEG-3350; 0.1 M NaCl; 0.1 M Hepes-NaOH, pH 7.5
FRB*rapamycin*FK1 FKBP52: 1.9 M Ammonium sulfate; 0,1 M BisTris, pH 6.5;
18% PEG-4000; 0.1 M BisTris, pH 6.5

Ammonium sulfate and PEG/PPG concentrations were varied systematically until growth of large and well shaped crystals was successful. In figure 4.5.2A, images of the crystals are presented. They grew under the following final buffer conditions:

FRB*rapamycin*FK1 FKBP51: 25% PEG-3350; 0.1 M NaCl; 0.1 M Hepes-NaOH, pH 7.5
FRB*rapamycin*FK1 FKBP52: 1.95 M NH_4SO_4; 0.1 M BisTris, pH 6.5

Each one of the crystals was used for data collection at the synchrotron in Grenoble at beamline ID29, yielding well-resolved diffraction patterns which could be used to solve the crystal structures (see figure 4.5.2B).

A

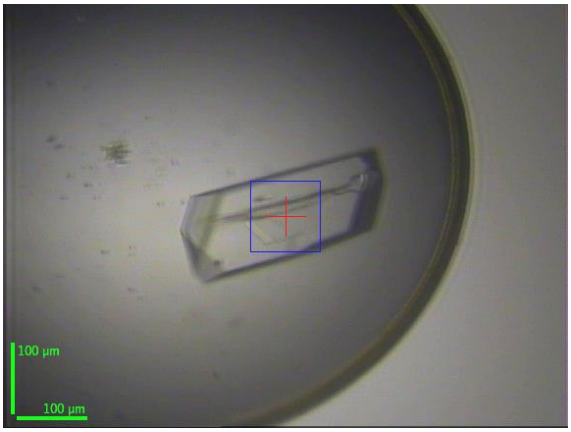

A262 B4
FRB*rapamycin*FK1 FKBP51

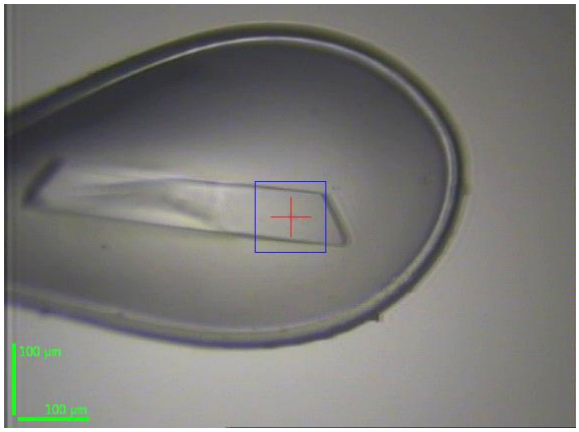

A263 B4
FRB*rapamycin*FK1 FKBP52

B

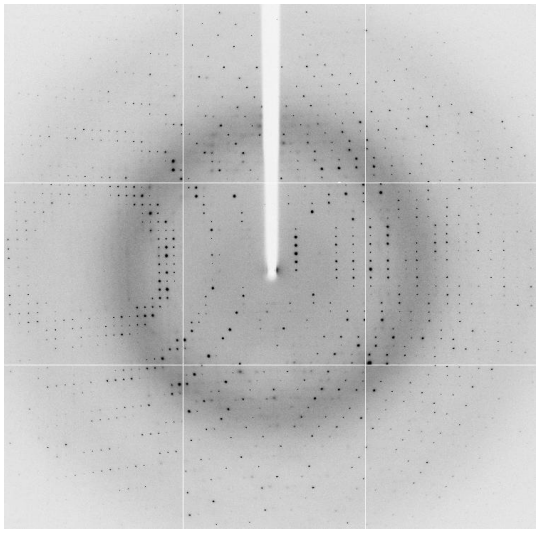

Figure 4.5.2: Protein crystals and X-ray diffraction pattern

(A) Microscopic image of the protein crystals used for x-ray crystallography
(B) Representative diffraction pattern recorded after X-ray exposure

4.5.2 – Crystals can be used for X-ray structure determination:

After computer-assisted analysis of the diffraction patterns, all key parameters of the final datasets were collected and are listed in table 4.5.1.

Parameter	FRB*rap*FK1 FKBP51 Crystal A262 B4	FRB*rap*FK1 FKBP52 Crystal A263 B4
Maximum resolution (Å)	1.45	1.8
Wavelength	0,9788	0,9788
Space group	$P2_12_12_1$	$P2_12_12_1$
Completeness	95.16%	98.6%
Cell dimensions (Å)	59.50 59.55 67.79	58.52 62.99 70.14
α, ß, gamma	90°, 90°, 90°	90°, 90°, 90°
Wilson B factor ($Å^2$)	21.767	32.313
Solvent content	44.6%	51.83%
Refinement (REFMAC)		
Resolution range (Å)	19.05 – 1.45	19.76 – 1.8
Reflections (test set)	39213	23105
Number of atoms	1995	1841
R_{free}	0.24054	0.24834
R	0.21173	0.22404
r.m.s.d. bonds (Å)	0.022	0.022
r.m.s.d. angles	2.001°	2.000°
Ramachandran Plot (determined by Procheck)		
Additionally allowed	5%	2.9%
Most favored region	94%	94.7%

Table 4.5.1: Crystal structures of the ternary complexes could be solved with resolutions of 1.45 and 1.8 Å
Characteristics of two crystals used for x-ray structure determination and results of computational analysis

There are two structures of the ternary complex of FRB*rapamycin*FKBP12 that have been solved at resolutions of 2.7 Å by Choi [23] and of 2.2 Å by Liang [111], using the rapamycin-derivative (C16)-ethoxy-rapamycin. Our datasets of the ternary complexes with FK1 51 and FK1 52 are substantially better and display resolutions of below 1.45 and 1.8 Å, respectively.

4.5.3 – Overall architecture of the ternary complexes is similar to the one of FKBP12:

4.5.3.1 – Structure of FKBPs does not differ significantly:

Generally, the overall structural arrangements in the ternary complexes FRB*rapamycin*FK1 FKBP51/52 are very similar to the complex containing FKBP12 (see figure 4.5.3): the ligand rapamycin can be found in the center of the complexes where it interacts via two defined areas with the FK1 domain on the one side, and with FRB on the other side. The FK1 domains of FKBP51 and FKBP52 are highly homologous to FKBP12 and display mainly ß-sheets as secondary structure element. Between one ß-sheet and a short α-helix, a hydrophobic pocket is located which represents the PPIase active site and the actual binding pocket of rapamycin.

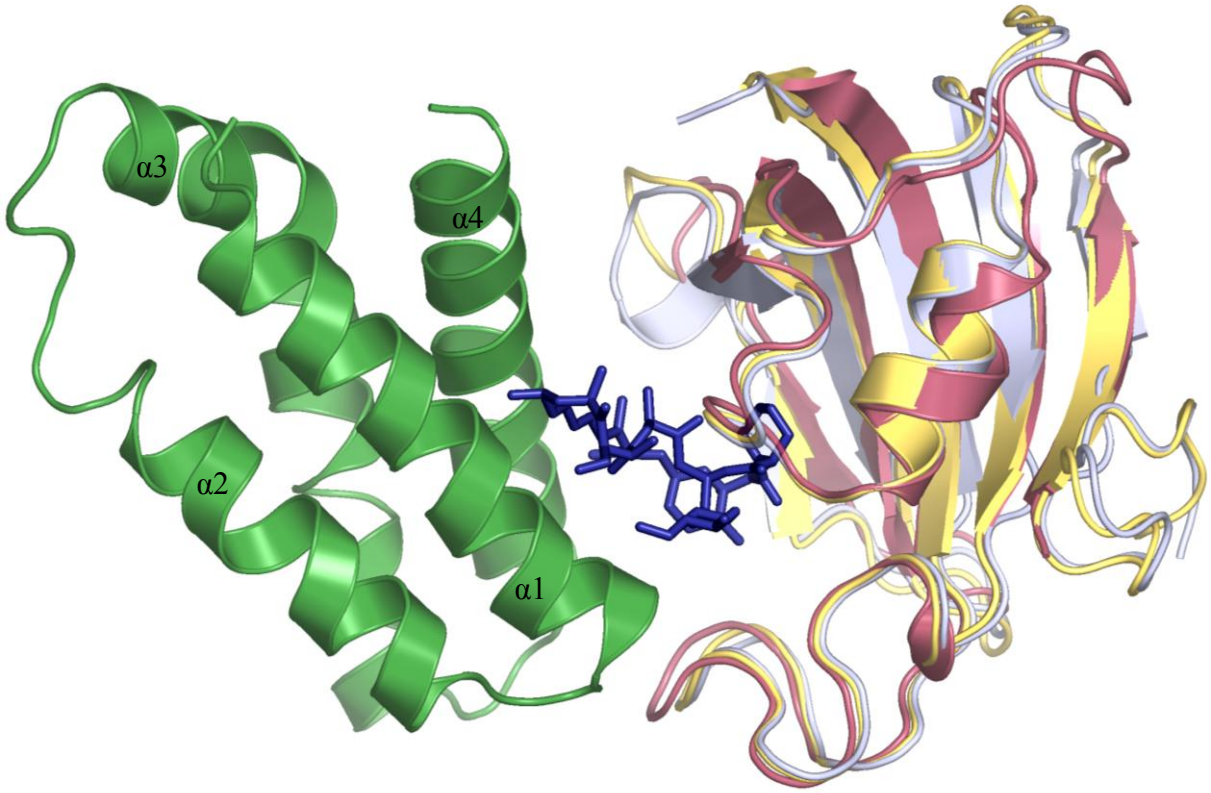

Figure 4.5.3: The three ternary complexes do not differ much and can be overlaid almost perfectly
Ribbon representation of the ternary complexes of FRB*rapamycin*FKBP12, FRB*rapamycin*FK1 FKBP51 and FRB*rapamycin*FK1 FKBP52. The FKBP parts of all three structures are overlaid, while one representative FRB (from 52 structure; α-helices 1-4 are indicated) and the central rapamycin (from the 51 complex) are shown.
Color scheme: Green: FRB; Red: FKBP12;
Blue: FK1 FKBP51; Yellow: FK1 FKBP52;
Dark Blue: Rapamycin

The FK1 domain of FKBP51 consists of 5 antiparallel ß-strands that are interconnected by loop regions (see figure 4.5.4). A large loop can be found between ß2 and ß3 (80S loop). ß5 is interrupted by a small loop (40S) and ends as the 50S loop region which is followed by a short α-helical structure. The binding pocket for rapamycin is located between ß5 and the α-helix; residues in the 40S, 50S and 80S loop contribute mainly to the interactions with rapamycin. It has been shown for both FKBP12 and FKBP51 that the loop regions are highly ordered only in complex with rapamycin, while they display much more flexibility in absence of the ligand [282].

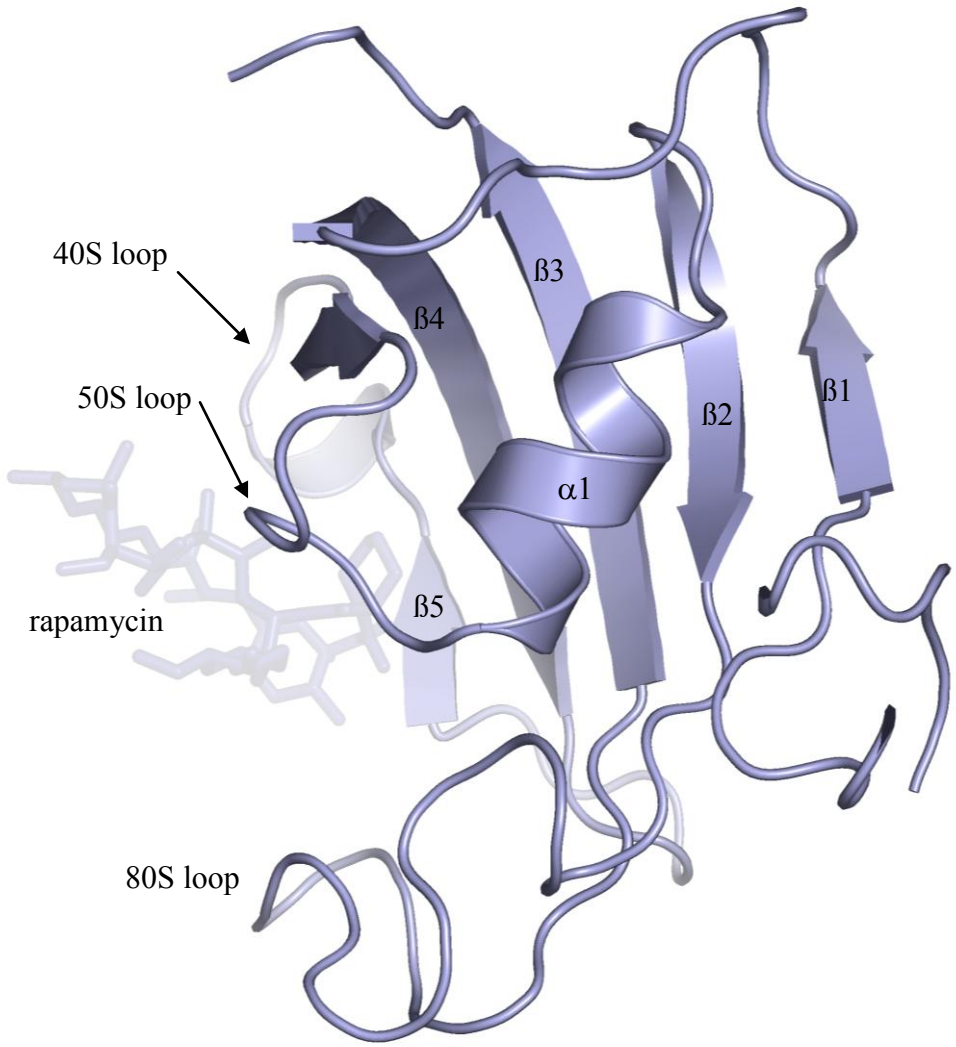

Figure 4.5.4: Overall structure of FK1 FKBP51 shows characteristic elements of all FKBPs

Cartoon representation of FK1 FKBP51; ß-sheet structures and α-helices are labeled (ß1 – ß5; α1); the ligand rapamycin is represented as a stick model (light blue).

When the three FKBP domains are overlaid, only minor structural deviations can be observed (see figure 4.5.3). These differences mainly concern the loop regions where larger discrepancies between the proteins can be detected. In contrast, the regions around the rapamycin-binding pocket show highly conserved structures which can be generally expected from these largely homologous proteins. Functional differentiation between the FKBPs is rather achieved by addition of independent domains.

4.5.3.2 – The FRB domain is structurally unchanged in all complexes:

The FK506-rapamycin-binding (FRB) domain of mTOR represents only around 3% of the total multi-domain protein (10 kDa vs. 290 kDa) and appears to be the mTOR domain that can be crystallized easily. Structurally, FRB consists of a compact bundle of four α-helices which are linked by short streaks of loops (α1-4, see figure 4.5.3, left part). At the regions that interact with rapamycin it forms a hydrophobic pocket, consisting of mainly aromatic residues. Here, the triene arm of rapamycin interacts with FRB (see figure 4.5.5A/C), and this happens exclusively via hydrophobic contacts. In detail, the residues S2035, F2039, Y2105, W2101 and F2108 can be found within a van-der-waals distance of 4 Å to rapamycin (see figure 4.5.5B). These amino acids form a total of 14 contacts to the triene arm C atoms (C17-24) of the ligand. The methyl group at C23 of rapamycin is responsible for another 8 contacts because it is located deep within the hollow space between the FRB residues Leu2031 and Phe2108 (see figure 4.5.5A/C). No direct H-bonds play a role in stabilizing the interaction between the natural compound and the FRB domain.
The rapamycin binding pockets of FRB are very similar in the ternary complexes of FKBP12 (in 2fap), FK1 FKBP51 and FKBP52. Only minor differences can be detected. For example, the location of the phenyl moiety of Y2105 seems to be variable: while it is closest to the rapamycin triene arm in the FKBP52 structure, it is significantly shifted out of the pocket in the FKBP51 ternary complex. For FRB*rapamycin*FKBP12, the residue is located in-between (see appendix section 6.6.4). This structural deviation results in the loss of hydrophobic contacts to the ligand: while the FKBP52 structure displays a total amount of 11 contacts between Y2105 and rapamycin, the number is reduced to 10 in 2fap, and goes down to 6 in the FKBP51 structure. Similarly, the residue R2036 interacts with C50 of rapamycin in the FKBP12 structure (2 contacts), while it is located beyond the 4 Å threshold in the FKBP52 ternary complex. For the FKBP51 structure, only one contact can be counted.

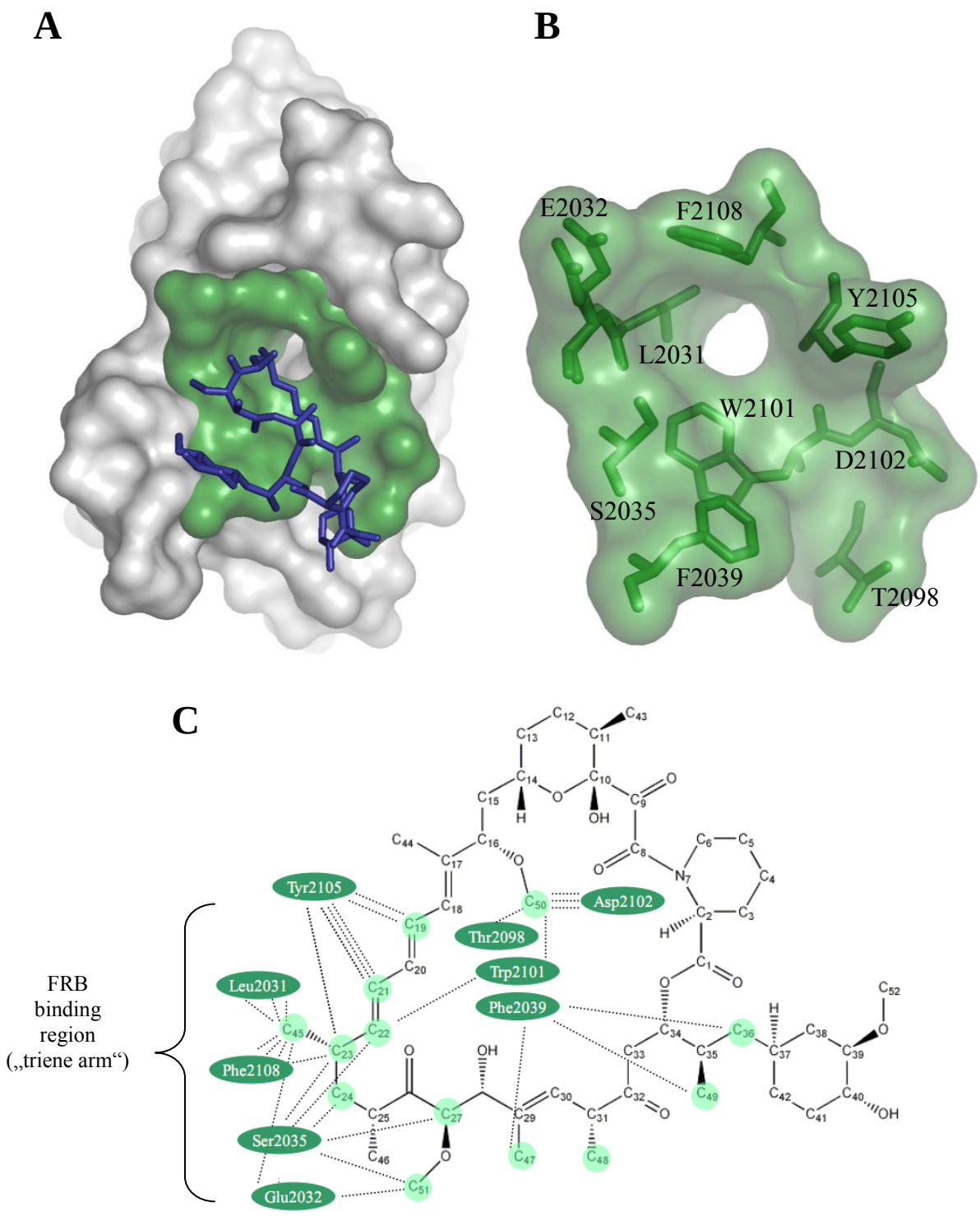

Figure 4.5.5: Interactions of rapamycin and the FRB domain are mainly hydrophobic

(A) Surface representation of the mTOR FRB domain (grey; from complex FRB*rapamycin*FK1 FKBP52) with rapamycin binding pocket (green) and rapamycin (dark blue).

(B) Binding pocket of FRB with aromatic amino acids as stick models. Rapamycin has been omitted.

(C) Graphical representation of the FRB residues interacting with rapamycin (carbon atoms involved in hydrophobic interactions are marked with a green circle).

4.5.3.3 – Rapamycin is bound to the FKBP binding sites in a similar manner:

Generally, the rapamycin binding site of all FKBPs is highly conserved: from the 13 residues involved in ligand binding, 10 are identical in the ternary complexes of FKBP12, FK1 FKBP51 and FK1 FKBP52. Between the latter two, only one residue, Q85 in 52 and E85 in 51, differs slightly. FKBP12 displays two additional mutations, namely Q53 (corresponding to G84 in 51/52) and I90 (K121 in 51/52) (see table 4.5.2). Thus, substantial differences in binding of rapamycin to the active site of the three FKBPs cannot be expected.
Just like in FKBP12, rapamycin interacts with FKBP51 and FKBP52 in a hydrophobic pocket that lies between an α-helix and a ß-sheet element. This binding site consists mainly of residues which can be found within three loop regions, namely the 40S, 50S and 80S loop. Only 5 or 6 direct H-bonds can be detected between the small molecule and the protein partner (involving D37, Q53, E54, I56, Y82 in FKBP12; D68, G84, Q85, I87, R73, Y113 in FK1 FKBP51; D68, G84, Q85, I87, Y113, K121 in FK1 FKBP52). Just like at the FRB-rapamycin interface, aromatic residues contribute mainly to the interactions between the pipecolyl ring of rapamycin and the FKBP protein. This heterocycle is the compound's moiety that reaches deepest into the binding pocket whose back wall consists of 4 aromatic residues (see figure 4.5.6). Again, stabilization of the binding is largely mediated by hydrophobic interactions. Altogether, 29 contacts (defined by proximity of less than 4 Å) are present between the FKBP-interacting portion of rapamycin and the residues Y57, F77, W90 and F130 in FK1 FKBP51, even 33 in FK1 FKBP52 (see appendix section 6.6.1 for a detailed register).

Structure	Number of residues	Unique residues	Contacts by unique residue	H-bonds	Non-conserved Residues
FKBP12 (2fap)	13	I90	1	5	Q53 (G84 in 51,52) I90 (K121 in 51, 52)
FK1 FKBP51	13	R73	9	6	Q85 (E85 in 51, E54 in 12)
FK1 FKBP52	13	K121	7	6	-

Table 4.5.2: Overview of differences in rapamycin binding pocket of three ternary complexes

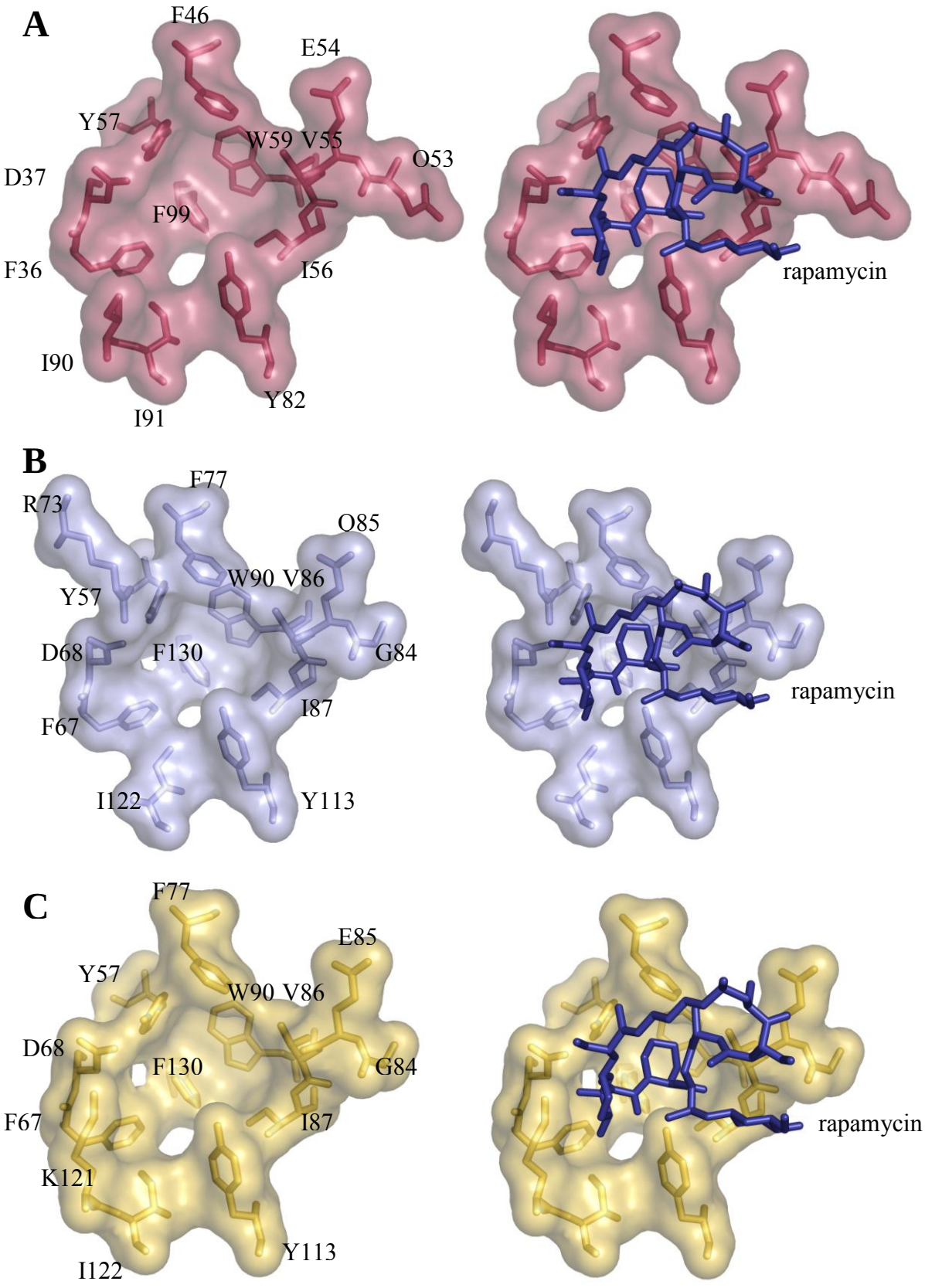

Figure 4.5.6: The rapamycin binding pockets of FKBP12, FKBP51 and FKBP52 are very similar

Surface representation of the rapamycin binding pockets of FKBP12 (from 2fap) (A), FK1 FKBP51 (B) and FK1 FKBP52 (C). Surface representation is laid over a stick model of the residues.

Dark blue: Rapamycin. Red: FKBP12. Blue: FK1 FKBP51. Yellow: FK1 FKBP52.

In FKBP51 and FKBP52, the residues G84, E/Q85, V86 and I87 form a hinge region which is involved in accommodation of the cyclohexyl moiety and the ester linkage of rapamycin. At the opposite site of the small molecule, Y57, F67, D68 and R73 contribute to binding of the pyranose moiety.

While 12 of 13 amino acids involved in rapamycin binding are totally conserved in the structures of FKBP51 and FKBP52, one lysine residues (K121) displays a clear exception: the FKBP52 species is engaged in interactions with rapamycin, whereas the FKBP51 counterpart is oriented away from the binding pocket. Like this, K121 of FKBP51 is unable to form contacts to the ligand. Compared to FKBP52, a total of 7 contacts (including 1 H-bond) are lost. The corresponding residue I90 is unique in FKBP12; it contributes only 1 contact to C10-14 of rapamycin (see figure 4.5.7).

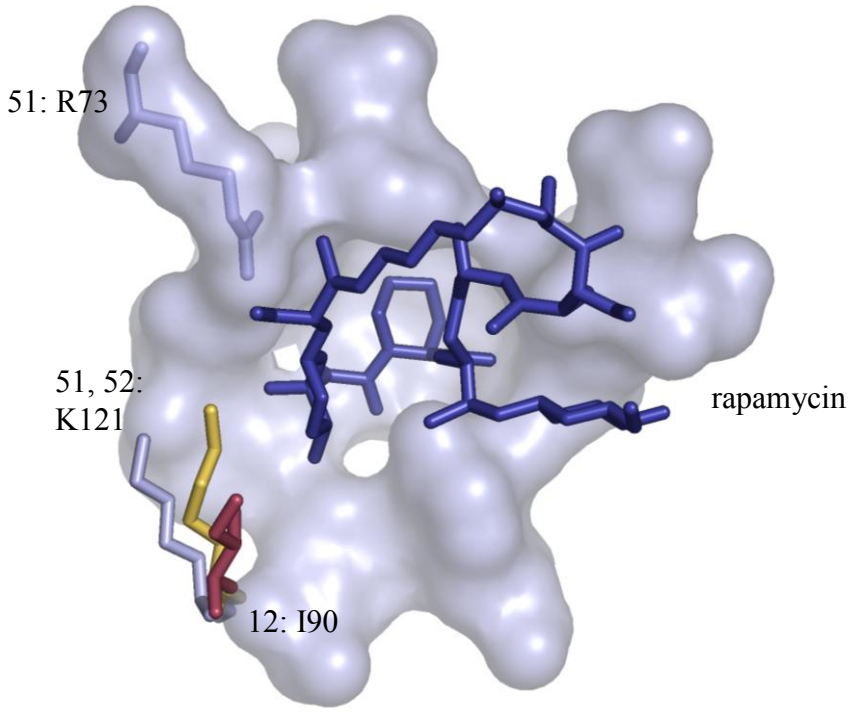

Figure 4.5.7: The rapamycin binding pockets of FKBP12, FKBP51 and FKBP52 differ in some details

Surface representation of the rapamycin binding pocket of FKBP51; residues that differ between FKBP12, FKBP51 and FKBP52 are shown. K121 of FKBP51 does not interact with rapamycin. The complementary residue I90 in FKBP12 is involved in such an interaction.

Dark blue: Rapamycin. Red: FKBP12. Blue: FK1 FKBP51. Yellow: FKBP52 FK1.

Interestingly, one arginine residue plays different roles in FKBP12, 51 and 52: an additional H-bond is present between arginine R73 of FK1 FKBP51 (NH2) and rapamycin (O7 next to C13). Furthermore, this residue is located within the 40S loop region which is crucial for rapamycin binding. Whether this interaction exerts stabilizing effects or whether affinity is reduced without R73 might be determined by mutational analysis. The side chain of the corresponding arginine residue in FK1 FKBP52 is not well defined; thus, no specific interactions and especially no H-bond can be assigned. In FKBP12, the corresponding residue R42 does not interact with rapamycin; it rather forms an intramolecular H-bond via a water molecule to the backbone of K44 (see figure 4.5.7).

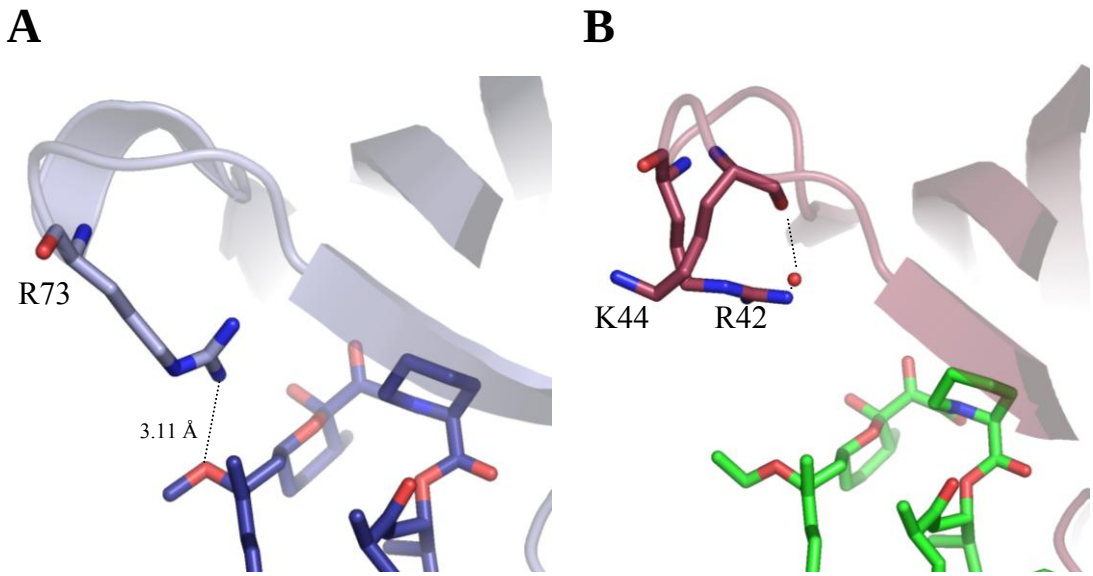

Figure 4.5.7: An additional H-bond is present between R73 and rapamycin in FK1 FKBP51

Ribbon representation of the 40S loop region of FK1 FKBP51 (A) and FKBP12 (B; taken from 2fap). The residues R73/R42/K44 are displayed as a stick model, with nitrogen atoms in blue and oxygen atoms in bright red. Dark blue, with oxygen atoms in red: Rapamycin; Green, with oxygen atoms in red: (C16)-ethoxy rapamycin.

Altogether, rapamycin interacts with the binding pocket of FKBP51 via 99 contacts. For FKBP52, 101 contacts can be observed, for FKBP12 (analyzed in 2fap) there are only 85. Most of these interactions are hydrophobic, while only a total 5 or 6 consists of H-bonds. A table listing all contacts can be found in the appendix (see section 6.6.1). In conclusion, rapamycin binding to FKBPs is strongly conserved, but differs in some interesting details.

4.5.3.4 – Interactions between the protein domains involve different residues:

Analysis of protein-protein contacts between the FKBP and the FRB domain within the ternary complex reveals that these contacts are quite rare: only the 40s and 80s loop regions of the FKBPs are involved in direct interactions with FRB. Thereby, the contacts mainly consist of hydrophobic interactions, while only few H-bonds are present. FK1 FKBP51 displays a sum of 48 contacts (4 H-bonds via R73, P76 and V78), while FK1 FKBP52 interacts with FRB only 21 times (1 H-bond via R52). FKBP12 ranges in-between with 27 total interactions (analyzed in 2fap; no H-bonds). A detailed list of all values can be found in the appendix (see section 6.6.2).

The differences regarding the number of interactions are also reflected by their distribution between the 40s and 80s loop regions (see figure 4.5.8). For FKBP12, only 3 contacts are located within the 40s loop. For FKBP51, 42 of 48 total interactions can be found in the 40s loop, while in FK1 FKBP52 there are only 5. Thus, FKBP12 interacts preferentially with the 80s loop, while FK1 FKBP51 makes much more contacts with its 40s loop. FK1 FKBP52 must be placed in-between (see table 4.5.3).

Strikingly, FK1 of FKBP51 displays the highest number of contacts to the FRB domain. Furthermore, there are two H-bonds which theoretically contribute up to 5-fold more binding enthalpy than typical van-der-waals interactions [283]. Thus, a hypothetical rapamycin-independent binding to FRB might be more probable for FKBP51 than for FKBP12 or FKBP52. Nevertheless, these few contacts might rather play a role in supporting rapamycin-mediated interaction; they are presumably much too weak to allow rapamycin-independent binding of FKBPs to FRB.

Structure	Total contacts	40S loop contacts	Percentage 40S loop contacts	H-bonds
FKBP12 (2fap)	27	3	11.1%	0
FK1 FKBP51	48	42	87.5%	4
FK1 FKBP52	21	13	61.9%	1

Table 4.5.3: Direct protein-protein contacts differ in localization and number

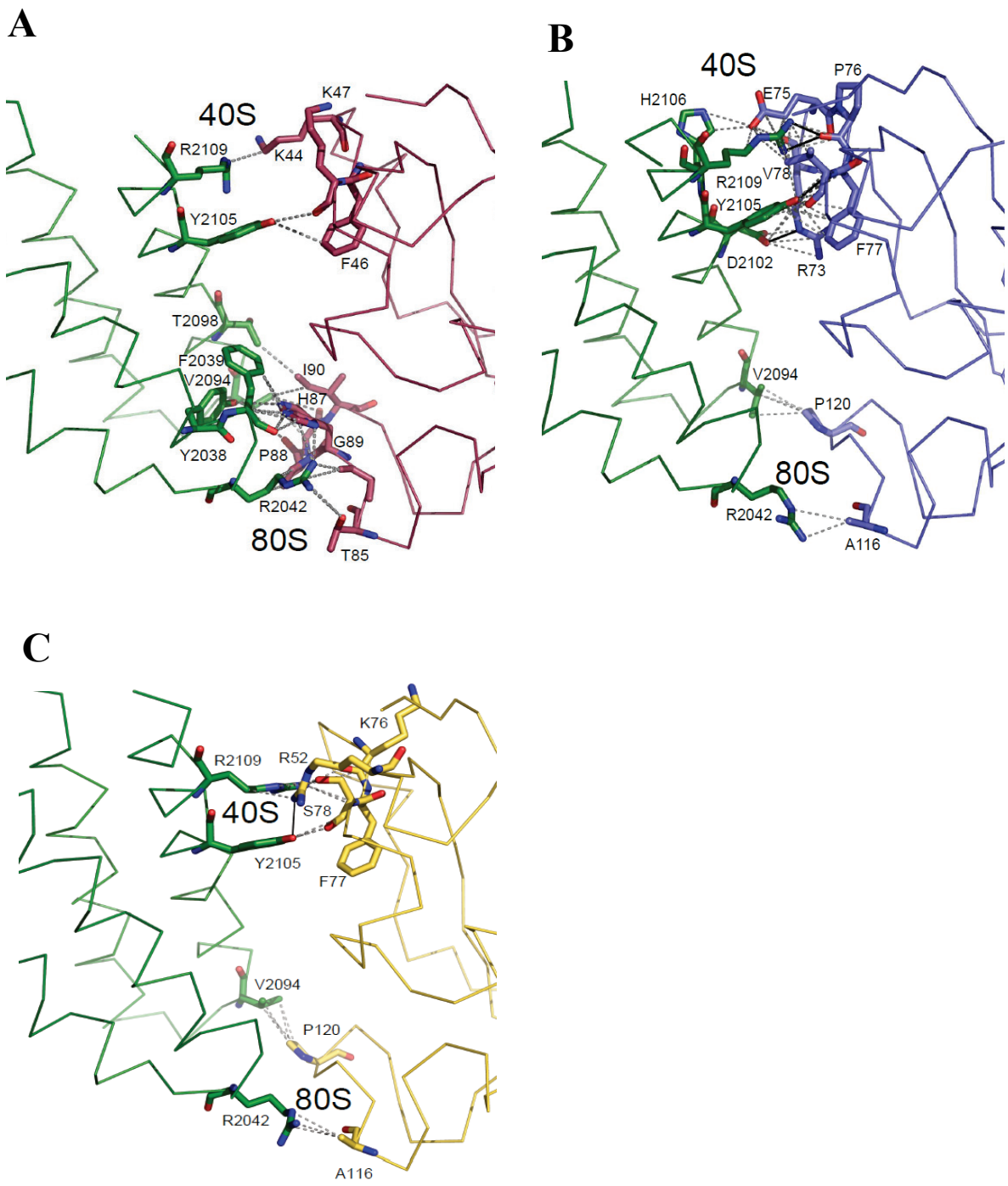

Figure 4.5.8: Direct protein-protein interactions between FK1 domains and FRB differ substantially

Representation of protein-protein interfaces of FRB (green; left side, ribbon) and FKBP (right side, ribbon). Ternary complexes of (A) FKBP12 (2fap), red (B) FK1 FKBP51, blue (C) FK1 FKBP52, yellow. H-bonds are shown as black lines, van-der-Waals contacts are shown as grey dashed lines.

Analysis of the residues involved in direct protein-protein contacts revealed striking differences between the three ternary complexes: importantly, the only residue which is totally conserved is F46 of FKBP12 (corresponding to F77 in FKBP51/52); it interacts with Y2105 (R2109 in FKBP52). 7 residues of FK1 FKBP51 are involved in contacts to 6 residues in FRB, while there are only 6 in FKBP52 (to 4 in FRB) and 10 in FKBP12 (to 7 in FRB). Notably, only 2 of these residues are identical between FKBP51 and 52 (P120 and A116), the others differ. Furthermore, the positions 76 and 78 are conserved in 51 and 52. In FKBP12, T85 corresponds to A116, G89 to P120, K44 to E75 and K47 to V/S78 in terms of sequence position. As an exclusive item of FKBP51, R73 interacts intensively with D2102, displaying 7 contacts to the FRB residue. Importantly, interactions of the FKBP12 residues H87 and I90 with FRB comprise 12 contacts which represent 44% of the total number of interactions. No comparable contacts can be found in the ternary complexes of FKBP51 and FKBP52 (see table 4.5.4).

Altogether, the protein-protein interface between FRB and the FKBPs can be considered as much more variant than the rapamycin-binding pockets because the interactions at the interface are maintained by different FKBP residues.

Residue in FRB with contact to…	**…FKBP12 residue (2fap)**	**…FK1 FKBP51 residue**	**…FK1 FKBP52 residue**
V2094	I90, G89, P88	P120	P120
R2042	H87, P88, G86, T85	A116	A116
R2109	K44	E75, P76, V78	K76, F77, S78
Y2105	F46, K47	F77, V78	R52, S78
H2109	-	E75	-
F2039	H87	-	-
Y2038	H87	-	-
T2098	I90	-	-
D2102	-	R73	-

Table 4.5.4: Overview of residues involved in protein-protein contacts between FRB and FKBPs in the respective ternary complexes

Contacts are defined as hydrophobic contacts or H-bonds between atoms that can be found within a proximity of 4 Å or less.

4.5.3.5 – Water molecules form an H-bond network across the protein-protein interface:

In all three ternary complexes, the interface between the two protein partners comprises mainly the 40S- and 80S-loop regions of FKBPs and the helices α4/1of FRB. At the centre of the interface, the ligand rapamycin can be found. Furthermore, plenty of well-defined water molecules are present in this area, bridging FRB residues with FKBPs residues via networks of H-bonds. The total number of water molecules in the interface differs little between the ternary complex of FKBP12 (2fap; ~30 waters) and the one of FK1 FKBP52 (~34 waters), whereas there are clearly more water molecules visible in the structure of FK1 FKBP51 (~47 waters).

Water molecules which function as direct mediators between the two protein domains are relatively rare: there are 2 in the FKBP12 complex, 2 in FKBP51 and 3 in FKBP52 (see figure 4.6.9, circles and appendix section 6.6.3). Interestingly, the FRB residues Y2105 and Y2038 act as H-bond acceptors in the complexes of FKBP12 and FKBP52, while F2039 is a shared feature of both FKBP51 and FKBP52 complexes. On the FKBP side, Ser118 mediates H-bonds in both FKBP51 and FKBP52, while E54 of FKBP12 corresponds to E85 in FKBP52. Thus, a certain degree of conservation between the residues involved in water-mediated H-bond formation can be observed.

Due to the high number of water molecules, the H-bond network between FK1 FKBP51 and FRB displays a high density: via one or several water molecules, residues in FKBP51 interact indirectly with residues in FRB. Most of the waters are involved in H-bond formation, either to neighboring waters or to amino acids; only few water molecules are isolated within the interface area (see figure 4.6.9B).

In contrast, the H-bond networks of the ternary complexes of FKBP12 and FKBP52 are much less defined. This could be explained by the smaller number of ordered water molecules in the interface. Furthermore, many of the water molecules stabilize intra-molecular contacts in FRB or the FKBP domains (see figure 4.6.9A/C). It also should be mentioned that the lower resolution of the structure 2fap might limit the number of detectable water molecules.

Importantly, one conserved water molecule mediates H-bond formation between the ligand rapamycin and the residue E2032 in FRB (H_2O 331 (in 2fap) [111], H_2O 71 (in 51 complex), H_2O 42 (in 52 complex; see figure 4.6.9D)). Since all the other contacts between the two binding partners are purely hydrophobic, it could be speculated that such an H-bond constitutes an important parameter for increasing affinity.

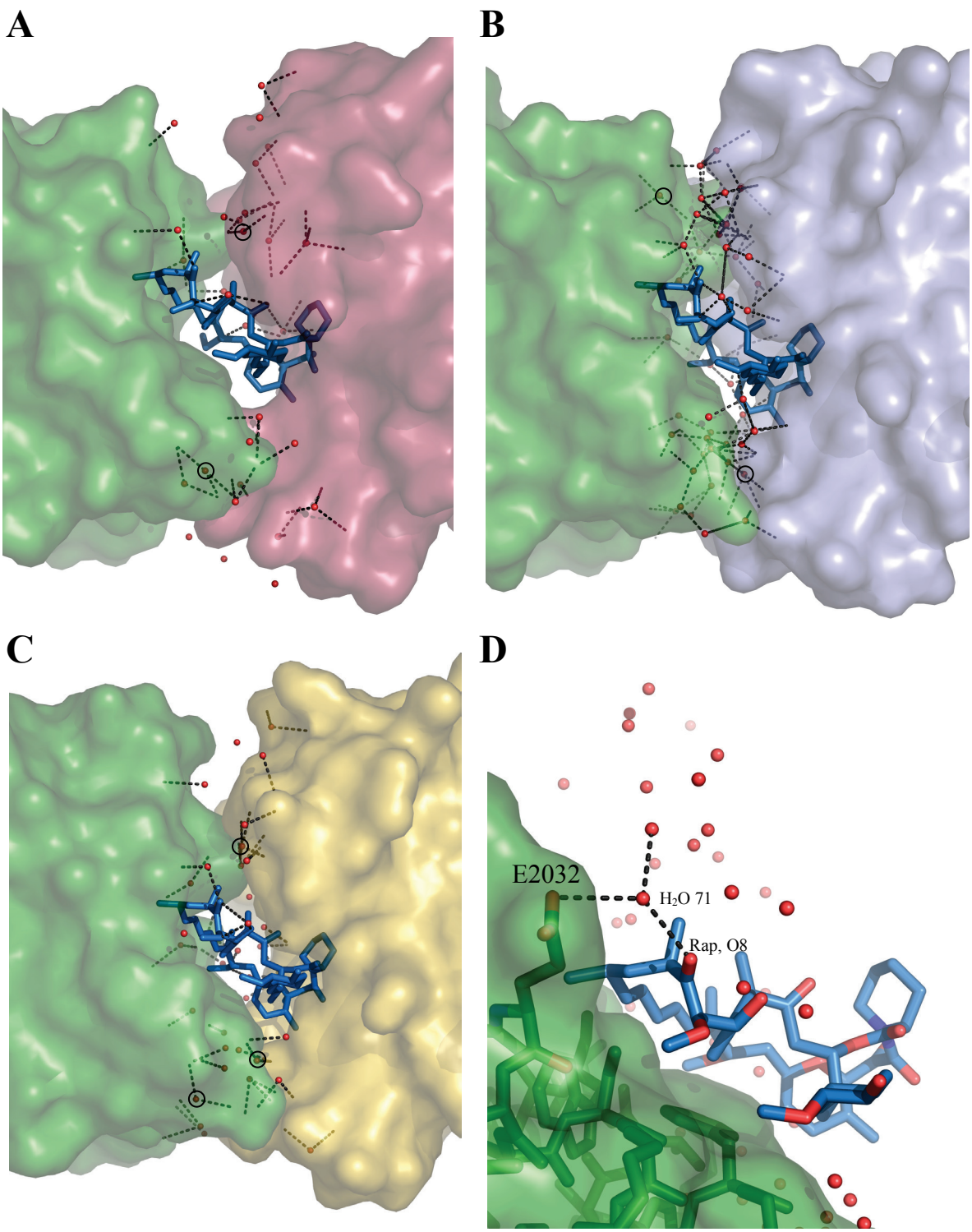

Figure 4.6.9: Water molecules bridge FRB and FKBP protein partners in the ternary complexes

Surface representation of the ternary complex FRB*rapamycin*FKBP12 (A; from 2fap)), FRB*rapamycin*FK1 FKBP51 (B) and FRB*rapamycin*FK1 FKBP52 (C) with water molecules in the interface region of the protein partners. Waters which directly mediate interaction between FRB and FKBP are marked (O).

(D) H-bonds between E2032 in FRB and O8 of rapamycin, mediated by the conserved H_2O 71 (in FRB*rapamycin*FK1 FKBP51).

Green: FRB (in (D): oxygen atoms of E2032 in red); blue: FK1 FKBP51; red: FKBP12; red dots: water molecules; grey dashes: H-bonds; blue sticks: rapamycin (in (D): oxygen atoms in red).

As water-mediated H-bonds between the two protein parts of the ternary complexes are quite frequent and as such interactions are known to have an effect on binding energetics [284], it is probable that they contribute to stabilization of the central rapamycin-mediated binding of FRB and FKBP. Similarly to the direct protein-protein contacts, the residues involved in these water-mediated interactions are rather variable.

Altogether, analysis of the crystal structures of the alternative ternary complexes of FK1 FKBP51 and FKBP52 reveal that they bind to FRB in a strictly rapamycin-dependent manner, and that the complexes are very similar to the one of FKBP12. These findings appear reasonable considering the high degree of homology of the three FKBPs' FK1 domains. Nevertheless, some details can be found in the binding patterns which are not conserved between the structures: an additional H-bond stabilizes rapamycin binding in FKBP51, and protein-protein contacts between FRB and FKBP are especially pronounced in FKBP51 compared to FKBP12 and FKBP52. Altogether, it seems that these variations do not have a significant impact on the overall affinity of rapamycin to the FKBP partner; such a differential binding would have been detected in *in vitro* binding assays. But as binding affinities and EC_{50} values of complex formation were relatively similar in the previous experiments for all three FKBPs, speculations about mechanistic differences in rapamycin binding or complex formation would be highly risky.

4.6 – FKBP51 interacts with mTORC1 and affects mTOR kinase activity:

4.6.1 – FKBP12 and FKBP51 interact with mTOR in a rapamycin-dependent way:

As all tested FKBPs bind to the FRB domain of mTOR under *in vitro* conditions, we were interested in detecting rapamycin-induced interactions in living cells. For this purpose we transfected HEK293 cells with a FLAG-mTOR or FLAG-mTORS2035T expression plasmid, treated them with rapamycin before lysis and subjected the lysates to immunoprecipitation using protein A affinity resin and an α-mTOR antibody. Endogenous proteins co-immunoprecipitating with FLAG-mTOR were characterized by immunoblotting. This procedure has been described in detail by others [139, 140]. Since FK506 competes for binding to the active sites of FKBP proteins with rapamycin [20], and since FK506*FKBP12 complex does not bind to mTOR-FRB [20, 285], co-immunoprecipitation experiments were performed either in presence of rapamycin, FK506 or DMSO.

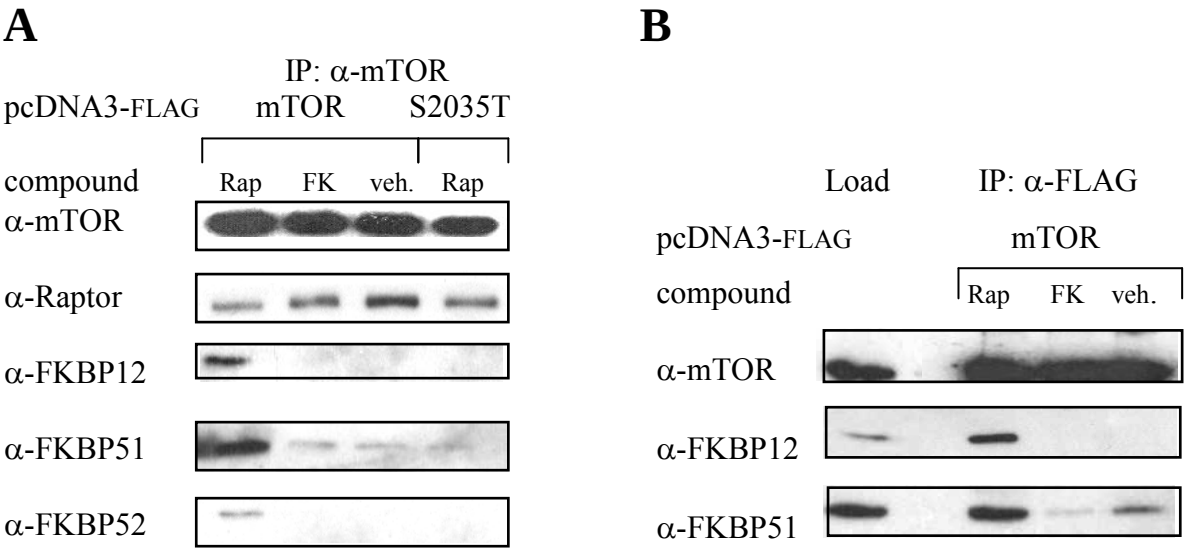

Figure 4.6.1: mTOR interacts with FKBP12 and FKBP51 in a rapamycin-dependent manner
(A) HEK293 and (B) HeLa cells were transfected with a FLAG-mTOR expression plasmid. 30 minutes prior to lysis, rapamycin, FK506 (final concentration: each 25 nM) or vehicle DMSO were added. The cell lysates were subjected to immunoprecipitation. The resin was washed and eluted by boiling for 5 minutes in SDS sample buffer. The eluates were separated by SDS-PAGE and analyzed by immunoblotting.

It turned out that FLAG-mTOR/mTORS2035T immunoprecipitation yields were similar in all samples (see figure 4.6.1A). The rapamycin-mediated interaction of FKBP12 with mTOR was used as positive control. As already known, FKBP12 only binds to the FRB domain of mTOR

if rapamycin is present. Without rapamycin or in the presence of FK506, no interaction could be expected. We replicated this control experiment in the co-IP assays. Furthermore, FKBP51 was clearly co-precipitated in the presence of rapamycin, while FK506 could not induce such a binding. This finding points to a rapamycin-induced interaction between mTOR and FKBP51. DMSO-treated HEK293 cells served as control and displayed merely weak binding. Similar results were obtained for FKBP52: rapamycin mediated an interaction with mTOR while it was totally absent in presence of FK506. The intensity of the co-IP signals was generally lower than for FKBP51. In the DMSO-treated controls there were no signals at all. As a negative control, we immunoprecipitated the mTOR mutant S2035T which is defective in rapamycin binding [21]. No rapamycin-dependent binding of FKBPs could be detected here.

Oshiro and Yoshino demonstrated that by rapamycin treatment the interaction between mTOR and Raptor is impaired: in co-IP experiments less Raptor could be detected in presence of rapamycin concentrations higher than 100 nM [131]. This result could be confirmed only partially; the used rapamycin doses in our experiments might be too low (25 nM).

Secondly, FLAG-mTOR was immunoprecipitated in HeLa cells, and endogenous FKBPs were detected as binding partners (see figure 4.6.1B). Western blot analysis revealed that rapamycin induces binding of both FKBP12 and FKBP51 to mTOR. Without rapamycin or in the presence of FK506, almost no interaction could be observed for FKBP12. FKBP51 displays a certain degree of binding even in absence of the compound. The nature of this interaction is largely unknown, because an interaction of the FK1 domain with FRB seems impossible without rapamycin.

In order to further verify the mTOR-FKBP interaction, HA-FKBPs und FLAG-mTOR were co-expressed in human cell systems. Immunoprecipitation was performed with HA-beads, and immunoblotting for interaction partners was done (as described in [113]). The addition or omission of 50 nM rapamycin to the cells prior to lysis allowed determination of rapamycin-dependency of binding.

Figure 4.6.2 demonstrates that immunoprecipitation of FKBPs in HEK293 cells was successful and yielded comparable amounts of protein per lane. In this case, a co-precipitation of mTOR could only be detected for FKBP12 and FKBP51. The interaction of FKBP52 and mTOR displays an intensity only slightly above background level. As Hsp90 recruits FKBP51 and FKBP52 by their TPR domains [36], the chaperone is enriched in IP samples of FKBP51

and (in parts) of FKBP52. While FKBP12 and mTOR seem to associate clearly in a rapamycin-dependent manner, this is not obvious for FKBP51: mTOR co-IP signals are comparable in the samples with and without rapamycin. Thus, rapamycin might not be necessary for this interaction, or the applied concentration was too low to allow proper binding.

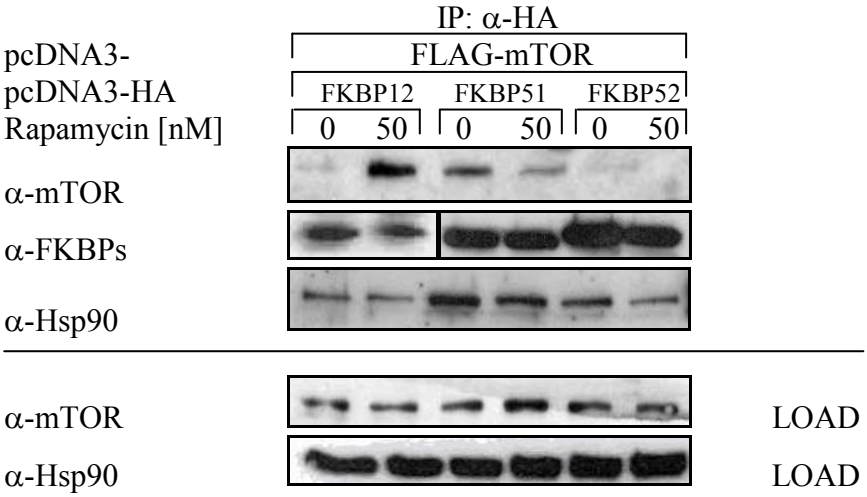

Figure 4.6.2: Immunoprecipitated FKBPs interact with mTOR

HEK293 cells were co-transfected with FLAG-mTOR and HA-FKBP12/51/52 expression plasmids. 30 minutes prior to lysis, rapamycin was added (final concentration: 50 nM) where indicated. The cell lysates were incubated for 2 hours with anti-HA affinity resin. After intensive washing, the resin was boiled in SDS sample buffer for 5 minutes. The supernatants were separated by SDS-PAGE and analyzed by immunoblotting.

Altogether, we were able to demonstrate in several independent co-immunoprecipitation experiments that both FKBP12 and FKBP51 interact with mTOR via its FRB domain. For FKBP12, this binding is largely rapamycin-dependent, while FKBP51 also displays an additional constitutive binding mode. Nevertheless, FK506 can be clearly excluded as a mediator of interactions between mTOR and FKBPs. As binding of FKBP52 turns out to be rather weak, we decided to focus on FKBP51 and compare its effects on mTOR with those of FKBP12.

4.6.2 – FKBP51 associates with Raptor in a rapamycin-dependent manner:

As FKBP51 has been found to interact with mTOR in a rapamycin-dependent as well as in a direct manner, we were interested in further examining the nature of this binding. First, one can differentiate between the two distinct mTOR complexes mTORC1 and mTORC2 that differ in their protein composition: while mTORC1 includes Raptor as the crucial recruiter of mTOR substrates [129], mTORC2 carries the protein Rictor [140]. By assessing interactions of FKBP proteins with Raptor and Rictor, it thus can be determined in which complex the FKBP binding occurs.

Co-immunoprecipitation experiments with FLAG-FKBPs and myc-Raptor were performed, and clear binding patterns could be detected (see figure 4.6.3): FKBP12 seems to interact with Raptor in a rapamycin-dependent manner. Compared to background signal caused by unspecific binding to the beads, this interaction appears rather weak. For FKBP51, a much stronger signal can be obtained. Again, binding seems to be increased by rapamycin. Altogether it could be concluded that FKBP12 and FKBP51 interact with Raptor, a component of the mTOR complex 1. This complex is known to be rapamycin-sensitive.

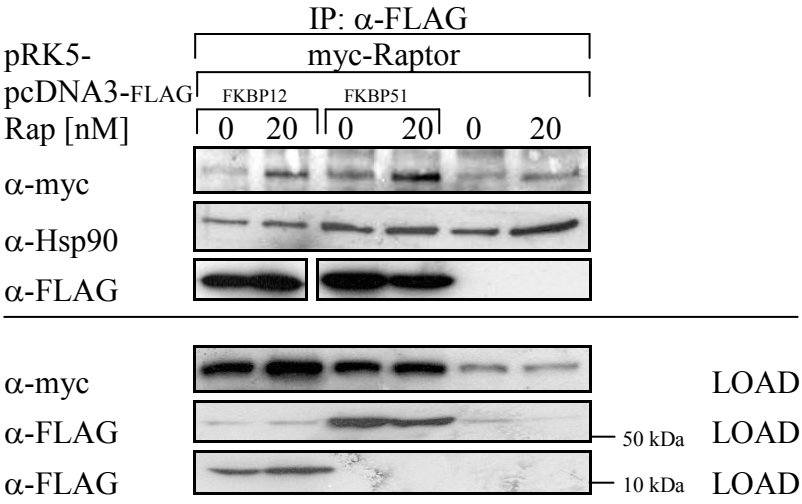

Figure 4.6.3: FKBP12 and FKBP51 interact with the mTORC1 component Raptor

HEK293 cells were transfected with myc-Raptor and FLAG-FKBPs, starved and stimulated with FCS in absence or presence of 20 nM rapamycin for 60 minutes. Cell lysates were subjected to FLAG-IP. Beads were washed four times with CHAPS-containing lysis buffer and eluted by boiling with SDS sample buffer for 5 minutes. Supernatants were analyzed by SDS-PAGE and immunoblotting.

4.6.3 – FKBP51 and FKBP52 interact with p70 S6Kinase:

As FKBP51 seems to interact with components of mTORC1, we performed further IP experiments to characterize the binding partners more precisely. As one candidate protein, p70 S6Kinase appears interesting because it is directly recruited into the complex by Raptor and phosphorylated by the kinase activity of mTOR [124].

When HA-S6Kinase and FLAG-FKBPs were co-expressed in HeLa cells, a robust interaction between FKBP51 and S6Kinase could be detected (see figure 4.6.4A). Similarly, FKBP52 was bound to the kinase. These effects seem to be mostly rapamycin-independent for FKBP52, while rapamycin enhanced the interaction of S6Kinase and FKBP51. For FKBP12, no obvious interaction could be observed.

In order to verify the results described above, we inverted the co-IP pattern by immunoprecipitating FLAG-FKBPs and detecting co-expressed S6Kinase. Thereby it turned out that HA-S6Kinase was detectable as an interaction partner for all tested FKBPs; nevertheless, clear differences in binding preference became obvious (see figure 4.6.4B): interaction of S6Kinase occurs mainly with FKBP51 while it is weakened for FKBP52 and even weaker for FKBP12. The Hsp90-binding defective TPR mutants of FKBP51 and FKBP52 did not display significantly different binding patterns. Thus, Hsp90 may not play a crucial role in modulating FKBP*S6Kinase interaction.

Interestingly, binding of FKBP51 to S6Kinase could be increased by rapamycin treatment. This effect is present for both wild type and TPR mutant FKBP51, and it is considerably strong: densitometric quantification revealed that rapamycin treatment elevates signal intensity by 200%. For FKBP52 proteins, the effect is less pronounced; for FKBP12, a signal indicating S6Kinase interaction is totally missing in absence of rapamycin. Treatment with the small molecule brings up a signal which is comparable to the one of untreated FKBP51.

Altogether, it can be concluded from the above experiments that FKBP12, FKBP51 and FKBP52 interact with S6Kinase. While this interaction can be increased by short-term rapamycin treatment especially for FKBP51, it tends to be equally strong under all conditions for FKBP52. FKBP12 seems to display a weak obligatorily rapamycin-induced binding to S6Kinase. Hsp90 recruitment may not be crucial for formation of this complex. From experiments that maintain integrity of mTORC1, no conclusions can be drawn concerning the question whether S6Kinase interacts with FKBPs within the mTOR complex or in an independent way.

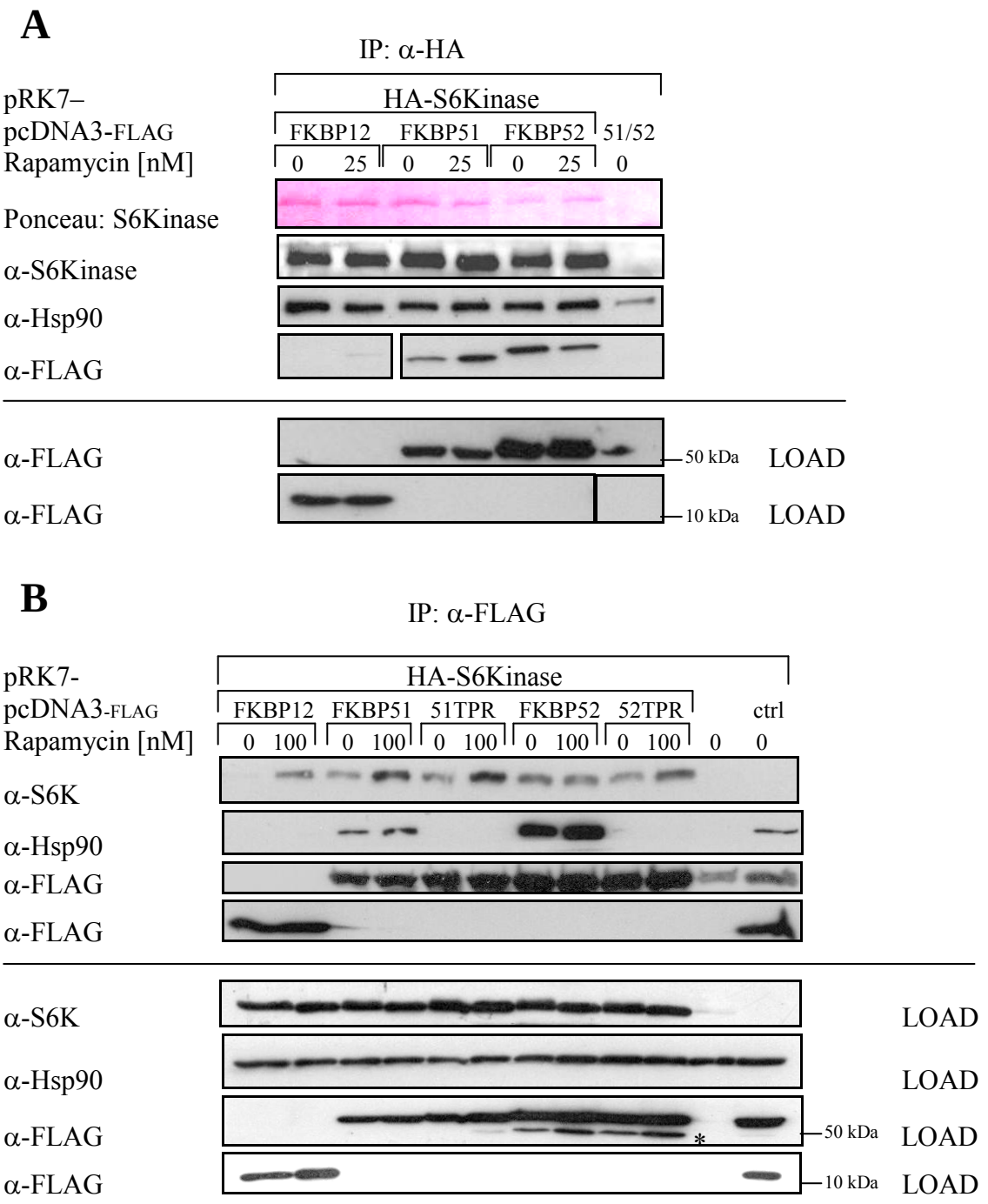

Figure 4.6.4: Co-IP assays demonstrate interaction between p70 S6Kinase and FKBP51/52

HeLa cells were co-transfected for expression of FLAG-FKBPs and HA-S6Kinase, treated with rapamycin for 60 minutes (where indicated) and lysed. Lysates were subjected to FLAG/HA-IP. Binging partners were analyzed by Western blotting. Unspecific signals are marked (*).

(A) HA-IP of HA-S6Kinase

(B) FLAG-IP of FLAG-FKBPs

Control lane (ctrl): expression of FLAG-FKBP12/51/52

4.6.4 – FKBPs influence interaction between S6Kinase and Raptor:

In order to assess a possible role of FKBP51 and FKBP52 in mediating and modulating the interaction of S6Kinase and Raptor in a rapamycin-dependent manner, we performed modified co-immunoprecipitation experiments: while FLAG-FKBP proteins were overexpressed, HA-S6 Kinase was precipitated from HeLa cells, and binding of co-expressed myc-Raptor was analyzed by Western blotting. Thus, a system of three simultaneously expressed and orthogonally tagged proteins could be studied in terms of rapamycin-dependent interaction.

Expression levels of all three putative interaction partners were verified, and unspecific binding to the HA-beads was checked (see figure 4.6.5). Overexpressed myc-Raptor binds to immunoprecipitated HA-S6Kinase. This binding was slightly increased in presence of overexpressed FKBP12 and FKBP52; only FKBP51 seemed to repress this interaction under basal conditions. For all three FKBPs, a rapamycin-induced binding of S6Kinase to Raptor could be observed, and co-IP signals of Raptor were increased compared to basal conditions (see quantification in figure 4.6.5B). Thus, S6Kinase seems to aggregate more efficiently with Raptor if FKBPs are overexpressed, and a rapamycin-dependency of this interaction is obvious.

This binding pattern seems contradictory to the classical model of rapamycin action which suggests a competition between Raptor and FKBP*rapamycin for mTOR binding. The interactions seen in our co-IP experiments rather suggest that after rapamycin application an mTOR*Raptor*rapamycin*FKBP complex exists that allows simultaneous binding of the two competing proteins. It could further be speculated whether FKBP*rapamycin prevents Raptor from being excluded from the complex, possibly blocking substrate turnover. Such a model is discussed in section 5.1.3.

Altogether, the above experiment indicates that FKBP51 and FKBP52 exert their influence on mTORC1 activity in a rapamycin-dependent manner similarly to FKBP12, namely by modulating interactions between mTOR/Raptor and its substrate S6Kinase. Assuming that overexpression of an individual FKBP renders it the dominant cellular FKBP species, our co-IP data suggest that the effects of FKBP51 and FKBP52 might be more pronounced.

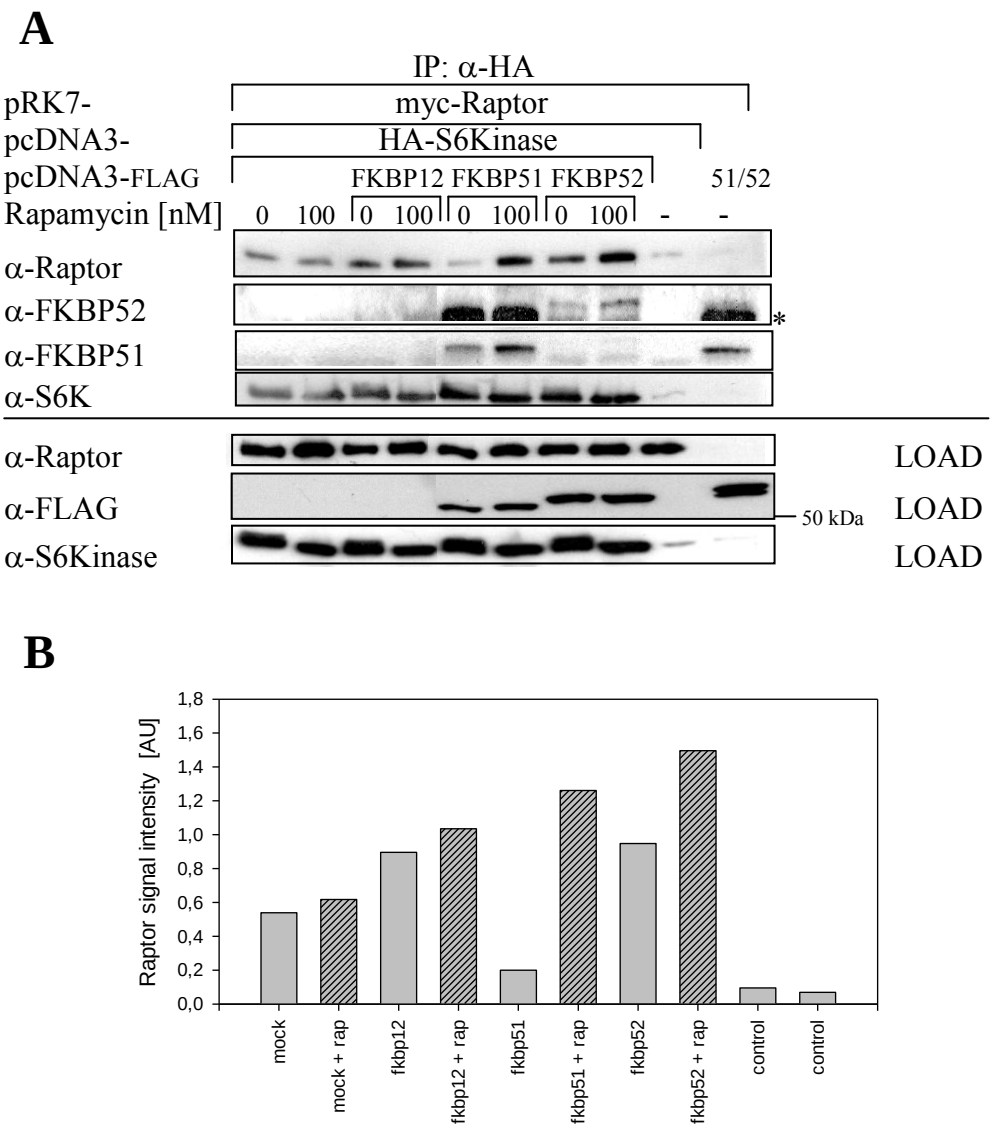

Figure 4.6.5: Rapamycin increases Raptor-S6Kinase interaction in presence of FKBPs

HeLa cells were transfected for expression of myc-Raptor, HA-S6 Kinase and FLAG-FKBPs as indicated. Cells were starved, stimulated with serum/insulin and treated with rapamycin for 60 minutes. Lysates were subjected to HA-immunoprecipitation, and binding partners were analyzed by Western blotting.

(A) Upper part: IP signals; lower part: Loads

Unspecific signals are marked (*)

(B) Densitometric quantification of α-Raptor IP signals (absolute signal intensities)

4.6.5 - FKBP51 overexpression affects S6Kinase phosphorylation:

In order to shed a light on the effects of different FKBPs on S6Kinase phosphorylation, we overexpressed human FKBPs in HeLa cells. S6Kinase phosphorylation was induced by starvation and subsequent stimulation with serum and insulin in the absence or presence of 0.25 nM rapamycin (as described in [119]). This rapamycin concentration is slightly below the concentration necessary for complete S6Kinase de-phosphorylation in mock-transfected cells. Phosphorylation status of differently treated samples was assessed by immunoblotting.

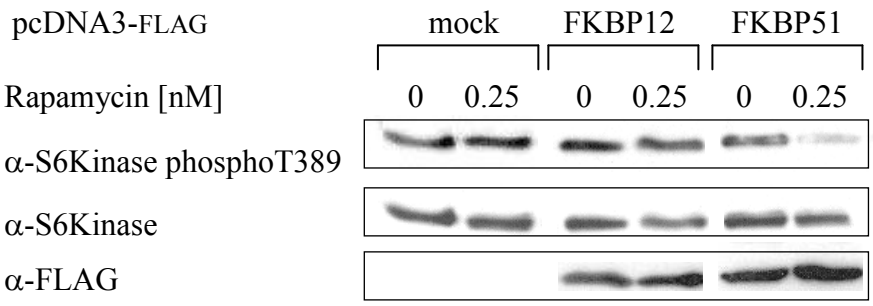

Figure 4.6.6: Overexpression of FKBP12 or FKBP51 has different effects on S6Kinase

HeLa cells were transfected with FKBP12/51 overexpression vectors, starved for 16 hours and stimulated with serum and insulin for 60 minutes in presence of rapamycin (concentrations as indicated). Then, cells were lysed and subjected to SDS-PAGE and Western blotting. The membrane was probed against the indicated proteins or antigens with appropriate antibodies.

Here, it turned out that FKBP expression indeed exerted effects on S6Kinase phosphorylation: when compared to mock-transfected cells, samples overexpressing FKBP12 displayed a slight rapamycin-dependent reduction in phospho-signal intensity (see figure 4.6.6). In cells transfected for FKBP51 overexpression, phosphorylation of the critical S6Kinase residue Thr389 was even lower at rapamycin concentrations of 0.25 nM, suggesting a more efficient mTOR kinase inhibition than observed for mock control or FKBP12 overexpression. As S6Kinase expression levels remain unaltered, it can be assumed that the protein‟s phosphorylation state is the actual effect.

The above results suggest that FKBP12 and FKBP51 influence S6Kinase phosphorylation and thus might have an effect on mTORC1 activity in HeLa cells: when overexpressed, the FKBP

proteins seem to cause a more effective rapamycin-induced mTOR inhibition, maybe by modulating interactions between S6Kinase and Raptor or by directly acting on mTOR kinase activity. Altogether the effect of FKBP51 appears stronger than the one of FKBP12. This may support a hypothesis in which parts of rapamycin action are carried out by FKBP51.

4.6.6 – FKBP12 knockdown does not abolish effects of rapamycin:

As it is difficult to assess the effects of other FKBPs on mTOR in presence of FKBP12, we performed siRNA knockdown experiments to reduce cellular FKBP12 content. In such a system, one would generally expect that rapamycin sensitivity is reduced.
Western blot analysis revealed that FKBP12 was knocked down efficiently: 90% less signal was detected for samples transfected with anti-FKBP12 siRNA. Mock-transfected cells with non-targeting siRNA did not show any altered FKBP12 expression levels.
S6Kinase phosphorylation was assessed, and only minor differences could be detected: in both cases, rapamycin caused a clear dose-dependent reduction in phosphoThr389 signal. For the control samples, no phosphorylation was detectable at 2 nM rapamycin, while the signals had disappeared for the FKBP12-siRNA samples at 2.5 nM. Thus, in spite of reduced FKBP12 concentration, rapamycin is still able to inhibit mTOR kinase activity, possibly by recruiting other FKBPs.

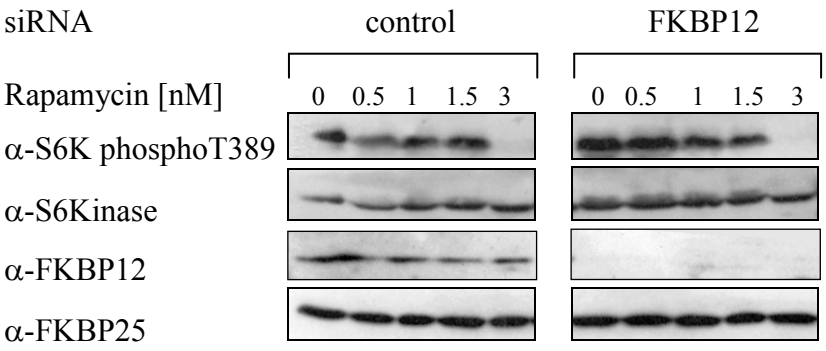

Figure 4.6.7: In FKBP12 knockdown HeLa cells, rapamycin still affects S6K phosphorylation
HeLa cells were transfected with siRNA (non-targeting control or anti-FKBP12), starved and stimulated with FCS and insulin for 60 minutes in presence of 0-3 nM rapamycin. Cells were lysed and analyzed by immunoblotting. FKBP25 was detected as additional loading control.

4.7 – FKBP51 associates with mTORC2 and influences phosphorylation status of Akt:

4.7.1 – FKBP51 interacts with Rictor in a stimulation-dependent way:

As previous experiments demonstrated that FKBP12 and FKBP51 interact with mTORC1 in a rapamycin-dependent manner, we were also interested in assessing binding to mTORC2 although this complex is generally considered to be rapamycin-independent upon acute treatment.

In order to perform co-IP experiments with HeLa cells, we transfected them for simultaneous expression of HA-FKBP51 and myc-Rictor. When we analyzed the binding partners of immunoprecipitated HA-FKBP51, we found myc-Rictor to robustly interact with FKBP51 (see figure 4.7.1). Compared to background binding of myc-Rictor to HA-beads, most IP-signals of Rictor were clearly stronger. We did not find an obvious rapamycin-dependency of these interactions. Rather it can be stated that FKBP51 preferentially binds to Rictor in unstimulated cells; after serum-stimulation, the signal intensity decreased. Hsp90 recruitment could be detected, too; it runs in parallel with the Rictor signal.

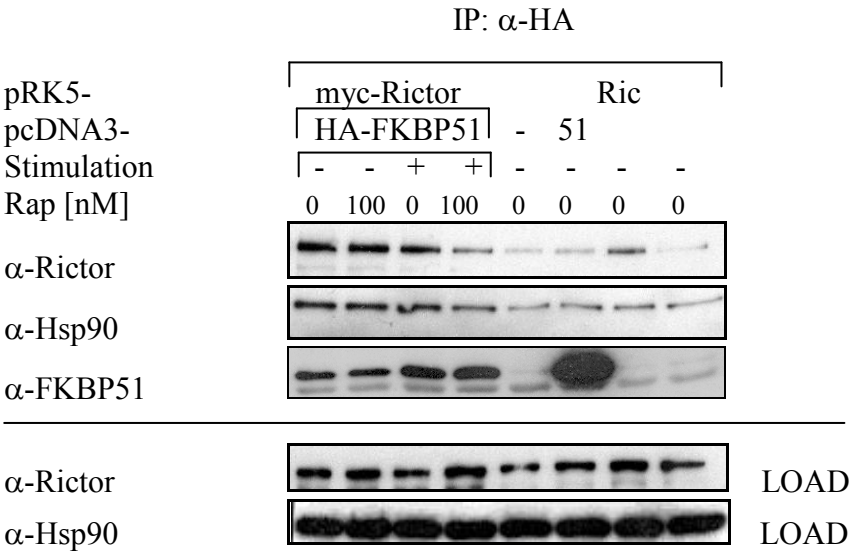

Figure 4.7.1: FKBP51 interacts with myc-Rictor in unstimulated HeLa cells

HeLa cells were transfected for expression of HA-FKBP51 and myc-Rictor. Cells were either starved or starved/stimulated with FCS for 24 h. Rapamycin was added as indicated for 60 minutes. Lysates were subjected to HA-IP. Beads were washed four times with CHAPS-containing lysis buffer and extracted by boiling. Eluates were analyzed by SDS-PAGE and immunoblotting.

We also performed this experiment with FKBP12. Here, binding to myc-Rictor was present mainly under conditions of serum-stimulation (see appendix, section 6.7).
In summary, these results suggest that FKBP51 interacts with the mTORC2 component Rictor. The interaction seems to be modulated by stimulation conditions, and a certain degree of Hsp90 recruitment might be involved in this process.

4.7.2 – FKBP51 mediates binding of the mTORC2 substrate Akt to Rictor:

As FKBP51 seems to associate with Rictor in mTORC2 complexes, we asked ourselves whether FKBP51 is involved in substrate recruitment. As the kinase Akt is the most prominent substrate of this TOR complex [141], we performed co-IP experiments in order to determine binding of Akt to Rictor in presence of FKBPs and rapamycin.
First, it turned out that Akt interacts with FKBP51. This finding was already described by Pei and colleagues [57], and we were able to verify it. Furthermore, we determined a clear rapamycin-dependency of this interaction which has not been demonstrated before (see figure 4.7.2A). Interestingly, endogenous FKBP51 was detectable as readily as overexpressed FLAG-FKBP51. As Hsp90 interacts strongly with FKBP51, the chaperone protein could be found in the complex, too. Under conditions of long-term rapamycin exposure, interaction with both FKBP51 and Hsp90 seemed to increase compared to short-term conditions.
More importantly, we checked for presence of the mTORC2 component Rictor in the Akt-FKBP complexes. Compared to background levels (lane 1, 2), Rictor protein was clearly enriched under conditions of FKBP51 overexpression. Strikingly, maximum Rictor signal intensity could only be detected in presence of rapamycin. This rapamycin-dependent binding pattern could be verified in 3 of 4 independent duplicates (marked as boxes in figure 4.7.2A; lanes 3,4 and 7,8 and 9,10) while it was inverted once (lanes 5,6). Nevertheless, rapamycin probably mediates an interaction of Akt, Rictor and FKBP51.
When we performed the same experiment with FLAG-FKBP12, 51TPRmut and 52, we realized that no comparable interaction with Akt and Rictor could be observed. Only for the FKBP51 TPR mutant, we detected some binding in absence of rapamycin; signal intensity was clearly below the one observed for FKBP51/rapamycin (see figure 4.7.2B).
In conclusion, these results demonstrate that interaction of Akt kinase with FKBP51 is rapamycin-dependent, and that the mTORC2 component Rictor can be found in the complex of Akt and FKBP51. To our knowledge, such an interaction of Akt and Rictor has not been described before.

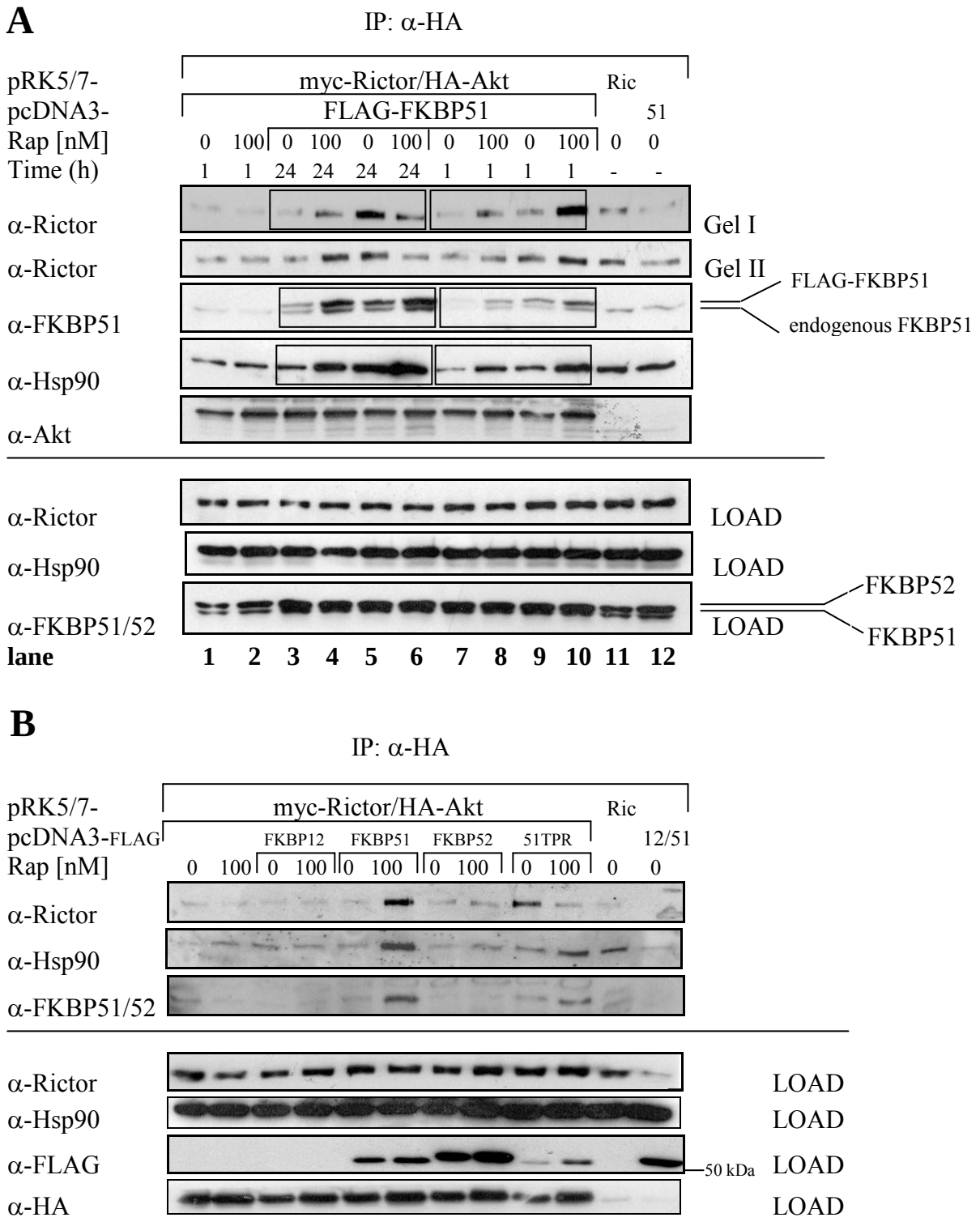

Figure 4.7.2: Rictor can be found associated with Akt in presence of FKBP51

(A) HeLa cells were transfected with myc-Rictor, HA-Akt and FLAG-FKBP12/51/51. After 24 h, medium was changed and cells were treated with rapamycin and insulin (each 100 nM) or vehicle for either 1 or 24 h, lysed and subjected to HA-IP. Beads were washed four times with TBS/0.3% CHAPS, extracted and analyzed by SDS-PAGE and immunoblotting. Lanes representing "load" are marked.

(B) Similar experiment as in (A), but only 1 h exposition to rapamycin (final concentration: 100 nM).

4.7.3 – In HeLa cells, FKBP51 overexpression increases Akt phosphorylation:

In order to assess whether FKBP51 is involved in Akt recruitment to mTORC2 via Rictor, we performed overexpression experiments in HeLa cells and determined phosphorylation of the mTORC2-dependent Akt residue S473. As rapamycin may be an essential mediator of Rictor/substrate assembly, we checked for Akt phosphorylation at different rapamycin concentrations.

The experiments revealed that FKBP51 overexpression generally raises rapamycin-dependent Akt phosphorylation: compared to mock conditions, FKBP51 overexpression increased mTORC2 activity toward Akt S473 up to 30% (see figure 4.7.3). This effect is clearly rapamycin-dependent, as basal phosphorylation levels are not significantly altered under conditions of FKBP51 overexpression. Importantly, these effects are short-term rapamycin effects: the small molecule was added for 1 h before cell lysis and analysis.

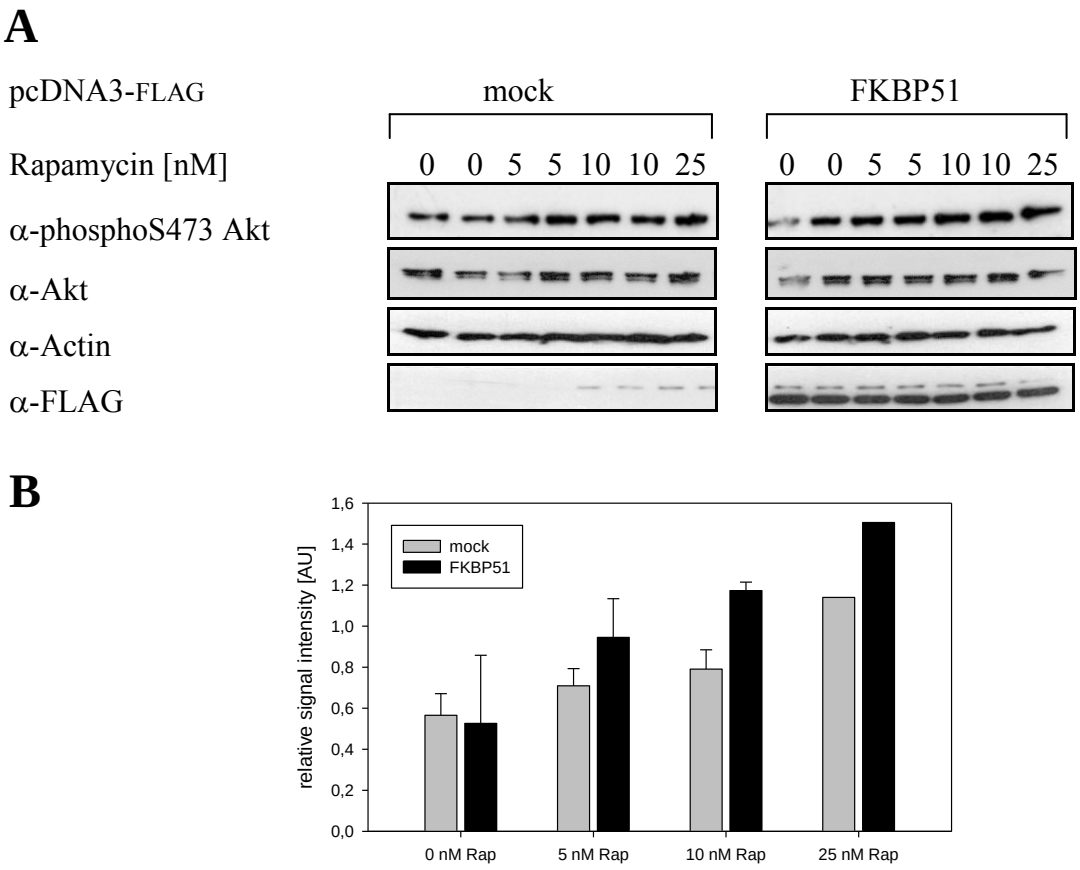

Figure 4.7.3: FKBP51 overexpression increases Akt phosphorylation in HeLa cells

HeLa cells were transfected for expression of FLAG-FKBP12/51/52. After 24 h, cells were starved (DMEM without serum). After another 24 h, cells were stimulated with serum and insulin for 60 minutes in presence of 0-25 nM rapamycin. Cells were lysed and subjected to immunoblotting analysis. (A) Western blot analysis and (B) densitometric analysis of phosphoS473 Akt signals (relative to load).

By increasing exposure time of rapamycin to 24 hours, the effect on Akt phosphorylation could be enhanced even more. As demonstrated in figure 4.7.4, FKBP51 overexpression resulted in a 90% increase in phosphoS473 signal compared to mock controls. For this effect, 3 nM rapamycin was sufficient. Control samples, supplemented with 5 nM torin1, displayed the expected reduction of Akt phosphorylation.

A

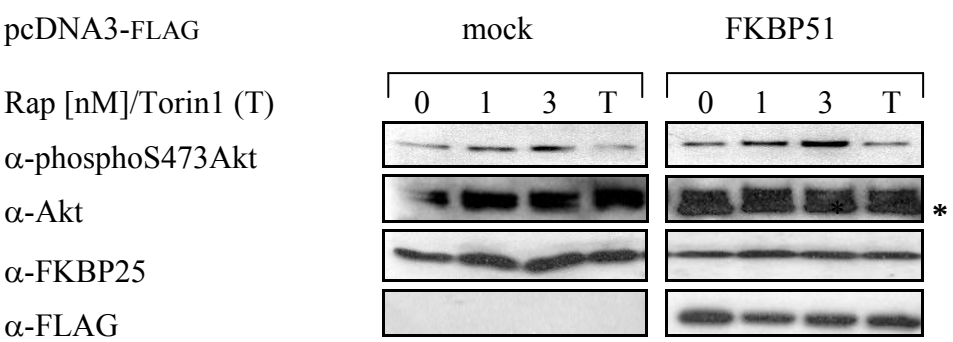

B

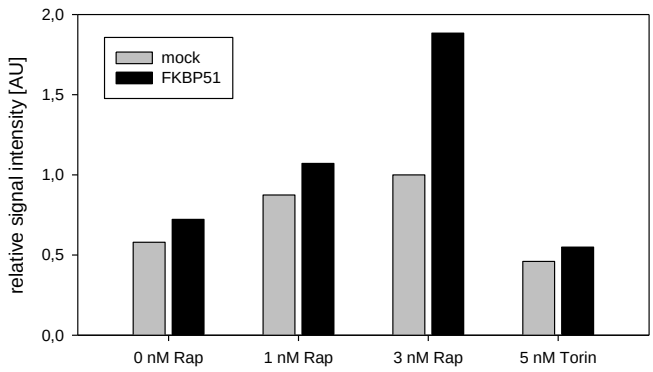

Figure 4.7.4: Effects of long-term rapamycin treatment on Akt phosphorylation are more pronounced

HeLa cells were transfected with human FLAG-FKBP51 and incubated for 24 h. Medium was changed (DMEM/FCS), and rapamycin/torin1 (T) was added (0-5 nM or 5 nM, as indicated). Cells were incubated for another 24 h, then lysed and subjected to immunoblotting analysis.

(A) Western blots; unspecific signals are marked (*).

(B) Quantification of phosphoS473 Akt signal intensities, relative to load (FKBP25)

Altogether, our results suggest that FKBP51 overexpression has increasing effects on rapamycin-dependent Akt phosphorylation in HeLa cells. While basal phosphoS473 signal is unaltered, intensity increases significantly after short- or long-term exposure to rapamycin. For this effect, rapamycin concentrations of 10 nM (short-term) and 3 nM (long-term) are sufficient.

5 – Discussion:

5.1 – Different FKBPs can be involved in rapamycin-dependent mTOR regulation:

5.1.1 – All ternary complexes of FRB*rapamycin*FKBP have similar structures:

Initially, we performed *in vitro* binding assays in order to determine binding of different FKBP proteins to the FRB domain of mTOR (see section 4.2). These experiments revealed that FKBP12 is just one of many FKBPs that form ternary complexes with FRB in presence of rapamycin: the large FKBPs FKBP51 and FKBP52 displayed comparably affine binding as the smaller FKBPs FKBP12.6, FKBP13 and FKBP25. Importantly, EC_{50} values for complex formation cluster below 30 nM, suggesting a possible competition for binding to FRB/mTOR *in vivo*.

Indeed, our structure determination of the alternative ternary complexes FRB*rapamycin*FK1 FKBP51/52 revealed that these FKBPs are able to form rapamycin-mediated complexes with the FRB domain of mTOR. Binding mode and structure architecture are very similar to FKBP12 (see section 4.5). Thus, it may be possible that these alternative complexes are present *in vivo* and might contribute to the effects generated by rapamycin in living cells.

Structural comparison of the three ternary complexes FRB*rapamycin*FKBP:

The FK1 domains of all immunophilins are highly conserved and very similar to the archetypical FKBP12 (see figure 5.1). Hereby, the overall residue similarity between FKBP12 and FK1 FKBP51 is 64%, while 50% of the residues are identical. For FK1 of FKBP52, 53% of the residues are identical to FKBP12, while similarity reaches 64%. When the FK1 domains of FKBP51 and FKBP52 are directly compared, an even higher identity of 62% is yielded with an overall similarity of 75%.

Our crystal structures demonstrate that the binding of rapamycin as observed in the FK1 domains of FKBP51 and FKBP52 is highly similar to FKBP12, involving mainly conserved residues. 12 of the 13 residues interacting with rapamycin are identical in FK1 FKBP51 and FKBP52 (K121 is unique in FK1 52, R73 in 51), and FKBP12 shares 9 interacting residues with 51/52 (apart from Q53, E54 and I91). The total number of hydrophobic contacts is very similar in all three cases, and the contribution of one additional H-bond in FKBP51 via R73 is

hard to estimate. In general, it is assumed that one H-bond can contribute up to 10-20 kJ/mol to the binding energy, while one hydrophobic interaction provides only around 2-5 kJ/mol [286]. Furthermore, hydrophobic contacts occur as clusters while H-bonds are well defined and directional. Thus, missing interactions of one kind could easily be compensated by other kinds of interactions.

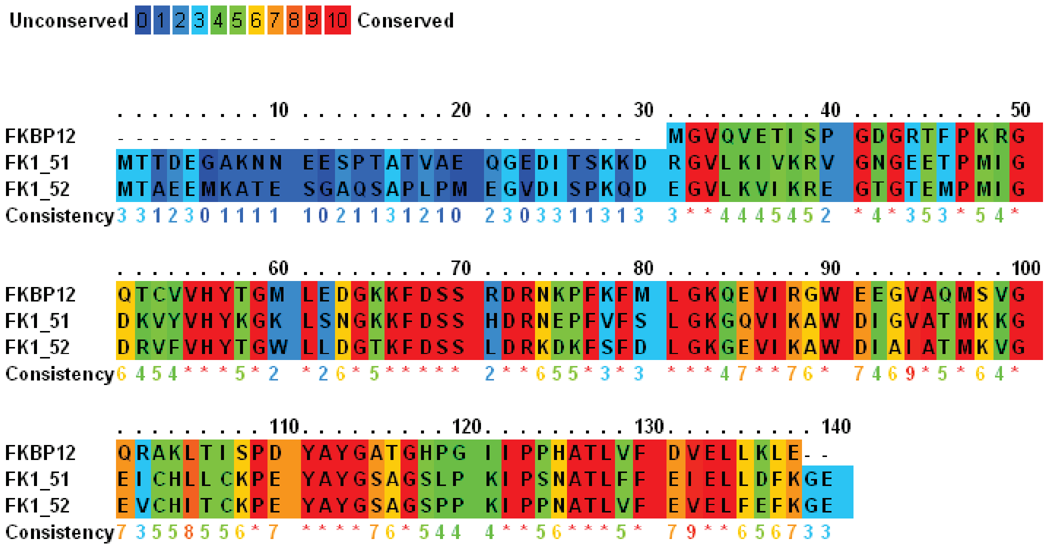

Figure 5.1: The protein sequences of the FK1 domains of human FKBPs are conserved

PRALINE representation of a multiple sequence alignment [287], indicating the degree of consistency for human FKBP12, FK1 FKBP51 (FK1_51) and FK1 FKBP52 (FK1_52).

As the complex formation with FRB is almost exclusively mediated by the small molecule rapamycin, no differences between the three complex structures were expected concerning this part of the complex: FRB interacts with the triene arm of rapamycin, and this interaction is apparently not influenced by the FKBP binding partner, resulting in a high degree of similarity of the binding mode for all three FKBPs. Some residues, for example Y2105, are slightly shifted and therefore display variations in the number of hydrophobic contacts (see appendix section 6.6.4). For R2036, contacts to rapamycin within 4 Å can be detected in the ternary complexes of FKBP12 and FKBP51, but they are located only slightly below the cut-off of the contact search engine. A minor shift of the arginine's position in FKBP52 locates it at 4.1 Å; thus, these contacts are not detected by the algorithm. Nevertheless, it is probable that these contacts are comparably important as the ones below 4 Å even if binding energy crucially depends on the distance. Since the contribution of these subtle variations can hardly be assessed, it must be assumed that missing contacts at one position are balanced by some additional ones at another position. This is also reflected in the fact that the total number of

FRB-rapamycin interactions is very similar (ternary complex FKBP12:42; FKBP51:42; FKBP52: 45).

Direct protein-protein interactions are underrepresented in the ternary complexes, and it must be hypothesized that crucial interactions are mediated by the shared ligand rapamycin. Nevertheless, direct contacts between FKBP and FRB might contribute to stabilization of the complexes. Importantly, the total number of direct protein-protein interactions is different between the three complexes, and in FKBP51 the 40S region seems to engage in an especially high number of contacts to FRB. As the pattern of direct contacts between FRB and FKBP12 and FKBP52 is well comparable, it appears that in both cases high-affine, direct binding of the protein partners is less probable. This hypothesis is also supported by the networks of water-mediated H-bonds which are much more expanded between the binding partners FKBP51 and FRB.

Strikingly, the residues involved in direct interactions of FRB and FKBPs differ significantly: only 2 of these residues are conserved in FKBP12, 51 and 52, although general similarity of FKBPs suggests a higher degree of conservation. The sequence position of the residues is more consistent, reflecting their position in the 40S and 80S loops. Nevertheless, structural heterogeneity seems to be big enough to favor one residue in one structure over the adjacent one in another ternary complex (see figure 5.2). Altogether, the substantial deviations in direct protein-protein contacts between FRB and FKBPs may indicate that these interactions act mainly as a supporting feature in order to strengthen the rapamycin-induced assembly of the ternary complex. Thus, these peripheral contacts might be much more tolerant towards variations in number, position and strength without affecting the central rapamycin binding in a negative manner.

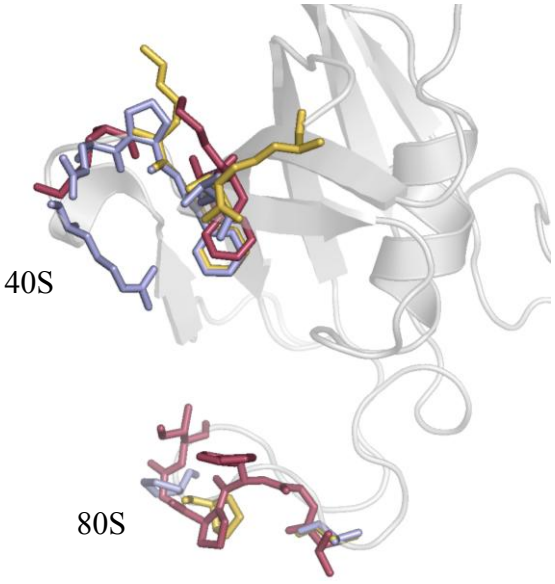

Figure 5.2: Residues involved in direct protein-protein contacts are less conserved
Amino acids of FKBP12 (red), FK1 FKBP51 (blue) and FK1 FKBP52 (yellow) that interact with FRB are shown as stick representation. A complete list can be found in the appendix, section 6.6.2.

We observed in our FP binding assays that the rapamycin-derivative CK97 binds to the isolated FRB domain of mTOR in absence of any FKBP binding partner (see appendix section 6.8). Normally, it is assumed that the pre-formed complex of FKBP and rapamycin binds to FRB with low nanomolar affinity, while rapamycin alone displays a much weaker binding (26 μM; 490 nM for Fluorescein-Rapamycin, as reported in [276]). We determined an EC_{50} value of 290 nM for CK97 and 1.04 μM for rapamycin (IC_{50} value, determined in competition experiments) which is relatively low compared to other reports; nevertheless, the values differs by two orders of magnitude from FKBP*rapamycin complex binding.

When the number of contacts between the protein domains and rapamycin is determined, there are strikingly less contacts between FRB and rapamycin (44 in structure "2fap") than between FKBPs and rapamycin (100 in "2fap"). Additionally, all these contacts are purely hydrophobic and therefore relatively week; H-bonds that contribute much stronger to increasing binding affinity are not present at all. Thus, these differences might be an explanation for the weaker binding of rapamycin to FRB.

Since the binding affinities of isolated rapamycin and the FKBP12*rapamycin complex differ a lot, it can be speculated whether the direct protein-protein contacts between FRB and FKBP are crucially involved in stabilizing the complex. Our analysis of the residues forming this interface in the three ternary complex rather suggest that due to the big variability these contacts have a more random character and are less conserved. Nevertheless, mutational analysis of the residues might be interesting in order to shed a light on their importance in interface formation.

Initially, FKBP12 was considered as the only cellular target mediating the inhibitory effects of rapamycin on mTOR. Apart from that, FKBP12.6, a highly related homologue to FKBP12 with partially overlapping functions, was also found to allow the ternary complex formation with rapamycin and FRB-mTOR [74]. Later, researchers tried to deduce the structure of alternative ternary complexes by superimposing structures of rapamycin-complexed FKBP13 and FKBP25 with the FKBP12*rapamycin crystal structure: they argued that within the 80S loop there are unfavorable sterical clashed that would not allow stable complex formation with FRB [111]. Although our results proof highly affine binding and thus indicate that complex formation with FRB is possible, FKBP13 and FKBP25 are probably not involved in complex formation *in vivo*: they are located mainly in the ER and in the nucleus, respectively. Only very recently, FKBP38 has been proposed as a player in rapamycin-independent mTOR inhibition by competition with Rheb GTPase for mTOR binding [113]. Here, a rapamycin-

independent binding to mTOR was implicated. Such binding presumably does not involve FRB but rather happens elsewhere in the mTOR complex.

Different FKBPs regulate calcineurin activity in presence of FK506:

The structure of the ternary complex FKBP12*FK506*calcineurin [288, 289] substantially differs from the complexes of FKBPs with rapamycin and FRB, although the small molecules are bound to the FKBP moiety in very similar manners. Due to the larger ring size of rapamycin, the distance between the two interacting proteins is bigger than in the complex with FK506 and calcineurin. Therefore, direct protein-protein contacts are limited in the first case, whereas FKBP12 and calcineurin engage in more intensive interactions (see figure 5.3). While FKBP12 binds to FRB mainly via its 40S and 80S regions, its interactions with calcineurin are more diverse, including some residues adjacent to the 80S loop. The ligand FK506 is almost completely buried between residues of FKBP12 and FRB that interact with each other; in contrast, big parts of rapamycin are solvent-accessible. Altogether, 18 residues in calcineurin engage with FKBP12 via direct protein-protein contacts, while there are only 9 in FRB (see section 4.5.3.2).

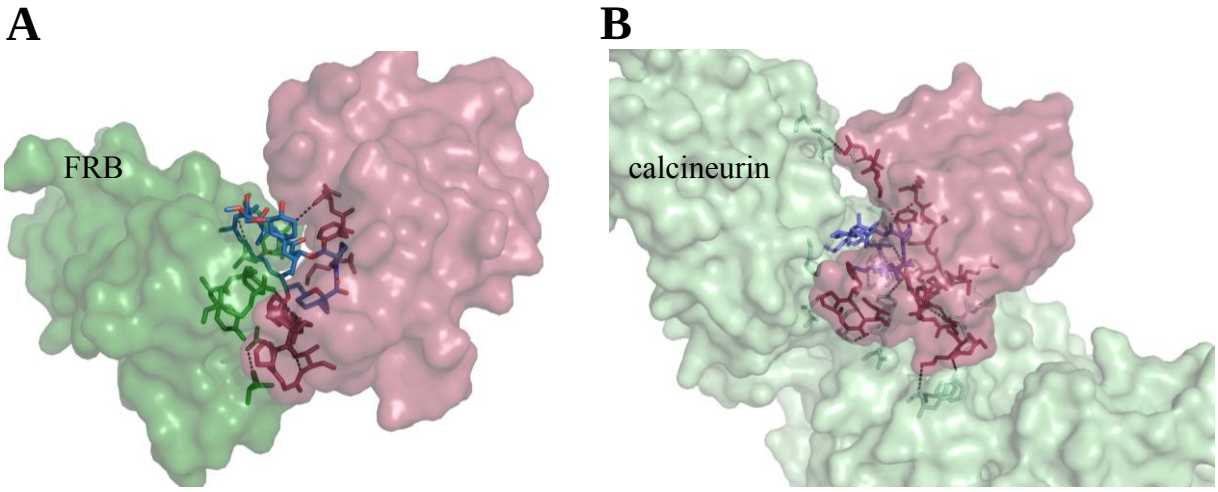

Figure 5.3: FKBP12*FK506 interacts more intensively with calcineurin than FKBP12*rapamycin does with FRB

(A) Surface representation of the ternary complex FRB*rapamycin*FKBP12 (2fap)

(B) Surface representation of the ternary complex calcineurin*FK506*FKBP12 (1tco)

Colour scheme: red: FKBP12; green: FRB; pale green: calcineurin; blue: rapamycin/FK506.

Weiwad and Edlich characterized calcineurin inhibition by different FKBPs in an *in vitro* assay [290]. Although binding to FK506 happens with high affinity, only FKBP12, 12.6 and 51 were able to form a complex with calcineurin and inhibit kinase activity effectively. These differences can be explained by substitution of two critical residues of FKBP12 that interfere with binding to calcineurin in some FKBPs. In contrast to these results, we observed comparable IC_{50} values for mTOR inhibition by all tested FKBP proteins (see section 4.3.1). This might be explained by a high degree of conservation between FKBP residues involved in rapamycin binding, in contrast to a putatively reduced importance and high variability of residues involved in direct contacts to FRB.

Similarly to our results for FRET mTOR activity assays, it has been found that FKBP51 can replace FKBP12 in inhibiting calcineurin activity *in vitro* in a weaker, but clearly FK506-dependent manner [34]. Later, it has been demonstrated in pulldown assays that FKBP51 can be bound to calcineurin even in absence of FK506, and that this alternative binding mode demands the C-terminal domain of FKBP51 [291]. Nevertheless, overexpression of FKBP51 did not affect calcineurin activity *in vivo*. In contrast, we were able to demonstrate rapamycin-dependent effects of FKBP51 on mTOR activity, assessed by quantification of S6Kinase phosphorylation (see section 4.6.5).

5.1.2 – FKBP51 is more abundant than FKBP12 in some tissues:

In all our *in vitro* experiments we demonstrate that FKBP51 can be involved in rapamycin-dependent inhibition of mTOR activity. Furthermore, the effects of the larger FKBP appear to be more pronounced than those of FKBP12 in terms of degree of *in vivo* inhibition (see section 4.6.5). Thus, it could be argued that actually FKBP51 might be a main mediator of rapamycin action in some tissues *in vivo*.

Most of FKBP family members bind to rapamycin with comparably high affinity. Consequently, a mixture of FKBP proteins will compete for binding to rapamycin when the compound is administered. While rapamycin-bound FKBP12 will certainly participate in FRB binding and mTOR inhibition, other FKBP proteins might form non-productive complexes with rapamycin due to their localization in the ER or the nucleus which results in sequestering the compound from its actual destination. Nevertheless, a small fraction of FKBP12*rapamycin seems to be sufficient for mTOR inhibition, as rapamycin exerts its action in a concentration range below 5 nM. Thus, the actual concentration of active complex

might be in the low nM range, sufficient for successful inhibition of the mTOR protein (80.000 - 200.000 copies per HeLa cell [292]). As very small amounts of FKBP*rapamycin complexes seem to be effective, it appears rather probable that FRB binding and mTOR inhibition is executed by the FKBP complex species that is most abundant in the cell. In the case of roughly similar concentration levels, these FKBPs might contribute equally to mTOR inhibition.

Whether this hypothesis is true depends largely on the abundance of FKBPs in living cells, comprising protein concentration and availability in the cytosol. Consequently, in the case of a high molar excess of one FKBP compared to another, the effect of the second should be more or less negligible.

Baughman and Wiederrecht characterized the tissue distribution and cellular concentration of FKBP51 and directly compared it to FKBP12 [19]. They found that FKBP51 is more abundant in 11 of 17 tissues, with rates of molar excess of 2-fold up to 12-fold. In kidneys, they quantified the ratio of FKBP51:FKBP12 with 3.5, while the value reaches 7.3 in the heart and even 11.6 in the liver. As FKBP51 and FKBP12 are both present in the cytosol, FKBP51 possibly competes with FKBP12 for binding to rapamycin, and FKBP51 might be the major component of the inhibitory rapamycin complex. Thus, it may be responsible for the majority of rapamycin-mediated effects in certain cell types that hitherto have been assigned to FKBP12.

Furthermore, mRNA quantification revealed that FKBP51 is highly overexpressed especially in adipocytes and in skeletal muscle cells, compared to median expression [293]. Therefore, these tissues might be especially rapamycin-sensitive. Furthermore, these cell types are linked to insulin action, and altered mTOR pathway activity plays a crucial role in development of insulin resistance and diabetes [294].

When we performed RNAi experiments for knockdown of FKBP12, we did not see a substantial decrease in mTOR inhibition by rapamycin: S6Kinase T389 phosphorylation was largely unaltered compared to control conditions (see section 4.6.6). This result further consolidates our hypothesis that FKBP51 is indeed able to replace FKBP12 function, and that FKBP51 mediates the inhibitory effect of rapamycin on mTOR kinase activity.

Nevertheless, it must be kept in mind that knockdown by means of siRNA is never quantitative. In our case, up to 10% of the total FKBP12 still might be present in knockdown cells, and this concentration might be sufficient for effective rapamycin-dependent mTOR inhibition, as discussed before. More reliable experiments could be performed with FKBP12KO MEF cells because they lack any background levels of FKBP12.

Generally, tissue-selective mTOR inhibition appears attractive, because classical, systemic rapamycin treatment causes potent immunosuppression in patients by acting on T cell proliferation [295]. Other side effect like nausea, fatigue and diarrhoea are quite common among patients [296]. Furthermore, the small molecule exerts toxic effects on the lungs, triggering severe pulmonary inflammation in some cases [297, 298]. In order to avoid global mTOR inhibition mainly mediated by FKBP12, a rapamycin analogue would be useful that binds selectively to FKBP51. Like this, cells that display high expression levels of FKBP51 could be selectively targeted for inhibition. In contrast, mTOR activity would remain unaffected in cells with FKBP51 levels that are insufficient for mediating the inhibitory effect of the rapamycin-derivative. Unfortunately, the rapalogues we tested in FRET binding assays did not show any selectivity for different FKBPs (see section 4.2.2). Also, considering the highly conserved rapamycin binding pocket of FKBP12 and FKBP51, it appears challenging to achieve total selectivity. Nevertheless, research with model compounds suggests that it might be possible to generate at least preferential binding to one FKBP (Steffen Gaali, MPI of Psychiatry, personal communication, May 2011). Our crystal structures of the alternative ternary complex can also be considered as excellent starting points for rational design of FKBP51-specific compounds.

5.1.3 – Possible mechanism of mTOR inhibition by large FKBPs:

Based on the cryo-EM mTOR complex structure:

Very recently, Yip and colleagues analyzed cryo-electron microscopic structures of mTOR complex 1 and proposed a model of rapamycin action on complex integrity [112]. They observed that FKBP12*rapamycin binds to the FRB domain of mTOR, just opposite to the substrate recruiter Raptor. Notably, one complex FKBP12*rapamycin is bound to one mTORC1 dimer (see figure 5.4). This initial binding results in a weakening of the mTOR-raptor interaction which forms the main interface of the dimer. Increasing structural fluctuation might trigger the binding of a second FKBP12*rapamycin complex, resulting in proceeding disassembly of mTORC1 dimers over time. Interestingly, S6Kinase can even be phosphorylated by monomeric mTOR, while the substrate 4E-BP1 is strictly obliged to the intact dimeric form.

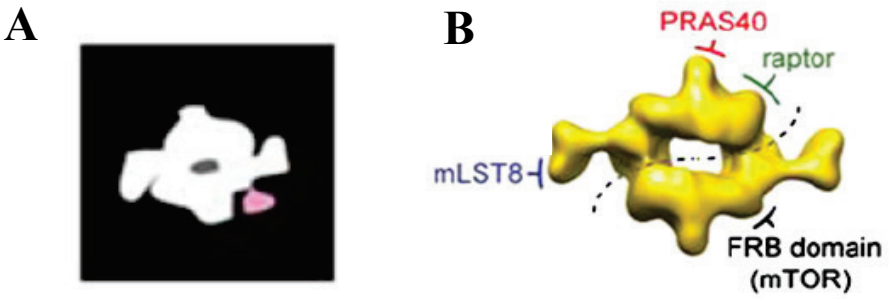

Figure 5.4: Model representation of dimeric mTOR and the FKBP12*rapamycin binding site
(A) Original cryo-EM image of mTORC1 dimers (white) in complex with FKBP12*rapamycin (pink)
(B) Model of mTOR dimers: dimer interface and individual components are indicated. Location of the FRB domain is shown. Taken from [112] , image 4A.

The EM image of mTORC1 in complex with FKBP12 and rapamycin shows clearly that FKBP12 is bound to the readily accessible FRB domain, and that this binding does not appear sterically challenging: both mLST8 and PRAS40 are also bound to mTOR in such a way that they do not interfere with FKBP12 binding. Thus, it might be concluded that this binding mode also allows accommodation of the larger multi-domain FKBP51 at the FRB site of mTOR.
The authors claim that binding of one FKBP12*rapamycin also may block the entry of big substrates like S6Kinase into the active site. Regarding this assumption, it could be speculated that a larger FKBP molecule might represent a more effective steric hindrance compared to small FKBP12. Unfortunately it is not known how the single domains of multi-domain FKBP51 are oriented within a complex with mTORC1.
As the degree of mTORC1 dimer dissociation cannot be estimated by SDS PAGE analysis, it is not clear whether binding of FKBP51/52 to the complex triggers disassembly differently than binding of FKBP12 does. It might be possible that the larger FKBPs affect the integrity of the complex more efficiently, resulting in a faster release of mTORC1 monomers. The degree of interaction with the monomers may also differ between the small and the large FKBPs.

<u>Based on the conventional mechanism of FKBP*rapamycin action:</u>

In all our co-immunoprecipitation experiments, we used detergents and salt concentrations that allow purification of intact mTORC1 complexes. As S6Kinase is recruited to mTOR

kinase by the scaffolding protein Raptor [129], and as S6Kinase therefore might be an intermittent part of the complex, it is unclear how interactions of S6Kinase and FKBPs occur. Several scenarios are possible: first, S6Kinase might be bound to mTORC1, and FKBPs interact with the FRB domain of mTOR. Thus, S6Kinase and FKBPs would not bind to each other; the interaction would be perfectly indirect. This option appears to be the most realistic one. Secondly, mTORC1-bound S6Kinase may recruit free FKBPs. Such a scenario demands a plausible explanation for the rapamycin-dependent binding mode which cannot be provided readily. Finally, free S6Kinase might directly interact with unbound FKBPs. Again, no mechanism is known that includes rapamycin in such a case.

As a fundamental mechanism of rapamycin action, a competition of binding to the mTOR complex 1 between Raptor and FKBP12*rapamycin has been proposed [131]: after FKBP12 has bound to the FRB domain of mTOR, Raptor is released from its binding site, resulting in abolishment of substrate phosphorylation by the mTOR kinase active site. Thus, at rapamycin concentrations of 100 nM and above, less Raptor is detected in immunoprecipitations of mTORC1. 500 nM rapamycin are necessary to reduce Raptor signal completely [299]. Presumably, the same result should be obtained for S6Kinase because this protein is recruited to mTORC1 by Raptor.

In contrast, the results of our co-IP experiments showed a different binding pattern: we observed that in presence of rapamycin Raptor interaction with S6Kinase was increased, and FKBPs were part of these complexes (see section 4.6.4). This might be explained by a mechanism that differs slightly from the one described above: instead of perfectly blocking the access to the active site in presence of rapamycin and therefore inducing the release and dissociation of the S6Kinase*Raptor complex, the FKBPs might bind to mTORC1 in a rapamycin-mediated manner. This binding is compatible with Raptor*S6Kinase remaining part of the complex, hypothetically accompanied by reduced S6Kinase release from Raptor (as the substrate remains unphosphorylated). Thus, in co-IP experiments, FKBPs interact only in presence of rapamycin (see scheme in figure 5.5), and the binding of Raptor and S6Kinase increases in a rapamycin-dependent manner.

Unfortunately, we were not able to determine whether Raptor remains part of the complex or whether it is rather expelled from mTORC1 as a consequence of FKBP binding. But as rapamycin-dependent FKBP binding is restricted to the FRB domain of mTOR, it must be assumed that Raptor stays an integral part of mTORC1.

Altogether, it can be concluded that our results from co-IP experiments rather support a mechanism of FKBP*rapamycin action that involves sequential binding of the FKBP to the

complex which does not result in an immediate dissociation of the complex (especially of the mTORC1 component Raptor).

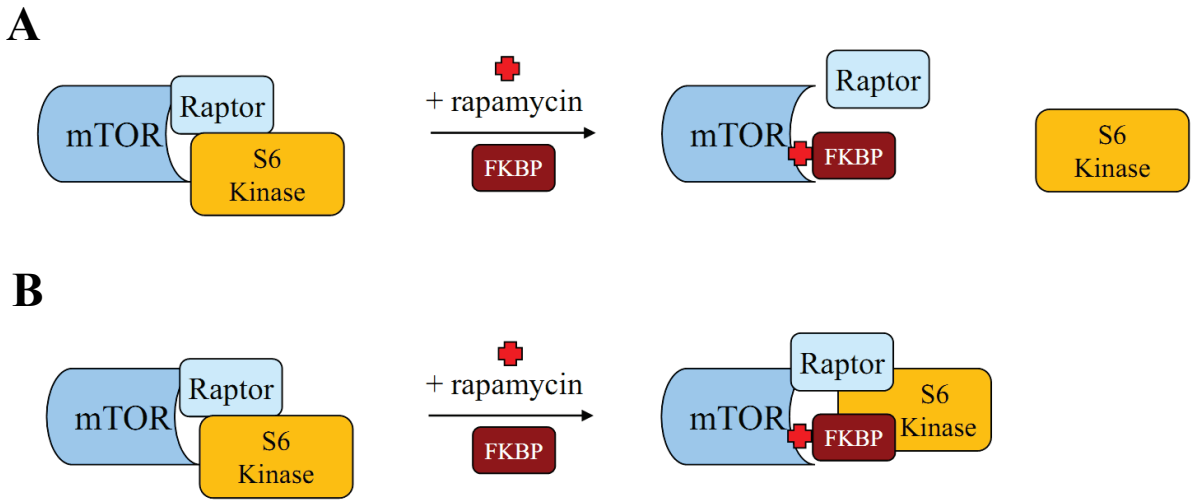

Figure 5.5: Schematic representation of rapamycin-mediated S6Kinase release from mTORC1

(A) Conventional mechanism of competitive binding of Raptor and FKBP*rapamycin to mTORC1

(B) Proposed mechanism for FKBP blocking S6Kinase phosphorylation at the active site

5.1.4 – mTOR inhibition in yeast: a valid model system?

In a FKBP-deficient yeast cell system which is resistant to growth inhibition by rapamycin, we expressed the FK1 domain of FKBP51 and observed restored rapamycin sensitivity (see section 4.4). This demonstrates that FKBP51 can mediate rapamycin-dependent mTOR inhibition in this model organism which may implicate that FKBP12 function in presence of rapamycin can generally be executed by FKBP51. Importantly, this finding is only conclusive under conditions of conserved mTOR structure and functionality between the species.

TOR was originally discovered in yeast cells represented by the two gene products TOR1 and TOR2, and two distinct complexes were characterized [126]. KOG1, the yeast homologue of Raptor, interacts with TOR1/2 to form TORC1, which controls different growth-associated downstream targets and is rapamycin-sensitive. The structure of this complex has been determined by EM [300], revealing a 1:1 stoichiometry: one TOR molecule engages intensively with one KOG1, and interactions comprise most of the domains in both proteins. The N-terminal domain of KOG1 is oriented toward the kinase domain of TOR and allows recruitment of substrates to the active site. Unlike in the mammalian complex, binding of FKBP12*rapamycin to yeast TORC1 does not weaken the binding of KOG1 to TOR [126].

The authors speculate whether in the yeast system binding of FKBP12*rapamycin to the FRB domain might either interfere with substrate presentation or might directly inhibit TOR kinase activity by interacting with the adjacent active site.
Altogether, it must be stated that the structure of yeast and mammalian TORC1 differs considerably, and that the proposed mechanism of inhibition of the mammalian form cannot be transferred to yeast conditions: while disruption of the dimeric state plays an important role in mammals, TOR complexes seems to be generally monomeric in yeast. Maybe the more advanced weakening of Raptor interactions with mTOR might be accompanied by the more archetypical direct interactions with the active site.
In yeast cells, no homologues of the larger human FKBPs are present [301], implicating that the FK1 domains of large FKBPs are sufficient for the inhibitory effect on TOR. Indeed, we observed this effect for human FKBP51, whose FK1 domain mediated growth arrest; the full-length variant turned out to be cytotoxic in yeast. Thus, rapamycin-dependent effects could not be fully separated from unspecific ones.

5.1.5 - mTOR *in vitro* kinase assay and its limitations:

By overexpressing different FKBPs and examining the phosphorylation state of S6Kinase in HeLa cells, we were able to demonstrate influences of FKBPs on mTOR activity *in vivo* (see section 4.6.5). On the one hand, it is very convenient to perform such an assay in a cellular system where all components of mTOR complexes and substrates are present. On the other hand, the unpredictability of cellular processes and the still limited knowledge of mTOR complex regulation *in vivo* make the assay difficult to control, and the results should be interpreted with caution.
In order to overcome these obstacles we performed an *in vitro* mTORC1 kinase assay with immunoprecipitated HA-S6Kinase and mTORC1. As the precipitate of HA-S6K was washed extensively with “triton X-100”-containing buffer, it was stripped and did not contain any additional proteins. mTORC1 preparation was purified with a CHAPS-containing buffer, maintaining complex integrity under these mild detergent conditions [129]. Thus, mTORC1 contains mTOR, Raptor and mLST8 [126, 157]. This well-defined composition allows the performance of *in vitro* kinase assays with addition or omission of recombinant FKBPs, therefore making reaction conditions much more controllable.

Nevertheless, it must be considered that immunoprecipitated and even carefully washed mTOR complex 1 might contain additional, maybe unknown proteins that are not present under all washing conditions. During our *in vitro* kinase assays we observed that addition of rapamycin inhibited mTOR activity toward 4E-BP1 even in absence of any FKBP (see figure 5.6).

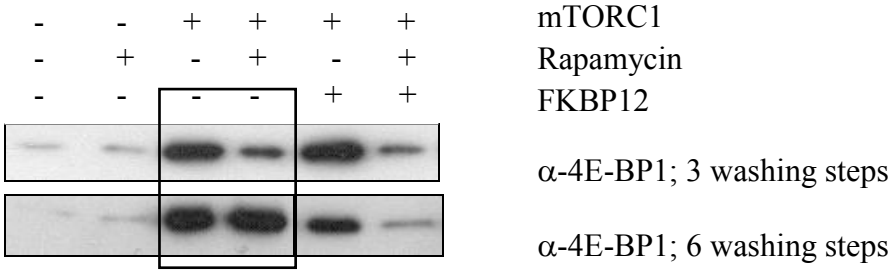

Figure 5.6: Influence of washing steps on mTOR *in vitro* kinase assay

In vitro kinase assay, performed with 4E-BP1 as substrate and mTORC1 preparations as described in section 4.3.2. mTORC1 immunoprecipitate has been washed 3 times or 6 times.

For troubleshooting, we doubled the number of washing steps and realized that excessive washing eliminated the artefact. Thus, we concluded that some endogenous FKBPs bind to mTORC1 even in absence of rapamycin, and that this interaction is strong enough to survive normal washing procedures.

5.2 – FKBP51 can exert rapamycin-independent effects on mTOR:

5.2.1 – Functions of FKBP51 within or outside of the mTOR complexes:

In our co-IP experiments, we were able to detect rapamycin-dependent interaction of FKBP12 and FKBP51 with mTOR (see section 4.6.1). Considering the crystal structure with its intensive rapamycin-mediated contacts and its few direct protein-protein interactions, rapamycin apparently represents the crucial mediator of binding.

Surprisingly, we also observed rapamycin-independent binding, especially in the case of FKBP51. As the mTOR complexes present themselves as multi-protein complexes, it seems probable that these kinds of interactions occur elsewhere in the big complex, but not necessarily within the FRB domain. Maybe rapamycin-independent binding does not involve

mTOR itself, but rather adaptor proteins (substrate recruiters like Raptor or Rictor) or even the mTOR substrates like S6Kinase and Akt kinase.
Also, it could be speculated that FKBPs might play a role in modifying the activity or affinity of certain parts of the complex. Co-chaperones like FKBP51 are considerably good candidates for assisting target proteins in maintaining or modifying their structure. This can be observed in the glucocorticoid receptor complex where alternative binding of FKBP51 and FKBP52 promotes maturation of the receptor [302]. Thus, multiple tasks can possibly be executed by FKBPs within a multi-protein complex.
Connected to the idea of chaperoning function, it has been reported recently that mTORC2 is involved in stabilization of Akt protein: the complex associates with polysomes, binds to newly synthesized Akt polypeptide and phosphorylates Akt at its turn motif residue T450. This co-translational modification assures proper folding of the kinase and prevents it from being ubiquitinylated [303]. A role of co-chaperones within such a complex appears reasonable.
Very recently, FKBP51 has been established as a negative regulator of the Akt signaling pathway: it functions as a scaffolding protein to recruit the phosphatase PHLPP to Akt, resulting in decreased survival signaling. Thus, certain cell lines are more susceptible to chemotherapeuticals. Interestingly, FKBP51 is downregulated in a number of cancer cell lines [57] and might be considered as a tumour suppressor protein.

The above findings indicate that the classical view of FKBP action being limited to rapamycin and the FRB domain of mTOR might be out-dated. As this function seems to be mainly connected to the ability of FKBPs to bind rapamycin, recent reports clearly suggest additional regulatory influences that focus on the original co-chaperone and scaffolding function of these proteins. Maybe both rapamycin-dependent and rapamycin-independent effects cooperate for mediating regulation of mTOR complexes and the substrates, respectively. Further research, especially including methods of FKBP truncation and PPIase inactivation, will be necessary in order to assess the underlying mechanisms of these processes.

5.2.2 – FKBP51 and Hsp90:

In T cells, Hsp90 has been reported to interact with Raptor. When the Hsp90 inhibitor geldanamycin is administered, Raptor expression is reduced, resulting in decreased mTORC1

signaling [299]. In co-IP experiments performed in HeLa cells, we observed a slight increase in Hsp90 recruitments when FKBP51 interaction with either Raptor or mTOR was assesses (see sections 4.6.1 and 4.6.2). This finding may point to a rapamycin-independent function of FKBP51: it might be involved in recruiting Hsp90 to the complex, where the heat shock protein interacts especially with Raptor.

Takai and colleagues proposed another important role for Hsp90 in mTOR complex maturation [292, 304]: together with Tel2, the chaperone is necessary for stabilization of immature mTOR until it has established the interactions with its partner proteins. Again, a rapamycin-independent role of FKBP51 as a co-chaperone could be possible, namely by mediating Hsp90 recruitment to the early mTOR*Raptor complex. As these processes occur during the maturation procedure, the involved chaperone proteins could not be detected in the complete mTOR complexes; thus, their detection is not possible with classical co-IP, but it demands more advanced pulse-chase techniques.

In osteosarcoma cells, the Hsp90 inhibitor 17-AAG (17-N-Allylamino-17-demethoxy-geldanamycin) was a potent inducer of apoptosis, in parts by inhibiting mTOR signaling and subsequent phosphorylation of all proteins involved [305]. Rapamycin was rather effective in affecting cell cycle progression, but it also reduced phosphorylation of Akt, mTOR and S6Kinase. The effects of 17-AAG clearly indicate that Hsp90 plays an important role in mTOR signaling. Again, a role of co-chaperones like FKBP51 or FKBP52 appears probable.

5.3 – Possible side-effects of FKBP51 on other signaling pathways:

When overexpressed in HeLa cells, we observed that FKBP51 decreases S6Kinase phosphorylation in a rapamycin-dependent manner (see section 4.6.5). This result indicates that FKBP51 exerts an inhibitory effect on mTOR in presence of the small molecule. Nevertheless, it must be considered that plasmid-based protein overexpression may influence different cellular processes and that such side-effects might influence the outcome of experiments.

In 2002, Giraudier and colleagues discovered that FKBP51 is overexpressed in patients with malignant bone marrow, and that overexpression of FKBP51 in these megakaryocytes renders them resistant to apoptosis [306]. They postulated that this effect may be caused by inhibition of the phosphatase calcineurin which is normally considered to be regulated by FKBP12*FK506. As calcineurin activates pro-apoptotic genes via NF-AT dephosphorylation,

FKBP51 suppresses programmed cell death and favors cell survival under cytokine deprivation. Other groups also discuss an involvement of the JAK/STAT pathway [307].

Unlike regulation of calcineurin or mTOR, the effects of FKBP51 on glucocorticoid receptor are well characterized [39, 41, 308]: presumably by binding to the receptor, FKBP51 reduces binding affinity of cortisol and thus inhibits transcriptional activation of GR-regulated genes. Glucocorticoids are used in clinical treatment of patients suffering from lymphoma and leukemia as these hormones slow down growth of malignant cells. Similarly, glucocorticoids display anti-proliferative action against different types of adenocarcinoma [309, 310], while they stimulate the growth of others [311].

Furthermore, a Japanese group reported that FKBP51 expression in colon cancer cells suppresses cell growth: when they knocked down the protein expression by means of siRNA, proliferation could be increased. This activating effect of FKBP51 was partially antagonized by the GR inhibitor mifepristone [312]. Thus, it could be concluded that tissue-specific expression levels of FKBP51 might influence glucocorticoid sensitivity which is reflected by expression level of downstream target genes.

Very recently, Shimizu and colleagues discovered that GR and mTOR pathways are interconnected in skeletal muscle cells: while glucocorticoids trigger katabolic processes in the cell, growth factors and insulin stimulate anabolism via PI3K/mTOR signaling. By a direct mutual crosstalk between the two antagonistic pathways, a fine-tuning of cellular metabolism can be achieved [313], mainly by modulating transactivation capacities of downstream transcription factors. Thus, a treatment of the muscle cells with dexamethasone (DEX) causes a reduction of S6Kinase and 4E-BP1 phosphorylation, while mTOR activation by amino acid supplementation results in repression of dexamethasone-mediated gene expression. Notably, rapamycin treatment caused an increased expression of the DEX-induced FKBP5 gene.

Furthermore, FKBP51 has already been proposed as a modulator of cell growth and rapamycin-sensitivity in glioma cells [314]: overexpression of FKBP51 caused a reduced response to rapamycin treatment while FKBP51 knockdown rendered the cells sensitive. Importantly, the protein is highly expressed in these cancer cells by default. When NF-κB activity was assessed, it was found that FKBP51 generally activates signaling via this transcription factor. The authors discuss that mTOR inhibition by rapamycin plays a minor role during this process.

Dan and Cooper demonstrated in prostate cancer cells that Akt is involved in NF-κB activation via IKK in an mTOR-dependent manner [315]. As Raptor is necessary for this

signaling pathway and as rapamycin suppresses IKK activity, it was assumed that Akt/mTORC1 signaling is crucially involved in regulating gene expression by modulating NF-κB activity.

Altogether, it must be considered that FKBP51 can be involved in the regulation of numerous cellular processes, including hormone receptor activation, cytokine signaling and co-chaperoning. In overexpression studies, one process cannot be favored against the others; thus, one might observe a combination of very different effects of FKBP51. Some of them may amplify each other, some of them may extinguish each other. As a consequence of this fact, it appears reasonable to modify only one parameter in a well-controlled way. Since mTOR activity might be negatively influenced by GR, GR inhibitors seem to be an important control to rule out those artefacts. As overexpression of wild type FKBP51 might modulate GR activity, the Hsp-binding defective TPR mutant could be used as a control to exclude a GR-dependent influence on mTOR. Probably, these issues do not play an important role in standard HEK293 or HeLa cells; but especially the GR effects of FKBP51 must be kept in mind in order to avoid false conclusions.

5.4 – FKBP51 mediates effects of rapamycin on mTORC2:

5.4.1 – FKBP51 increases Akt binding to Rictor in a rapamycin-dependent manner:

Originally, the mTOR complex 2 was considered to be insensitive to short-term rapamycin treatment [140]. In co-IP experiments performed in HeLa cells, we clearly demonstrated that Akt forms a complex with the mTORC2 component Rictor in a rapamycin-dependent manner (see section 4.7.2). FKBP51 seems to be part of that complex, too. These results might question the classical paradigm of rapamycin not being directly involved in regulation of mTORC2. Recently, more and more evidence was found which strengthens the role of this small molecule:
Sarbassov and colleagues claimed that in some cell types (especially in PC3 or in Jurkat cells) long-term treatment with rapamycin inhibits mTORC2 assembly, resulting in reduced Akt phosphorylation [139]. They observed that the amount of Rictor was dramatically reduced in mTORC immunoprecipitations, indicating a lack of intact and active complexes. This effect on the mTORC2 complex was thought to be mainly caused by binding of

FKBP12*rapamycin to free mTOR protein and thus sequestering it from complex assembly. As the pre-assembled active complexes have a certain life time, rapamycin action does not take place immediately. This explains the requirement for long-term treatment.

Our results suggest that FKBP51 increases interaction of Akt with Rictor in a rapamycin-dependent manner. As Rictor is a component of the mTOR complex 2, it can be assumed that Rictor is at least temporarily associated with the complex. Experiments performed by Pei and Li [57] indicate that FKBP51 might directly interact with Akt in a constitutive way. In contrast, we rather found a rapamycin-induced binding of FKBP51 to Akt. Thus, it could be speculated that FKBP51 binding to the mTORC2 complex is triggered by rapamycin, and that the resulting complex increases recruitment of Akt by Rictor (see scheme in figure 5.7).

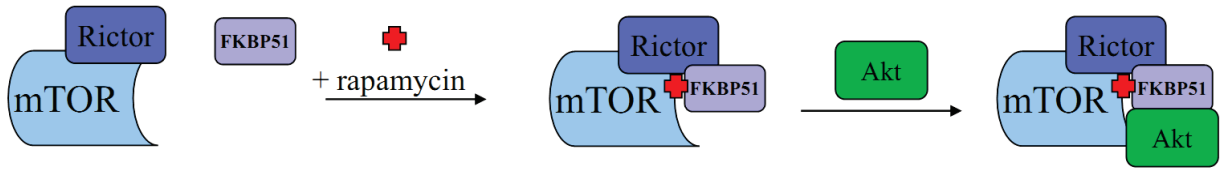

Figure 5.7: Rapamycin modulates interaction of Akt with the mTORC2 component Rictor
Schematic representation of a proposed mechanism of Akt recruitment to mTORC2 via Rictor.

Similar to S6Kinase, a direct binding of FKBP51 to Akt appears questionable, especially if it happens in a rapamycin-dependent manner. Nevertheless, *in vitro* pull-down experiments performed in our lab indicate that there may be a certain degree of constitutive, direct binding of Akt and FKBP51 in an environment that lacks mTOR (Anne Fabian, personal communication, April 2011).

In contrast to the well-established interaction of S6Kinase and Raptor, binding of Akt to Rictor has not yet been studied intensively. Only one report can be found, describing an immunoprecipitation of Rictor which failed to demonstrate binding of Akt in HEK293 cells [316]. As we invested a lot of effort in optimizing our immunoprecipitation experiments in terms of stimulation (serum/insulin), incubation time, detergents and expression levels, it can be speculated that the simple co-IPs done by others were not elaborate enough. They also used a different cell system and pulled down endogenous Rictor without overexpressing the protein. Furthermore, they stimulated the cells with serum; our results indicate that insulin is necessary to increases interaction of Rictor and Akt significantly. Most importantly, this

interaction might be detectable only if it is amplified by rapamycin treatment; hence we did not observe increased complex formation under basal conditions. Altogether, our data indicate a rapamycin-dependent interaction, but they are insufficient to claim a general role of FKBP51 in recruitment of Akt to the mTOR complex 2.

This conclusion is also supported by several observations in FKBP51 knockout mice: these animals show no differences in phenotype or behavior compared to wild type controls. Consequently, essential functions of the missing FKBP51 might be taken over by other proteins or might be compensated by other processes.

5.4.2 – FKBP51 is involved in regulation of Akt phosphorylation:

In 2009, FKBP51 was found to act as a scaffold protein that mediates an interaction of the phosphatase PHLPP with Akt kinase, resulting in reduced Akt phosphorylation when the FKBP is overexpressed [57]. Thus, a role of FKBP51 in Akt phosphorylation is established.

When we overexpressed FKBP51 in HeLa cells, we observed that short-term treatment with rapamycin increases Akt phosphorylation. This effect was clearly rapamycin-dependent and more pronounced compared to mock-transfected cells (see section 4.7.3). While FKBP51 recruits PHLPP to Akt under basal conditions, we did not observe any changes in Akt phosphorylation in absence of rapamycin. Maybe, the phosphatase does not play a big role in HeLa cells.

Generally, Akt activation via the PI3K/Akt/mTOR signaling pathway is essential for regulation of cell growth and survival, and it is regulated in a very strict manner by feedback loops [317]. Rapamycin-induced Akt hyperphosphorylation can be explained by blockage of these negative feedbacks [139]: one signals via S6Kinase and the insulin receptor substrate IRS [318], while the second less characterized one is based on mTOR-dependent expression of the protein phosphatase PHLPP [319].

Concerning the latter, the expression of PHLPP is based on mTOR-mediated protein translation in colon carcinoma cells. Normally, PHLPP is available in sufficient amounts, associates with Akt kinase and inactivates it by dephosphorylation. If mTOR signaling is blocked by rapamycin treatment or mTOR depletion, PHLPP protein concentration decreases, resulting in Akt hyperactivation. This is one mechanism that renders cancer cells rapamycin-resistant [319]. Nevertheless, the effects of such a long-term regulation are unlikely to be triggered by a rapamycin exposure of 60 minutes (as done in our experiments).

In human lung cancer cell lines, rapamycin does not exert any inhibitory effect on cell growth, although mTORC1 signaling is clearly suppressed (resulting in reduced S6K and 4E-BP1 phosphorylation) [320]. Surprisingly, survival signaling pathways involving Akt and eIF4E were hyperactive in presence of rapamycin or analogues, providing a possible explanation for missing growth arrest. The role of PI3Kinase in Akt activation was proven by administration of the inhibitor LY294002 which reduced cell growth when co-administered with rapamycin.
In contrast, Gupta and co-authors reported that PI3K inhibitors were not successful in suppressing the rapamycin-induced increase in Akt phosphorylation in a lymphoma cell culture [321]. Furthermore, Raptor knockdown did not affect Akt phosphorylation, arguing against an involvement of the mTORC1-dependent feedback in mTORC2 regulation. In contrast, a knockdown of Rictor abolished Akt phosphorylation.
Wan and colleagues also reported that rapamycin treatment increases Akt phosphorylation in some cancer cell lines (especially in human rhabdomyosarcoma cell lines) [322]. In contrast to our findings, rapamycin must be administered for at least 3 hours at a relatively high dose (10-100 nM). The authors assume that Akt activity is increased by signaling via the insulin-like growth factor 1 (IGF-1) receptor, but they also admit a scenario in which mTORC2 is directly activated by rapamycin. Importantly, it can be stated that for a possible negative feedback via mTORC1 and IRS-1 both time and necessary rapamycin concentration are suspiciously high; this might indicate that the mTORC1-dependent feedback is not necessarily involved in this regulatory circuit.

Generally, it must be conceded that the above mentioned feedback mechanisms can influence Akt phosphorylation significantly. Concerning our experiments analyzing short-term effects of rapamycin on Akt phosphorylation (see section 4.7.3), it appears possible that increased Akt phosphorylation is simply caused by mTORC1 inhibition and subsequent abolishment of S6Kinase/IRS-1 negative feedback. In case of FKBP51 overexpression, rapamycin might be more effective in mediating its inhibitory effect on mTORC1, resulting in total shut-down of S6Kinase activity. Thus, FKBP51 might be superior to FKBP12 in generating rapamycin-induced Akt hyperphosphorylation.
As the involvement of mTORC1-mediated negative feedback via PI3Kinase seems to be inconsistent between different cancer cell lines, no conclusion can be drawn about its role in HeLa cells. To overcome this obstacle, it will be necessary to perform experiments which allow control of mTORC1 signaling, e.g. by combining rapamycin treatment with administration of the PI3Kinase inhibitor Wortmannin.

5.4.3 – Possible mechanism of FKBP51 affecting Akt phosphorylation:

Altogether, rapamycin-mediated Akt activation can be based on several, different mechanisms. It also cannot be estimated whether these mechanisms act independently, or whether they influence each other. Nevertheless, based on the above research findings, a hypothesis can be created that integrates two mechanisms of FKBP51 influencing mTORC2 activity and Akt phosphorylation, maybe resulting in a rapamycin-resistant phenotype in cancer cell lines.
In such a scenario, FKBP51 initially binds to mTORC1 in a rapamycin-dependent manner and prevents phosphorylation of the mTOR substrate S6Kinase. This causes downregulation of cap-dependent protein biosynthesis via S6Kinase and 4E-BP1, combined with a reduction of the negative feedback loop provided by IRS-1. As a result, signaling via PI3Kinase becomes highly active, and Akt is phosphorylated in an mTORC2-dependent manner. Importantly, FKBP51 is also directly involved in this process by increasing recruitment of Akt kinase to mTORC2 via Rictor in a rapamycin-dependent way. Thus, Akt is hyperphosphorylated at S473, causing increased pro-survival signaling via downstream substrates. Altogether, FKBP51 and rapamycin co-operate in rendering Akt hyperactive by affecting the two mTOR complexes differently (see scheme in figure 5.8). As a consequence, the cancer cells might display rapamycin-resistance, and their growth in rapamycin-containing medium should be unchanged or even increased compared to control conditions.

Maybe, FKBP51 expression levels could be assessed in order to predict rapamycin-sensitivity of cancer cell lines. It could be expected that cells that contain high concentrations of FKBP51 are able to mediate rapamycin-induced effects more efficiently than cells that express less FKBP51. Supporting this idea, Staibano and colleagues collected reports on FKBP51 expression in cancer cells and concluded that there is generally an overexpression of the protein, especially in prostate, skin and colon cancer [323]. These finding are in contrast to the role of FKBP51 as a PHLPP-dependent tumour suppressor protein which has been proposed by Pei for breast and pancreatic cancer cell lines [57, 324, 325]; here, FKBP51 expression levels are especially low.

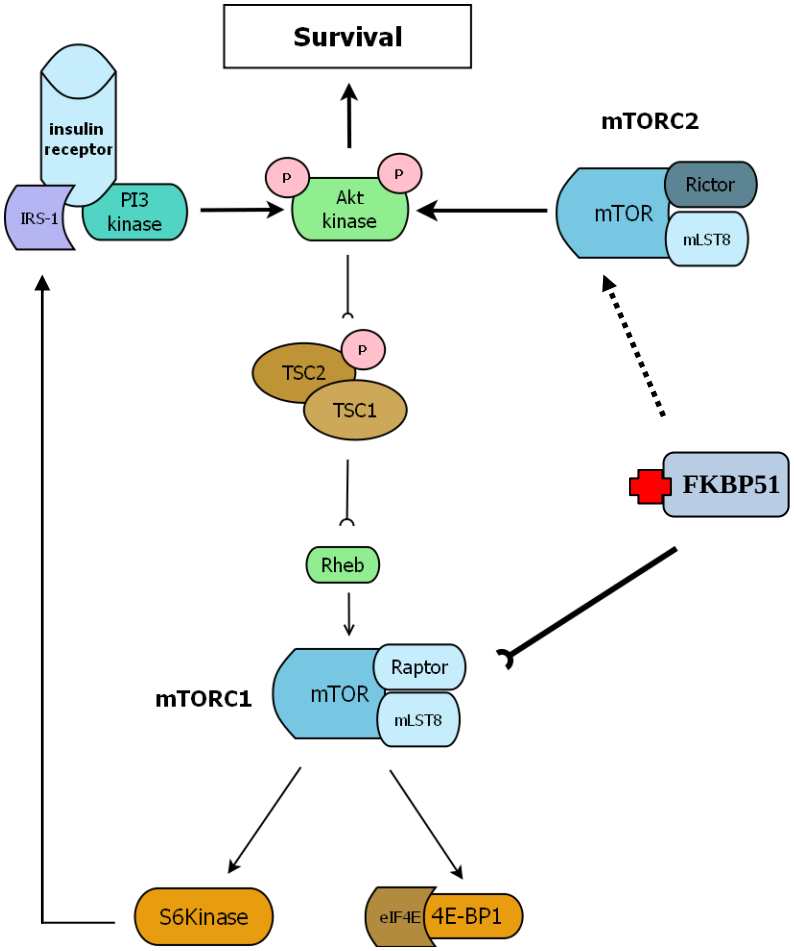

Figure 5.8: Model of rapamycin-mediated FKBP51 effects on mTOR signaling

FKBP51 potentially exerts distinct rapamycin-dependent effects on both mTOR complexes. While it inhibits mTORC1 and thus shuts down S6Kinase negative feedback, it might enhance substrate recruitment of mTORC2 and may increase Akt-dependent survival signaling.

5.5 – Summary:

The kinase "mammalian Target of Rapamycin" (mTOR) plays a crucial role in the regulation of cell cycle progression and cell growth by integrating signals of growth factors, energy levels and amino acid availability. mTOR activity can be inhibited potently by a complex of rapamycin and FKBP12 leading to growth arrest in immune and cancer cell lines. FKBP51, another member of the family of FK506-binding proteins, is best known for its function in glucocorticoid receptor maturation and for its influence on antidepressive treatment**.**

Rapamycin tightly binds to most members of the FKBP protein family. To examine the effect of the larger FKBP homologues on mTOR regulation, we tested different FKBP proteins for mTOR binding and kinase inhibition *in vitro*. In the presence of rapamycin all FKBPs exhibited high affinity to the FRB domain of mTOR (EC_{50} < 30 nM) and inhibited mTOR activity (IC_{50} < 10 nM) in a rapamycin-dependent manner.

In order to elucidate the structural basis of these interactions, we solved the high-resolution crystal structures of two alternative ternary complexes (FRB*rapamycin*FK1 FKBP51/52). The overall architecture of the complexes was very similar to the one known for FKBP12. However, FKBP51 showed novel intensive contacts to FRB via its 40S loop region while for FKBP52 these protein-protein interactions were more prominent within the 80S loop. A large number of water-mediated H-bonds were identified that bridge residues of FRB with those in FKBP51 and contribute to stabilization of the complex. Furthermore, an additional H-bond to rapamycin and between the protein domains could be observed in the complex with FKBP51.

To assess FKBP action *in vivo*, we transformed FKBP12-deficient yeast cells with human FKBPs. In this complementation assay, FKBP51 restored rapamycin sensitivity similar to FKBP12. In mammalian cells treated with rapamycin, FKBP51 could be found in mTORC1 complexes, implying a functional role of the larger FKBP. By overexpressing FKBP51 in HeLa cells, we observed decreased p70S6K phosphorylation, resulting from reduced mTOR activity in presence of rapamycin compared to FKBP12-overexpressing cells. When FKBP12 was knocked down, rapamycin still inhibited mTOR kinase activity, indicating that FKBP12 might be dispensable.

Co-IP experiments in HeLa cells revealed that the mTORC2 component Rictor binds to Akt kinase in a rapamycin- and FKBP51-dependent manner. When FKBP51 is overexpressed, Akt phosphorylation by mTORC2 is elevated compared to mock conditions. Thus, FKBP51 might be involved in substrate recruitment.

Altogether, our results demonstrate that mTOR is able to form stable and inhibitory ternary complexes with different FKBPs *in vitro* and in eukaryotic cells. FKBP51 might contribute to classical rapamycin-dependent inhibition of mTORC1, and tissues with high FKBP51 expression levels may be attractive targets for pharmacological effects of rapamycin. Furthermore, FKBP51 may also play a more exclusive role in modulating Akt phosphorylation by mTORC2. Potentially, the effects on mTORC1 and mTORC2 might cooperate in rendering cancer cells resistant to chemotherapeuticals like rapamycin.

6 – Appendix:

6.1 – Extinction coefficients for expressed proteins:

In order to determine concentration of protein preparations, we calculated the extinction coefficients based on the protein sequence, using a web-based application (protein calculator, see http://www.mrc-lmb.cam.ac.uk/ms/methods/proteincalculator.html).

Protein	Molecular weight [kDa]	Extinction coefficient [mol cm $^{-1}$]
FKBP12	15.2	15930
FKBP12.6	15.1	9065
FKBP13	15.8	14565
FKBP25	28.5	33900
FK1 FKBP51	18.6	17545
FKBP51	55.5	48290
FK1 FKBP52	18.6	21555
FKBP52	56.1	53540
EGFP-FKBP12	42.6	34420
EGFP-FKBP12.6	46.8	27450
EGFP-FKBP13	47.8	33140
EGFP-FKBP25	55.4	52770
EGFP-FKBP51	82.5	63700
EGFP-FKBP52	83.1	69400
EGFP-4E-BP1	43.3	27450
FRB	14.7	29910
GST-FRB	37.2	65800

Table 6.1: Overview of extinction coefficients used for calculation of protein concentrations

6.2 – Active site titration:

Active site titration has been performed for FKBP13 and FKBP25, too. Experimental procedures were the same as described for FKBP12, 12.6, 51 and 52. The resulting graph is shown in figure 6.1.

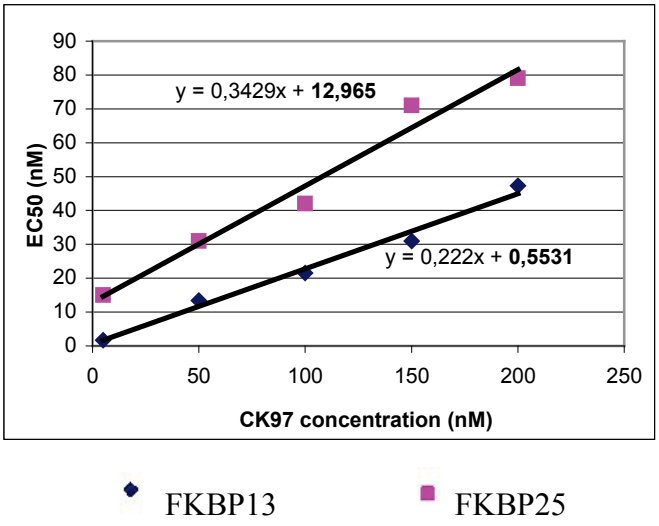

Figure 6.1: Active site titration reveals high affinity of tracers to recombinant FKBP13 and FKBP25
Plot of calculated EC_{50} values against corresponding tracer concentration; linear equation is shown, intersection with y-axis is printed in bold.

6.3 – Formula for curve fitting and K_d determination:

A formula for determination of K_d values in protein-ligand titration experiments has been described before [326]:

$$[LR] = [([R]_t + [L]_t + K_d)/2] - \{[([R]_t + [L]_t + K_d)/2]^2 - [L]_t[R]_t\}^{0.5}$$

As fluorescence anisotropy (A) increases with increasing concentrations of the receptor-ligand complex [LR], it can be expressed as follows:

$$A = (\Delta A / [L]_t)\,[LR] + A_{min}$$

Finally, the terms can be combined, resulting in the formula used for K_d fitting:

$$A = [(A_{max} - A_{min}) / [L]_t] \times \{[([R]_t + [L]_t + K_d)/2] - \{[([R]_t + [L]_t + K_d)/2]^2 - [L]_t[R]_t\}^{0.5}\} + A_{min}$$

A formula for determination of K_d values in two-ligand competition experiments was published by Wang [327]. In this formula, anisotropy values were introduced by combining it with $A = (\Delta A / [L]_t)\,[LR] + A_{min}$. The final term was used for K_d fitting of competition assays [274] and reads as follows:

$$A = (A_{max} - A_{min}) / [L]_t \times (([L]_t \times ((2x((K_{lig} + K_{comp} + [L]_t + [I]_t - [R]_t)^2 - 3x(K_{comp} \times ([L]_t - [R]_t) + K_{lig} \times ([I]_t - [R]_t) + K_{lig} \times K_{comp}))^{0.5} \times \cos(\arccos((-2x(K_{lig} + K_{comp} + [L]_t + [I]_t - [R]_t)^3 + 9x(K_{lig} + K_{comp} + [L]_t + [I]_t - [R]_t) \times (K_{comp} \times ([L]_t - [R]_t) + K_{lig} \times ([I]_t - [R]_t) + K_{lig} \times K_{comp}) - 27x(-1x\,K_{lig} \times K_{comp} \times [R]_t)) / (2x((((K_{lig} + K_{comp} + [L]_t + [I]_t - [R]_t)^2 - 3x(K_{comp} \times ([L]_t - [R]_t) + K_{lig} \times ([I]_t - [R]_t) + K_{lig} \times K_{comp}))^3)^{0.5}))) / 3)) - (K_{lig} + K_{comp} + [L]_t + [I]_t - [R]_t))) / ((3x\,K_{lig}) + ((2x((K_{lig} + K_{comp} + [L]_t + [I]_t - [R]_t)^2 - 3x(K_{comp} \times ([L]_t - [R]_t) + K_{lig} \times ([I]_t - [R]_t) + K_{lig} \times K_{comp}))^{0.5} \times \cos(\arccos((-2x(K_{lig} + K_{comp} + [L]_t + [I]_t - [R]_t)^3 + 9x(K_{lig} + K_{comp} + [L]_t + [I]_t - [R]_t) \times (K_{comp} \times ([L]_t - [R]_t) + K_{lig} \times ([I]_t - [R]_t) + K_{lig} \times K_{comp}) - 27x(-1x\,K_{lig} \times K_{comp} \times [R]_t)) / (2x((((K_{lig} + K_{comp} + [L]_t + [I]_t - [R]_t)^2 - 3x(K_{comp} \times ([L]_t - [R]_t) + K_{lig} \times ([I]_t - [R]_t) + K_{lig} \times K_{comp}))^3)^{0.5})))/3)) - (K_{lig} + K_{comp} + [L]_t + [I]_t - [R]_t)))) + A_{min}$$

being: K_{lig}: K_d values of the used tracer

K_{comp}: K_d values of the competitor

$[I]_t$: total concentration of the inhibitor

6.4 – FRET binding: controls

In order to test for unspecific FRET events, we performed the FRET binding assay with GST-FRB and EGFP-FKBP12 in absence of rapamycin. As figure 6.2 shows, no increase in FRET ratio could be observed. If simple EGFP was used instead of the EGFP-FKBP12 fusion protein, rapamycin was unable to induce any binding; thus, a flat line was observed when FRET ratio was plotted against the rapamycin concentration.

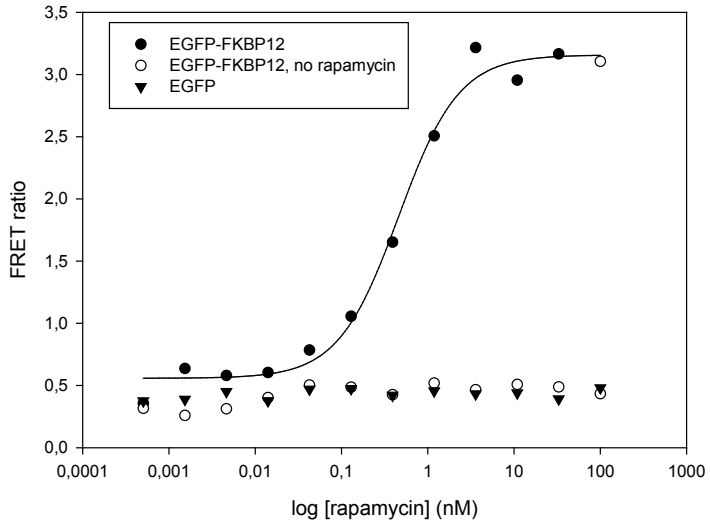

Figure 6.2: Rapamycin and FKBP12 are essential components of FRET binding assay
Half-logarithmic plot of the rapamycin concentration vs. the observed FRET ratio. 5 nM GST-FRB, 25 nM EGFP-FKBPs and 2.5 nM anti-GST antibody were used. Rapamycin was titrated from 0 to 100 nM.

6.5 – mTOR activity assay

6.5.1 – FRET mTOR activity assay: LY294002 and PI-103 controls

In order to verify the reliability of the mTOR FRET activity assay, different known mTOR/PI3K inhibitors were used as a control. For the assay, the compounds were pre-diluted in DMSO, and a fixed amount of DMSO dilution was added to the FRET samples. LY294002 inhibited 4E-BP1 phosphorylation with an IC_{50} value of 170 nM which is considerably lower than a reported value of 2 µM [328]. PI-103 was even more potent; an IC_{50} of 12 nM was determined (literature value: 20 nM [329]).

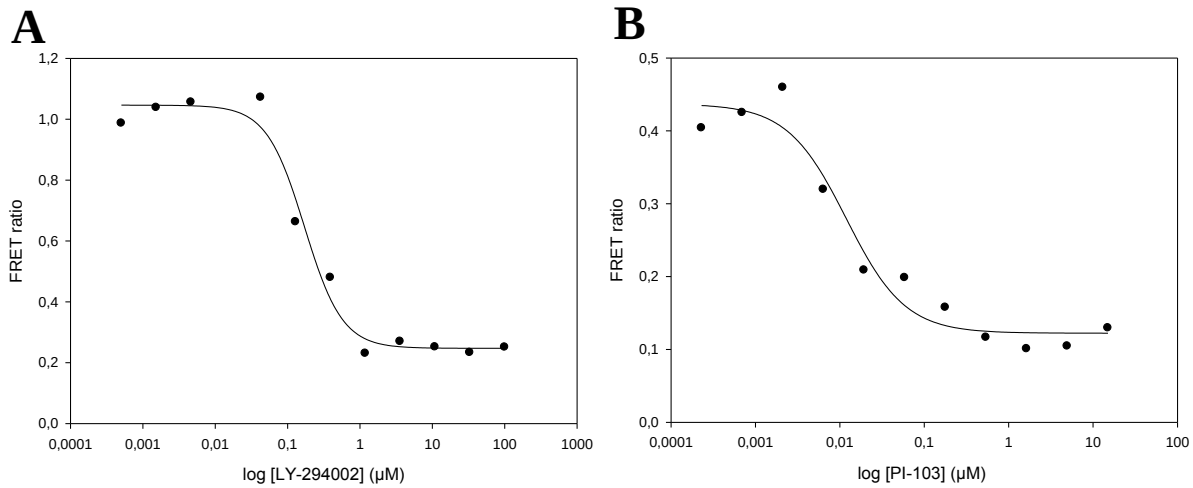

Figure 6.3: LY294002 and PI-103 potently inhibit 4E-BP1 phosphorylation

Half-logarithmic plot of the inhibitor concentration against the FRET ratio. Assay was performed as described before. (A) LY-294002 (B) PI-103

6.5.2 – *In vitro* kinase assay: rapamycin control

In order to exclude effects that are exerted by rapamycin alone, we included a sample that contains mTORC1 and 500 nM rapamycin. Unlike torin1, rapamycin did not induce a dramatic reduction of S6Kinase phosphorylation (see figure 6.4).

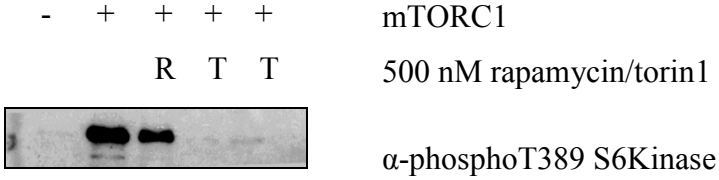

Figure 6.4: Rapamycin alone has only minor effects on S6Kinase phosphorylation

6.6 – Crystal structures: interaction data:

Analysis of molecular contacts was performed using the program CONTACT which is part of the CCP4 suite. H-bonds were detected using the program FindHBond of the Chimera package.

6.6.1 – Interactions between rapamycin and protein domains:

All interactions between rapamycin and the FRB domain (in the structure FRB*rapamycin* FK1 FKBP52) with a range of up to 4 Å are listed in the following table.

Residue in FRB (FKBP52 ternary complex)	**Atom in rapamycin**	**Distance (Å)**	**Number of contacts**
Leu2031 C, O, CB	Rap C45, C45, C45	3.64 – 3.76	3
Glu2032 O, N	Rap C51, C45	3.47 – 3.92	2
Ser2035 OG, OG, OG, OG, OG, OG, CB	Rap C27, O9, C51, C24, C23, C22, C22	3.35 – 3.99	7
Phe2039 CG, CD2, CZ, CE1, CD1, CB, CE2	Rap C47, C47, C18, C13, C49, C36, C18	3.76 – 3.96	7
Thr2098 O, CG2	Rap C50, C50	3.36; 3.66	2
Trp2101 CB, CZ3	Rap C50, C22	3.72; 3.98	2
Asp2102 OD1, N, OD1, CG	Rap O7, C50, C50, C50	3.34 – 3.95	4
Tyr2105 CZ, CE2, CE1, CD1, CB, CG, CD1, CE1, CB, CG, CD2	Rap C48, C48, C46, C23, C21, C21, C21, C21, C19, C19, C19	3.36 – 3.99	11
Phe2108 CD2, CB, CG, CD1, CE1, CD2	Rap C23, C45, C45, C45, C45, C45	3.42 – 3.90	6
		Total contacts	**44**

Table 6.2: Interactions between rapamycin and FRB

Interactions between rapamycin and FKBP12, the FK1 domains of FKBP51 and FKBP52 are listed in the following tables:

Residue in FKBP12	Atoms in (C16)-ethoxy rapamycin (RAD)	Distance (Å)	Number of contacts
Tyr26 CE1, CE2, CZ	RAD 04, C5, C5	3.66-3.81	3
Phe36 CD1, CD1, CE1, CE1, CE1	RAD O4, C42, C8, O4, C42	3.23-3.86	5
Asp37 CB, CB, CG, CG, OD2 (6x)	RAD O4, O6, O4, O6, O5, C13, C8, C9, O4, O6	2.74-3.95	10
Phe46 CE2, CZ (3x)	RAD C4, C4, C5, O11	3.69-3.99	4
Gln53 C, O (4x), CB	RAD O13, C38, C39, C40, O13, O13	2.65-3.91	6
Glu54 CA, C, O (7x), CB	RAD O10, O10, C27, C28, O10, C29, C31, O11, C36, O10	2.82-3.96	10
Val55 CA, CA, C, C, O, CB, CG1 (3x)	RAD O2, C40, O2, C40, C40, O2, C4, O2, O11	3.28-3.96	9
Ile56 N (3x), CA, CG1, CG2, CG2	RAD O2, C41, C40, C40, O2, O2, C41	3.00-3.99	7
Trp59 CG, CD1, CD2, NE1, CE2, CE2, CE3, CZ2, CZ2, CZ3, CH2	RAD C3, C3, C4, C3, C3, C4, C3, C4, C4, C3, C4, C4	3.35-3.92	12
Tyr82 CE1, CE2, CZ, OH (10x)	RAD C34, O3, O3, C1, O1, O2, C33, C34, C48, C2, N7, O3, C7	2.75-3.95	13
Ile90 CG2	RADC42	3.82	1
Ile91 CG1, CD1	RAD C42, C42	3.89-3.90	2
Phe99 CE1, CZ, CZ	RAD O4, O3, C7	3.68-3.89	3
		Total contacts	**85**

Table 6.3: Interactions between (C16)-ethoxy rapamycin and FKBP12 (analyzed in 2fap)

Residue in FK1 FKBP51	Atom in rapamycin	Distance (Å)	Number of contacts
Tyr57 CE1, CZ, OH, OH, CZ, OH, CE2	Rap O4, O4, O4, C6, C5, C5, C5	3.49 – 3.92	7
Phe67 CD1, CE1, CE1	Rap O4, O4, C9	3.43 - 3.94	3
Asp68 OD2, OD2, CB, CG, OD2, OD2, CB, CG, OD2	Rap O5, C10, O6, O6, O6, C9, O4, O4, O4	2.73 – 3.85	9
Arg73 NE, CZ, NH2, NH3, NE, CZ, NH2, NH2, NH2, (NH2)	Rap C44, C44, C44, C16, O7, O7, O7, C15, C14,	3.02 – 3.97	9
Phe77 CZ, CZ, CZ, CE2, CZ, CE2	Rap O11, C48, C5, C5, C4, C4	3.32 – 3.88	6
Gly84 O, O, C, O, O	Rap C41, C40, O13, O13, C39	2.66 – 3.80	5
Gln85 O, O, O, O, O, CG, CA, CB, C, O, CG, O, O, O	Rap C32, O11, C30, C29, C28, O10, O10, O10, O10, O10, O8, C37, C41, C41	2.69 – 3.92	14
Val86 CG1, CG1, CA, CB, CG1, C, O, CA, C	Rap O11, C4, O2, O2, O2, O2, C41, C41, C41	3.21 – 3.99	9
Ile87 N, CG1, CG2, CA, N	Rap O2, O2, O2, O2, C41	2.87 – 4.00	5
Trp90 CH2, CZ2, CE3, CD2, CZ3, CH2, CE2, CZ2, CG, CD1, CD1, NE1, CE2, CZ2	Rap C5, C5, C4, C4, C4, C4, C4, C4, C3, C3, C3, C3, C3, C3	3.49 – 3.93	14
Tyr113 OH, CE1, OH, CE1, OH, OH, OH, OH, CZ, OH, CE2, OH, OH, OH, OH	Rap C34, C35, C35, C49, C49, O1, C11, C8, O3, O3, O3, N7, C2, C1, O2	2.65 – 3.99	15
Ile122 CD1	Rap C43	3.46	1
Phe130 CE1, CZ	Rap O4, O3	3.69 - 3.93	2
		Total contacts	**99**

Table 6.4: Interactions between rapamycin and FK1 FKBP51

Residue in FK1 FKBP52	Atom in rapamycin	Distance (Å)	Number of contacts
Tyr57 OH, CZ, OH, CZ, OH, CZ, OH, CE2, CE1	Rap O5, O4, O4, C6, C6, C5, C5, C5, O4	3.54 – 3.93	9
Phe67 CE1, CE1	Rap C9, O4	3.47; 4.00	2
Asp68 OD2, OD2, CG, OD2, CB, OD2, CG, OD2, CB	Rap O5, C10, O6, O6, O6, C9, O4, O4, O4	2.68 – 3.90	9
Phe77 CZ, CE1, CZ, CZ, CE2, CZ, CE2	Rap O11, C48, C48, C5, C5, C4, C4	3.32 – 3.89	7
Gly84 O, O, C, O, O	Rap C41, C40, O13, O13, C39	2.68 – 3.79	5
Glu85 O, O, O, O, O, CA, CB, C, O, O, O	Rap C32, O11, C30, C29, C28, O10, O10, O10, O10, C37, C41	2.74 – 3.99	11
Val86 CG1, CA, C, O, C, CG2, CB, CG1, CA, C	Rap O11, C41, C41, C41, C42, C4, O2, O2, O2, O2	2.85 – 3.99	10
Ile87 N, N, N, CA, CG2, CG1, CB	Rap C41, C42, O2, O2, O2, O2, O2	2.85 – 4.00	7
Trp90 CH2, CZ2, CZ3, CE2, CD2, CE3, CH2, CZ2, CG, CD1 NE1, CE2, CD2, CZ2	Rap C5, C5, C4, C4, C4, C4, C4, C4, C3, C3, C3, C3, C3, C3	3.47 – 3.99	14
Tyr113 OH, OH, CZ, OH, CE2, OH, OH, OH, OH, OH, CE1, OH, CE1, OH, OH	Rap C11, C8, O3, O3, O3, N7, C2, C1, O1, C34, C35, C35, C49, C49, O2	2.64 – 3.94	15
Lys121 NZ, NZ, CE, NZ, NZ, CE	Rap C14, C12, C12, C43, C10, O6, O6	2.76 – 4.00	7
Ile122 CG1, CD1	Rap C43, C43	3.78 – 3.99	2
Phe130 CE1, CZ, CZ	Rap O4, C8, O3	3.72 – 3.95	3
		Total contacts	**101**

Table 6.5: Interactions between rapamycin and FK1 FKBP52

6.6.2 – Interactions between protein domains:

All direct contacts between the FKBP and the corresponding FRB domain are listed below. Atoms involved in H-bond formation are underlined. H-bonds have been defined as contacts between the classical H-donor and H-acceptor atoms N and O. Distance between donor and acceptor must be less than 4 Å.

Residue in FKBP12 (2fap)	Residue in FRB	Distance (Å)	Number of contacts
Lys44 CE	Arg2109 NH2	3.68	1
Phe46 CE1	Tyr2105 OH	3.87	1
Lys47 O	Tyr2105 OH	3.57	1
Thr85 OG1	Arg2042 CZ, NH2	3.92 – 3.98	2
Gly86 O	Arg2042 CZ, NH1	3.08 – 3.91	2
His87 NE2	Tyr2038 OH	3.94	1
His87 CE1, NE2, CE1, NE2, CE1, NE2, NE2	Phe2039 CA, CA, O, O, CD1, CD1, CD1	3.25 – 3.96	7
His87 ND1, CE1	Arg2042 NH1, NH1	3.47 – 3.93	3
Pro88 CD, CG, CD	Arg2042 CG, CG, CD	3.75 – 4.0	3
Pro88 O	Val2094 CG2	3.45	1
Gly89 CA, C, O	Val2094 CG1	3.58 – 3.98	3
Ile90 CG1	Val2094 CG1	3.95	1
Ile90 CD1	Thr2098 CG2	3.74	1
		Total contacts	**27**

Table 6.6: Interactions between FKBP12 and FRB (determined from structure 2fap)

Residue in FK1 FKBP51	Residue in FRB	Distance (Å)	Number of contacts
Arg73 CD, NE, CG, CD, NE, CZ, NH2	Asp2102 CG, CG, OD1, OD1, OD1, OD1, OD1	2.72 - 3.97	7
Glu75 OE2, OE2	His2106 NE2, CD2	3.26 – 3.91	2
Glu75 OE2, OE2, CD, OE2, CG, CD, OE2, CB, CG	Arg2109 CD, NE, CZ, CZ, CZ, NH1, NH1, NH1	3.57 – 3.90	8
Pro76 O, C, O, C, O	Arg2109 CZ, NH1, NH1, NH2, NH2	2.78 – 3.92	5
Phe77 CD1, CE1, CA, C, CD1, CG, CE1, CD1	Tyr2105 CZ, CZ, OH, OH, OH, OH, OH, CE2	3.38 - 3.92	8
Val78 O, O, CA, CG1, C, O, N	Tyr2105 CE1, CZ, OH, OH, OH, OH, OH	2.60 – 3.87	7
Val78 CG1, CG1, CG1, CB, CG1	Arg2109 NE, CZ, NH1, NH2, NH2	3.42 – 3.86	5
Ala116 CB, CB	Arg2042 NE, NH2	3.59 – 3.97	2
Pro120 CG, CD, CD, CD	Val2094 CB, CB, CG1, CG2	3.67 – 3.98	4
		Total contacts	**48**

Table 6.7: Interactions between FK1 FKBP51 and FRB

Residue in FK1 FKBP52	Residue in FRB	Distance (Å)	Number of contacts
Arg52 NH2	Tyr2105 OH	3.14	1
Arg52 NH2	Arg2109 CG	3.81	1
Lys76 C, O	Arg2109 NH2, NH2	2.83 – 3.92	2
Phe77 CA	Arg2109 NH2	3.94	1
Ser78 C, O, O, O	Tyr2105 OH, OH, CE2, CZ	2.36 – 3.72	4
Ser78 OG, OG, N, OG	Arg2109 NE, CZ, NH2, NH2	3.20 – 3.66	4
Ala116 CB, CB, CB	Arg2042 NE, CZ, NH2	3.68 – 3.90	3
Pro120 CG, CD, CG, CD, CD	Val2094 CB, CB, CG, CG1, CG2	3.53 – 3.83	5
		Total contacts	**21**

Table 6.8: Interactions between FK1 FKBP52 and FRB

6.6.3 – Waters involved in interactions between the protein domains:

A list of water molecules that are involved in mediating protein-protein interactions via H-bonds can be found below:

Water number	Residue in FKBP12	Residue in FRB	Distances (A)
317	Lys47, Glu54	Tyr2105	2.7; 2.9
422	Pro88	Tyr2038	2.7; 2.9

Table 6.9: Water molecules that mediate protein-protein interactions between FRB and FKBP12 (from 2fap)

Water number	Residue in FK1 FKBP51	Residue in FRB	Distances (A)
94	Glu75	His2106	3.5; 3.1
107	Ser118	Phe2039	2.7; 3.6

Table 6.10: Water molecules that mediate protein-protein interactions between FRB and FK1 FKBP51

Water number	Residue in FK1 FKBP52	Residue in FRB	Distances (A)
22	Glu85	Tyr2105	2.7; 3.2
27	Pro119	Tyr2038	3.1; 2.8
47	Ser118	Phe2039	2.9; 2.7

Table 6.11: Water molecules that mediate protein-protein interactions between FRB and FK1 FKBP52

6.6.4 – Small differences are present in the rapamycin binding pockets of FRBs:

An overlay of the residues involved in binding of rapamycin reveals a high degree of structural conservation between the FRB domains of the three ternary complexes. Nevertheless, some minor differences can be seen, especially involving the residues Y2105 and R2036. Also, only G2040 in the FKBP12 structure seems to be involved in rapamycin binding, while the residue does not play such a role in the FK1 FKBP51 and the FK1 FKBP52 ternary complex.

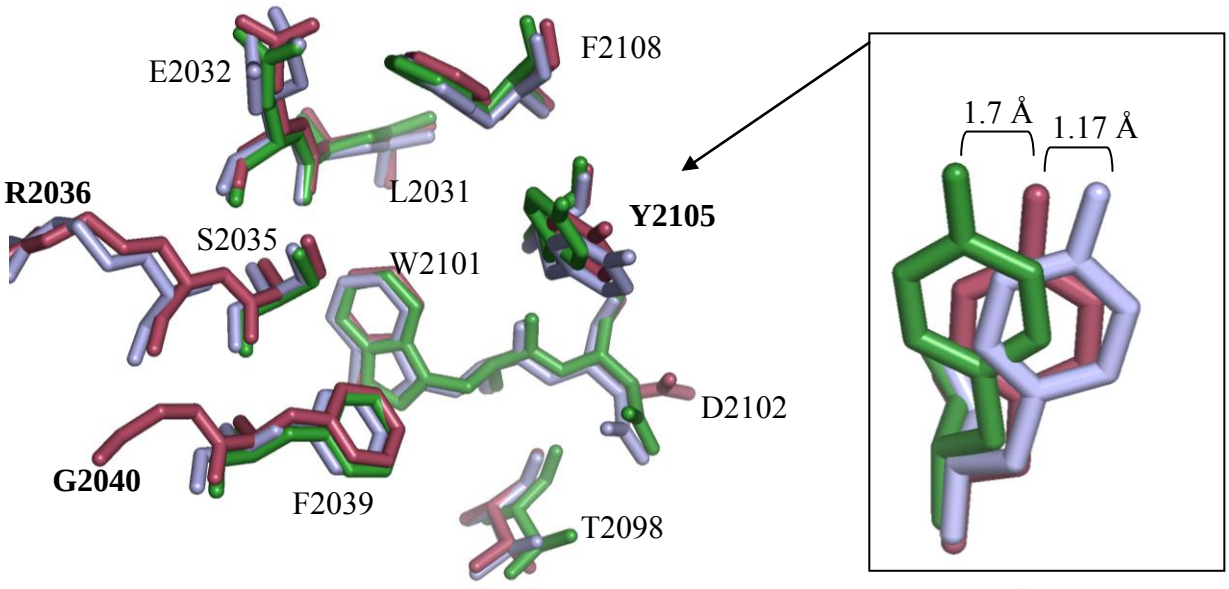

Figure 6.5: Overlay of the residues in FRB involved in rapamycin binding

Color scheme: FRB of FKBP12 (2fap): red
FRB of FK1 FKBP51 complex: light blue
FRB of FK1 FKBP52 complex: green

In box: magnification of Y2105 which is shifted. Distances are indicated.

6.7 – Rictor interacts with FKBP12 in a constitutive manner:

Co-IP experiments were also performed with FLAG-FKBP12 and myc-Rictor. Here, interaction mainly appeared under conditions of serum stimulation. Again, no obvious rapamycin-dependence could be observed.

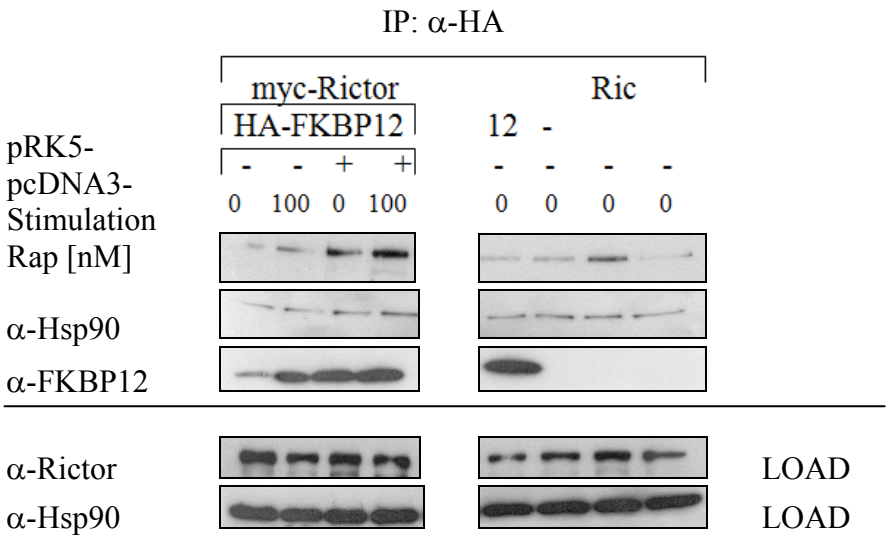

Figure 6.6: FKBP12 interacts with myc-Rictor in stimulated HeLa cells

HeLa cells were transfected for expression of HA-FKBP12 and myc-Rictor. Cells were either starved or starved and stimulated with FCS for 24 h. Lysates were subjected to HA-IP. Beads were washed four times with CHAPS-containing lysis buffer and extracted by boiling. Eluates were analyzed by SDS-PAGE and immunoblotting.

6.8 – Rapamycin binds to His-FRB:

In FP assays using the fluorescein-labeled rapamycin derivative CK97, we observed binding of the tracer to His-tagged FRB with an EC_{50} value of 290 nM ±17.4 (see figure 6.7). No FKBP component was present in the assay.

By performing competition binding experiments with fixed concentrations of CK97 and His-FRB and increasing concentrations of rapamycin, we determined an IC_{50} value for rapamycin of 1.04 µM ± 0.11.

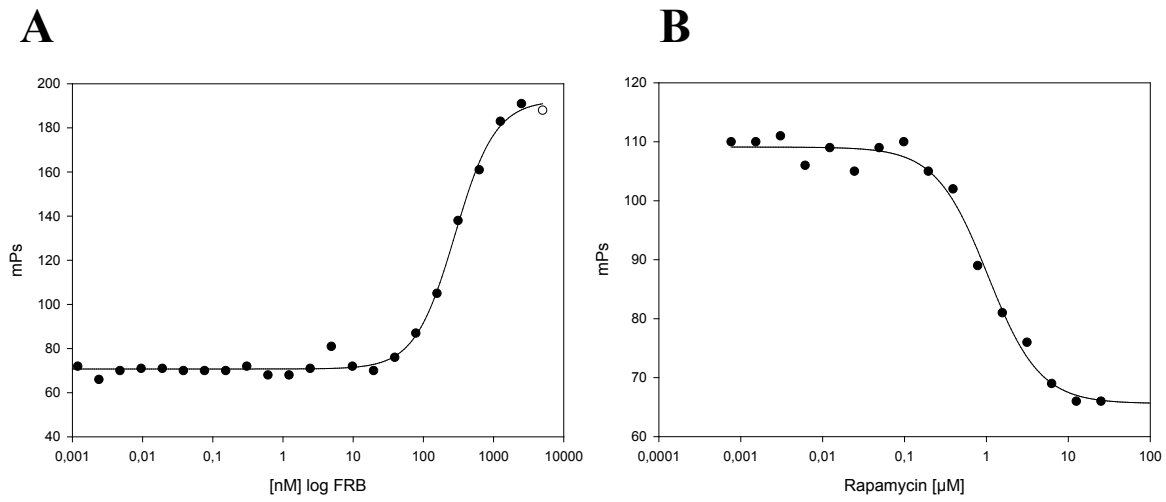

Figure 6.7: CK97 binds to the FRB domain of mTOR in absence of FKBPs

(A) 5 nM CK97 was titrated to increasing concentrations of His-FRB. An EC_{50} value of 290 nM was determined by fitting the curve with "Four Parameter Logistic" in SigmaPlot.

(B) Competitive FP assays were performed with 5 nM CK97 and 750 nM His-FRB. Rapamycin was titrated from 0 – 20 µM. Curve fitting was performed using "Four Parameter Logistic" in SigmaPlot.

6.9 - Immunoblotting proves galactose-dependent FKBP expression in yeast cells:

As the expression activity of transfected plasmids can vary dramatically in yeast, the FKBP protein levels were checked by immunoblotting. During this procedure, a definite amount of yeast cells (determined by OD_{600}) was harvested and analyzed. Thus, FKBP protein levels can be quantified by blotting against the protein tag.

It turned out that all checked clones exhibited heterologous expression of the transformed plasmid. No expressed protein could be detected for clones grown in glucose-containing medium, while expression is strong in presence of the inducer galactose (see figure 6.8). Thus, the expression system seems to be tight.

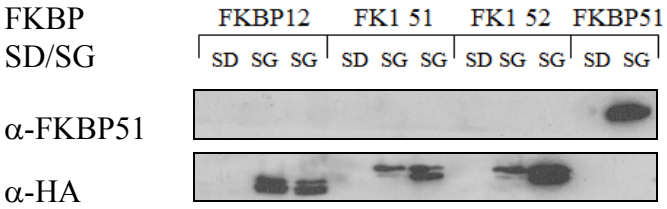

Figure 6.8: Western blot quantification of yeast clone expression

For quantification of protein expression, yeast cell lysates were boiled in SDS sample buffer and subjected to SDS PAGE. HA-tagged proteins were detected by immunoblotting. For FKBP12, FK1 FKBP51 and FK1 FKBP52 each two SG clones are represented.

SD: growth in medium containing glucose

SG: growth in medium containing galactose

When protein expression levels of different clones are compared, it is obvious that the amount of HA-tagged protein differs a lot. Even two clones containing the same plasmid display big variations in protein expression. This is especially pronounced for the two samples of clones expressing the FK1 domain of FKBP52. For FKBP12 and FK1 FKBP51, these differences are less distinct. Probably, copy numbers of these 2-µm plasmids differ considerably in the selected clones and thus create varying expression levels.

For the FK1 domains, an additional band appears in all the samples, representing either a truncated product or another variant of the protein. It could not be determined whether protein degradation occurred *in vivo* or during preparation of the samples. Only one species could be observed for the full-length FKBP51 expressing clone.

6.10 – Abbreviations:

Å	Angstrom (1 Å = 10^{-10} m)
AP	Alkaline Phosphatase
aa	amino acid
ATP	adenosine-5'-triphosphate
bp	base pair(s)
BSA	bovine serum albumin
CIP	calf intestine phosphatase
CV	column volume
d	day
Da	Dalton
bidest. H2O	double distilled water
DMSO	dimethylsulfoxide
DNA	deoxyribonucleic acid
dNTP	2'-deoxynucleoside 5'-triphosphate
dsDNA	double strand DNA
E. coli	*Escherichia coli*
EDTA	ethylendiamine-tetraacetic acid
EtOH	ethanol
FCS	fetal calf serum
g	gram(s)
h	hour(s)
HEPES	4-(2-hydroxyethyl)-1-piperazineethanesulfonic acid
FPLC	Fast Performance Liquid Chromatography
IPTG	Isopropyl-β-D-1-thiogalactopyranoside
kb	kilo base pair(s)
kDa	kilo Dalton
l	litre
LB Medium	lysogeny broth
M	molar (mol/l)
m	metre(s)
mA	milliAmpere(s)

min	minute(s)
ml	millilitre(s)
mM	millimolar
MW	molecular weight
nM	nanomolar
OD	optical density
ORF	open reading frame
PCR	polymerase chain reaction
pM	picomolar
RNase A	Ribonuclease A
rpm	round(s) per minute
Rap	Rapamycin
RT	room temperature
SDS	sodium dodecyl sulfate
s	second(s)
ssDNA	single strand DNA
Tris	tris(hydroxymethyl)aminomethane
Triton X-100	polyethylene glycol p-(tetramethylbutyl)-phenyl ether
U	enzymatic unit(s)
UV	ultraviolet
V	Volt
v/v	volume per volume
w/v	weight per volume
wt	wild type
µl	microlitre(s)
µM	micromolar

7 – Bibliography:

1. Siekierka, J.J., et al., *A cytosolic binding protein for the immunosuppressant FK506 has peptidyl-prolyl isomerase activity but is distinct from cyclophilin.* Nature, 1989. **341**(6244): p. 755-7.
2. Siekierka, J.J., et al., *The cytosolic-binding protein for the immunosuppressant FK-506 is both a ubiquitous and highly conserved peptidyl-prolyl cis-trans isomerase.* J Biol Chem, 1990. **265**(34): p. 21011-5.
3. Fischer, G., H. Bang, and C. Mech, *[Determination of enzymatic catalysis for the cis-trans-isomerization of peptide binding in proline-containing peptides].* Biomed Biochim Acta, 1984. **43**(10): p. 1101-11.
4. Fischer, S., S. Michnick, and M. Karplus, *A mechanism for rotamase catalysis by the FK506 binding protein (FKBP).* Biochemistry, 1993. **32**(50): p. 13830-7.
5. Lang, K., F.X. Schmid, and G. Fischer, *Catalysis of protein folding by prolyl isomerase.* Nature, 1987. **329**(6136): p. 268-70.
6. Liu, J., et al., *Calcineurin is a common target of cyclophilin-cyclosporin A and FKBP-FK506 complexes.* Cell, 1991. **66**(4): p. 807-15.
7. Mukai, H., et al., *FKBP12-FK506 complex inhibits phosphatase activity of two mammalian isoforms of calcineurin irrespective of their substrates or activation mechanisms.* J Biochem, 1993. **113**(3): p. 292-8.
8. Liu, J., et al., *Inhibition of T cell signaling by immunophilin-ligand complexes correlates with loss of calcineurin phosphatase activity.* Biochemistry, 1992. **31**(16): p. 3896-901.
9. Sabatini, D.M., et al., *RAFT1: a mammalian protein that binds to FKBP12 in a rapamycin-dependent fashion and is homologous to yeast TORs.* Cell, 1994. **78**(1): p. 35-43.
10. Chung, J., et al., *Rapamycin-FKBP specifically blocks growth-dependent activation of and signaling by the 70 kd S6 protein kinases.* Cell, 1992. **69**(7): p. 1227-36.
11. Burnett, P.E., et al., *RAFT1 phosphorylation of the translational regulators p70 S6 kinase and 4E-BP1.* Proc Natl Acad Sci U S A, 1998. **95**(4): p. 1432-7.
12. Dawson, T.M., et al., *The immunophilins, FK506 binding protein and cyclophilin, are discretely localized in the brain: relationship to calcineurin.* Neuroscience, 1994. **62**(2): p. 569-80.
13. Lyons, W.E., et al., *Neuronal regeneration enhances the expression of the immunophilin FKBP-12.* J Neurosci, 1995. **15**(4): p. 2985-94.
14. Sharkey, J. and S.P. Butcher, *Immunophilins mediate the neuroprotective effects of FK506 in focal cerebral ischaemia.* Nature, 1994. **371**(6495): p. 336-9.
15. Lyons, W.E., et al., *Immunosuppressant FK506 promotes neurite outgrowth in cultures of PC12 cells and sensory ganglia.* Proc Natl Acad Sci U S A, 1994. **91**(8): p. 3191-5.
16. Sinars, C.R., et al., *Structure of the large FK506-binding protein FKBP51, an Hsp90-binding protein and a component of steroid receptor complexes.* Proc Natl Acad Sci U S A, 2003. **100**(3): p. 868-73.
17. Wu, B., et al., *3D structure of human FK506-binding protein 52: implications for the assembly of the glucocorticoid receptor/Hsp90/immunophilin heterocomplex.* Proc Natl Acad Sci U S A, 2004. **101**(22): p. 8348-53.
18. Michnick, S.W., et al., *Solution structure of FKBP, a rotamase enzyme and receptor for FK506 and rapamycin.* Science, 1991. **252**(5007): p. 836-9.
19. Baughman, G., et al., *Tissue distribution and abundance of human FKBP51, and FK506-binding protein that can mediate calcineurin inhibition.* Biochem Biophys Res Commun, 1997. **232**(2): p. 437-43.

20. Bierer, B.E., et al., *Two distinct signal transmission pathways in T lymphocytes are inhibited by complexes formed between an immunophilin and either FK506 or rapamycin.* Proc Natl Acad Sci U S A, 1990. **87**(23): p. 9231-5.
21. Chen, J., et al., *Identification of an 11-kDa FKBP12-rapamycin-binding domain within the 289-kDa FKBP12-rapamycin-associated protein and characterization of a critical serine residue.* Proc Natl Acad Sci U S A, 1995. **92**(11): p. 4947-51.
22. Van Duyne, G.D., et al., *Atomic structure of FKBP-FK506, an immunophilin-immunosuppressant complex.* Science, 1991. **252**(5007): p. 839-42.
23. Choi, J., et al., *Structure of the FKBP12-rapamycin complex interacting with the binding domain of human FRAP.* Science, 1996. **273**(5272): p. 239-42.
24. Jayaraman, T., et al., *FK506 binding protein associated with the calcium release channel (ryanodine receptor).* J Biol Chem, 1992. **267**(14): p. 9474-7.
25. Samso, M., X. Shen, and P.D. Allen, *Structural characterization of the RyR1-FKBP12 interaction.* J Mol Biol, 2006. **356**(4): p. 917-27.
26. Brillantes, A.B., et al., *Stabilization of calcium release channel (ryanodine receptor) function by FK506-binding protein.* Cell, 1994. **77**(4): p. 513-23.
27. Cameron, A.M., et al., *FKBP12 binds the inositol 1,4,5-trisphosphate receptor at leucine-proline (1400-1401) and anchors calcineurin to this FK506-like domain.* J Biol Chem, 1997. **272**(44): p. 27582-8.
28. Okadome, T., et al., *Characterization of the interaction of FKBP12 with the transforming growth factor-beta type I receptor in vivo.* J Biol Chem, 1996. **271**(36): p. 21687-90.
29. Wang, T., et al., *The immunophilin FKBP12 functions as a common inhibitor of the TGF beta family type I receptors.* Cell, 1996. **86**(3): p. 435-44.
30. Chen, Y.G., F. Liu, and J. Massague, *Mechanism of TGFbeta receptor inhibition by FKBP12.* EMBO J, 1997. **16**(13): p. 3866-76.
31. Hoeffer, C.A., et al., *Removal of FKBP12 enhances mTOR-Raptor interactions, LTP, memory, and perseverative/repetitive behavior.* Neuron, 2008. **60**(5): p. 832-45.
32. Gerard, M., et al., *Inhibition of FK506 binding proteins reduces alpha-synuclein aggregation and Parkinson's disease-like pathology.* J Neurosci, 2010. **30**(7): p. 2454-63.
33. Tanaka, K., et al., *Neuroprotective and antioxidant properties of FKBP-binding immunophilin ligands are independent on the FKBP12 pathway in human cells.* Neurosci Lett, 2002. **330**(2): p. 147-50.
34. Baughman, G., et al., *FKBP51, a novel T-cell-specific immunophilin capable of calcineurin inhibition.* Mol Cell Biol, 1995. **15**(8): p. 4395-402.
35. Yeh, W.C., et al., *Identification and characterization of an immunophilin expressed during the clonal expansion phase of adipocyte differentiation.* Proc Natl Acad Sci U S A, 1995. **92**(24): p. 11081-5.
36. Nair, S.C., et al., *Molecular cloning of human FKBP51 and comparisons of immunophilin interactions with Hsp90 and progesterone receptor.* Mol Cell Biol, 1997. **17**(2): p. 594-603.
37. Barent, R.L., et al., *Analysis of FKBP51/FKBP52 chimeras and mutants for Hsp90 binding and association with progesterone receptor complexes.* Mol Endocrinol, 1998. **12**(3): p. 342-54.
38. Young, J.C., W.M. Obermann, and F.U. Hartl, *Specific binding of tetratricopeptide repeat proteins to the C-terminal 12-kDa domain of hsp90.* J Biol Chem, 1998. **273**(29): p. 18007-10.
39. Reynolds, P.D., et al., *Glucocorticoid resistance in the squirrel monkey is associated with overexpression of the immunophilin FKBP51.* J Clin Endocrinol Metab, 1999. **84**(2): p. 663-9.

40. Scammell, J.G., et al., *Overexpression of the FK506-binding immunophilin FKBP51 is the common cause of glucocorticoid resistance in three New World primates.* Gen Comp Endocrinol, 2001. **124**(2): p. 152-65.
41. Denny, W.B., et al., *Squirrel monkey immunophilin FKBP51 is a potent inhibitor of glucocorticoid receptor binding.* Endocrinology, 2000. **141**(11): p. 4107-13.
42. Denny, W.B., et al., *Structure-function analysis of squirrel monkey FK506-binding protein 51, a potent inhibitor of glucocorticoid receptor activity.* Endocrinology, 2005. **146**(7): p. 3194-201.
43. Vermeer, H., et al., *An in vitro bioassay to determine individual sensitivity to glucocorticoids: induction of FKBP51 mRNA in peripheral blood mononuclear cells.* Mol Cell Endocrinol, 2004. **218**(1-2): p. 49-55.
44. Hubler, T.R. and J.G. Scammell, *Intronic hormone response elements mediate regulation of FKBP5 by progestins and glucocorticoids.* Cell Stress Chaperones, 2004. **9**(3): p. 243-52.
45. Cheung, J. and D.F. Smith, *Molecular chaperone interactions with steroid receptors: an update.* Mol Endocrinol, 2000. **14**(7): p. 939-46.
46. Hubler, T.R., et al., *The FK506-binding immunophilin FKBP51 is transcriptionally regulated by progestin and attenuates progestin responsiveness.* Endocrinology, 2003. **144**(6): p. 2380-7.
47. Binder, E.B., et al., *Polymorphisms in FKBP5 are associated with increased recurrence of depressive episodes and rapid response to antidepressant treatment.* Nat Genet, 2004. **36**(12): p. 1319-25.
48. Kirchheiner, J., et al., *Genetic variants in FKBP5 affecting response to antidepressant drug treatment.* Pharmacogenomics, 2008. **9**(7): p. 841-6.
49. Ising, M., et al., *Polymorphisms in the FKBP5 gene region modulate recovery from psychosocial stress in healthy controls.* Eur J Neurosci, 2008. **28**(2): p. 389-98.
50. Roy, A., et al., *Interaction of FKBP5, a stress-related gene, with childhood trauma increases the risk for attempting suicide.* Neuropsychopharmacology, 2010. **35**(8): p. 1674-83.
51. Willour, V.L., et al., *Family-based association of FKBP5 in bipolar disorder.* Mol Psychiatry, 2009. **14**(3): p. 261-8.
52. Pratt, W.B. and D.O. Toft, *Steroid receptor interactions with heat shock protein and immunophilin chaperones.* Endocr Rev, 1997. **18**(3): p. 306-60.
53. Ni, L., et al., *FKBP51 promotes assembly of the Hsp90 chaperone complex and regulates androgen receptor signaling in prostate cancer cells.* Mol Cell Biol, 2010. **30**(5): p. 1243-53.
54. Periyasamy, S., et al., *The immunophilin ligands cyclosporin A and FK506 suppress prostate cancer cell growth by androgen receptor-dependent and -independent mechanisms.* Endocrinology, 2007. **148**(10): p. 4716-26.
55. Soontornniyomkij, V., et al., *Short-term recognition memory impairment is associated with decreased expression of FK506 binding protein 51 in the aged mouse brain.* Age (Dordr), 2010.
56. Jinwal, U.K., et al., *The Hsp90 cochaperone, FKBP51, increases Tau stability and polymerizes microtubules.* J Neurosci, 2010. **30**(2): p. 591-9.
57. Pei, H., et al., *FKBP51 affects cancer cell response to chemotherapy by negatively regulating Akt.* Cancer Cell, 2009. **16**(3): p. 259-66.
58. Wiederrecht, G., et al., *Characterization of high molecular weight FK-506 binding activities reveals a novel FK-506-binding protein as well as a protein complex.* J Biol Chem, 1992. **267**(30): p. 21753-60.

59. Lebeau, M.C., et al., *P59, an hsp 90-binding protein. Cloning and sequencing of its cDNA and preparation of a peptide-directed polyclonal antibody.* J Biol Chem, 1992. **267**(7): p. 4281-4.
60. Peattie, D.A., et al., *Expression and characterization of human FKBP52, an immunophilin that associates with the 90-kDa heat shock protein and is a component of steroid receptor complexes.* Proc Natl Acad Sci U S A, 1992. **89**(22): p. 10974-8.
61. Callebaut, I., et al., *An immunophilin that binds M(r) 90,000 heat shock protein: main structural features of a mammalian p59 protein.* Proc Natl Acad Sci U S A, 1992. **89**(14): p. 6270-4.
62. Miyata, Y., et al., *Phosphorylation of the immunosuppressant FK506-binding protein FKBP52 by casein kinase II: regulation of HSP90-binding activity of FKBP52.* Proc Natl Acad Sci U S A, 1997. **94**(26): p. 14500-5.
63. Qing, K., et al., *Adeno-associated virus type 2-mediated gene transfer: role of cellular FKBP52 protein in transgene expression.* J Virol, 2001. **75**(19): p. 8968-76.
64. Qing, K., et al., *Adeno-associated virus type 2-mediated gene transfer: role of cellular T-cell protein tyrosine phosphatase in transgene expression in established cell lines in vitro and transgenic mice in vivo.* J Virol, 2003. **77**(4): p. 2741-6.
65. Massol, N., et al., *Promoter activity and gene structure of rabbit FKBP52.* DNA Cell Biol, 2003. **22**(8): p. 505-11.
66. Pratt, W.B. and D.O. Toft, *Regulation of signaling protein function and trafficking by the hsp90/hsp70-based chaperone machinery.* Exp Biol Med (Maywood), 2003. **228**(2): p. 111-33.
67. Riggs, D.L., et al., *The Hsp90-binding peptidylprolyl isomerase FKBP52 potentiates glucocorticoid signaling in vivo.* EMBO J, 2003. **22**(5): p. 1158-67.
68. Silverstein, A.M., et al., *Different regions of the immunophilin FKBP52 determine its association with the glucocorticoid receptor, hsp90, and cytoplasmic dynein.* J Biol Chem, 1999. **274**(52): p. 36980-6.
69. Galigniana, M.D., et al., *Evidence that the peptidylprolyl isomerase domain of the hsp90-binding immunophilin FKBP52 is involved in both dynein interaction and glucocorticoid receptor movement to the nucleus.* J Biol Chem, 2001. **276**(18): p. 14884-9.
70. Galigniana, M.D., et al., *Binding of hsp90-associated immunophilins to cytoplasmic dynein: direct binding and in vivo evidence that the peptidylprolyl isomerase domain is a dynein interaction domain.* Biochemistry, 2002. **41**(46): p. 13602-10.
71. Davies, T.H., Y.M. Ning, and E.R. Sanchez, *A new first step in activation of steroid receptors: hormone-induced switching of FKBP51 and FKBP52 immunophilins.* J Biol Chem, 2002. **277**(7): p. 4597-600.
72. Chambraud, B., et al., *A role for FKBP52 in Tau protein function.* Proc Natl Acad Sci U S A, 2010. **107**(6): p. 2658-63.
73. Sewell, T.J., et al., *Inhibition of calcineurin by a novel FK-506-binding protein.* J Biol Chem, 1994. **269**(33): p. 21094-102.
74. Lam, E., et al., *A novel FK506 binding protein can mediate the immunosuppressive effects of FK506 and is associated with the cardiac ryanodine receptor.* J Biol Chem, 1995. **270**(44): p. 26511-22.
75. Timerman, A.P., et al., *Selective binding of FKBP12.6 by the cardiac ryanodine receptor.* J Biol Chem, 1996. **271**(34): p. 20385-91.
76. Timerman, A.P., et al., *Characterization of an exchange reaction between soluble FKBP-12 and the FKBP.ryanodine receptor complex. Modulation by FKBP mutants deficient in peptidyl-prolyl isomerase activity.* J Biol Chem, 1995. **270**(6): p. 2451-9.
77. Xin, H.B., et al., *Oestrogen protects FKBP12.6 null mice from cardiac hypertrophy.* Nature, 2002. **416**(6878): p. 334-8.

78. Jin, Y.J., et al., *Molecular cloning of a membrane-associated human FK506- and rapamycin-binding protein, FKBP-13.* Proc Natl Acad Sci U S A, 1991. **88**(15): p. 6677-81.
79. Nigam, S.K., et al., *Localization of the FK506-binding protein, FKBP 13, to the lumen of the endoplasmic reticulum.* Biochem J, 1993. **294 (Pt 2)**: p. 511-5.
80. Nielsen, J.B., et al., *Yeast FKBP-13 is a membrane-associated FK506-binding protein encoded by the nonessential gene FKB2.* Proc Natl Acad Sci U S A, 1992. **89**(16): p. 7471-5.
81. Partaledis, J.A. and V. Berlin, *The FKB2 gene of Saccharomyces cerevisiae, encoding the immunosuppressant-binding protein FKBP-13, is regulated in response to accumulation of unfolded proteins in the endoplasmic reticulum.* Proc Natl Acad Sci U S A, 1993. **90**(12): p. 5450-4.
82. Bush, K.T., B.A. Hendrickson, and S.K. Nigam, *Induction of the FK506-binding protein, FKBP13, under conditions which misfold proteins in the endoplasmic reticulum.* Biochem J, 1994. **303 (Pt 3)**: p. 705-8.
83. Walensky, L.D., et al., *The 13-kD FK506 binding protein, FKBP13, interacts with a novel homologue of the erythrocyte membrane cytoskeletal protein 4.1.* J Cell Biol, 1998. **141**(1): p. 143-53.
84. Jin, Y.J., S.J. Burakoff, and B.E. Bierer, *Molecular cloning of a 25-kDa high affinity rapamycin binding protein, FKBP25.* J Biol Chem, 1992. **267**(16): p. 10942-5.
85. Galat, A., et al., *A rapamycin-selective 25-kDa immunophilin.* Biochemistry, 1992. **31**(8): p. 2427-34.
86. Hung, D.T. and S.L. Schreiber, *cDNA cloning of a human 25 kDa FK506 and rapamycin binding protein.* Biochem Biophys Res Commun, 1992. **184**(2): p. 733-8.
87. Liang, J., Hung, D. T, Schreiber, S. L, and, Clardy, J., *X-ray fragment of hFKBP-25 (residues 116 to 224)* PDB entry: 1PKB, 1995.
88. Jin, Y.J. and S.J. Burakoff, *The 25-kDa FK506-binding protein is localized in the nucleus and associates with casein kinase II and nucleolin.* Proc Natl Acad Sci U S A, 1993. **90**(16): p. 7769-73.
89. Ahn, J., et al., *Down-regulation of the stathmin/Op18 and FKBP25 genes following p53 induction.* Oncogene, 1999. **18**(43): p. 5954-8.
90. Yang, W.M., Y.L. Yao, and E. Seto, *The FK506-binding protein 25 functionally associates with histone deacetylases and with transcription factor YY1.* EMBO J, 2001. **20**(17): p. 4814-25.
91. Leclercq, M., F. Vinci, and A. Galat, *Mammalian FKBP-25 and its associated proteins.* Arch Biochem Biophys, 2000. **380**(1): p. 20-8.
92. Vezina, C., A. Kudelski, and S.N. Sehgal, *Rapamycin (AY-22,989), a new antifungal antibiotic. I. Taxonomy of the producing streptomycete and isolation of the active principle.* J Antibiot (Tokyo), 1975. **28**(10): p. 721-6.
93. Sehgal, S.N., H. Baker, and C. Vezina, *Rapamycin (AY-22,989), a new antifungal antibiotic. II. Fermentation, isolation and characterization.* J Antibiot (Tokyo), 1975. **28**(10): p. 727-32.
94. Singh, K., S. Sun, and C. Vezina, *Rapamycin (AY-22,989), a new antifungal antibiotic. IV. Mechanism of action.* J Antibiot (Tokyo), 1979. **32**(6): p. 630-45.
95. Baker, H., et al., *Rapamycin (AY-22,989), a new antifungal antibiotic. III. In vitro and in vivo evaluation.* J Antibiot (Tokyo), 1978. **31**(6): p. 539-45.
96. Houchens, D.P., et al., *Human brain tumor xenografts in nude mice as a chemotherapy model.* Eur J Cancer Clin Oncol, 1983. **19**(6): p. 799-805.
97. Martel, R.R., J. Klicius, and S. Galet, *Inhibition of the immune response by rapamycin, a new antifungal antibiotic.* Can J Physiol Pharmacol, 1977. **55**(1): p. 48-51.

98. Collier, D.S., et al., *Rapamycin in experimental renal allografts in dogs and pigs.* Transplant Proc, 1990. **22**(4): p. 1674-5.
99. Kahan, B.D., et al., *Immunosuppressive effects and safety of a sirolimus/cyclosporine combination regimen for renal transplantation.* Transplantation, 1998. **66**(8): p. 1040-6.
100. Kronsteiner, E., et al., *Outcomes of overlapping bare-metal stents with sirolimus-eluting stents for long lesions in small coronary vessels.* J Invasive Cardiol, 2010. **22**(2): p. 76-9.
101. Mehilli, J., et al., *Randomized trial of paclitaxel- and sirolimus-eluting stents in small coronary vessels.* Eur Heart J, 2006. **27**(3): p. 260-6.
102. Meier, B., et al., *Sirolimus-eluting coronary stents in small vessels.* Am Heart J, 2006. **151**(5): p. 1019 e1-7.
103. Bierer, B.E., et al., *Probing immunosuppressant action with a nonnatural immunophilin ligand.* Science, 1990. **250**(4980): p. 556-9.
104. Heitman, J., N.R. Movva, and M.N. Hall, *Targets for cell cycle arrest by the immunosuppressant rapamycin in yeast.* Science, 1991. **253**(5022): p. 905-9.
105. Kunz, J., et al., *Target of rapamycin in yeast, TOR2, is an essential phosphatidylinositol kinase homolog required for G1 progression.* Cell, 1993. **73**(3): p. 585-96.
106. Barbet, N.C., et al., *TOR controls translation initiation and early G1 progression in yeast.* Mol Biol Cell, 1996. **7**(1): p. 25-42.
107. Sabers, C.J., et al., *Isolation of a protein target of the FKBP12-rapamycin complex in mammalian cells.* J Biol Chem, 1995. **270**(2): p. 815-22.
108. Beretta, L., et al., *Rapamycin blocks the phosphorylation of 4E-BP1 and inhibits cap-dependent initiation of translation.* EMBO J, 1996. **15**(3): p. 658-64.
109. Brown, E.J., et al., *Control of p70 s6 kinase by kinase activity of FRAP in vivo.* Nature, 1995. **377**(6548): p. 441-6.
110. Murakami, M., et al., *mTOR is essential for growth and proliferation in early mouse embryos and embryonic stem cells.* Mol Cell Biol, 2004. **24**(15): p. 6710-8.
111. Liang, J., J. Choi, and J. Clardy, *Refined structure of the FKBP12-rapamycin-FRB ternary complex at 2.2 A resolution.* Acta Crystallogr D Biol Crystallogr, 1999. **55**(Pt 4): p. 736-44.
112. Yip, C.K., et al., *Structure of the human mTOR complex I and its implications for rapamycin inhibition.* Mol Cell, 2010. **38**(5): p. 768-74.
113. Bai, X., et al., *Rheb activates mTOR by antagonizing its endogenous inhibitor, FKBP38.* Science, 2007. **318**(5852): p. 977-80.
114. Wang, X., et al., *Re-evaluating the roles of proposed modulators of mammalian target of rapamycin complex 1 (mTORC1) signaling.* J Biol Chem, 2008. **283**(45): p. 30482-92.
115. Uhlenbrock, K., et al., *Reassessment of the role of FKBP38 in the Rheb/mTORC1 pathway.* FEBS Lett, 2009. **583**(6): p. 965-70.
116. Thoreen, C.C., et al., *An ATP-competitive mammalian target of rapamycin inhibitor reveals rapamycin-resistant functions of mTORC1.* J Biol Chem, 2009. **284**(12): p. 8023-32.
117. Thoreen, C.C. and D.M. Sabatini, *Rapamycin inhibits mTORC1, but not completely.* Autophagy, 2009. **5**(5): p. 725-6.
118. Garcia-Martinez, J.M., et al., *Ku-0063794 is a specific inhibitor of the mammalian target of rapamycin (mTOR).* Biochem J, 2009. **421**(1): p. 29-42.
119. Feldman, M.E., et al., *Active-site inhibitors of mTOR target rapamycin-resistant outputs of mTORC1 and mTORC2.* PLoS Biol, 2009. **7**(2): p. e38.

120. Knutson, B.A., *Insights into the domain and repeat architecture of target of rapamycin.* J Struct Biol, 2010. **170**(2): p. 354-63.
121. Alarcon, C.M., M.E. Cardenas, and J. Heitman, *Mammalian RAFT1 kinase domain provides rapamycin-sensitive TOR function in yeast.* Genes Dev, 1996. **10**(3): p. 279-88.
122. Sabatini, D.M., et al., *The rapamycin and FKBP12 target (RAFT) displays phosphatidylinositol 4-kinase activity.* J Biol Chem, 1995. **270**(36): p. 20875-8.
123. Leone, M., et al., *The FRB domain of mTOR: NMR solution structure and inhibitor design.* Biochemistry, 2006. **45**(34): p. 10294-302.
124. Nojima, H., et al., *The mammalian target of rapamycin (mTOR) partner, raptor, binds the mTOR substrates p70 S6 kinase and 4E-BP1 through their TOR signaling (TOS) motif.* J Biol Chem, 2003. **278**(18): p. 15461-4.
125. Dames, S.A., et al., *The solution structure of the FATC domain of the protein kinase target of rapamycin suggests a role for redox-dependent structural and cellular stability.* J Biol Chem, 2005. **280**(21): p. 20558-64.
126. Loewith, R., et al., *Two TOR complexes, only one of which is rapamycin sensitive, have distinct roles in cell growth control.* Mol Cell, 2002. **10**(3): p. 457-68.
127. Wang, L., C.J. Rhodes, and J.C. Lawrence, Jr., *Activation of mammalian target of rapamycin (mTOR) by insulin is associated with stimulation of 4EBP1 binding to dimeric mTOR complex 1.* J Biol Chem, 2006. **281**(34): p. 24293-303.
128. Kim, D.H., et al., *GbetaL, a positive regulator of the rapamycin-sensitive pathway required for the nutrient-sensitive interaction between raptor and mTOR.* Mol Cell, 2003. **11**(4): p. 895-904.
129. Hara, K., et al., *Raptor, a binding partner of target of rapamycin (TOR), mediates TOR action.* Cell, 2002. **110**(2): p. 177-89.
130. Kim, D.H., et al., *mTOR interacts with raptor to form a nutrient-sensitive complex that signals to the cell growth machinery.* Cell, 2002. **110**(2): p. 163-75.
131. Oshiro, N., et al., *Dissociation of raptor from mTOR is a mechanism of rapamycin-induced inhibition of mTOR function.* Genes Cells, 2004. **9**(4): p. 359-66.
132. Guertin, D.A., et al., *Ablation in mice of the mTORC components raptor, rictor, or mLST8 reveals that mTORC2 is required for signaling to Akt-FOXO and PKCalpha, but not S6K1.* Dev Cell, 2006. **11**(6): p. 859-71.
133. Pause, A., et al., *Dominant negative mutants of mammalian translation initiation factor eIF-4A define a critical role for eIF-4F in cap-dependent and cap-independent initiation of translation.* EMBO J, 1994. **13**(5): p. 1205-15.
134. Pause, A., et al., *Insulin-dependent stimulation of protein synthesis by phosphorylation of a regulator of 5'-cap function.* Nature, 1994. **371**(6500): p. 762-7.
135. Holz, M.K., et al., *mTOR and S6K1 mediate assembly of the translation preinitiation complex through dynamic protein interchange and ordered phosphorylation events.* Cell, 2005. **123**(4): p. 569-80.
136. Schalm, S.S. and J. Blenis, *Identification of a conserved motif required for mTOR signaling.* Curr Biol, 2002. **12**(8): p. 632-9.
137. Frias, M.A., et al., *mSin1 is necessary for Akt/PKB phosphorylation, and its isoforms define three distinct mTORC2s.* Curr Biol, 2006. **16**(18): p. 1865-70.
138. Yang, Q., et al., *Identification of Sin1 as an essential TORC2 component required for complex formation and kinase activity.* Genes Dev, 2006. **20**(20): p. 2820-32.
139. Sarbassov, D.D., et al., *Prolonged rapamycin treatment inhibits mTORC2 assembly and Akt/PKB.* Mol Cell, 2006. **22**(2): p. 159-68.
140. Sarbassov, D.D., et al., *Rictor, a novel binding partner of mTOR, defines a rapamycin-insensitive and raptor-independent pathway that regulates the cytoskeleton.* Curr Biol, 2004. **14**(14): p. 1296-302.

141. Sarbassov, D.D., et al., *Phosphorylation and regulation of Akt/PKB by the rictor-mTOR complex.* Science, 2005. **307**(5712): p. 1098-101.
142. Lawlor, M.A. and D.R. Alessi, *PKB/Akt: a key mediator of cell proliferation, survival and insulin responses?* J Cell Sci, 2001. **114**(Pt 16): p. 2903-10.
143. Jacinto, E., et al., *Mammalian TOR complex 2 controls the actin cytoskeleton and is rapamycin insensitive.* Nat Cell Biol, 2004. **6**(11): p. 1122-8.
144. Zinzalla, V., et al., *Activation of mTORC2 by association with the ribosome.* Cell. **144**(5): p. 757-68.
145. Cantley, L.C., *The phosphoinositide 3-kinase pathway.* Science, 2002. **296**(5573): p. 1655-7.
146. Banfic, H., et al., *A novel integrin-activated pathway forms PKB/Akt-stimulatory phosphatidylinositol 3,4-bisphosphate via phosphatidylinositol 3-phosphate in platelets.* J Biol Chem, 1998. **273**(1): p. 13-6.
147. McManus, E.J., et al., *The in vivo role of PtdIns(3,4,5)P3 binding to PDK1 PH domain defined by knockin mutation.* EMBO J, 2004. **23**(10): p. 2071-82.
148. Gao, X., et al., *Tsc tumour suppressor proteins antagonize amino-acid-TOR signalling.* Nat Cell Biol, 2002. **4**(9): p. 699-704.
149. Kwiatkowski, D.J., *Tuberous sclerosis: from tubers to mTOR.* Ann Hum Genet, 2003. **67**(Pt 1): p. 87-96.
150. Tee, A.R., et al., *Tuberous sclerosis complex-1 and -2 gene products function together to inhibit mammalian target of rapamycin (mTOR)-mediated downstream signaling.* Proc Natl Acad Sci U S A, 2002. **99**(21): p. 13571-6.
151. Tee, A.R., et al., *Tuberous sclerosis complex gene products, Tuberin and Hamartin, control mTOR signaling by acting as a GTPase-activating protein complex toward Rheb.* Curr Biol, 2003. **13**(15): p. 1259-68.
152. Long, X., et al., *Rheb binds and regulates the mTOR kinase.* Curr Biol, 2005. **15**(8): p. 702-13.
153. Kovacina, K.S., et al., *Identification of a proline-rich Akt substrate as a 14-3-3 binding partner.* J Biol Chem, 2003. **278**(12): p. 10189-94.
154. Vander Haar, E., et al., *Insulin signalling to mTOR mediated by the Akt/PKB substrate PRAS40.* Nat Cell Biol, 2007. **9**(3): p. 316-23.
155. Sancak, Y., et al., *PRAS40 is an insulin-regulated inhibitor of the mTORC1 protein kinase.* Mol Cell, 2007. **25**(6): p. 903-15.
156. Oshiro, N., et al., *The proline-rich Akt substrate of 40 kDa (PRAS40) is a physiological substrate of mammalian target of rapamycin complex 1.* J Biol Chem, 2007. **282**(28): p. 20329-39.
157. Wang, L., et al., *PRAS40 regulates mTORC1 kinase activity by functioning as a direct inhibitor of substrate binding.* J Biol Chem, 2007. **282**(27): p. 20036-44.
158. Inoki, K., T. Zhu, and K.L. Guan, *TSC2 mediates cellular energy response to control cell growth and survival.* Cell, 2003. **115**(5): p. 577-90.
159. Shaw, R.J., et al., *The LKB1 tumor suppressor negatively regulates mTOR signaling.* Cancer Cell, 2004. **6**(1): p. 91-9.
160. Um, S.H., et al., *Absence of S6K1 protects against age- and diet-induced obesity while enhancing insulin sensitivity.* Nature, 2004. **431**(7005): p. 200-5.
161. Greene, M.W., et al., *Modulation of insulin-stimulated degradation of human insulin receptor substrate-1 by Serine 312 phosphorylation.* J Biol Chem, 2003. **278**(10): p. 8199-211.
162. Peterson, T.R., et al., *DEPTOR is an mTOR inhibitor frequently overexpressed in multiple myeloma cells and required for their survival.* Cell, 2009. **137**(5): p. 873-86.
163. Proud, C.G., *Dynamic balancing: DEPTOR tips the scales.* J Mol Cell Biol, 2009. **1**(2): p. 61-3.

164. Sancak, Y., et al., *The Rag GTPases bind raptor and mediate amino acid signaling to mTORC1.* Science, 2008. **320**(5882): p. 1496-501.
165. Li, L., et al., *Regulation of mTORC1 by the Rab and Arf GTPases.* J Biol Chem. **285**(26): p. 19705-9.
166. Sancak, Y., et al., *Ragulator-Rag complex targets mTORC1 to the lysosomal surface and is necessary for its activation by amino acids.* Cell, 2010. **141**(2): p. 290-303.
167. Mizushima, N., et al., *Autophagy fights disease through cellular self-digestion.* Nature, 2008. **451**(7182): p. 1069-75.
168. Hosokawa, N., et al., *Nutrient-dependent mTORC1 association with the ULK1-Atg13-FIP200 complex required for autophagy.* Mol Biol Cell, 2009. **20**(7): p. 1981-91.
169. Hara, T., et al., *FIP200, a ULK-interacting protein, is required for autophagosome formation in mammalian cells.* J Cell Biol, 2008. **181**(3): p. 497-510.
170. Yang, X., et al., *The mammalian target of rapamycin-signaling pathway in regulating metabolism and growth.* J Anim Sci, 2008. **86**(14 Suppl): p. E36-50.
171. Marcotrigiano, J., et al., *Cocrystal structure of the messenger RNA 5' cap-binding protein (eIF4E) bound to 7-methyl-GDP.* Cell, 1997. **89**(6): p. 951-61.
172. Marcotrigiano, J., et al., *X-ray studies of the messenger RNA 5' cap-binding protein (eIF4E) bound to 7-methyl-GDP.* Nucleic Acids Symp Ser, 1997(36): p. 8-11.
173. Haghighat, A., et al., *Repression of cap-dependent translation by 4E-binding protein 1: competition with p220 for binding to eukaryotic initiation factor-4E.* EMBO J, 1995. **14**(22): p. 5701-9.
174. Matsuo, H., et al., *Structure of translation factor eIF4E bound to m7GDP and interaction with 4E-binding protein.* Nat Struct Biol, 1997. **4**(9): p. 717-24.
175. Mader, S., et al., *The translation initiation factor eIF-4E binds to a common motif shared by the translation factor eIF-4 gamma and the translational repressors 4E-binding proteins.* Mol Cell Biol, 1995. **15**(9): p. 4990-7.
176. Fadden, P., T.A. Haystead, and J.C. Lawrence, Jr., *Identification of phosphorylation sites in the translational regulator, PHAS-I, that are controlled by insulin and rapamycin in rat adipocytes.* J Biol Chem, 1997. **272**(15): p. 10240-7.
177. Proud, C.G., *Signalling to translation: how signal transduction pathways control the protein synthetic machinery.* Biochem J, 2007. **403**(2): p. 217-34.
178. Schalm, S.S., et al., *TOS motif-mediated raptor binding regulates 4E-BP1 multisite phosphorylation and function.* Curr Biol, 2003. **13**(10): p. 797-806.
179. Gingras, A.C., et al., *Regulation of 4E-BP1 phosphorylation: a novel two-step mechanism.* Genes Dev, 1999. **13**(11): p. 1422-37.
180. Ayuso, M.I., et al., *New hierarchical phosphorylation pathway of the translational repressor eIF4E-binding protein 1 (4E-BP1) in ischemia-reperfusion stress.* J Biol Chem, 2010. **285**(45): p. 34355-63.
181. Ferguson, G., I. Mothe-Satney, and J.C. Lawrence, Jr., *Ser-64 and Ser-111 in PHAS-I are dispensable for insulin-stimulated dissociation from eIF4E.* J Biol Chem, 2003. **278**(48): p. 47459-65.
182. Mothe-Satney, I., et al., *Mammalian target of rapamycin-dependent phosphorylation of PHAS-I in four (S/T)P sites detected by phospho-specific antibodies.* J Biol Chem, 2000. **275**(43): p. 33836-43.
183. Wang, X., et al., *Distinct signaling events downstream of mTOR cooperate to mediate the effects of amino acids and insulin on initiation factor 4E-binding proteins.* Mol Cell Biol, 2005. **25**(7): p. 2558-72.
184. McMahon, L.P., et al., *The rapamycin-binding domain governs substrate selectivity by the mammalian target of rapamycin.* Mol Cell Biol, 2002. **22**(21): p. 7428-38.

185. Choo, A.Y., et al., *Rapamycin differentially inhibits S6Ks and 4E-BP1 to mediate cell-type-specific repression of mRNA translation.* Proc Natl Acad Sci U S A, 2008. **105**(45): p. 17414-9.
186. Choo, A.Y. and J. Blenis, *Not all substrates are treated equally: implications for mTOR, rapamycin-resistance and cancer therapy.* Cell Cycle, 2009. **8**(4): p. 567-72.
187. Gwinn, D.M., et al., *AMPK phosphorylation of raptor mediates a metabolic checkpoint.* Mol Cell, 2008. **30**(2): p. 214-26.
188. Carriere, A., et al., *Oncogenic MAPK signaling stimulates mTORC1 activity by promoting RSK-mediated raptor phosphorylation.* Curr Biol, 2008. **18**(17): p. 1269-77.
189. Grove, J.R., et al., *Cloning and expression of two human p70 S6 kinase polypeptides differing only at their amino termini.* Mol Cell Biol, 1991. **11**(11): p. 5541-50.
190. Reinhard, C., et al., *Nuclear localization of p85s6k: functional requirement for entry into S phase.* EMBO J, 1994. **13**(7): p. 1557-65.
191. Shima, H., et al., *Disruption of the p70(s6k)/p85(s6k) gene reveals a small mouse phenotype and a new functional S6 kinase.* EMBO J, 1998. **17**(22): p. 6649-59.
192. Montagne, J. and G. Thomas, *S6K integrates nutrient and mitogen signals to control cell growth.* Cold Spring Harbor Monograph Series 42. Cold Spring Harbor Press, 2004(Hall M, Raff M, Thomas G (eds) Cell growth: control of cell size.): p. 265-298.
193. Pearce, L.R., D. Komander, and D.R. Alessi, *The nuts and bolts of AGC protein kinases.* Nat Rev Mol Cell Biol, 2010. **11**(1): p. 9-22.
194. Frodin, M., et al., *A phosphoserine/threonine-binding pocket in AGC kinases and PDK1 mediates activation by hydrophobic motif phosphorylation.* EMBO J, 2002. **21**(20): p. 5396-407.
195. Panasyuk, G., et al., *Nuclear export of S6K1 II is regulated by protein kinase CK2 phosphorylation at Ser-17.* J Biol Chem, 2006. **281**(42): p. 31188-201.
196. Song, Q. and L.I. Gilbert, *S6 phosphorylation results from prothoracicotropic hormone stimulation of insect prothoracic glands: a role for S6 kinase.* Dev Genet, 1994. **15**(4): p. 332-8.
197. Raught, B., et al., *Phosphorylation of eucaryotic translation initiation factor 4B Ser422 is modulated by S6 kinases.* EMBO J, 2004. **23**(8): p. 1761-9.
198. Jastrzebski, K., et al., *Coordinate regulation of ribosome biogenesis and function by the ribosomal protein S6 kinase, a key mediator of mTOR function.* Growth Factors, 2007. **25**(4): p. 209-26.
199. Valentinis, B., et al., *Insulin receptor substrate-1, p70S6K, and cell size in transformation and differentiation of hemopoietic cells.* J Biol Chem, 2000. **275**(33): p. 25451-9.
200. Westphal, R.S., et al., *Identification of kinase-phosphatase signaling modules composed of p70 S6 kinase-protein phosphatase 2A (PP2A) and p21-activated kinase-PP2A.* J Biol Chem, 1999. **274**(2): p. 687-92.
201. Wang, M.L., et al., *Regulation of ribosomal protein S6 kinases by ubiquitination.* Biochem Biophys Res Commun, 2008. **369**(2): p. 382-7.
202. Park, S., et al., *RIP1 activates PI3K-Akt via a dual mechanism involving NF-kappaB-mediated inhibition of the mTOR-S6K-IRS1 negative feedback loop and down-regulation of PTEN.* Cancer Res, 2009. **69**(10): p. 4107-11.
203. Selman, C., et al., *Evidence for lifespan extension and delayed age-related biomarkers in insulin receptor substrate 1 null mice.* FASEB J, 2008. **22**(3): p. 807-18.
204. Cho, I., et al., *Age- and Diet-Specific Effects of Variation at S6 Kinase on Life History, Metabolic, and Immune Response Traits in Drosophila melanogaster.* DNA Cell Biol, 2010.

205. Selman, C., et al., *Ribosomal protein S6 kinase 1 signaling regulates mammalian life span.* Science, 2009. **326**(5949): p. 140-4.
206. Spilman, P., et al., *Inhibition of mTOR by rapamycin abolishes cognitive deficits and reduces amyloid-beta levels in a mouse model of Alzheimer's disease.* PLoS One, 2010. **5**(4): p. e9979.
207. Lee, N.Y., et al., *The prolyl isomerase Pin1 interacts with a ribosomal protein S6 kinase to enhance insulin-induced AP-1 activity and cellular transformation.* Carcinogenesis, 2009. **30**(4): p. 671-81.
208. Dummler, B. and B.A. Hemmings, *Physiological roles of PKB/Akt isoforms in development and disease.* Biochem Soc Trans, 2007. **35**(Pt 2): p. 231-5.
209. Ananthanarayanan, B., Q. Ni, and J. Zhang, *Signal propagation from membrane messengers to nuclear effectors revealed by reporters of phosphoinositide dynamics and Akt activity.* Proc Natl Acad Sci U S A, 2005. **102**(42): p. 15081-6.
210. Bellacosa, A., et al., *Akt activation by growth factors is a multiple-step process: the role of the PH domain.* Oncogene, 1998. **17**(3): p. 313-25.
211. Alessi, D.R., et al., *Characterization of a 3-phosphoinositide-dependent protein kinase which phosphorylates and activates protein kinase Balpha.* Curr Biol, 1997. **7**(4): p. 261-9.
212. Datta, S.R., et al., *Akt phosphorylation of BAD couples survival signals to the cell-intrinsic death machinery.* Cell, 1997. **91**(2): p. 231-41.
213. Tran, H., et al., *The many forks in FOXO's road.* Sci STKE, 2003. **2003**(172): p. RE5.
214. Cardone, M.H., et al., *Regulation of cell death protease caspase-9 by phosphorylation.* Science, 1998. **282**(5392): p. 1318-21.
215. Manning, B.D., et al., *Identification of the tuberous sclerosis complex-2 tumor suppressor gene product tuberin as a target of the phosphoinositide 3-kinase/akt pathway.* Mol Cell, 2002. **10**(1): p. 151-62.
216. Liang, J., et al., *PKB/Akt phosphorylates p27, impairs nuclear import of p27 and opposes p27-mediated G1 arrest.* Nat Med, 2002. **8**(10): p. 1153-60.
217. Cho, H., et al., *Akt1/PKBalpha is required for normal growth but dispensable for maintenance of glucose homeostasis in mice.* J Biol Chem, 2001. **276**(42): p. 38349-52.
218. Chen, W.S., et al., *Growth retardation and increased apoptosis in mice with homozygous disruption of the Akt1 gene.* Genes Dev, 2001. **15**(17): p. 2203-8.
219. Garofalo, R.S., et al., *Severe diabetes, age-dependent loss of adipose tissue, and mild growth deficiency in mice lacking Akt2/PKB beta.* J Clin Invest, 2003. **112**(2): p. 197-208.
220. Cho, H., et al., *Insulin resistance and a diabetes mellitus-like syndrome in mice lacking the protein kinase Akt2 (PKB beta).* Science, 2001. **292**(5522): p. 1728-31.
221. Tschopp, O., et al., *Essential role of protein kinase B gamma (PKB gamma/Akt3) in postnatal brain development but not in glucose homeostasis.* Development, 2005. **132**(13): p. 2943-54.
222. Dummler, B., et al., *Life with a single isoform of Akt: mice lacking Akt2 and Akt3 are viable but display impaired glucose homeostasis and growth deficiencies.* Mol Cell Biol, 2006. **26**(21): p. 8042-51.
223. Vivanco, I. and C.L. Sawyers, *The phosphatidylinositol 3-Kinase AKT pathway in human cancer.* Nat Rev Cancer, 2002. **2**(7): p. 489-501.
224. Wang, S.I., et al., *Somatic mutations of PTEN in glioblastoma multiforme.* Cancer Res, 1997. **57**(19): p. 4183-6.
225. Celebi, J.T., et al., *Identification of PTEN mutations in metastatic melanoma specimens.* J Med Genet, 2000. **37**(9): p. 653-7.

226. Kawamura, N., et al., *PTEN/MMAC1 mutations in hepatocellular carcinomas: somatic inactivation of both alleles in tumors.* Jpn J Cancer Res, 1999. **90**(4): p. 413-8.
227. Dahia, P.L., et al., *Somatic deletions and mutations in the Cowden disease gene, PTEN, in sporadic thyroid tumors.* Cancer Res, 1997. **57**(21): p. 4710-3.
228. Alimov, A., et al., *Somatic mutation and homozygous deletion of PTEN/MMAC1 gene of 10q23 in renal cell carcinoma.* Anticancer Res, 1999. **19**(5B): p. 3841-6.
229. Philp, A.J., et al., *The phosphatidylinositol 3'-kinase p85alpha gene is an oncogene in human ovarian and colon tumors.* Cancer Res, 2001. **61**(20): p. 7426-9.
230. Bellacosa, A., et al., *Molecular alterations of the AKT2 oncogene in ovarian and breast carcinomas.* Int J Cancer, 1995. **64**(4): p. 280-5.
231. Guba, M., et al., *Rapamycin inhibits primary and metastatic tumor growth by antiangiogenesis: involvement of vascular endothelial growth factor.* Nat Med, 2002. **8**(2): p. 128-35.
232. Shor, B., et al., *A new pharmacologic action of CCI-779 involves FKBP12-independent inhibition of mTOR kinase activity and profound repression of global protein synthesis.* Cancer Res, 2008. **68**(8): p. 2934-43.
233. Mabuchi, S., et al., *RAD001 inhibits human ovarian cancer cell proliferation, enhances cisplatin-induced apoptosis, and prolongs survival in an ovarian cancer model.* Clin Cancer Res, 2007. **13**(14): p. 4261-70.
234. O'Reilly T, V.J., Muller M,, *In vivo activity of RAD001, an orally active rapamycin derivative, in experimental tumor models.* Proc Am Assoc Cancer Res, 2002. **43**(71).
235. Couderc, C., et al., *Targeting the PI3K/mTOR pathway in murine endocrine cell lines: in vitro and in vivo effects on tumor cell growth.* Am J Pathol, 2011. **178**(1): p. 336-44.
236. Ikezoe, T., et al., *Longitudinal inhibition of PI3K/Akt/mTOR signaling by LY294002 and rapamycin induces growth arrest of adult T-cell leukemia cells.* Leuk Res, 2007. **31**(5): p. 673-82.
237. Werzowa, J., et al., *Suppression of mTOR complex 2-dependent AKT phosphorylation in melanoma cells by combined treatment with rapamycin and LY294002.* Br J Dermatol, 2009. **160**(5): p. 955-64.
238. Hudes, G., et al., *Temsirolimus, interferon alfa, or both for advanced renal-cell carcinoma.* N Engl J Med, 2007. **356**(22): p. 2271-81.
239. Motzer, R.J., et al., *Phase I/II trial of temsirolimus combined with interferon alfa for advanced renal cell carcinoma.* J Clin Oncol, 2007. **25**(25): p. 3958-64.
240. Shariat, S.F., J.A. Karam, and P.I. Karakiewicz, *Words of wisdom. Re: Temsirolimus, interferon alfa, or both for advanced renal-cell carcinoma. Hudes G, Carducci M, Tomczak P, Dutcher J, Figlin R, Kapoor A, Staroslawska E, Sosman J, McDermott D, Bodrogi I, Kovacevic Z, Lesovoy V, Schmidt-Wolf IG, Barbarash O, Gokmen E, O'Toole T, Lustgarten S, Moore L, Motzer RJ; Global ARCC Trial. N Engl J Med 2007;356:2271-81.* Eur Urol, 2009. **55**(1): p. 250-2.
241. Yu, K., et al., *mTOR, a novel target in breast cancer: the effect of CCI-779, an mTOR inhibitor, in preclinical models of breast cancer.* Endocr Relat Cancer, 2001. **8**(3): p. 249-58.
242. Chan, H.Y., A.B. Grossman, and R.M. Bukowski, *Everolimus in the treatment of renal cell carcinoma and neuroendocrine tumors.* Adv Ther, 2010.
243. Noh, W.C., et al., *Determinants of rapamycin sensitivity in breast cancer cells.* Clin Cancer Res, 2004. **10**(3): p. 1013-23.
244. Fasolo, A. and C. Sessa, *mTOR inhibitors in the treatment of cancer.* Expert Opin Investig Drugs, 2008. **17**(11): p. 1717-34.

245. Dutcher, J.P., et al., *Effect of temsirolimus versus interferon-alpha on outcome of patients with advanced renal cell carcinoma of different tumor histologies.* Med Oncol, 2009. **26**(2): p. 202-9.
246. Witzig, T.E., et al., *Phase II trial of single-agent temsirolimus (CCI-779) for relapsed mantle cell lymphoma.* J Clin Oncol, 2005. **23**(23): p. 5347-56.
247. Molhoek, K.R., D.L. Brautigan, and C.L. Slingluff, Jr., *Synergistic inhibition of human melanoma proliferation by combination treatment with B-Raf inhibitor BAY43-9006 and mTOR inhibitor Rapamycin.* J Transl Med, 2005. **3**: p. 39.
248. Wang, T. and P.K. Donahoe, *The immunophilin FKBP12: a molecular guardian of the TGF-beta family type I receptors.* Front Biosci, 2004. **9**: p. 619-31.
249. Wang, T., P.K. Donahoe, and A.S. Zervos, *Specific interaction of type I receptors of the TGF-beta family with the immunophilin FKBP-12.* Science, 1994. **265**(5172): p. 674-6.
250. Fruman, D.A., et al., *FK506 binding protein 12 mediates sensitivity to both FK506 and rapamycin in murine mast cells.* Eur J Immunol, 1995. **25**(2): p. 563-71.
251. Dumont, F.J., et al., *Dominant mutations confer resistance to the immunosuppressant, rapamycin, in variants of a T cell lymphoma.* Cell Immunol, 1995. **163**(1): p. 70-9.
252. Nathan, C.O., et al., *Elevated expression of eIF4E and FGF-2 isoforms during vascularization of breast carcinomas.* Oncogene, 1997. **15**(9): p. 1087-94.
253. Dilling, M.B., et al., *4E-binding proteins, the suppressors of eukaryotic initiation factor 4E, are down-regulated in cells with acquired or intrinsic resistance to rapamycin.* J Biol Chem, 2002. **277**(16): p. 13907-17.
254. Huang, S., et al., *Sustained activation of the JNK cascade and rapamycin-induced apoptosis are suppressed by p53/p21(Cip1).* Mol Cell, 2003. **11**(6): p. 1491-501.
255. Kerr, K.M., Z.E. Sauna, and S.V. Ambudkar, *Correlation between steady-state ATP hydrolysis and vanadate-induced ADP trapping in Human P-glycoprotein. Evidence for ADP release as the rate-limiting step in the catalytic cycle and its modulation by substrates.* J Biol Chem, 2001. **276**(12): p. 8657-64.
256. Arceci, R.J., K. Stieglitz, and B.E. Bierer, *Immunosuppressants FK506 and rapamycin function as reversal agents of the multidrug resistance phenotype.* Blood, 1992. **80**(6): p. 1528-36.
257. Humar, R., et al., *Hypoxia enhances vascular cell proliferation and angiogenesis in vitro via rapamycin (mTOR)-dependent signaling.* FASEB J, 2002. **16**(8): p. 771-80.
258. Majumder, P.K., et al., *mTOR inhibition reverses Akt-dependent prostate intraepithelial neoplasia through regulation of apoptotic and HIF-1-dependent pathways.* Nat Med, 2004. **10**(6): p. 594-601.
259. Kurmasheva, R.T. and P.J. Houghton, *IGF-I mediated survival pathways in normal and malignant cells.* Biochim Biophys Acta, 2006. **1766**(1): p. 1-22.
260. Cox, M.B., et al., *FK506-binding protein 52 phosphorylation: a potential mechanism for regulating steroid hormone receptor activity.* Mol Endocrinol, 2007. **21**(12): p. 2956-67.
261. Pettersen, E., et al., *UCSF Chimera -- a visualization system for exploratory research and analysis.* J Comput Chem., 2004. **13**(25): p. 1605-12.
262. Laemmli, U.K., *Cleavage of structural proteins during the assembly of the head of bacteriophage T4.* Nature, 1970. **227**(5259): p. 680-5.
263. Bradford, M.M., *A rapid and sensitive method for the quantitation of microgram quantities of protein utilizing the principle of protein-dye binding.* Anal Biochem, 1976. **72**: p. 248-54.
264. Winn, M.D., et al., *Overview of the CCP4 suite and current developments.* Acta Crystallogr D Biol Crystallogr. **67**(Pt 4): p. 235-42.

265. Leslie, A.G.W., *Recent changes to the MOSFLM package for processing film and image plate data* Joint CCP4 + ESF-EAMCB Newsletter on Protein Crystallography, 1992. **26**.
266. Evans, P., *Scaling and assessment of data quality.* Acta Crystallogr D Biol Crystallogr, 2006. **62**(Pt 1): p. 72-82.
267. Cohen, S.X., et al., *ARP/wARP and molecular replacement: the next generation.* Acta Crystallogr D Biol Crystallogr, 2008. **64**(Pt 1): p. 49-60.
268. Emsley, P., et al., *Features and development of Coot.* Acta Crystallogr D Biol Crystallogr. **66**(Pt 4): p. 486-501.
269. Murshudov, G.N., A.A. Vagin, and E.J. Dodson, *Refinement of macromolecular structures by the maximum-likelihood method.* Acta Crystallogr D Biol Crystallogr, 1997. **53**(Pt 3): p. 240-55.
270. Jameson, D.M. and S.E. Seifried, *Quantification of protein-protein interactions using fluorescence polarization.* Methods, 1999. **19**(2): p. 222-33.
271. Förster, T., *Zwischenmolekulare Energiewanderung und Fluoreszenz.* Annalen der Physik, 1948. **437**(1-2): p. 55-75.
272. Graham, F.L. and A.J. van der Eb, *A new technique for the assay of infectivity of human adenovirus 5 DNA.* Virology, 1973. **52**(2): p. 456-67.
273. Standaert, R.F., et al., *Molecular cloning and overexpression of the human FK506-binding protein FKBP.* Nature, 1990. **346**(6285): p. 671-4.
274. Kozany, C., et al., *Fluorescent probes to characterise FK506-binding proteins.* Chembiochem, 2009. **10**(8): p. 1402-10.
275. Vilella-Bach, M., et al., *The FKBP12-rapamycin-binding domain is required for FKBP12-rapamycin-associated protein kinase activity and G1 progression.* J Biol Chem, 1999. **274**(7): p. 4266-72.
276. Banaszynski, L.A., C.W. Liu, and T.J. Wandless, *Characterization of the FKBP.rapamycin.FRB ternary complex.* J Am Chem Soc, 2005. **127**(13): p. 4715-21.
277. van Rossum, H.H., et al., *Everolimus and sirolimus antagonize tacrolimus based calcineurin inhibition via competition for FK-binding protein 12.* Biochem Pharmacol, 2009. **77**(7): p. 1206-12.
278. Reichling, L.J., et al., *Pharmacological characterization of purified recombinant mTOR FRB-kinase domain using fluorescence-based assays.* J Biomol Screen, 2008. **13**(3): p. 238-44.
279. Reichling, L., et al., *A Homogenous Fluorescence-Based Assay for mTOR Kinase Activity*.
280. Koltin, Y., et al., *Rapamycin sensitivity in Saccharomyces cerevisiae is mediated by a peptidyl-prolyl cis-trans isomerase related to human FK506-binding protein.* Mol Cell Biol, 1991. **11**(3): p. 1718-23.
281. Melendez, H.G., et al., *Role of the Botrytis cinerea FKBP12 ortholog in pathogenic development and in sulfur regulation.* Fungal Genet Biol, 2009. **46**(4): p. 308-20.
282. Wilson, K.P., et al., *Comparative X-ray structures of the major binding protein for the immunosuppressant FK506 (tacrolimus) in unliganded form and in complex with FK506 and rapamycin.* Acta Crystallogr D Biol Crystallogr, 1995. **51**(Pt 4): p. 511-21.
283. Jiang, L. and L. Lai, *CH...O hydrogen bonds at protein-protein interfaces.* J Biol Chem, 2002. **277**(40): p. 37732-40.
284. Covell, D.G. and A. Wallqvist, *Analysis of protein-protein interactions and the effects of amino acid mutations on their energetics. The importance of water molecules in the binding epitope.* J Mol Biol, 1997. **269**(2): p. 281-97.
285. Dumont, F.J., et al., *The immunosuppressive macrolides FK-506 and rapamycin act as reciprocal antagonists in murine T cells.* J Immunol, 1990. **144**(4): p. 1418-24.
286. Stenesh, J., *Biochemistry.* Springer, 1998.

287. Simossis, V.A. and J. Heringa, *PRALINE: a multiple sequence alignment toolbox that integrates homology-extended and secondary structure information.* Nucleic Acids Res, 2005. **33**(Web Server issue): p. W289-94.
288. Kissinger, C.R., et al., *Crystal structures of human calcineurin and the human FKBP12-FK506-calcineurin complex.* Nature, 1995. **378**(6557): p. 641-4.
289. Griffith, J.P., et al., *X-ray structure of calcineurin inhibited by the immunophilin-immunosuppressant FKBP12-FK506 complex.* Cell, 1995. **82**(3): p. 507-22.
290. Weiwad, M., et al., *Comparative analysis of calcineurin inhibition by complexes of immunosuppressive drugs with human FK506 binding proteins.* Biochemistry, 2006. **45**(51): p. 15776-84.
291. Li, T.K., et al., *Calcium- and FK506-independent interaction between the immunophilin FKBP51 and calcineurin.* J Cell Biochem, 2002. **84**(3): p. 460-71.
292. Takai, H., et al., *Tel2 structure and function in the Hsp90-dependent maturation of mTOR and ATR complexes.* Genes Dev, 2010. **24**(18): p. 2019-30.
293. Su, A.I., et al., *A gene atlas of the mouse and human protein-encoding transcriptomes.* Proc Natl Acad Sci U S A, 2004. **101**(16): p. 6062-7.
294. Pasini, E., et al., *Intracellular molecular effects of insulin resistance in patients with metabolic syndrome.* Cardiovasc Diabetol, 2010. **9**: p. 46.
295. Dumont, F.J., et al., *Distinct mechanisms of suppression of murine T cell activation by the related macrolides FK-506 and rapamycin.* J Immunol, 1990. **144**(1): p. 251-8.
296. Amato, R.J., et al., *Pilot study of rapamycin in patients with hormone-refractory prostate cancer.* Clin Genitourin Cancer, 2008. **6**(2): p. 97-102.
297. Feagans, J., et al., *Interstitial pneumonitis in the transplant patient: consider sirolimus-associated pulmonary toxicity.* J La State Med Soc, 2009. **161**(3): p. 166, 168-72.
298. Pham, P.T., et al., *Sirolimus-associated pulmonary toxicity.* Transplantation, 2004. **77**(8): p. 1215-20.
299. Delgoffe, G.M., et al., *Enhanced interaction between Hsp90 and raptor regulates mTOR signaling upon T cell activation.* Mol Immunol, 2009. **46**(13): p. 2694-8.
300. Adami, A., et al., *Structure of TOR and its complex with KOG1.* Mol Cell, 2007. **27**(3): p. 509-16.
301. Arevalo-Rodriguez, M., et al., *Prolyl isomerases in yeast.* Front Biosci, 2004. **9**: p. 2420-46.
302. Davies, T.H., Y.M. Ning, and E.R. Sanchez, *Differential control of glucocorticoid receptor hormone-binding function by tetratricopeptide repeat (TPR) proteins and the immunosuppressive ligand FK506.* Biochemistry, 2005. **44**(6): p. 2030-8.
303. Oh, W.J., et al., *mTORC2 can associate with ribosomes to promote cotranslational phosphorylation and stability of nascent Akt polypeptide.* EMBO J, 2010. **29**(23): p. 3939-51.
304. Takai, H., et al., *Tel2 regulates the stability of PI3K-related protein kinases.* Cell, 2007. **131**(7): p. 1248-59.
305. Gazitt, Y., et al., *Targeted therapy of human osteosarcoma with 17AAG or rapamycin: characterization of induced apoptosis and inhibition of mTOR and Akt/MAPK/Wnt pathways.* Int J Oncol, 2009. **34**(2): p. 551-61.
306. Giraudier, S., et al., *Overexpression of FKBP51 in idiopathic myelofibrosis regulates the growth factor independence of megakaryocyte progenitors.* Blood, 2002. **100**(8): p. 2932-40.
307. Komura, E., et al., *Spontaneous STAT5 activation induces growth factor independence in idiopathic myelofibrosis: possible relationship with FKBP51 overexpression.* Exp Hematol, 2003. **31**(7): p. 622-30.

308. Westberry, J.M., et al., *Glucocorticoid resistance in squirrel monkeys results from a combination of a transcriptionally incompetent glucocorticoid receptor and overexpression of the glucocorticoid receptor co-chaperone FKBP51.* J Steroid Biochem Mol Biol, 2006. **100**(1-3): p. 34-41.
309. Yemelyanov, A., et al., *Tumor suppressor activity of glucocorticoid receptor in the prostate.* Oncogene, 2007. **26**(13): p. 1885-96.
310. Hatakeyama, S., et al., *Glucocorticoid-induced growth inhibition with enhanced expression of ductal epithelium of human salivary gland adenocarcinoma cells transplanted into athymic nude mice.* Cancer, 1988. **62**(4): p. 716-22.
311. Tutton, P.J. and D.H. Barkla, *Effects of glucocorticoid hormones on cell proliferation in dimethylhydrazine-induced tumours in rat colon.* Virchows Arch B Cell Pathol Incl Mol Pathol, 1981. **38**(2): p. 247-51.
312. Mukaide, H., et al., *FKBP51 expressed by both normal epithelial cells and adenocarcinoma of colon suppresses proliferation of colorectal adenocarcinoma.* Cancer Invest, 2008. **26**(4): p. 385-90.
313. Shimizu, N., et al., *Crosstalk between Glucocorticoid Receptor and Nutritional Sensor mTOR in Skeletal Muscle.* Cell Metab, 2011. **13**(2): p. 170-82.
314. Jiang, W., et al., *FK506 binding protein mediates glioma cell growth and sensitivity to rapamycin treatment by regulating NF-kappaB signaling pathway.* Neoplasia, 2008. **10**(3): p. 235-43.
315. Dan, H.C., et al., *Akt-dependent regulation of NF-{kappa}B is controlled by mTOR and Raptor in association with IKK.* Genes Dev, 2008. **22**(11): p. 1490-500.
316. Jacinto, E., et al., *SIN1/MIP1 maintains rictor-mTOR complex integrity and regulates Akt phosphorylation and substrate specificity.* Cell, 2006. **127**(1): p. 125-37.
317. Hay, N., *The Akt-mTOR tango and its relevance to cancer.* Cancer Cell, 2005. **8**(3): p. 179-83.
318. Shah, O.J., Z. Wang, and T. Hunter, *Inappropriate activation of the TSC/Rheb/mTOR/S6K cassette induces IRS1/2 depletion, insulin resistance, and cell survival deficiencies.* Curr Biol, 2004. **14**(18): p. 1650-6.
319. Liu, J., P.D. Stevens, and T. Gao, *mTOR-dependent regulation of PHLPP expression controls the rapamycin sensitivity in cancer cells.* J Biol Chem, 2010.
320. Sun, S.Y., et al., *Activation of Akt and eIF4E survival pathways by rapamycin-mediated mammalian target of rapamycin inhibition.* Cancer Res, 2005. **65**(16): p. 7052-8.
321. Gupta, M., et al., *Inhibition of histone deacetylase overcomes rapamycin-mediated resistance in diffuse large B-cell lymphoma by inhibiting Akt signaling through mTORC2.* Blood, 2009. **114**(14): p. 2926-35.
322. Wan, X., et al., *Rapamycin induces feedback activation of Akt signaling through an IGF-1R-dependent mechanism.* Oncogene, 2007. **26**(13): p. 1932-40.
323. Staibano, S., et al., *Immunohistochemical analysis of FKBP51 in human cancers.* Curr Opin Pharmacol, 2011.
324. Pei, H., Z. Lou, and L. Wang, *Emerging role of FKBP51 in AKT kinase/protein kinase B signaling.* Cell Cycle, 2010. **9**(1): p. 6-7.
325. Dibble, C.C. and B.D. Manning, *A molecular link between AKT regulation and chemotherapeutic response.* Cancer Cell, 2009. **16**(3): p. 178-80.
326. Wang, Z.X., N.R. Kumar, and D.K. Srivastava, *A novel spectroscopic titration method for determining the dissociation constant and stoichiometry of protein-ligand complex.* Anal Biochem, 1992. **206**(2): p. 376-81.
327. Wang, Z.X., *An exact mathematical expression for describing competitive binding of two different ligands to a protein molecule.* FEBS Lett, 1995. **360**(2): p. 111-4.
328. Brunn, G.J., et al., *Direct inhibition of the signaling functions of the mammalian target of rapamycin by the phosphoinositide 3-kinase inhibitors, wortmannin and LY294002.* EMBO J, 1996. **15**(19): p. 5256-67.
329. Knight, Z.A., et al., *A pharmacological map of the PI3-K family defines a role for p110alpha in insulin signaling.* Cell, 2006. **125**(4): p. 733-47.

8 – Acknowledgement:

I would like to thank.....

..... Dr. Felix Hausch who invested a tremendous amount of time and effort in supervising my PhD thesis. While directing my work, he constantly provided exciting ideas and hypotheses, and he always aimed to integrate details into a big picture. Being a chemist, he turned out to be extremely experienced in establishing biological assays. Furthermore, he taught me how to analyze critically both own results and other people's publications.

.... Prof. Dr. Christoph W. Turck for precious feedback during the work-in-progress sessions and for representing my PhD thesis at the LMU.

.... Prof. Dr. Dr. Florian Holsboer for giving me the opportunity to work at his institute and for supporting my work financially for such a long time.

.... Dr. Andreas Bracher who familiarized me with protein crystallization and supervised the whole process of crystal structure determination. He also gave me the opportunity to join him for the synchrotron in Grenoble and performed critical steps of diffraction data analysis.

.... all the colleagues in the lab who provided help with daily lab-work, who gave advice about scientific and personal questions and who contributed to a nice atmosphere during work. I acknowledge Christian Kozany for sharing his huge experience in protein purification, and Serena Cuboni for providing help with mammalian cell cultures and transfection methods. I also want to thank Alexander Kirschner for kindly providing FKBP51KO MEF cells, Anne Fabian for her support during the Akt project and Bas Hoogeland for maintaining the cell culture and keeping the lab alive.
I am grateful to the colleagues in the chemistry lab, namely Steffen Gaali, Christian Devigny, Yansong Wang and Ranganath Gopalakrishnan, for providing compounds and small molecules for different assays and for accompanying me for lunch every day.

.... my parents who supported me financially during the years of study. More importantly, they always encouraged me to continue my work even when it was difficult. Thanks to my sister Martina and to my brother Josef for taking me as a role model (at least concerning the academic career...). Thanks to my aunt Elfriede for providing a lot of encouragement and a nice suit for the final exam. :-)